# Deciphering the Notch Pathway:

## A Bioinformatics Analysis of the RBPJ/Notch Axis

---

**Dissertation**

zur Erlangung des Doktorgrades der Naturwissenschaften

(Dr. rer. nat.)

vorgelegt von

**Tobias Friedrich**

angefertigt am

Institut für Genetik und

Institut für Biomedizinische Informatik und Systemmedizin

Justus-Liebig-Universität Giessen

2023

**Dekan:**

Prof. Dr. Thomas Wilke

Department of Animal Ecology & Systematics, Justus-Liebig-University Giessen

**1. Gutachter:**

Prof. Dr. Sandra B. Hake

Institute for Genetics, Justus-Liebig-University Giessen

**2. Gutachter:**

Prof. Dr. Marek Bartkuhn

Biomedical Informatics and Systems Medicine, Justus-Liebig-University Giessen

## Eidesstattliche Versicherung

Ich erkläre: Ich habe die vorgelegte Dissertation selbstständig und ohne unerlaubte fremde Hilfe und nur mit den Hilfen angefertigt, die ich in der Dissertation angegeben habe. Alle Textstellen, die wörtlich oder sinngemäß aus veröffentlichten Schriften entnommen sind, und alle Angaben, die auf mündlichen Auskünften beruhen, sind als solche kenntlich gemacht. Ich stimme einer evtl. Überprüfung meiner Dissertation durch eine Antiplagiat-Software zu. Bei den von mir durchgeführten und in der Dissertation erwähnten Untersuchungen habe ich die Grundsätze guter wissenschaftlicher Praxis, wie sie in der „Satzung der Justus-Liebig-Universität Gießen zur Sicherung guter wissenschaftlicher Praxis“ niedergelegt sind, eingehalten.

## Statement of authorship

I declare that I have completed this dissertation single-handedly without the unauthorized help of a second party and only with the assistance acknowledged therein. I have appropriately acknowledged and cited all text passages that are derived verbatim from or are based on the content of published work of others, and all information relating to verbal communications. I consent to the use of an anti-plagiarism software to check my thesis. I have abided by the principles of good scientific conduct laid down in the charter of the Justus Liebig University Giessen „Satzung der Justus-Liebig-Universität Gießen zur Sicherung guter wissenschaftlicher Praxis“ in carrying out the investigations described in the dissertation.

_____ _____

Ort, Datum (Tobias Friedrich)

# Abstract

Notch-mediated signal transduction plays a pivotal role for multiple biological processes in development, differentiation and cell homeostasis. Its dysregulation has been linked to several diseases, including different types of cancer. RBPJ is the central transcription factor in Notch signaling, which functions as a molecular switch acting either as an activator or a repressor depending on the activation state of Notch signaling. The RBPJ/Notch complex recruits different co-factors influencing the adjacent chromatin structure and thereby controls transcription. The transcriptional outcome of the Notch pathway is highly context-dependent and therefore difficult to define. In addition, the repressive function of RBPJ and the role of RBPJ in chromatin regulation and signaling dynamics still remain enigmatic.

In this study, transcriptomics and epigenomics approaches were used to characterize both the repressive and activating function of RBPJ. Surprisingly, only a small subset of RBPJ sites act as repressors or activators of Notch target genes and can alter chromatin structure accordingly. I was able to show that RBPJ does not appear to act as a repressor and activator of all Notch target genes equally, rather there are distinct clusters of RBPJ/Notch-mediated transcriptional responses. These Notch-dependent or Notch-independent clusters are associated with distinct biological functions. Furthermore, the responsive RBPJ sites are characterized by comparable features like genomic location and binding strength. Strikingly, these features turned out to be evolutionary conserved, cell-type independent and allowed to computationally predict the responsiveness of RBPJ sites using only RBPJ ChIP-seq data in several cellular models. Taken together, my studies of the repressive and activating functions of RBPJ provide a redefined model for the transcriptional response mediated by Notch. Ultimately, this leads to a better understanding of distinct functions of RBPJ and a more accurate identification of Notch target genes. It is likely that the rules for Notch responsiveness and RBPJ binding, or at least comparable ones, are valid to be applied for several other inducible systems and their corresponding transcription factors.

# Zusammenfassung

Der Notch-Signalweg spielt eine wichtige Rolle für zahlreiche biologische Prozesse in der Entwicklung, Differenzierung und Zellhomöostase. Seine Dysregulation wurde mit unterschiedlichen Krankheiten, einschließlich verschiedener Krebsarten, in Verbindung gebracht. RBPJ ist der zentrale Transkriptionsfaktor des Notch-Signalweges und fungiert als molekularer Schalter, der je nach Aktivierungszustand des Notch-Signalweges entweder als Aktivator oder als Repressor wirkt. Der RBPJ/Notch-Komplex rekrutiert verschiedene Kofaktoren, die die angrenzende Chromatinstruktur beeinflussen und dadurch die Transkription regulieren können. Die transkriptionellen Folgen des Notch-Signalweges sind stark vom zellulären Kontext abhängig und daher schwer zu verallgemeinern. Darüber hinaus sind die repressive Funktion von RBPJ und die Rolle von RBPJ bei der Chromatinregulation immer noch nicht vollständig verstanden.

In meiner Thesis wurden verschiedene transkriptomische und epigenomische Datensätze verwendet, um sowohl die repressive als auch die aktivierende Funktion von RBPJ zu charakterisieren. Überraschenderweise wirkt nur eine kleine Gruppe von RBPJ-Bindungen als Repressoren oder Aktivatoren von Notch-Zielgenen und kann die Chromatinstruktur entsprechend verändern. Ich konnte zeigen, dass RBPJ nicht als Repressor und Aktivator für alle Notch-Zielgene gleichermaßen wirkt, sondern dass es verschiedene Cluster von RBPJ/Notch-vermittelten transkriptionellen Reaktionen gibt. Diese Notch-abhängigen oder Notch-unabhängigen Cluster repräsentieren unterschiedlichen biologischen Funktionen. Des Weiteren haben transkriptionell responsive RBPJ-Bindungen vergleichbare Merkmale wie genomische Lage und Bindungsstärke. Diese Merkmale erwiesen sich als evolutionär konserviert, zelltypunabhängig und ermöglichten eine Vorhersage der transkriptionell responsiven RBPJ-Bindungen. Hierfür sind RBPJ ChIP-seq Daten ausreichend. Zusammengefasst liefern meine Ergebnisse der repressiven und aktivierenden Funktionen von RBPJ ein neu definiertes Modell für die von Notch vermittelte Transkriptionsantwort. Letztendlich führt dies zu einem besseren Verständnis der verschiedenen Funktionen von RBPJ und zu einer genaueren Identifizierung von Notch-Zielgenen. Es ist wahrscheinlich, dass die Regeln für die transkriptionell responsiven RBPJ-Bindungen, oder zumindest vergleichbare Regeln, auch für andere induzierbare Systeme und die entsprechenden Transkriptionsfaktoren gelten.

# TABLE OF CONTENTS

# List of tables



# List of figures

# 1. Introduction

## 1.1. The mammalian genome

Deoxyribonucleic acid (DNA) encodes the genetic information, which is the basis of all life as we know it. It is composed of nucleic acid base pairs whose sequence are ciphering the code of life. The genome itself can be divided into different regions with distinct functions. The most prominent regions are so called protein-coding genes (Crick et al. 1961). Genes can be transcribed into messenger RNA (mRNA) by the RNA polymerase. The resulting mRNA is translocated from the nucleus into the cytoplasm. Here, these mRNAs are translated at the ribosome to synthesize functional proteins needed to catalyze biological processes (Roeder and Rutter 1969; Boeger et al. 2005). The rate at which genes are transcribed is regulated by specific proteins, the so-called transcription factors (TFs). These TFs can recognize specific DNA sequences, e.g. at promoter regions of genes or distal regulatory regions (enhancers), bind to them and thus initiate or enhance the transcription of the associated genes (Latchman 1993). However, protein coding genes are making up only around 1.5% of the whole DNA sequence (Lander et al. 2001; Pennisi 2001; Venter et al. 2001). The vast majority of the DNA is referred to as noncoding regions, which include highly repetitive elements and regulatory regions amongst others (ENCODE Project Consortium 2012; Perenthaler et al. 2019).

The human genome contains about 3.2 billion base pairs, which is equivalent to 2 meters in length if it would be stretched out (Alberts et al. 2002). That is why, in order to fit into a nucleus of roughly 6 µm, the DNA needs to be tightly packed (Bloomfield 1996). In eukaryotes, this is achieved by wrapping the DNA around a protein complex called a nucleosome. The nucleosome consists of eight core histone proteins, two of each H2A, H2B, H3 and H4 and the linker histone H1 (Kornberg 1974; Olins and Olins 1974; Woodcock et al. 1976). These complexes are wrapped by 147 base pairs of DNA and are referred to as a “beads on a string” structure (Olins and Olins 2003). This structure can be further condensed until it becomes a chromosome during the metaphase (Finch and Klug 1976; Sedat and Manuelidis 1978). The entire complex of DNA and the above-mentioned histone proteins is called chromatin.

In mammals, all somatic cells are descendants of one fertilized ovum and therefore contain the same genetic code (Nanney 1958; Jacob and Monod 1961). Nevertheless, the cells of different tissues differ drastically regarding their function and structure. This is possible

because different cells express specific genes and thus possess a cell-specific composition of proteins. The underlying mechanism is called transcriptional regulation and can explain the phenotypic differences between cells even though they share the same genetic code. Transcriptional regulation is not only critical for cellular differentiation during the development of a multicellular organism, but also plays a major role in cellular responses to various stimuli. In addition, dysregulation of transcription is associated with many disease (Lee and Young 2013).

## 1.2. Regulation of transcription

The precise regulation of gene transcription is of utmost importance to the fundamental processes of cells, tissues and whole multicellular organisms. In the next chapter, some of the known mechanisms for regulating transcription in eukaryotes will be highlighted.

### 1.2.1. Chromatin conformation

Chromatin plays the central role in the condensation of DNA during cell division, however, it plays an important role in the transcriptional regulation, as well. As early as the 1920s, the observation of the differently strongly stained parts of chromatin during cell division was made. These two different forms of chromatin were described by Emil Heitz as euchromatin and heterochromatin (Heitz 1928). Due to their different densities, the hypothesis was formulated that euchromatic regions are genetically active, while heterochromatic regions are not (Heitz 1929). Subsequent studies confirmed that euchromatin consists of the looser regions, whereas heterochromatin is more compacted and that euchromatic regions are generally more transcriptionally active compared to heterochromatic regions (Trojer and Reinberg 2007). As a result of their less dense packing, euchromatic regions are much more accessible for proteins, like TFs, hence enabling transcription. In contrast, the compact packing of heterochromatin prevents the binding of proteins and thus hinders transcription. Heterochromatin can be further divided into facultative or constitutive heterochromatin (Brown 1966). Constitutive heterochromatin is found at gene-poor regions, that contain a lot of repetitive elements like in the telomeric or centromeric regions. Furthermore, it was shown that constitutive heterochromatic regions are in general conserved between different cell types. In contrast, facultative heterochromatin can be converted into euchromatin and vice

versa and is found at genes that need to be silenced after certain developmental processes (Trojer and Reinberg 2007; Saksouk et al. 2015).

As described, heterochromatic and euchromatic regions differ strongly in their function and structure. Multiple mechanisms were identified that are known to influence the structure of chromatin.

First, there are specific variants of histones, such as H2A.Z, that can replace the canonical histones within the nucleosome (Raisner et al. 2005; Giaimo et al. 2018) (Fig. 1A). To achieve this, various chaperones and chromatin remodelers can incorporate the variants into the nucleosome. These variants can deviate significantly from their canonical counterparts in regards of their amino acid sequence and thus in their associated function. Histone variants can directly or indirectly affect the nucleosome structure and are known to be involved in lineage commitment, transcriptional regulation, DNA repair, chromosome segregation and more (Buschbeck and Hake 2017; Giaimo et al. 2019).

Next, are ATP-dependent chromatin remodelers (Swygert and Peterson 2014) (Fig. 1B). These proteins consume energy to alter the chromatin structure. In addition to the incorporation of histone variants, they can lead to a relocalization (“sliding”) of the nucleosomes by detaching the DNA resulting in more or less accessible DNA. Furthermore, chromatin remodelers can interact with the posttranslational modifications of histones (Reyes et al. 2021).

Finally, the posttranslational modifications (PTMs) of the N-terminal tail of histones have a profound influence on the structure of the chromatin (Cheung et al. 2000; Bannister and Kouzarides 2011) (Fig. 1C). Over the time multiple modifications were identified, including acetylation, methylation, phosphorylation, ubiquitination and SUMOylation. These modifications can be localized at various amino acids of different histone tails. Depending on the modification and the affected amino acids, the PTMs have different effects. Conserved combination of histone PTMs are associated with distinct regions and/or functions of the chromatin (Fig. 1D). In addition, there are different groups of enzymes that can interact with those PTMs. In simple terms, these can be divided into “readers” which recognize and interact with a particular histone PTM, “writers” and “erasers” which set or remove histone PTMs, respectively (Strahl and Allis 2000; Gillette and Hill 2015).

In general, acetylation of lysines at the histones tails is associated with more active chromatin. Acetylation neutralizes the positive charge of lysine, resulting in weaker binding

of DNA to histones. This weaker binding is accompanied by a more accessible DNA and allows for better interaction with proteins such as TFs. Acetylation is regulated by two opposing families of enzymes. The histone acetyltransferases (HAT) are able to catalyze the transfer of an acetyl group to the histone tail, while the histone deacetylases (HDAC) do the opposite. (Allfrey et al. 1964; Hebbes et al. 1988; Thorne et al. 1990; Sterner and Berger 2000; Kouzarides 2007)

Histone methylation typically occurs at lysines or arginines at the histone tails. Lysines can be mono-, di-, or trimethylated. The function of lysine methylation is more diverse compared to acetylation, as it does not affect the charge of the histone itself and subsequently does not directly regulate the structure of chromatin. Methylation is associated with both activation and repression of transcription and plays an important role in the formation of heterochromatin and X-chromosome inactivation. This can be achieved by chromatin binding proteins that recognize and bind the methylated histones and subsequently affect the chromatin structure or gene transcription. Lysine methylation is catalyzed by lysine methyltransferases and demethylation by histone demethylase (Rea et al. 2000; Shi et al. 2004; Whetstine et al. 2006; Bannister and Kouzarides 2011; Huang and Zhu 2018).

In summary, several mechanisms are known to alter the chromatin conformation including histone variants, PTMs and chromatin remodelers. Importantly, these mechanisms are interrelated and can regulate each other.

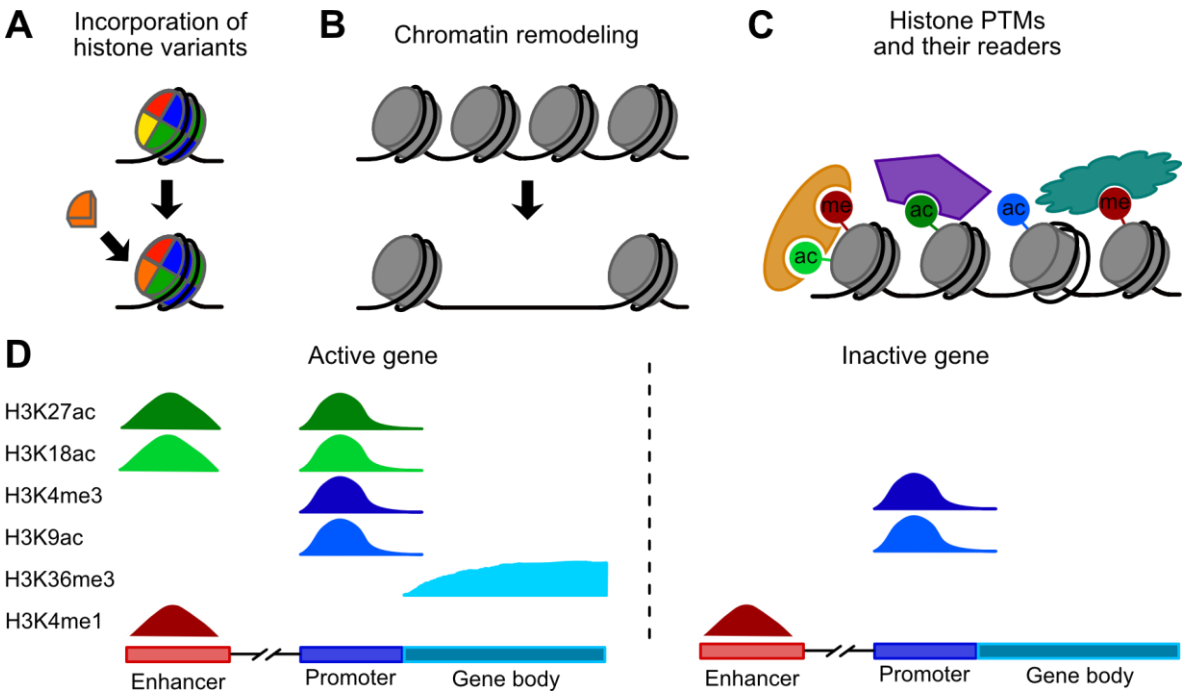


**Figure 1) Schematic representation of mechanisms that influence the chromatin conformation and gene regulation.** A) Incorporation of histone variants, B) ATP-dependent remodeling and C) histone PTMs and their readers (ac = acetylation of histone tails, me = methylation of histone tails). D) Schematic of conserved combinations of histone PTMs, which are associated with distinct functions or genomic regions leading to different activation state of the associated genes.

### 1.2.2. Transcription factors

The term transcription factor was initially chosen for proteins that can alter the expression (transcription) of genes or are involved in this process (Matsui et al. 1980). Nowadays, the definition of a TF has been refined. While the ability to affect transcription is still a prerequisite, an equally important feature of a TF is its ability to bind to a specific DNA sequence, a so-called motif (Latchman 1993).

The combinatory network of multiple TFs, orchestrating the expression of thousands of genes, plays a pivotal role in the precise regulation of different transcriptional programs (Sonawane et al. 2017). These programs, and therefore their associated TFs, are required for many biological processes, such as different developmental stages or as a response upon stimuli. Thus, aberrant expression and regulation of TFs is frequently found as the cause for various diseases, from cancer to developmental disorders (Alitalo et al. 1983; Spitz

and Furlong 2012; Bushweller 2019). Overall, TFs can be divided into ubiquitously expressed ones, like CCCTC-binding factor (CTCF) or the specificity protein 1 (SP1), that play an important role in many cell types or specific TFs, which are only expressed in a tissue-specific manner (Pugh and Tjian 1990; Filippova et al. 1996; Zhou et al. 2017). It has to be noted that TF expression is not binary (expressed or not expressed), but the graded degree of expression is important. Moreover, TFs can regulate their own expression, thus adding an additional layer of fine tuning the transcription (Ravasi et al. 2010).

In general, TFs can either act as an activator or a repressor of transcription by binding directly to the promoter regions of genes or at distal regulatory regions (Heintzman et al. 2007; Palstra and Grosveld 2012). To exert their effect on transcription, TFs have several modes of function, which often involve interactions with additional proteins to form a multiprotein complex. On the one hand, TFs are crucial for the initiation of gene expression by regulating the interaction of DNA with the RNA polymerase (Horikoshi et al. 1988; Tsai and Sigler 2000; Kornberg 2007). On the other hand, TFs are also able to inhibit the interaction of the RNA polymerase with the promoter regions, thereby repressing transcription (Ohkuma et al. 1990; Um et al. 1995; Gaston and Jayaraman 2003).

Additionally, TFs can modify the adjacent chromatin to regulate the transcription. This can be achieved by the recruitment of additional co-factors. These modifications of the chromatin include the ATP-dependent remodeling, PTM of histones, incorporation of histone variants and more, which in turn affects levels of transcription (Weber and Henikoff 2014; Zhang et al. 2018; Jian et al. 2021).

TFs can also act as insulators inhibiting long-range interactions between enhancers and promoters or protect open chromatin regions by blocking the spread of heterochromatin (Brasset and Vaury 2005).

Finally, the pioneer TFs can bind to the inaccessible heterochromatic regions and recruit ATP-dependent remodelers, resulting in less condensed chromatin and thus enabling the binding of further TFs. Additionally, some pioneering TFs bind to inactive regulatory regions (e.g. primed enhancer), allowing the binding of further TFs to activate them. In summary, pioneer factors are important for the initiation of transcription, especially in condensed chromatin (Zaret and Carroll 2011; Zaret 2020).

### 1.2.3. Methylation of DNA

DNA methylation represents also an important mechanism for the transcriptional regulation (Miller and Grant 2013). In this case, a methyl group is transferred onto the C5 position of the cytosine resulting in a 5-methylcytosine. This is accomplished by a family of enzymes called DNA methyltransferases (Bestor et al. 1988). Demethylation of cytosine can be achieved by TET methylcytosine dioxygenases (Tahiliani et al. 2009). Typically, DNA methylation is associated with the repression of genes and has critical functions in imprinting, X-chromosome inactivation and the repression of germline-specific genes. The methylation of cytosines usually occurs at symmetrical CpG dinucleotides. CpGs are generally rarely found in the mammalian genome, except in so-called CpG islands (CGI) (Ehrlich et al. 1982). CGIs are highly enriched at promoter regions, especially at housekeeping genes. In contrast to typical CpG sites, CpG islands are rarely methylated (Bird et al. 1985; Miller and Grant 2013).

### 1.2.4. Super enhancers

Enhancer regions are central for the precise regulation of gene transcription. Genome-wide binding studies (e.g. ChIP-seq) for typical enhancer marks have revealed a subset of atypical enhancers. These enhancer clusters have been termed "super-enhancers" (SEs) by Young and colleagues (Lovén et al. 2013; Whyte et al. 2013) and "stretch enhancers" by Collins and colleagues (Parker et al. 2013). SEs contain multiple enhancer clusters, span broader regions than the average enhancer and are more strongly associated with active enhancer marks such as H3K27ac or the Mediator complex (Whyte et al. 2013). Several studies linked SEs to basic processes such as regulation of genes vital for cell identity. In addition, dysregulation of SEs have been linked to various diseases, including cancer (Lovén et al. 2013; Liu et al. 2022; Yoshino and Suzuki 2022). Although some groups find the use of the term SE problematic due to the lack of functional definition and arbitrary chosen cutoffs of binding strength between “normal” and “super” enhancers, these regions clearly represent the most active enhancers within a cell and therefore appear to be important for transcriptional regulation (Pott and Lieb 2015).

## 1.3. The Notch signal transduction pathway

The development of a single zygote into a multicellular organism containing many different cell types organized in complex tissues is an intricate process that needs to be precisely regulated (Sanz-Ezquerro et al. 2017). Essential for developmental processes are signaling pathways that lead to the execution of the respective transcriptional programs, which orchestrate cell differentiation and determination. A set of highly conserved signaling pathways including Notch are pivotal for the correct regulation of the development process in many species (Artavanis-Tsakonas et al. 1999; Sanz-Ezquerro et al. 2017).

### 1.3.1. A brief history of the Notch pathway

In 1914, John S. Dexter described the Notch phenotype in *Drosophila melanogaster* as a small notch in the wing margin (Dexter 1914). Shortly thereafter, the alleles of the associated gene were identified by Thomas Hunt Morgan (Morgan 1917). In the 1980s, the group of Spyros Artavanis-Tsakonas succeeded in elucidating the structure of the *Notch* gene and the Notch protein. They were able to isolate (Artavanis-Tsakonas et al. 1983) and sequence (Wharton et al. 1985) the *Notch* gene and identified that the putative Notch protein spans the membrane and contains epidermal growth factor (EGF)-like repeats (Kidd et al. 1986). Notch homologs were found in other species including *lin-12* (Yochem et al. 1988) and *glp-1* (Austin and Kimble 1989) in *Caenorhabditis elegans, Xotch* (Coffman et al. 1990) in Xenopus, *LvNotch* (Sherwood and McClay 1997) in sea urchin, *int-3* (Robbins et al. 1992; del Amo et al. 1993) in mouse or *TAN-1* (Ellisen et al. 1991; Aster et al. 1994) in humans. Later studies have shown that Notch is highly conserved in metazoans (Gazave et al. 2009; Theodosiou et al. 2009).

An important milestone in understanding the Notch signaling pathway was the 1991 finding that the Notch transmembrane receptor can interact with another transmembrane receptor called Delta (Rebay et al. 1991). Based on this discovery, Notch was hypothesized to be important for cell-cell interactions, which was later confirmed by several groups (reviewed in (Artavanis-Tsakonas et al. 1999).

Over the decades, numerous functions for the Notch signaling pathway were unraveled. As early as the 1930s, Donald F. Poulson showed that Notch is essential for embryonic development (Poulson 1937). This was later confirmed by Artavanis-Tsakonas and colleagues when they described that a complete deletion of Notch resulted in failure of correct neurogenic tissue development (Artavanis-Tsakonas et al. 1983).

### 1.3.2. The role of the Notch pathway in mammalian development

Notch signaling is important in many biological processes, including the development and homeostasis of somite-derived organs, vasculature, heart, nervous system, hematopoietic systems and other tissues. (reviewed in (Siebel and Lendahl 2017; Zhou et al. 2022) (Fig. 2A & B). In addition, Notch signaling has important functions in the maintenance of progenitor stem cells (VanDussen et al. 2012; Dray et al. 2021), temporal and spatial expression of Notch during e.g. organogenesis (Mishra et al. 2001; Tokunaga et al. 2004) and damage repair of organs (Minnis-Lyons et al. 2021). One of the best described functions of Notch is its activity in the development of T-cells (Fig. 2C).

Several studies have shown that T-cell development does not occur in the absence of Notch1. Instead, there is even an accumulation of B-cells (Radtke et al. 1999; Han et al. 2002). Accordingly, hyperactivation of Notch leads to an increase of T-cell numbers and a reduction of B-cell numbers (Pui et al. 1999). This highlights the importance of the Notch pathway for the T-cell lineage commitment and the T-cell development. T-cells have their origin in hematopoietic stem cells (HSCs), which reside in the bone marrow (T-cell development is reviewed in (Rothenberg et al. 2008). The HSCs migrate into the thymus, colonize there and then are called immature thymocytes. Interaction between immature thymocytes and thymic epithelial cells (TECs), which constitutively express the Notch ligand DLL4, leads to differentiation into early T-cell precursors (ETP). The expression of DLL4 in TECs is a prerequisite for the differentiation of T-cells and its depletion leads to an ectopic appearance of immature B-cells (Koch et al. 2008). The ETPs, still double negative stages for CD4 and CD8 coreceptors (DN; CD4- & CD8-), develop further through DN1 and DN2 stages, which also depends on Notch expression (Schmitt et al. 2004; Taghon et al. 2005). Interestingly, artificial expression of the Notch inhibitor NRAP leads to a stop of progression during maturation (Yun and Bevan 2003). DN3 stage cells express the pre T-cell receptor (TCR) and are now completely committed for T-cells. Next, the TCR gene rearrangement takes place, which is followed by the decision for the either αβ or γδ T-cell lineages. Again, Notch plays a role in this decision, here lower levels of Notch are associated with a decreased likelihood to become αβ T-cells (Garbe et al. 2006; Ciofani et al. 2006). αβ T-cells develop into CD4 & CD8 double positive (DP) thymocytes, which later differentiate into CD4 or CD8 single positive (SP) thymocytes.

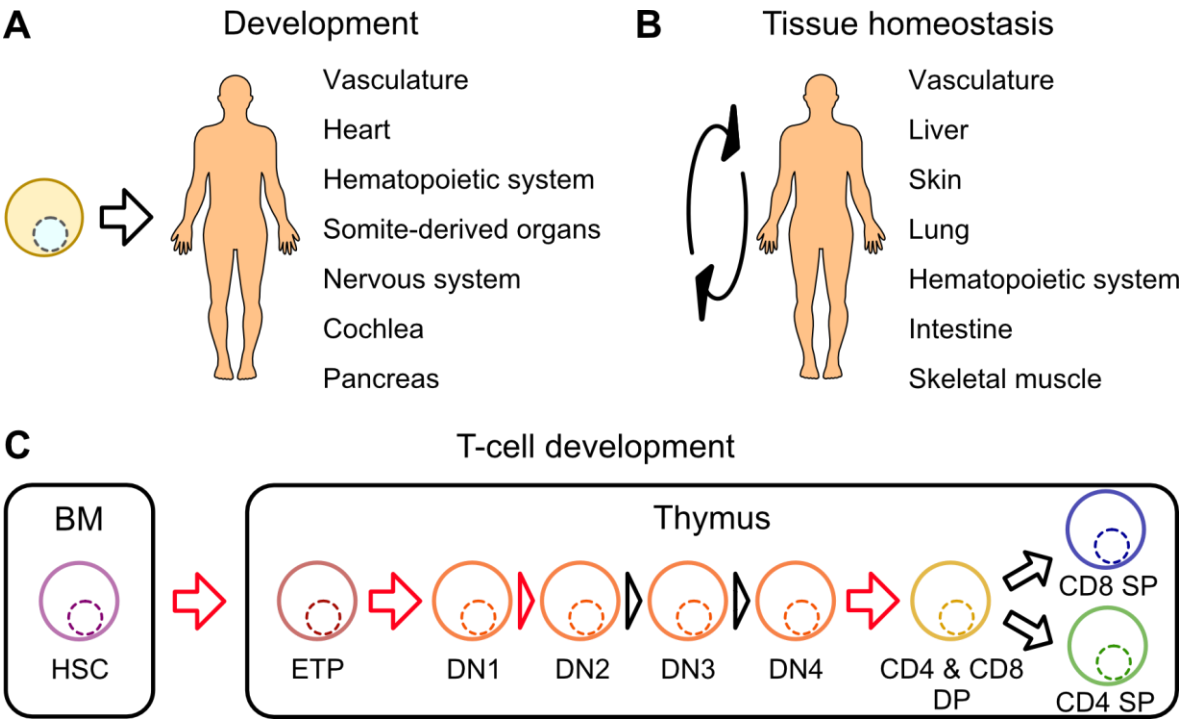


**Figure 2) Schematic representation of the functions of the Notch signaling pathway.** Functions associated with A) developmental processes, B) tissue homeostasis or C) T-cell development. BM = bone marrow, ETP = early T-cell precursors, DN = double negative, DP = double positive, HSC = hematopoietic stem cells, SP = single positive. Red arrows indicate developmental steps that have been associated with Notch signaling.

### 1.3.3. The role of the Notch pathway in cancer and other diseases

In the last three decades, the Notch pathway has been frequently linked to cancer. Often Notch directs the decision between differentiation and proliferation. Thus, it can take either an oncogenic or tumor-suppressive role, depending on the context. Notch can have an oncogenic function in most leukemias (Pear et al. 1996; Weng et al. 2004; Herranz et al. 2014), breast cancer (Reedijk et al. 2005; Stylianou et al. 2006) and hepatocellular cancer (Razumilava and Gores 2013; Zhu et al. 2021). In contrast, Notch acts as a tumor suppressor in squamous cell carcinoma (Pickering et al. 2014) and neuroendocrine tumors (Rekhtman et al. 2016). In 2017, Aster, Pear and Blacklow summarized that Notch signaling affects all cancer hallmarks (Aster et al. 2017), as described by Hanahan and Weinberg (Hanahan and Weinberg 2011). In this context, the function and contribution of Notch signaling in a specific cancer depends strongly on the type of cancer.

In 1991, it was first discovered that patients with T-cell acute lymphoblastic leukemia (T-ALL) suffer from a chromosomal translocation of the *NOTCH1* gene (Ellisen et al. 1991). This was confirmed in mice (Pear et al. 1996) and later it was identified that over 50% of all T-ALL patients have activation mutations of *NOTCH1* (Weng et al. 2004). These mutations result in a ligand-independent activation or a prolonged half-life, respectively. However, the previously described translocation of *NOTCH1* occurs in only less than 1% of the patients. Similar to Notch1, hyperactivating mutations of the *NOTCH3* gene have also been discovered in T-ALL, which results in a comparable Notch signature as the mentioned *NOTCH1* mutations (Bernasconi-Elias et al. 2016).

Triple negative breast cancer (TNBC) is a subtype of breast cancer (BC) characterized by the lack of estrogen receptor (ER), progesterone receptor (PR) and human epidermal growth factor receptor 2 (HER2) (Abramson et al. 2015). Patients with TNBC have a higher mortality rate and an increased likelihood of relapsing rate within the first five years compared to other types of BC (Dent et al. 2007). Furthermore, expression of a constitutively active form of Notch1 has been shown to contribute to breast cancer development in mice (Kiaris et al. 2004) and high level of NOTCH1 is associated with poor patients survival (Reedijk et al. 2005). Additionally, NOTCH1 and NOTCH4 are valid biomarkers for TNBC compared to hormone positive breast cancer, as they are much stronger expressed and subcellular localized in the nucleus (Speiser et al. 2012). Approximately 13% of TNBC patients have mutations of *NOTCH1,* that results in a ligand-independent activation or an increased half-life of the protein (Wang et al. 2015). This is comparable to the mutations identified in T-ALL patients. Furthermore, other studies showed a positive correlation between Notch expression and pAKT and nuclear NF-κB signaling (Zhu et al. 2013).

Moreover, mutations of the Notch receptors, their ligands or the downstream components of Notch signaling lead various noncancerous diseases such as CADASIL (Joutel et al. 1996), Alagille syndrome (Li et al. 1997) or Adams-Oliver syndrome (Hassed et al. 2012; Stittrich et al. 2014).

### 1.3.4. Activation of the Notch pathway

In contrast to *Drosophila*, mammals have four paralogous Notch genes (Larsson et al. 1994; Sugaya et al. 1997). These encode four transmembrane receptors that have both redundant and unique functions. The overall structure of the four Notch proteins is similar and each receptor contains three domains: The Notch extracellular domain (NECD), the transmembrane (TM) domain and the Notch intracellular domain (NICD) (Kojika and Griffin 2001).

The NECD consists of 29-36 tandem epidermal growth factor (EGF)-like repeats, depending on the Notch receptor (Wharton et al. 1985; Lardelli et al. 1994; Uyttendaele et al. 1996; Gallahan and Callahan 1997). These EGF-like repeats are necessary for the interaction with the ligands that initiate the activation of Notch signaling (Rebay et al. 1991). Structurally, EGF is followed by a unique negative regulatory region (NRR) that contains three cysteine-rich Lin12 Notch repeats, as well as the heterodimerization domain. This NRR harbors the S2 cleavage sites for metalloproteases (Brou et al. 2000; Stephenson and Avis 2012). The TM domain contains the S3 cleave site for the γ-secretase complex. The NICD contains an N-terminal RAM (recombination binding protein-J -associated module) domain, followed by seven ankyrin repeats (ANK), the NOTCH cytokine response (NCR) region and the transactivation domain (TAD). At the very C-terminus is the PEST (proline/glutamic acid/serine/threonine) region, which is required for recruitment of the ubiquitin ligase complex, which is necessary for proteasome-dependent degradation of the NICD (Rechsteiner and Rogers 1996; Gupta-Rossi et al. 2001; Fryer et al. 2004; Carrieri and Dale 2016). The overall structure of the Notch receptor is reviewed in depth in (Gordon et al. 2008) (Fig. 3).

Five different Notch ligands have been described in mice and humans: Delta-like ligand 1 (DLL1), delta-like ligand 3 (DLL3), delta-like ligand 4 (DLL4), Jagged1 (JAG1) and Jagged2 (JAG2) (Fig. 3). All of these ligands are also transmembrane proteins with extracellular domains that harbor multiple EGF-like repeats. The EGF-like repeats, along with other motifs, form the interaction point of Notch receptors with their ligand (D'Souza et al. 2010). Each individual ligand is associated with different biological functions, including typical cell-cell communication, but also specific ones such as the induction of apoptosis (Maemura et al. 2013).

After translation in the endoplasmic reticulum, the Notch receptor is processed at the S1 cleavage site by furin-like convertase in the Golgi compartment, followed by the

translocation to the cell membrane lake (Lake et al. 2009). Here, upon binding of the ligand to the NECD, the conformation of the NECD changes, leading to an exposition of the S2 cleavage site. This S2 site is then recognized and cleaved by the metalloprotease (ADAM), resulting in the removal of the NECD (van Tetering et al. 2009). The remaining protein, composed of the TM domain and the NICD, is called NOTCH extracellular truncation (NEXT). NEXT is subsequently cleaved at the S3 site by the γ-secretase complex, leading to the release of the NICD from the membrane (Mumm et al. 2000). The NICD is then translocated into the nucleus and interacts with the transcription factor recombination binding protein-J (RBPJ) via the NICDs RAM domain (Tamura et al. 1995). An inactivation of the Notch signaling is mediated through proteasomal degradation of the NICD, after poly-ubiquitylation by FBWX7 (Fig. 4).

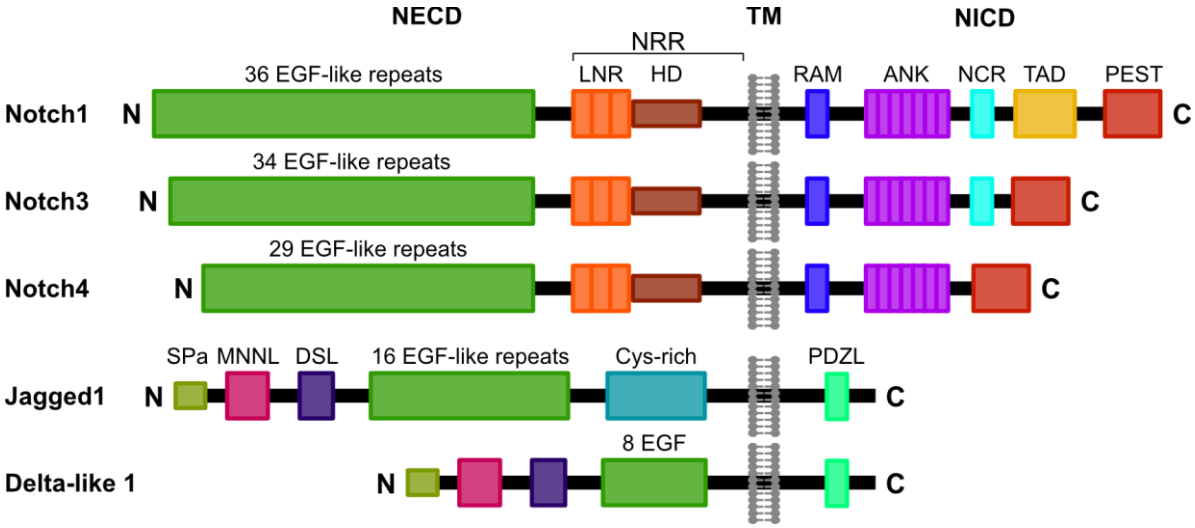


**Figure 3) Illustration of the Notch1, Notch3 and Notch4 receptors, as well as their ligands Jagged1 and Delta-like 1.** Abbreviations: NECD = Notch extracellular domain; TM = transmembrane domain; NICD = Notch intracellular domain; EGF = epidermal growth factor; NRR = negative regulatory region; LNR = Lin12 Notch repeats; HD = heterodimerization domain; RAM = recombination binding protein-J -associated module; ANK = ankyrin repeats; NCR = NOTCH cytokine response; TAD = transactivation domain; PEST = proline/glutamic acid/serine/threonine; SPa = single-pass; MNNL = NOTCH ligand N-terminal domain; DSL = Delta/Serrate/LAG-2 domain; Cys = cysteine, PDZL = post-synaptic density protein ligand. Modified after (Arruga et al. 2018).

### 1.3.5. Transcriptional response upon Notch activation

RBPJ, also known as CSL (CBF1/Su(H)/Lag-1), is the central transcription factor in Notch signal transduction (Lake et al. 2014). It is ubiquitously expressed (Hamaguchi et al. 1992) and is already essential for embryonic developmental (Oka et al. 1995). RBPJ consists of three domains, the NTD (N-terminal domain), BTD (β-trefoil domain) and CTD (C-terminal domain) and binds to DNA via the NTD and BTD (Nam et al. 2006; Wilson and Kovall 2006). Genome-wide binding studies have shown that RBPJ can bind to either promoter or enhancer regions in order to regulate transcription (Wang et al. 2011; Wang et al. 2014).

In the absence of the NICD, the transcription factor RBPJ acts as an active repressor of transcription (Hsieh et al. 1996; Furriols and Bray 2001). Over the years, several repressive mechanisms of RBPJ have been identified. RBPJ can either directly repress transcription by directly interacting with TFIID/TFIIA (Olave et al. 1998) or is able to recruit various co-repressors to from a repressive complex. Known co-repressors include SHARP (Oswald et al. 2002), KyoT2 (Taniguchi et al. 1998) and L3MBTL3 (Xu et al. 2017). Although they do not share identical sequences, many co-repressors interact with the same domains of RBPJ (Hall et al. 2022). The repressor complexes include histone modifying enzymes like HDACs and the histone H3K4me3 demethylase KDM5A, that inactivate the surrounding chromatin (Kao et al. 1998; Liefke et al. 2010; Oswald et al. 2016).

Upon ligand binding the NICD translocates into the nucleus and binds to RBPJ (Tamura et al. 1995). The interaction of the NICDs and RBPJ leads to recruitment of the co-activator Mastermind-like (MAML) (Jeffries et al. 2002). The MAML/NICD/RBPJ ternary complex (Nam et al. 2006; Wilson and Kovall 2006) leads to the recruitment of the HATs p300 and PCAF (Oswald et al. 2001; Wallberg et al. 2002; Guarani et al. 2011) and chromatin remodelers (Pillidge and Bray 2019). This results in an active chromatin state, leading to the transcription of Notch target genes. In addition, the binding of MAML with NICD/RBPJ increases the DNA binding capabilities of the complex (Wu et al. 2000; Rogers et al. 2020).

However, several studies have revealed another layer of regulation of Notch target genes. It was found that two RBPJ binding motifs in a head-to-head arrangement are located at some regulatory regions of known Notch target genes (Nam et al. 2007). These sites lead to the formation of a dimeric Notch transcription complexes, which is more stable compared to a single bound RBPJ. This dimeric complexes play an important role in leukemogenesis and T-cell development (Liu et al. 2010).

Furthermore, the Stunnenberg group has found that RBPJ binds DNA in a methylation-dependent manner (Bartels et al. 2011). More specifically, RBPJ can bind strongly to a methylated and mutated consensus motif (GCmGGGAA), which is only weakly bound in its unmethylated form. Following publications identified that RBPJ binds methylated GC repressor elements, resulting in a specific gene expression pattern in the smooth muscle cell context (Rozenberg et al. 2014; Rozenberg et al. 2018).

Finally, the canonical model implies that RBPJ is constantly bound to the DNA (Borggrefe and Oswald 2009), independent of the Notch activity status. Several studies refined this model and revealed in part distinct dynamic binding behavior of RBPJ. In *Drosophila*, the group of Sarah J. Bray unveiled that RBPJs binding capability to the DNA is stronger when the Notch signaling pathway is active (Krejčí and Bray 2007). Furthermore, an "assisted loading" of the MAML/NICD/RBPJ complex to the DNA was described, which additionally displayed a longer dwell time (Gomez-Lamarca et al. 2018). In humans, the groups of Stunnenberg and Aster identified two distinct groups of RBPJ binding sites based on their response upon changes in the Notch pathway (Castel et al. 2013; Wang et al. 2014). In the first group, the genomic RBPJ binding strength does not change whether the Notch signaling pathway is active or inactive. These sites, however, were less associated with the co-activator p300 and active chromatin mark H3K27ac in the background of an active Notch signaling pathway. This contrasts with the second group of binding sites, to which RBPJ binds more strongly when the Notch signaling pathway is active. These sites were stronger associated with active chromatin marks and p300 (Castel et al. 2013). This leads to an active transcription of associated Notch target genes. Furthermore, those sites with activating capabilities are often located within super-enhancers, which have strong transcriptional potential themselves and RBPJ may even further increase the activation levels of the aforementioned SEs (Wang et al. 2014).

Several recent studies have shown that NICD can also interact with various other signaling pathways independently of RBPJ. Interactions with the NF-κB (Song et al. 2008; Jin et al. 2013), PTEN (Yue et al. 2017), AKT (Li et al. 2020), Wnt (Axelrod et al. 1996; Hayward et al. 2005; Mangolini et al. 2018) or TGF-β (Blokzijl et al. 2003; Zavadil et al. 2004) pathways have been described. The interaction with NF-κB pathway has been shown to play a role in colorectal (Fernández-Majada et al. 2007), cervical (Song et al. 2008), breast (Hossain et al. 2018) and small-cell lung cancer (Kuramoto et al. 2012).

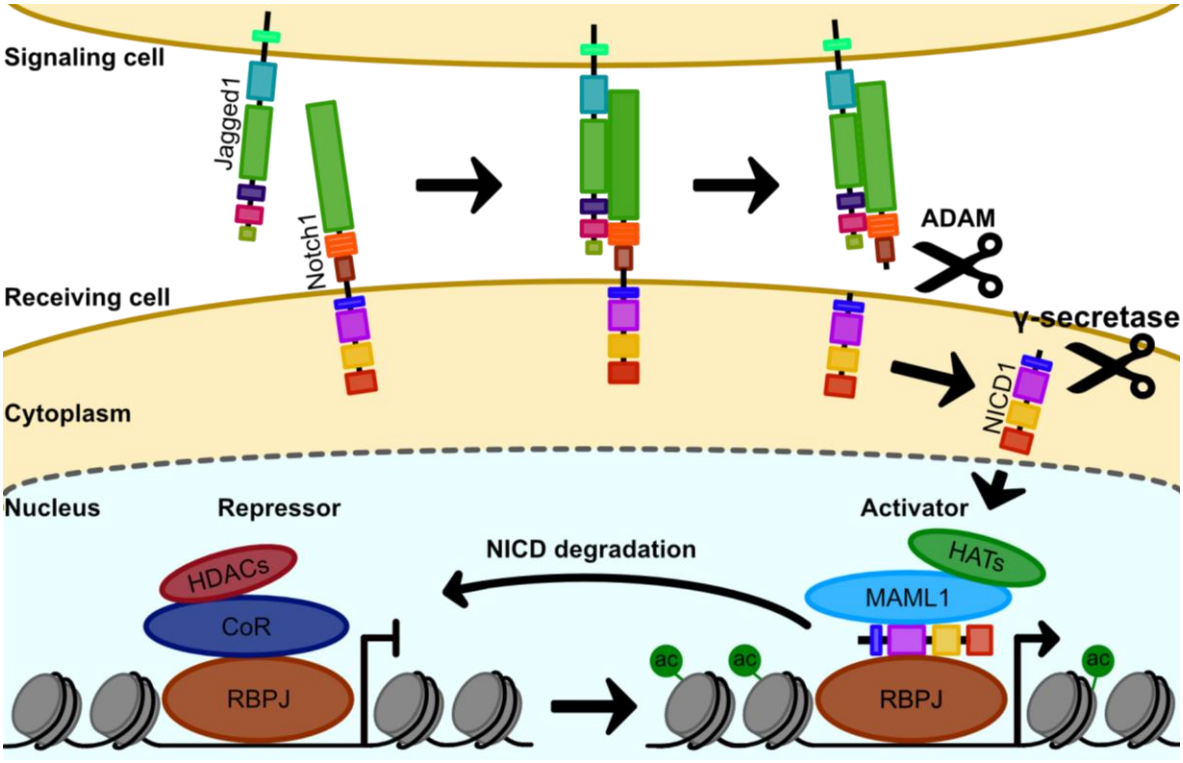


**Figure 4) Molecular model of the Notch pathway.** Notch signaling pathway is activated upon interaction of Jagged1 and the Notch1 receptor. Abbreviations: ac = acetylation of histone tails; ADAM = a disintegrin and metalloprotease; CoR = co-repressors; HAT = histone acetyltransferase; HDAC = histone deacetylase; NICD1 = Notch1 intracellular domain.

### 1.3.6. Diversity in tissue-specific expression of Notch target genes

Although the Notch signaling pathway plays an important role in development and homeostasis and its dysregulation has been linked to diseases and carcinogenesis, there are only a few comprehensive studies focusing on Notch target genes (Agrawal et al. 2009; Canté-Barrett et al. 2020; Xue et al. 2021). Canonical direct Notch target genes are characterized by an RBPJ-mediated activation upon Notch signaling. One difficulty is that sets of Notch target genes sometimes differ widely between various cell types (Borggrefe and Oswald 2009; Siebel and Lendahl 2017). This suggests a complex gene regulatory network (GRN) that is influenced by Notch, but also influences the transcriptional Notch response, as well (Sánchez-Iranzo et al. 2022). Over the past decade, genome-wide studies of RBPJ binding have dramatically increased our knowledge of the Notch gene regulatory network.

Importantly, genome-wide studies of Notch binding have shown that the majority of genes whose promoters are bound do not respond to perturbations of the Notch pathway, i.e., activation or inhibition (Wang et al. 2011). In addition, many known Notch target genes are characterized by Notch binding to enhancer elements. Studies have identified several additional TF binding sites at RBPJ/Notch bound enhancer elements. These include ZNF143, ETS and RUNX1, leading to the hypothesis of a combinatorial regulation of transcription (Wang et al. 2011; Wang et al. 2014). Later, Aster and colleagues validated that functional RBPJ/Notch target sites were strongly association with RUNX1 binding in a T-lymphoblastic leukemia cell line (Wang et al. 2014). Other known proteins that are described to coregulate Notch via direct binding at NICD/RBPJ sites are Ikaros or zinc finger protein 143 (Beverly and Capobianco 2003; Dumortier et al. 2006; Ngondo-Mbongo et al. 2013).

Furthermore, different other pathways are known to synergistically regulate the expression of Notch target genes. Here, HIF signaling pathways (Gustafsson et al. 2005; Ferrante et al. 2022), the Wnt signaling pathway (Axelrod et al. 1996; Hayward et al. 2005) or BMP/ TGFβ (Blokzijl et al. 2003; Itoh et al. 2004) are among the best described ones.

Despite the above-mentioned aspects that potentially indicate a cell type specific Notch response, some genes are commonly regulated in almost all scenarios (Table 1). Among the most prominent and well-characterized Notch target genes are the basic helix-loop-helix (bHLH) TF family, which are the mammalian homolog to the *Drosophila hairy and enhancer of split* (*Hes*) genes (Sasai et al. 1992). In *Drosophila*, *hairy and enhancer of split* was described to act as a repressor that inhibits neural differentiation (Giebel and Campos-Ortega 1997). This was later validated in mammalians for the genes *Hes1*, *Hes3* and *Hes5* (Nakamura et al. 2000; Hatakeyama et al. 2004). Furthermore, *Hes1* plays a role in lymphocyte development, as well as more general processes including cell cycle arrest, apoptosis and self-renewal ability (Murata et al. 2005; Wendorff et al. 2010; Gao et al. 2014; Zhang et al. 2022). The remaining *Hes* genes are also associated with functions during the development, differentiation and proliferation (Fischer and Gessler 2007). Other studies revealed a Notch-independent regulation of the *Hes* genes by c-jun N-terminal protein kinase (JNK) signaling (Curry et al. 2006).

*Hes* TFs can form heterodimers with another bHLH TF family called Hes-related with YRPW motif (*Hey*), resulting in higher binding affinity (Iso et al. 2001; Iso et al. 2003). The *Hey* TFs have important functions in somitogenesis and in the cardiovascular system (William et al.

2007; Wiese et al. 2010). Both the *Hes* and *Hey* families are also coregulated by additional pathways such as BMP/ TGFβ, JAK-STAT, Ras, PI3K, ERK and HIF signaling (Zhou et al. 2012). Both, *Hes* and *Hey* genes have been identified as Notch targets by different biological approaches in various cell types (Canté-Barrett et al. 2020).

The Notch-regulated ankyrin repeat protein (*NRARP*) and deltex-1 (*Dtx1*) are both direct Notch target genes that have been described as negative feedback regulators of Notch signaling (Lamar et al. 2001; Yamamoto et al. 2001; Izon et al. 2002; Jarrett et al. 2019). Furthermore, Notch1 itself and Notch3 are also a Notch1 target genes, resulting in an autoregulatory mechanism (Yashiro-Ohtani et al. 2009).

Other known direct Notch target genes include: both Interleukin receptors *Il2ra*/CD25 (Adler et al. 2003) and *Il7ra (González-García et al. 2009)*, cluster of differentiation 44 (CD44) (García-Peydró et al. 2018), the protooncogene MYC (Weng et al. 2006), the peptidylprolyl isomerases PIN1 (Rustighi et al. 2009) and the TF SOX9 (Martini et al. 2013).

In summary, the GRN associated to the Notch signaling pathway is far more complex than the relatively simple pathway itself. Cooperative regulation of Notch target genes with other pathways or transcription factors, autoregulation and much more contribute to the diverse and cell type specific Notch response.

**Table 1: Example of Notch genes and their evidence.** Taken from (Canté-Barrett et al. 2020).

| Gene | Evidence |
|---|---|
| *CD44* | Response element, ChIP, GSI treatment |
| *DTX1* | GSI treatment, Notch1 knockdown, Notch1 induction (mouse) |
| *EPHB3* | Response element, ChIP, GSI treatment, Luciferase (Depending on cell line), dnMAML induction |
| *HES1* | Response element, ChIP, GSI treatment, dnMAML induction, Luciferase, Luciferase (mouse), Delta1+CHX (mouse) |
| *HES4* | Response element, ChIP, GSI treatment |
| *HES5* | Response element, Notch mutant (mouse), GSI treatment, NICD transfection (mouse) |
| *HES7* | GSI treatment, Response element (mouse), Luciferase assay (mouse) |
| *HEY1* | Response element, Luciferase (mouse), Cycloheximide (mouse), ChIP, GSI treatment |
| *HEY2* | Response element, Luciferase (mouse), Promoter deletions (mouse), GSI treatment, NICD4 overexpression, RBPJ mutation, immobilized Dll1, NICD1 transfection (mouse), ChIP (mouse), ChIP (human), EMSA |

| | |
|---|---|
| *HEYL* | Response element, GSI treatment, Notch1 knockout (mice), Notch activation (mouse), Promoter deletion (mouse) |
| *MYC* | Response element, GSI treatment, GSI treatment (mouse), Cycloheximide treatment, ChIP, ChIP (mouse), EMSA, Notch1 knockdown |
| *NFKB2* | Response element, EMSA, luciferase, ChIP |
| *NOX1* | Response element, ChIP, GSI treatment |
| *NRARP* | Response element, GSI treatment, Luciferase (mouse), EMSA, NICD Mutation (mouse), NICD3 transfection |
| *PBX1* | Response element, Cycloheximide treatment, GSI treatment, NICD3 inhibition |
| *PIN1* | Response element, Luciferase assay, ChIP, GSI treatment, NICD1 overexpression |
| *PLXND1* | Response element, Luciferase assay, dnRBPj, NICD1 overexpression |
| *SOX9* | Response element, ChIP, GSI treatment, Notch1 signaling induction, Cycloheximide treatment |

### 1.4. Next generation sequencing and comprehensive genomics / transcriptomics

In 1977, Frederick Sanger and colleagues published their protocol for sequencing DNA using chain-terminating inhibitors (Sanger et al. 1977). This method became the gold standard for DNA sequencing for the next several decades and was so groundbreaking that it is nowadays known as Sanger sequencing. Sanger sequencing was used to achieve countless milestones in genetics and molecular biology, most famously the Human Genome Project, which took 13 years and $2.7 billion to complete (Lander et al. 2001). Although Sanger sequencing still has its uses today, it has been largely replaced over time by newer and more efficient methods (Slatko et al. 2018).

Increasing knowledge and understanding of DNA, as well as advances in robotics and microtechnology, have given rise to modern microarray analyses. In microarray analyses, the hybridization of the fixed DNA probes on the array with the labeled (e.g. fluorophore) input target DNA is used for the analysis of expression, protein binding or genotypes (Solomon et al. 1988; Wang et al. 1998; Richter et al. 2002). Microarrays are easy to use and relatively inexpensive, which is why they have been and continue to be used in both research and clinical applications (Ahrendt et al. 1999; Wu et al. 2005). The predominate use case for microarrays is the analysis of the whole transcriptome, which can elucidate complex transcriptional networks (Lockhart et al. 1996; Bumgarner 2013). However, microarrays have some fundamental disadvantages such as the limitation of the probes. Microarrays can only analyze sequences for which they were designed to detect, making it

impossible to identify new genes, undescribed spliced genes or unknown non-coding RNAs (Bumgarner 2013).

A more modern approach is the massive parallel sequencing of large numbers of short reads, known as next generation sequencing (NGS). Here, relatively short reads (300 - 500 bp) are analyzed by applying the sequencing by synthesis (SBS) method (Zhang et al. 2011; McCombie et al. 2019). While there are several techniques available, the most commonly used one is provided by Illumina (Hu et al. 2021). Although there are several Illumina systems or those from other companies, a common disadvantage is that all of these SBS methods inherently have higher error rates. To overcome this problem, vast numbers (up to a billion) of DNA fragments must be sequenced (Slatko et al. 2018). Nonetheless, the cost and time needed for NGS has decreased dramatically over time and nowadays a sequencing of the human genome takes less than two days and costs less than 1000$.

The possibilities of NGS gave rise to many techniques including the typical RNA-seq (Wang et al. 2009), ChIP-seq (Furey 2012) and ATAC-seq (Buenrostro et al. 2015), but also more specialized or refined approaches like CUT&Tag (Kaya-Okur et al. 2019), HiChIP (Mumbach et al. 2016), GRO-seq (Lopes et al. 2017) and several more. Nowadays, NGS is also utilized for the analysis of individual cells (single cell analysis), which allows an even more precise and detailed understanding of molecular biological processes (Wang and Bodovitz 2010).

The use of ChIP-seq and RNA-seq has dramatically expanded the understanding of genetics and molecular biology by providing comprehensive insides into regulatory networks and greatly impacted projects such as the ENCyclopedia Of DNA Elements (The ENCODE (ENCyclopedia Of DNA Elements) Project 2004; ENCODE Project Consortium 2012).

The single-molecule sequencing techniques are a more modern approach compared to SBS methods (Thompson and Steinmann 2010). They circumvented the problematic amplification step that is required for the SBS techniques by analyzing only single molecules. However, SMS reads currently have a higher error rate than SBS, which is why few instruments have achieved commercial status (McCombie et al. 2019).

### 1.5. Aims of the study

Despite significant progress, unraveling the specificity of the transcriptional response mediated by Notch remains one of the central questions in the field. In particular, the function of the transcription factor RBPJ, which can act as either an activator or a repressor demands further investigation. Addressing this, the genome-wide function of RBPJ, particularly its currently poorly characterized repressive function, in the context of Notch signaling is critical for further understanding of the Notch response.

In this study, I aim to elucidate the genome-wide function of RBPJ, both repressive, Notch-independent, and activating, Notch-dependent. This is achieved by analyzing different transcriptomic and (epi)genomic datasets. Initially, the switch of RBPJ from a repressor to an activator and vice versa is analyzed by activation and inactivation of the Notch pathway, followed by a thorough examination of the resulting impact on transcription and chromatin structure. This exploration aims to ascertain whether RBPJ regulates (activates or represses) all genes equally or whether distinct regulatory patterns emerge. In addition, it is tested if different transcriptional programs are associated with possible distinct functions of RBPJ. Subsequently, I identify the transcriptional functional RBPJ binding sites in the context of Notch signaling. Lastly, I focus on the identification of distinct features, which characterize transcriptional functional RBPJ binding sites and test these features in different cell types.

# 2. Material and Methods

## 2.1. Wet lab experiments

All wet lab experiments were performed by Dr. Benedetto Daniele Giaimo and Dr. Francesca Ferrante in the lab of Prof. Dr. Tilman Borggrefe (Institute of Biochemistry, Justus-Liebig University, Giessen). Detailed protocols, kits, plasmids and chemicals used in this study have been previously published in (Giaimo et al. 2017; Yuan et al. 2019; Ferrante et al. 2022; Friedrich et al. 2022).

### 2.1.1. Cell culture and treatment

Mouse hybridoma mature T (MT) E2-10HA cells and mouse leukemia progenitor T-cells (Beko) were grown in Iscove's Modified Dulbecco Medium supplemented with 2% fetal bovine serum, 5 mg/l insulin, 0.3 mg/ml Primatone, nonessential amino acids and penicillin/streptomycin at 37°C under 5% $CO_2$. *Phoenix*™ cells were cultured in Dulbecco's modified Eagle's medium added with 10% fetal calf serum (FCS) and penicillin/streptomycin at 37°C under 5% $CO_2$.

MT cells and Beko cells were treated with 20 µg/ml GSI or with DMSO as control for 24 h. For the washout of GSI in Beko cells, the cells were treated with 10 µg/ml GSI for 48 h, followed by the washout of GSI and culturing for additional 24 h. In addition, Beko cells were treated with 0.01 µg/ml apicidin. MT NICD1-ER cells were induced with (Z)-4-hydroxytamoxifen (4-OHT) at 1 µM final concentration or ethanol as control.

### 2.1.2. Infection of MT

*Phoenix*™ cells were used to generate retrovirus containing the plasmid DNA of interest. 20 µg of DNA of interest, 860 µL of $H_2O$ and 120 µL of 2 M $CaCl_2$ were mixed and transferred to 1 mL of 2 × HBS buffer, followed by 20 min of incubation at room temperature. In parallel, 25 µM Chloroquine solution was added to the *Phoenix*™ cells (1 µl/ml) and incubated for 20 min. The DNA containing solution was added to the cells and after 12 h the medium was replaced. The medium containing the retroviral suspension was filtered after 24 h and polybrene solution was added. The retroviral solution was used for the infection of the MT cells by centrifugation, followed by selection with puromycin or blasticidin.

### 2.1.3. RNA extraction and library preparation

The total RNA was purified with the RNeasy Mini Kit, the QIAshredder and the DNase I. Subsequently the libraries were prepared using the TruSeq® Stranded Total RNA LT-Ribo-Zero Gold kit.

### 2.1.4. CUT&Tag and ATAC-seq preparation

CUT&Tag was performed using the CUT&Tag kit (Active Motif 53160) and ATAC-seq with the ATAC-Seq kit (Active Motif 53150) accordingly to manufacturer´s instructions.

### 2.1.5. ChIP-seq preparation

Cells were fixed for 30 min in 1% FMA at room temperature, followed by 5 min of blocking by 1/8 volume of 1 M glycine pH 7.5. Next, cells were two times washed with PBS and resuspended in 1 ml of SDS Lysis Buffer, followed by 10 min of incubation on ice. Subsequently, the cells were sonicated and the chromatin was diluted in ChIP Dilution Buffer. Next, the samples were 30 min pre-cleared using protein-A-Sepharose beads at 4°C, followed by overnight incubation with the needed antibody and 1 h of antibody immobilization with 40 µl protein-A-Sepharose beads at 4°C. Subsequently, the chromatin was eluted using Elution Buffer and the crosslink was reverted at 65°C over night. Next, the SDS was diluted with TE buffer, the samples were 2 h incubated with RNAse A at 37°C and for 2 h with Proteinase K at 55°C. Lastly, the DNA was extracted using phenol/chloroform/isoamylic alcohol and purified with the Qiaquick PCR cleanup kit. Libraries were prepared with the Diagenode MicroPlex Library Preparation kit v2 or the Diagenode MicroPlex Library Preparation kit v3 and subsequently purified using Agencourt AMPure XP Beads.

### 2.1.6. Protein extraction and Western blotting

The cells were washed twice in PBS and then resuspended in a Hypotonic buffer (20 mM Hepes pH 7.9, 20 mM NaCl, 5 mM MgCl2, 10% glycerol, 0.2 mM PMSF). After incubating the samples on ice for 20 min, they were centrifuged at 4.000 rpm and 4°C for 10 min and the resulting nuclei were washed twice with ice-cold PBS. Next, the isolated nuclei were lysed in a Hypertonic buffer (20 mM Hepes pH 7.9, 1 mM MgCl2, 300 mM NaCl, 0.2% NP-40, 25% glycerol, 0.2 mM PMSF, 1x Protease inhibitor mix, 0.3 mM DTT). The lysates were incubated on ice for an additional 20 min and then centrifuged at 14.000 rpm and 4°C for 5

min. The supernatants were collected for further analysis. The protein concentration in the nuclear extracts was determined using the Bradford assay (Sigma-Aldrich). To prepare the extracts for Western blotting, they were boiled in the presence of SDS loading buffer.

The proteins were dissolved in SDS polyacrylamide gels and then transferred to a Nitrocellulose membrane (Amersham) using wet blotting. Next, membranes were then blocked in 5% milk / TBST (1x TBS, 0.1% Tween 20) and subsequently overnight incubated with the antibody of interest diluted (1:1000) in 5% milk / TBST. Membranes were washed in TBST, followed by incubation at room temperature for 1 hour with secondary antibody (IgG HRP) diluted 1:5000 in 5% milk / TBST. Membranes were washed in TBST and subsequently incubated at room temperature with ECL solution. Finally, chemiluminescence was detected using a Vilber Fusion FX7 system.

### 2.2. Antibodies

**Table 2: List of all antibodies used in this study.**

| Target | Company | Number |
|---|---|---|
| H3 | abcam | ab1791 |
| H3K4me1 | abcam | ab8895 |
| H3K4me3 | Diagenode | pAb-003-050 |
| H3K9ac | abcam | ab4441 |
| H3K18ac | Cell Signaling | #9675 |
| H3K27ac | Diagenode | pAb-174-050 |
| H3K36me3 | Cell Signaling | #4909 |
| IgG | Diagenode | C15410206 |
| IgG HRP | Cell Signaling | #7074 |
| NICD1 | Cell Signaling | #4147 |
| RBPJ | Cell Signaling | #5313 |

### 2.3. Cell types

**Table 3: List of all cell lines from the Borggrefe lab.**

| Name | Origin | Species |
|---|---|---|
| Beko | Progenitor T-cells | Mouse |
| Mature T-cells | Hybridoma mature T-cells | Mouse |
| Mature T-cells RBPJ depletion | Hybridoma mature T-cells | Mouse |

**Table 4: List of all cell lines from publicly available data.**

| Name | Origin | Species | Publication |
|---|---|---|---|
| T6E | Murine T-ALL | Mouse | (Severson et al. 2017) |
| Phase I T-cells | Primary T-cells | Mouse | (Romero-Wolf et al. 2020) |
| Phase II T-cells | Primary T-cells | Mouse | |
| KP1 | Small cell lung cancer | Mouse | (George et al. 2015) |
| HCC1599 | TNBC | Human | (Petrovic et al. 2019) |
| MB157 | TNBC | Human | |
| CUTLL1 | T-ALL | Human | (Wang et al. 2011) |
| IC8 | Squamous cell carcinoma | Human | (Pan et al. 2020) |

## 2.4. Genomes

Both UCSC mouse (mm9) and human (hg19) genomes together with their corresponding genome transfer file (GTF) were downloaded from Illumina's iGenomes website.

(https://emea.support.illumina.com/sequencing/sequencing_software/igenome.html)

## 2.5. Publicly available and self-generated data sets

**Table 5: List of all NGS / microarray data sets used in chapter I (Suppl. Table S1).**

| Name | Type | GEO Entry | PMID |
|---|---|---|---|
| **Mature T-cells** | | | |
| Control_sgRbpj_Rep_1 | RNA-seq | GSM5705476 | 35848919 |
| Control_sgRbpj_Rep_2 | RNA-seq | GSM5705477 | 35848919 |
| sgRbpj_2-12_Rep_1 | RNA-seq | GSM5705478 | 35848919 |
| sgRbpj_2-12_Rep_2 | RNA-seq | GSM5705479 | 35848919 |
| sgRbpj_2-14_Rep_1 | RNA-seq | GSM5705480 | 35848919 |
| sgRbpj_2-14_Rep_2 | RNA-seq | GSM5705481 | 35848919 |
| NICD1-ER_24h_EtOH_Rep_1 | RNA-seq | GSM5705482 | 35848919 |
| NICD1-ER_24h_EtOH_Rep_2 | RNA-seq | GSM5705483 | 35848919 |
| NICD1-ER_24h_EtOH_Rep_3 | RNA-seq | GSM5705484 | 35848919 |
| NICD1-ER_24h_OHT_Rep_1 | RNA-seq | GSM5705485 | 35848919 |
| NICD1-ER_24h_OHT_Rep_2 | RNA-seq | GSM5705486 | 35848919 |
| NICD1-ER_24h_OHT_Rep_3 | RNA-seq | GSM5705487 | 35848919 |
| NICD1-ER_4h_OHT_Rep_1 | RNA-seq | GSM5705488 | 35848919 |
| NICD1-ER_4h_OHT_Rep_2 | RNA-seq | GSM5705489 | 35848919 |

| | | | |
|---|---|---|---|
| NICD1-ER_4h_OHT_Rep_3 | RNA-seq | GSM5705490 | 35848919 |
| NICD1-ER_8h_OHT_Rep_1 | RNA-seq | GSM5705491 | 35848919 |
| NICD1-ER_8h_OHT_Rep_2 | RNA-seq | GSM5705492 | 35848919 |
| NICD1-ER_8h_OHT_Rep_3 | RNA-seq | GSM5705493 | 35848919 |
| GSI_Rep_1 | RNA-seq | GSM5705503 | 35848919 |
| GSI_Rep_2 | RNA-seq | GSM5705504 | 35848919 |
| DMSO_Rep_1 | RNA-seq | GSM5705505 | 35848919 |
| DMSO_Rep_2 | RNA-seq | GSM5705506 | 35848919 |
| Control_sgRbpj+Biocontrol_Rep_1_1 | RNA-seq | GSM5705507 | 35848919 |
| Control_sgRbpj+Biocontrol_Rep_2_1 | RNA-seq | GSM5705508 | 35848919 |
| Control_sgRbpj+Biocontrol_Rep_3_1 | RNA-seq | GSM5705509 | 35848919 |
| Control_sgRbpj+BioNICD1_WT_Rep_1_1 | RNA-seq | GSM5705510 | 35848919 |
| Control_sgRbpj+BioNICD1_WT_Rep_2_1 | RNA-seq | GSM5705511 | 35848919 |
| Control_sgRbpj+BioNICD1_WT_Rep_3_1 | RNA-seq | GSM5705512 | 35848919 |
| sgRbpj+Biocontrol_Rep_1_1 | RNA-seq | GSM5705513 | 35848919 |
| sgRbpj+Biocontrol_Rep_2_1 | RNA-seq | GSM5705514 | 35848919 |
| sgRbpj+Biocontrol_Rep_3_1 | RNA-seq | GSM5705515 | 35848919 |
| sgRbpj+BioNICD1_WT_Rep_1_1 | RNA-seq | GSM5705516 | 35848919 |
| sgRbpj+BioNICD1_WT_Rep_2_1 | RNA-seq | GSM5705517 | 35848919 |
| sgRbpj+BioNICD1_WT_Rep_3_1 | RNA-seq | GSM5705518 | 35848919 |
| Biocontrol_Rep_1 | RNA-seq | This study | This study |
| Biocontrol_Rep_2 | RNA-seq | This study | This study |
| BioNICD1_WT_Rep_1 | RNA-seq | GSM3020596 | 29986055 |
| BioNICD1_WT_Rep_2 | RNA-seq | GSM3020597 | 29986055 |
| NICD1-ER_24h_OHT_Rep_4 | RNA-seq | GSM3020602 | 29986055 |
| NICD1-ER_24h_OHT_Rep_5 | RNA-seq | GSM3020603 | 29986055 |
| NICD1-ER_24h_EtOH_Rep_4 | RNA-seq | GSM3020600 | 29986055 |
| NICD1-ER_24h_EtOH_Rep_5 | RNA-seq | GSM3020601 | 29986055 |
| MT_sgH2afv/H2afz_#12_rep1 | RNA-seq | GSM3020594 | 29986055 |
| MT_sgH2afv/H2afz_#12_rep2 | RNA-seq | GSM3020595 | 29986055 |
| MT_sgH2afv/H2afz_#12_rep3 | RNA-seq | GSM3143012 | 29986055 |
| MT_sgH2afv/H2afz_#12_rep4 | RNA-seq | GSM3143013 | 29986055 |
| MT_sgH2afv/H2afz_#12_rep5 | RNA-seq | GSM3143014 | 29986055 |
| MT_sgH2afv/H2afz_#12_rep6 | RNA-seq | GSM3143015 | 29986055 |
| MT_CRISPR_Control_rep1 | RNA-seq | GSM3020592 | 29986055 |
| MT_CRISPR_Control_rep2 | RNA-seq | GSM3020593 | 29986055 |
| MT_CRISPR_Control_rep3 | RNA-seq | GSM3143016 | 29986055 |
| MT_CRISPR_Control_rep4 | RNA-seq | GSM3143017 | 29986055 |

| | | | |
|---|---|---|---|
| MT_CRISPR_Control_rep5 | RNA-seq | GSM3143018 | 29986055 |
| MT_CRISPR_Control_rep6 | RNA-seq | GSM3143019 | 29986055 |
| sgRbpj_2-12_RBPJ_Rep_1 | ChIP-seq | GSM5705534 | 35848919 |
| sgRbpj_2-12_RBPJ_Rep_2 | ChIP-seq | GSM5705535 | 35848919 |
| Control_sgRbpj_RBPJ_Input | ChIP-seq | GSM5705536 | 35848919 |
| sgRbpj_2-12_RBPJ_Input | ChIP-seq | GSM5705537 | 35848919 |
| Biocontrol_RBPJ_Input | ChIP-seq | GSM5705538 | 35848919 |
| Biocontrol_RBPJ_Rep_1 | ChIP-seq | GSM5705539 | 35848919 |
| Biocontrol_RBPJ_Rep_2 | ChIP-seq | GSM5705540 | 35848919 |
| BioNICD1_DEP_RBPJ_Input | ChIP-seq | GSM5705541 | 35848919 |
| BioNICD1_DEP_RBPJ_Rep_1 | ChIP-seq | GSM5705542 | 35848919 |
| BioNICD1_DEP_RBPJ_Rep_2 | ChIP-seq | GSM5705543 | 35848919 |
| BioNICD1_WT_RBPJ_Input | ChIP-seq | GSM5705544 | 35848919 |
| BioNICD1_WT_RBPJ_Rep_1 | ChIP-seq | GSM5705545 | 35848919 |
| BioNICD1_WT_RBPJ_Rep_2 | ChIP-seq | GSM5705546 | 35848919 |
| Control_sgRbpj_H3K27ac_Rep_1_1 | ChIP-seq | GSM5705547 | 35848919 |
| Control_sgRbpj_H3K27ac_Rep_2_1 | ChIP-seq | GSM5705548 | 35848919 |
| Control_sgRbpj_H3K4me1_Rep_1_1 | ChIP-seq | GSM5705549 | 35848919 |
| Control_sgRbpj_H3K4me1_Rep_2_1 | ChIP-seq | GSM5705550 | 35848919 |
| Control_sgRbpj_H3K4me3_Rep_1_1 | ChIP-seq | GSM5705551 | 35848919 |
| Control_sgRbpj_H3K4me3_Rep_2_1 | ChIP-seq | GSM5705552 | 35848919 |
| sgRbpj_2-12_H3K27ac_Rep_1_1 | ChIP-seq | GSM5705553 | 35848919 |
| sgRbpj_2-12_H3K27ac_Rep_2_1 | ChIP-seq | GSM5705554 | 35848919 |
| sgRbpj_2-12_H3K4me1_Rep_1_1 | ChIP-seq | GSM5705555 | 35848919 |
| sgRbpj_2-12_H3K4me1_Rep_2_1 | ChIP-seq | GSM5705556 | 35848919 |
| sgRbpj_2-12_H3K4me3_Rep_1_1 | ChIP-seq | GSM5705557 | 35848919 |
| sgRbpj_2-12_H3K4me3_Rep_2_1 | ChIP-seq | GSM5705558 | 35848919 |
| Input_Control_sgRbpj_histone_marks_Rep_1_1 | ChIP-seq | GSM5705559 | 35848919 |
| Input_Control_sgRbpj_histone_marks_Rep_2_1 | ChIP-seq | GSM5705560 | 35848919 |
| Input_sgRbpj_2-12_histone_marks_Rep_1_1 | ChIP-seq | GSM5705561 | 35848919 |
| Input_sgRbpj_2-12_histone_marks_Rep_2_1 | ChIP-seq | GSM5705562 | 35848919 |
| sgRbpj_2-12_ATAC_Rep_1_1 | ATAC-seq | GSM5705563 | 35848919 |
| sgRbpj_2-12_ATAC_Rep_2_1 | ATAC-seq | GSM5705564 | 35848919 |
| sgRbpj_2-12_ATAC_Rep_3_1 | ATAC-seq | GSM5705565 | 35848919 |
| Control_sgRbpj_ATAC_Rep_1_1 | ATAC-seq | GSM5705566 | 35848919 |
| Control_sgRbpj_ATAC_Rep_2_1 | ATAC-seq | GSM5705567 | 35848919 |
| Control_sgRbpj_ATAC_Rep_3_1 | ATAC-seq | GSM5705568 | 35848919 |

| | | | |
|---|---|---|---|
| **T6E** | | | |
| T6E MigR1-DMSO-rep 1 | Microarray | GSM2565735 | GSE97465 |
| T6E MigR1-DMSO-rep 2 | Microarray | GSM2565736 | GSE97465 |
| T6E MigR1-DMSO-rep 3 | Microarray | GSM2565737 | GSE97465 |
| T6E ICN1-DMSO-rep 1 | Microarray | GSM2565747 | GSE97465 |
| T6E ICN1-DMSO-rep 2 | Microarray | GSM2565748 | GSE97465 |
| T6E ICN1-DMSO-rep 3 | Microarray | GSM2565749 | GSE97465 |
| **KP1** | | | |
| Empty vector transfected cells, biological rep1 | Microarray | GSM1692708 | 26168399 |
| Empty vector transfected cells, biological rep2 | Microarray | GSM1692709 | 26168399 |
| Empty vector transfected cells, biological rep3 | Microarray | GSM1692710 | 26168399 |
| Notch1-ICD transfected cells, biological rep 1 | Microarray | GSM1692711 | 26168399 |
| Notch1-ICD transfected cells, biological rep 2 | Microarray | GSM1692712 | 26168399 |
| Notch1-ICD transfected cells, biological rep 3 | Microarray | GSM1692713 | 26168399 |
| **Primary T-cells** | | | |
| GSE148441_Phase1_Notch_KO_DLL1.txt.gz | RNA-seq | GSE148441 | 32756905 |
| GSE148441_Phase2_Notch_KO_DLL1.txt.gz | RNA-seq | GSE148441 | 32756905 |

**Table 6: List of all NGS / microarray data sets used in chapter II (Suppl. Table S8).**

| Name | Type | GEO Entry | Publication |
|---|---|---|---|
| **Beko** | | | |
| Apicidin_Rep1 | RNA-seq | GSM2836561 | 32107550 |
| Apicidin_Rep2 | RNA-seq | GSM2836562 | 32107550 |
| DMSO_Apicidin_Rep1 | RNA-seq | GSM2836563 | 32107550 |
| DMSO_Apicidin_Rep2 | RNA-seq | GSM2836564 | 32107550 |
| GSI_Rep1 | RNA-seq | GSM2836565 | 32107550 |
| GSI_Rep2 | RNA-seq | GSM2836566 | 32107550 |
| DMSO_Rep1 | RNA-seq | GSM2836567 | 32107550 |
| DMSO_Rep2 | RNA-seq | GSM2836568 | 32107550 |
| GSI_washout_Rep1 | RNA-seq | This study | This study |
| GSI_washout_Rep2 | RNA-seq | This study | This study |
| GSI_Rep1 | RNA-seq | This study | This study |
| GSI_Rep2 | RNA-seq | This study | This study |

| | | | |
|---|---|---|---|
| DMSO_Input_RBPJ | ChIP-seq | GSM3383946 | 32107550 |
| DMSO_RBPJ_Rep1 | ChIP-seq | GSM3383948 | 32107550 |
| DMSO_RBPJ_Rep2 | ChIP-seq | GSM3383949 | 32107550 |
| GSI_Input_RBPJ | ChIP-seq | GSM3383947 | 32107550 |
| GSI_RBPJ_Rep1 | ChIP-seq | This study | This study |
| GSI_RBPJ_Rep2 | ChIP-seq | This study | This study |
| Apicidin_Input_RBPJ | ChIP-seq | GSM3383945 | 32107550 |
| Apicidin_RBPJ_Rep1 | ChIP-seq | This study | This study |
| Apicidin_RBPJ_Rep2 | ChIP-seq | This study | This study |
| DMSO_RBPJ_Rep3 | ChIP-seq | GSM5825470 | 35821235 |
| DMSO_RBPJ_Rep4 | ChIP-seq | GSM5825471 | 35821235 |
| DMSO_RBPJ_Rep5 | ChIP-seq | GSM5825472 | 35821235 |
| DMSO_Input_RBPJ | ChIP-seq | GSM5825469 | 35821235 |
| GSI_RBPJ_Rep3 | ChIP-seq | This study | This study |
| GSI_RBPJ_Rep4 | ChIP-seq | This study | This study |
| GSI_RBPJ_Rep5 | ChIP-seq | This study | This study |
| GSI_Input_RBPJ | ChIP-seq | This study | This study |
| DMSO_H3K9ac_Rep1 | ChIP-seq | This study | This study |
| DMSO_H3K18ac_Rep1 | ChIP-seq | This study | This study |
| DMSO_H3K36me3_Rep1 | ChIP-seq | This study | This study |
| DMSO_H3K36me3_Rep2 | ChIP-seq | This study | This study |
| DMSO_H3K9ac_Rep2 | ChIP-seq | This study | This study |
| DMSO_H3K18ac_Rep2 | ChIP-seq | This study | This study |
| DMSO_Input_H3K36me_H3K9ac_H3K18ac_Rep1 | ChIP-seq | This study | This study |
| DMSO_Input_H3K36me_H3K9ac_H3K18ac_Rep2 | ChIP-seq | This study | This study |
| GSI_H3K36me3_Rep1 | ChIP-seq | This study | This study |
| GSI_H3K36me3_Rep2 | ChIP-seq | This study | This study |
| GSI_H3K9ac_Rep1 | ChIP-seq | This study | This study |
| GSI_H3K18ac_Rep1 | ChIP-seq | This study | This study |
| GSI_H3K9ac_Rep2 | ChIP-seq | This study | This study |
| GSI_H3K18ac_Rep2 | ChIP-seq | This study | This study |
| GSI_Input_H3K36me_H3K9ac_H3K18ac_Rep1 | ChIP-seq | This study | This study |
| GSI_Input_H3K36me_H3K9ac_H3K18ac_Rep2 | ChIP-seq | This study | This study |
| DMSO_H3K4me1_Rep1 | ChIP-seq | This study | This study |
| DMSO_H3K4me3_Rep1 | ChIP-seq | This study | This study |
| DMSO_H3K4me1_Rep2 | ChIP-seq | This study | This study |
| DMSO_H3K4me3_Rep2 | ChIP-seq | This study | This study |
| DMSO_Input_H3K4me_Rep1 | ChIP-seq | This study | This study |

| | | | |
|---|---|---|---|
| DMSO_Input_H3K4me_Rep2 | ChIP-seq | This study | This study |
| GSI_H3K4me1_Rep1 | ChIP-seq | This study | This study |
| GSI_H3K4me3_Rep1 | ChIP-seq | This study | This study |
| GSI_H3K4me1_Rep2 | ChIP-seq | This study | This study |
| GSI_H3K4me3_Rep2 | ChIP-seq | This study | This study |
| GSI_Input_H3K4me_Rep1 | ChIP-seq | This study | This study |
| GSI_Input_H3K4me_Rep2 | ChIP-seq | This study | This study |
| DMSO_H3K27ac_Rep1 | ChIP-seq | GSM3383941 | 32107550 |
| DMSO_H3K27ac_Rep2 | ChIP-seq | GSM3383942 | 32107550 |
| DMSO_Input_Rep1 | ChIP-seq | GSM3383946 | 32107550 |
| GSI_H3K27ac_Rep1 | ChIP-seq | GSM3383943 | 32107550 |
| GSI_H3K27ac_Rep2 | ChIP-seq | GSM3383944 | 32107550 |
| GSI_Input_Rep1 | ChIP-seq | GSM3383947 | 32107550 |
| Apicidin_H3K27ac_Rep1 | ChIP-seq | GSM3383939 | 32107550 |
| Apicidin_H3K27ac_Rep2 | ChIP-seq | GSM3383940 | 32107550 |
| Apicidin_Input_Rep1 | ChIP-seq | GSM3383945 | 32107550 |
| Normoxia_RBPJ_Rep1 | ChIP-seq | GSM5825493 | 35821235 |
| Normoxia_RBPJ_Rep2 | ChIP-seq | GSM5825494 | 35821235 |
| Hypoxia_RBPJ_Rep1 | ChIP-seq | GSM5825487 | 35821235 |
| Hypoxia_RBPJ_Rep2 | ChIP-seq | GSM5825488 | 35821235 |
| Normoxia_Input_Rep1 | ChIP-seq | GSM5825491 | 35821235 |
| Normoxia_Input_Rep2 | ChIP-seq | GSM5825492 | 35821235 |
| Hypoxia_Input_Rep1 | ChIP-seq | GSM5825485 | 35821235 |
| Hypoxia_Input_Rep2 | ChIP-seq | GSM5825486 | 35821235 |
| DMSO_Rep1 | ATAC-seq | This study | This study |
| DMSO_Rep2 | ATAC-seq | This study | This study |
| DMSO_Rep3 | ATAC-seq | This study | This study |
| GSI_Rep1 | ATAC-seq | This study | This study |
| GSI_Rep2 | ATAC-seq | This study | This study |
| GSI_Rep3 | ATAC-seq | This study | This study |
| CT_H3K27ac_DMSO_Rep1 | CUT&Tag | This study | This study |
| CT_H3K27ac_DMSO_Rep2 | CUT&Tag | This study | This study |
| CT_H3K27ac_GSI_Rep1 | CUT&Tag | This study | This study |
| CT_H3K27ac_GSI_Rep2 | CUT&Tag | This study | This study |
| Beko_DNMAML_Eth | Microarray | GSM1528411 | 25805888 |
| Beko_DNMAML_OHT | Microarray | GSM1528412 | 25805888 |

| | | | |
|---|---|---|---|
| **HCC1599** | | | |
| HCC1599_WO_RNAseq_rep1 | RNA-seq | GSM3263171 | 30745086 |
| HCC1599_WO_RNAseq_rep2 | RNA-seq | GSM3263172 | 30745086 |
| HCC1599_WO_RNAseq_rep3 | RNA-seq | GSM3263173 | 30745086 |
| HCC1599_GSI_RNAseq_rep1 | RNA-seq | GSM3263174 | 30745086 |
| HCC1599_GSI_RNAseq_rep2 | RNA-seq | GSM3263175 | 30745086 |
| HCC1599_WO_H3K27ac_ChIPseq_rep1 | ChIP-seq | GSM3263177 | 30745086 |
| HCC1599_WO_H3K27ac_ChIPseq_rep2 | ChIP-seq | GSM3263178 | 30745086 |
| HCC1599_GSI_H3K27ac_ChIPseq_rep1 | ChIP-seq | GSM3263179 | 30745086 |
| HCC1599_GSI_H3K27ac_ChIPseq_rep2 | ChIP-seq | GSM3263180 | 30745086 |
| HCC1599_WO_NICD1_ChIPseq_rep1 | ChIP-seq | GSM3263189 | 30745086 |
| HCC1599_WO_NICD1_ChIPseq_rep2 | ChIP-seq | GSM3263190 | 30745086 |
| HCC1599_GSI_NICD1_ChIPseq_rep1 | ChIP-seq | GSM3263191 | 30745086 |
| HCC1599_GSI_NICD1_ChIPseq_rep2 | ChIP-seq | GSM3263192 | 30745086 |
| HCC1599_WO_RBPJ_ChIPseq_rep1 | ChIP-seq | GSM3263193 | 30745086 |
| HCC1599_WO_RBPJ_ChIPseq_rep2 | ChIP-seq | GSM3263194 | 30745086 |
| HCC1599_GSI_RBPJ_ChIPseq_rep1 | ChIP-seq | GSM3263195 | 30745086 |
| HCC1599_GSI_RBPJ_ChIPseq_rep2 | ChIP-seq | GSM3263196 | 30745086 |
| HCC1599_ChIPseq_input_GSI | ChIP-seq | GSM3263198 | 30745086 |
| HCC1599_ChIPseq_input_WO | ChIP-seq | GSM3263199 | 30745086 |
| **MB157** | | | |
| MB157_WO_RNAseq_rep1 | RNA-seq | GSM3263137 | 30745086 |
| MB157_WO_RNAseq_rep2 | RNA-seq | GSM3263138 | 30745086 |
| MB157_WO_RNAseq_rep3 | RNA-seq | GSM3263139 | 30745086 |
| MB157_GSI_RNAseq_rep1 | RNA-seq | GSM3263140 | 30745086 |
| MB157_GSI_RNAseq_rep2 | RNA-seq | GSM3263141 | 30745086 |
| MB157_GSI_RNAseq_rep3 | RNA-seq | GSM3263142 | 30745086 |
| MB157_GSI_H3K27ac_ChIPseq_rep1 | ChIP-seq | GSM3263143 | 30745086 |
| MB157_GSI_H3K27ac_ChIPseq_rep2 | ChIP-seq | GSM3263144 | 30745086 |
| MB157_WO_H3K27ac_ChIPseq_rep1 | ChIP-seq | GSM3263145 | 30745086 |
| MB157_WO_H3K27ac_ChIPseq_rep2 | ChIP-seq | GSM3263146 | 30745086 |
| MB157_WO_NICD1_ChIPseq_rep1 | ChIP-seq | GSM3263155 | 30745086 |
| MB157_WO_NICD1_ChIPseq_rep2 | ChIP-seq | GSM3263156 | 30745086 |
| MB157_GSI_NICD1_ChIPseq_rep1 | ChIP-seq | GSM3263157 | 30745086 |
| MB157_GSI_NICD1_ChIPseq_rep2 | ChIP-seq | GSM3263158 | 30745086 |
| MB157_WO_RBPJ_ChIPseq_rep1 | ChIP-seq | GSM3263159 | 30745086 |
| MB157_WO_RBPJ_ChIPseq_rep2 | ChIP-seq | GSM3263160 | 30745086 |

| | | | |
|---|---|---|---|
| MB157_GSI_RBPJ_ChIPseq_rep1 | ChIP-seq | GSM3263161 | 30745086 |
| MB157_GSI_RBPJ_ChIPseq_rep2 | ChIP-seq | GSM3263162 | 30745086 |
| MB157_ChIPseq_input | ChIP-seq | GSM3263167 | 30745086 |
| **CUTLL1** | | | |
| CUTLL_GSI_1 | RNA-seq | GSM1446780 | 25104330 |
| CUTLL_GSI_2 | RNA-seq | GSM1446781 | 25104330 |
| CUTLL_GSI_3 | RNA-seq | GSM1446782 | 25104330 |
| CUTLL_Washout_1 | RNA-seq | GSM1446783 | 25104330 |
| CUTLL_Washout_2 | RNA-seq | GSM1446784 | 25104330 |
| CUTLL_Washout_3 | RNA-seq | GSM1446785 | 25104330 |
| CUTLL-RBPJ-1 | ChIP-seq | GSM732905 | 21737748 |
| CUTLL-RBPJ-2 | ChIP-seq | GSM732906 | 21737748 |
| CUTLL-Input-1 | ChIP-seq | GSM732908 | 21737748 |
| CUTLL-Input-2 | ChIP-seq | GSM732909 | 21737748 |
| input DNA GSI | ChIP-seq | GSM1252932 | 24374627 |
| RBPJ GSI | ChIP-seq | GSM1252934 | 24374627 |
| input DNA w4h | ChIP-seq | GSM1252935 | 24374627 |
| RBPJ w4h | ChIP-seq | GSM1252937 | 24374627 |
| H3K27ac GSI | ChIP-seq | GSM1252939 | 24374627 |
| H3K27ac w4h | ChIP-seq | GSM1252940 | 24374627 |
| **IC8** | | | |
| IC8-L1597H-0h-RBPJ | ChIP-seq | GSM4732255 | 32936072 |
| IC8-L1597H-4h-RBPJ | ChIP-seq | GSM4732256 | 32936072 |
| IC8-L1597H-0h-RBPJ-input | ChIP-seq | GSM4732257 | 32936072 |
| IC8-L1597H-4h-RBPJ-input | ChIP-seq | GSM4732258 | 32936072 |
| H3K27Ac_0h | ChIP-seq | GSM4732247 | 32936072 |
| H3K27Ac_4h | ChIP-seq | GSM4732250 | 32936072 |
| H3K27Ac_0h_input | ChIP-seq | GSM4732251 | 32936072 |
| H3K27Ac_4h_input | ChIP-seq | GSM4732254 | 32936072 |

### 2.6. The systemPipeR workflow

The systemPipeR (H Backman and Girke 2016) R package provides a great pipeline for the basic analysis of NGS based techniques (e.g. RNA-seq, ChIP-seq) in R. The concept of systemPipeR v.2.2.2. includes a “target” file that contains the path to the input files, names of the samples, groups of the sample, comparison of interest and more (Fig. 5). The other

important file type is the parameter (.param) file. The information from both files is used to create system calls within the R environment for every individual sample in order to automatically run system tools (e.g. trimming, alignment, peak calling). Required parameters and the full paths to the data samples are preselected and extracted from the target files. Several new param files for the corresponding tools used in this study were created (Appendix/ Parameter_files).

In R, the *systemArgs* function generates the system calls for each input file or for multiple input files, e.g. for paired-end data. These system calls can be executed using the *runCommandline* function. The function also checks if the output files already exist and is able to convert Sequence Alignment Maps (SAM) to Binary Alignment Maps (BAM) using Rsamtools (Morgan et al. 2017). To note, I expanded and modified the function to be able to recognize more output formats and generate multiple outputs needed for some specific tools (Appendix/R_code/Functions/SysArgs_New). In a last step, a new target file is generated using the *writeTargetsout* function. This new target file will be used as an input for the next step of the pipeline containing adjusted sample names and paths.

In addition, systemPipeR includes functions for visualization of the quality FASTQ files (*seeFastq*) and the calculation of the alignment percentage (*alignStats*).

Finally, systemPipeR is able to perform some of the downstream analysis for RNA-seq, ChIP-seq and other techniques.

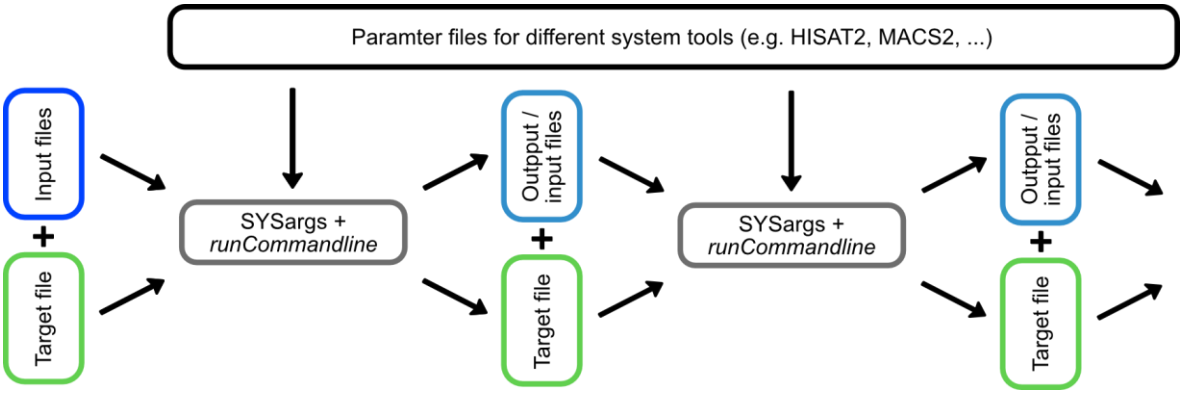


**Figure 5) The systemPipeR workflow.** The systemPipeR workflow includes input files, target files and the *runCommandline* function.

## 2.7. Data analysis

### 2.7.1. Unix / R

All analyses were performed on a computer with 64GB RAM and 24 threads (Ryzen 9 3900x) running Ubuntu 20.04. LTS as an operating system. R version 4.2.1 (R Core Team 2022) together with RStudio (RStudio Team 2022) was used for R-based analyses.

### 2.7.2. Primary analysis (from raw FASTQ file to final BAM file)

Publicly available NGS data sets were downloaded from the Gene Expression Omnibus (GEO) (Edgar et al. 2002) database using the *fasterq-dump* function provided by the SRA-Toolkit (https://github.com/ncbi/sra-tools) and saved as FASTQ files.

The first step of the analysis of NGS data was to trim the raw FASTQ files. This includes trimming of the bases with insufficient quality or leftover sequencing adapters. Finally, reads below a certain length were removed (Fig. 6). For this purpose, the TrimGalore (Krueger 2019) tool was used with "--phred33" parameter. It combines the two tools Cutadapt (Martin 2011) for adapter, primer and poly-A trimming and FastQC (Andrews et al. 2020) for quality control. Without providing a specific adapter parameter (e.g. Ilumina, Nextera), the default method is to automatically detect the used sequencing adapter. For the automatic adapter detection TrimGalore uses the first 1 million reads and search for known sequencing adapters, which are subsequently removed from the reads in the entire file. TrimGalore provides detailed statistics on the effectiveness of trimming for each file. Furthermore, systemPipeR's *seeFastq* function was used to provide a visual representation of the quality for given FASTQ files.

The next step, the alignment, was based on the trimmed FASTQ files. Here, varying tools were used for the alignment of individual samples (Suppl. Table S1 & S8). The first few analyses (RBPJ binding in MT cells - RBPK KO in MT cells) were aligned with bowtie2 (Langmead and Salzberg 2012) for ChIP-seq or the splice-aware tophat2 (Kim et al. 2013) for RNA-seq. All other files were aligned with HISAT2 (Kim et al. 2019), which provides a much faster alignment and can be used for both spliced and non-spliced reads. To increase the speed of the alignment in case of spliced reads, a maximum intron length of 3000 bp was set. In this way, over 70% of all introns in the mouse genome can still be detected, and no significant disadvantage was shown compared to considering all intron lengths when analyzing typical differentially expressed genes (tested on multiple data sets, data not shown). All three alignment tools provide a detailed statistics on the quality of the alignment

for each individual SAM/BAM file. For a simpler and more lucid comparison, systemPipeR's *alignStats* function was used. This function counted the successfully aligned reads, compared them to the number of unmappable reads and provided a compact list of those values for multiple files at once.

The generated SAM files were directly converted to BAM files by the parameter "make_bam = T" when using systemPipeR's *runCommandline* function, which uses Rsamtools for the conversion (Morgan et al. 2017).

For the ChIP-seq, ATAC-seq, CUT&TAG and some RNA-seq (MT cells RBPJ depletion) analyses, the aligned reads were filtered for potential PCR duplicates. For this, I used Picard tools *MarkDuplicates* function with "REMOVE_SEQUENCING_DUPLICATES = true REMOVE_DUPLICATES = true" parameters (http://broadinstitute.github.io/picard/) and saved the output as BAM file. These filtered BAM files were indexed using samtools' (Li et al. 2009) *index* function. For the generation of normalized coverage tracks (bigWigs), the filtered BAM files were converted with deepTools' *bamCoverage* function (Ramírez et al. 2014). In case of cross-sample normalization of the coverage track files, DESeq2's (Love et al. 2014) size factors were used as scaling factors with the parameter "--scaleFactor".

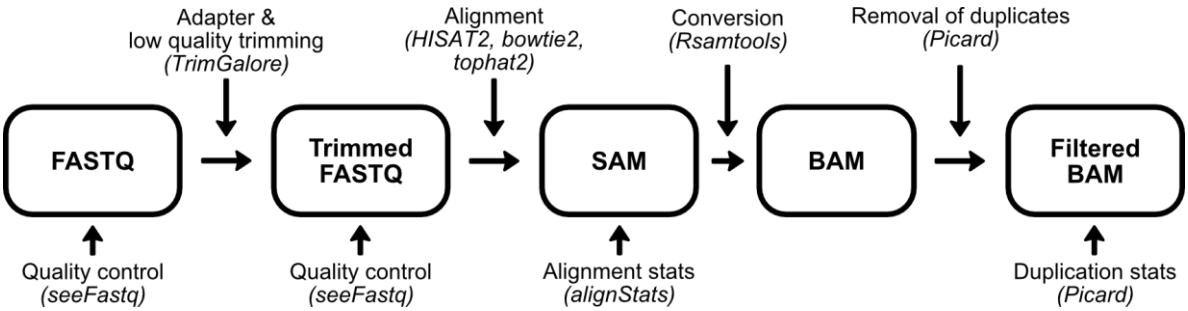


**Figure 6) Illustration of the NGS primary analysis.** SAM = Sequence Alignment Map, BAM = Binary Alignment Map.

### 2.7.3. Downstream analysis of RNA-seq

The GTF file for each organism was imported into R and converted directly into a TxDb object using the *makeTxDBfromGFF* function (Lawrence et al. 2013) (Fig. 7). The genomic position information for the exons of each gene was extracted from the corresponding TxDB object and stored as a GRanges object. The *summarizedOverlaps* function with the "mode

= 'Union'" and the specific parameter for single-end or paired-end samples was used to count reads of the BAM files for the genomic ranges of all exons, yielding absolute numbers of reads aligned to individual genes. These counts were used as input for the differential gene expression analysis with DESeq2 (Love et al. 2014). DESeq2's median of ratio normalization was used for the cross-sample normalization over all samples. In the cases where samples from different experiments were pooled (NICD1-ER) to identify differentially expressed genes (DEGs), additional batch normalization was applied. The quality of the normalization was validated by plotting the normalized read counts of all samples as box plots. The overall quality and comparability of the replicates was visualized and tested by both Pearson correlation coefficient (PCC) or principal component analysis. Unless otherwise indicated, genes with a $\log_2$ fold change (FC) < -1 or > 1 and adjusted p-value (Benjamini and Hochberg 1995) < 0.05 were identified as significantly deregulated. Heat maps for expression changes ($\log_2$ FC), z-scaled expression values or PCC were generated using gplots' *heatmap.2* function. Line plots visualizing the expression were plotted using ggplot2 (Wickham 2016). Volcano plots for gene expression changes and adjusted p-values were created using the EnhancedVolcano package (github.com/kevinblighe/EnhancedVolcano).

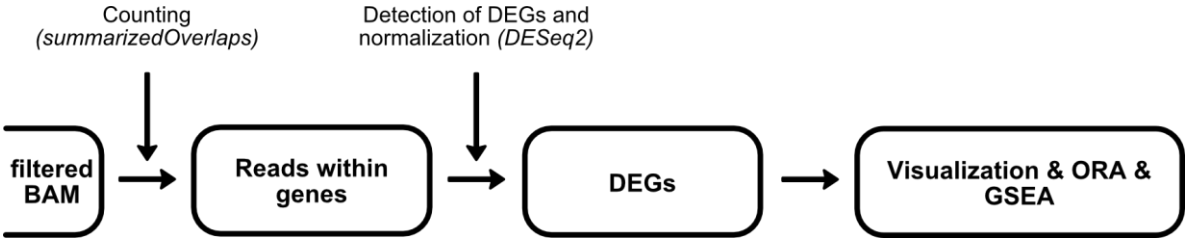


**Figure 7) Schematic representation of the downstream analysis of RNA-seq.** BAM = Binary Alignment Map, DEGs = differentially expressed genes, ORA = over representation analysis, GSEA = gene set enrichment analysis.

### 2.7.4. Downstream analysis of ChIP-seq, ATAC-seq and CUT&Tag

To obtain the optimal peak set, peak calling based on the final BAM files was performed with both MACS2 (Zhang et al. 2008) and Peakranger (Feng et al. 2011) (Fig. 8). The resulting peak sets were compared by optical inspection and the peak caller with the more convincing results was used. For ChIP-seq classical input (without AB) was used, while ATAC-seq was analyzed without any input. For CUT&Tag, both no AB and IgG input was tested as an input

for the peak calling. For the final peak sets of the CUT&Tag data, I used the peaks for which IgG was used as input because they looked more convincing on visual inspection.

Due to the "poor" signal-to-noise ratio in the case of the RBPJ ChIP-seq data, the peak sets from multiple replicates were combined using the MSPC tool (Jalili et al. 2015) with parameters “-r bio -w 1e-6 -s 1e-10”. The basic idea of this approach is to perform a less stringent peak calling on the individual samples to get a larger and less specific set of peaks for the individual samples. These weaker peaks were then cross-validated between the different samples, allowing weaker peaks to be identified as "true positive peaks” if they were conserved between replicates. These “true positive peaks” were taken for the next steps.

To increase the confidence in the final set of peaks of the other data sets (except for RBPJ ChIP-seq), the overlap between replicates was used to generate the final set of peaks. For ATAC-seq or ChIP-seq of histone modifications (H3K27ac, H3K4me1, H3K4me3, H3K18ac, H3K9ac), a peak had to be conserved in 3 out of 4 (Control/*sgRBPJ*, DMSO/GSI or GSI/Washout) replicates. These final peak sets were filtered for the ENCODE blacklisted regions, which contain “…anomalous, unstructured, or high signal in next-generation sequencing experiments independent of cell line or experiment” (Amemiya et al. 2019). Final peak sets were validated by optical inspection in the IGV browser (Robinson et al. 2011).

In case of mature T-cell data, the csaw R package (Lun and Smyth 2016) was used to quantify binding of RBPJ and associated histone modifications. The *windowCounts* function with parameters “ext = 110, width = 10” generated windows with a width of 10 bp and a spacing between each window of 50 bp (default). Next, a sliding window approach was then used to count the number of reads (based on the BAM files) that overlap with each window. The minimum allowable mapping score for the reads was set to 20. As a control to the sites of interest (identified RBPJ binding sites) an additional 150000 random sites with an equal length as the RBPJ sites were used. These reads were normalized to achieve a comparable background level (average reads at 150000 random sites) of reads.

For the identification of differentially bound regions (DBRs) or differential accessibility regions (DARs) for Beko or human data sets, the *summarizedOverlaps* (see 2.7.3. Downstream analysis of RNA-seq) function was used to count reads based on the BAM files and the regions of interest e.g. peaks. Normalization of the counts and identification of DBRs/DARs was performed using DESeq2.

Heat maps for binding intensity of ChIP-seq, ATAC-seq or CUT&Tag were generated using deepTools' (Ramírez et al. 2014) *computeMatrix* and *plotHeatmap* functions. Input for these functions included the peak set and the normalized coverage tracks (bigWigs). Line plots were generated using ggplot2 based on the matrix files from deepTools' *computeMatrix* function. The plotted lines indicated the mean and outlines standard deviation for the used replicates. Snapshots were generated using Gviz (Hahne and Ivanek 2016) with the normalized coverage tracks as input. Association of binding sites to genes was performed using an inhouse tool that works in a comparable manner like GREAT's (McLean et al. 2010) basal plus extension mode that allows mapping to two genes but prioritizes transcription start site (TSS) regions (5 kb upstream, 1 kb downstream). Identification of genomic features at RBPJ binding sites and distance to the next TSS were calculated using ChIPseeker's (Yu et al. 2015) *annotatePeak* function with the corresponding GTF file. Motif analysis of RBPJ sites (summits + / - 50 bp) was performed using the Meme suite v5.05 (Bailey et al. 2009) running in a docker container (memesuite/memesuite). Different numbers of states were tested for the description of the chromatin landscape with ChromHMM (Ernst and Kellis 2017) on H3K4me1, H3K27ac, H3K4me3 ChIP-Seq, and ATAC-Seq data sets.

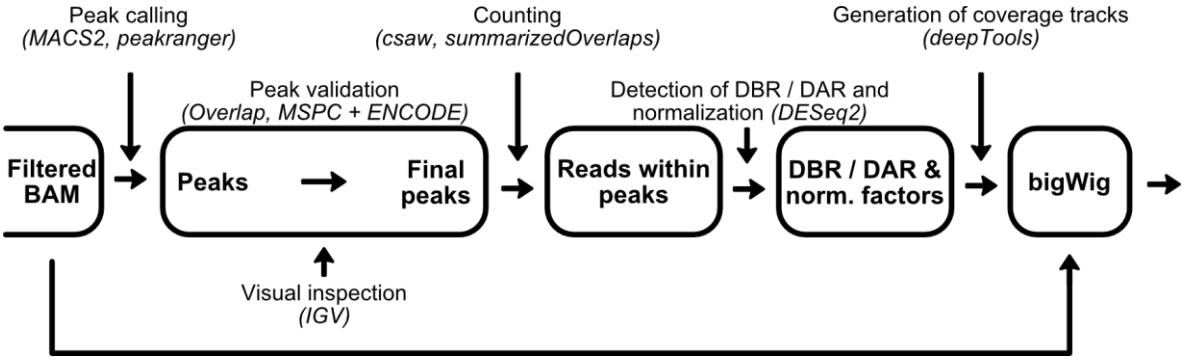


**Figure 8) The downstream analysis of ChIP-seq, ATAC-seq and CUT&Tag.** BAM = Binary Alignment Map, DBR = differentially bound regions, DAR = differential accessibility regions.

### 2.7.5. Microarray analysis

Microarray data sets (SCLC, T6E and Beko) were analyzed in R. The data was downloaded and imported in R from GEO (GSE97465, GSE69091 and GSE62528) using the *getGEO* function from the GEOquery R package (Davis and Meltzer 2007). The limma (Ritchie et al. 2015) R package was used to scale normalize the raw data and detect DEGs.

### 2.8. Identification of "Super Enhancers" in Beko cells

While there are several methods to identify super enhancers, the basic idea is the same for all of them. The first step involves identifying active enhancer regions by performing a genome-wide binding assay (e.g., ChIP-seq or CUT&Tag). Several targets are known for the identification of such enhancer regions, including histone modifications such as H3K27ac, BRD4 or subunits of the Mediator complex such as MED1. Subsequently, enhancers that are located at a certain distance from each other are assigned to larger enhancer clusters. These enhancer clusters are sorted according to their activity level, which is characterized by the strength of binding of the enhancer factor. With this approach, there should be a small group of enhancers characterized by a much higher activity level than the vast majority of others. This group is referred to as super-enhancers.

In this study, I used the ROSE tool (Whyte et al. 2013) for identifying super-enhancers, which was developed by the Young lab. The ROSE tool needs two input files, first the identified enhancer regions as a General Feature Format (GFF) file and second the associated aligned reads as a BAM file. Due to the two replicates of H3K27ac ChIP-seq in control Beko cells (DMSO), I first merged the two BAM files using samtools' merge function. To keep consistent, this merged BAM file was used for a new peak calling using MACS2 with the single input control. The resulting narrow peaks were converted to a GFF file within R. This GFF file together with the merged BAM file was used as an input for ROSE. The typical output of ROSE includes a file for the identified enhancer clusters (stitched enhancers), super enhancers and the curve showing the strength of all enhancer clusters. The resulting 935 super enhancers in Beko cells were optically validated within the IGV browser and compared to known super enhancers in T-cells.

### 2.9. GO / GSEA functions

Many RNA-seq analyses involve the same basic questions. The typical questions are: Which genes are significantly deregulated? With which known signaling pathways / GO terms are these genes associated? Which gene sets are significantly regulated?

To answer these questions in an automated way, I have developed a set of functions that can answer these questions and automatically generate publication ready figures (Appendix/R_code/Functions/my_GO_analysis). These functions need only the generated DESeq2 object and the contrast of interest defined in systemPipeR's targets file. The first step is to translate the human-readable Gene Symbols to Entrez Gene IDs using bitr. These

Entrez Gene IDs are used as input for the over representation analysis (ORA) with either the Gene Ontology (GO) (BP, MF, CC) or the KEGG database. The ORA analysis is based on the clusterProfiler (Yu et al. 2012) package (*enrichGO* / *enrichKEGG*). All genes with at least one read in one sample are defined as the background (universe) for the ORA.

For the gene set enrichment analysis (GSEA), all genes are ranked by their Wald test statistic (max to min) provided by DESeq2. Genes without values are removed. These ranked gene lists are used as an input for the *gseGO* or *gseKEGG* functions.

The results of all analyses are tables including all significant pathways with p-values, associated genes and other statistics. Furthermore, dot plots for the top 10 significant pathways, GSEA plots and KEGG maps are generated. Additionally, .rds objects store all necessary information to reproduce all plots with specific pathways of interest. To increase the speed of the analysis, there are parameters that define which part of the analyses should be performed.

### 2.10. Prediction of dynamic RBPJ binding sites

I tested the prediction of dynamic or static binding behavior of RBPJ sites in Beko cells based on several features. These features included min-max normalized MSPC's negative decadal log p-values (proxy for the quality of binding), distance relative to the nearest TSS, genomic feature (see ChIP-seq section), association with different histone marks, occurrence of the canonical RBPJ motif and more. To create and test different prediction approaches the caret package was used (Kuhn 2008). First, the raw data set was split into two data sets (training and test) using the *createDataPartition* function from the caret package. Due to the strong imbalance in the classifications (5% dynamic, 95% static), I tested random subsets with varying percentage of static sites as an input for the training set. 158, 500, 1000, 1500, 2500, 3000 and all static sites were tested as an input for the model (Suppl. Table S15). Therefore, random subsampling of static sites was used. The *createDataPartition* function of the caret (Kuhn 2008) package was used to split the data set (all dynamic sites + variable number of static sites) into 80% training data and 20% test data. Finally, 1500 static sites represent the sweet spot for the best prediction.

Various machine learning algorithms were tested for the prediction, including random forest, generalized linear model and others. The most accurate prediction was using the random forest algorithm with over 95% overall accuracy. The random forest model was generated based on the training data using the *randomForest* function of the randomForest (Liaw 2002)

package. Mean accuracy (fraction of correctly predicted sites in test data) was measured over 500 random forest models based randomly subsampled static sites. Finally, one random model with an accuracy over the mean of all 500 models was chosen as the final one. This exact same model was used for the prediction of dynamic or static binding behavior of RBPJ sites in other cell types.

Lastly, the two features that showed the strongest predictive power for dynamic or static sites were MSPC's p-value and the associated genomic feature (defined by the ChIPseeker's *annotatePeaks* function), while all other features had only a minor impact on the overall accuracy.

Receiver operating characteristic (ROC) curve showing the true vs. false positive rates for both static and dynamic site prediction was calculated using the ROCR package (Sing et al. 2005).

### 2.11. System tools and R environment

All system tools, R code and the R "sessionInfo" that were used for bioinformatics analysis are in the appendix.

# 3. Results

## Chapter I: Notch-dependent and -independent functions of transcription factor RBPJ

### 3.1.1. Characterization of RBPJ binding sites in mature T-cells

The transcriptional response of the Notch pathway is mediated by the transcription factor RBPJ, which is the major interaction partner of the Notch intracellular domain (NICD) (Siebel and Lendahl 2017). Depending on the activation state of the Notch pathway, RBPJ can act as an activator or a repressor by interaction either with co-activators (Notch active) or co-repressors (Notch inactive). To elucidate the molecular mechanism of RBPJ-mediated repression genome-wide, I analyzed different ChIP-seq and ATAC-seq data sets in a mature T-cell line (MT) displaying no Notch signaling (Notch-OFF) (Xu et al. 2017). In MT cells the role of RBPJ was described to repress Notch target gene expression (Yuan et al. 2019).

First, I identified RBPJ binding sites in MT cells by analyzing RBPJ ChIP-seq data in control (eV) MT cells. I was able to identify 1753 RBPJ binding sites that were shared between two replicates (Fig. 9A, Appendix Fig. 1A, Suppl. Table S2). To test the function of RBPJ and validate the ChIP-seq signals, I additionally analyzed data from MT cells with CRISPR-meditated depletion of RBPJ (KO). Some groups suggest using depletion experiments in ChIP-seq to eliminate “phantom peaks”, regions that are not enriched due to specific immunoprecipitation but are rather identified nonspecifically (Jain et al. 2015). Thus, I removed all peaks that still had a detectable signal in either replicate of RBPJ depleted MT cells. (Fig. 9A).

It is known that many TFs, including RBPJ, bind to open chromatin regions (Tsompana and Buck 2014). ATAC-seq provides a useful tool to identify open chromatin regions on genome-wide scale. Analysis of ATAC-seq data derived from control MT cells revealed 47763 open chromatin regions (Fig. 9C, Suppl. Table S2). As expected, the vast majority of RBPJ sites (1735/1753) were within these accessible regions. Noteworthy, the visual inspection of the 18 non-overlapping sites indicated that these regions were nonetheless enriched for ATAC-seq signals, but the stringency of peak calling resulted in the failure to detect these as accessible regions. Nevertheless, these regions were removed from the set of RBPJ sites.

Typically, TFs recognize and bind specific DNA motifs to regulate their target regions. To identify motifs at RBPJ sites, I performed a DNA binding motif identification analysis. As

expected, I found the canonical RBPJ binding motif significantly (E-value = $8.2\times10^{-31}$) enriched at these sites (Fig. 9D). Surprisingly, only 340 of the 1735 sites carried the canonical RBPJ motif. The most enriched and frequently identified motif was not the RBPJ consensus binding sequence but the transcription factor specificity protein 1 (SP1) motif (E-value = $8.1\times10^{-170}$), which is mainly found at promoter regions (Hasegawa and Struhl 2021). In addition, other motifs such as RUNX2, NRF1, SP2, and others were identified as significantly enriched (Suppl. Table S3).

In summary, the above findings supported the specificity of the identified RBPJ binding sites in MT cells and showed that the SP1 and RBPJ consensus binding sequence, among others, were enriched at RBPJ sites.

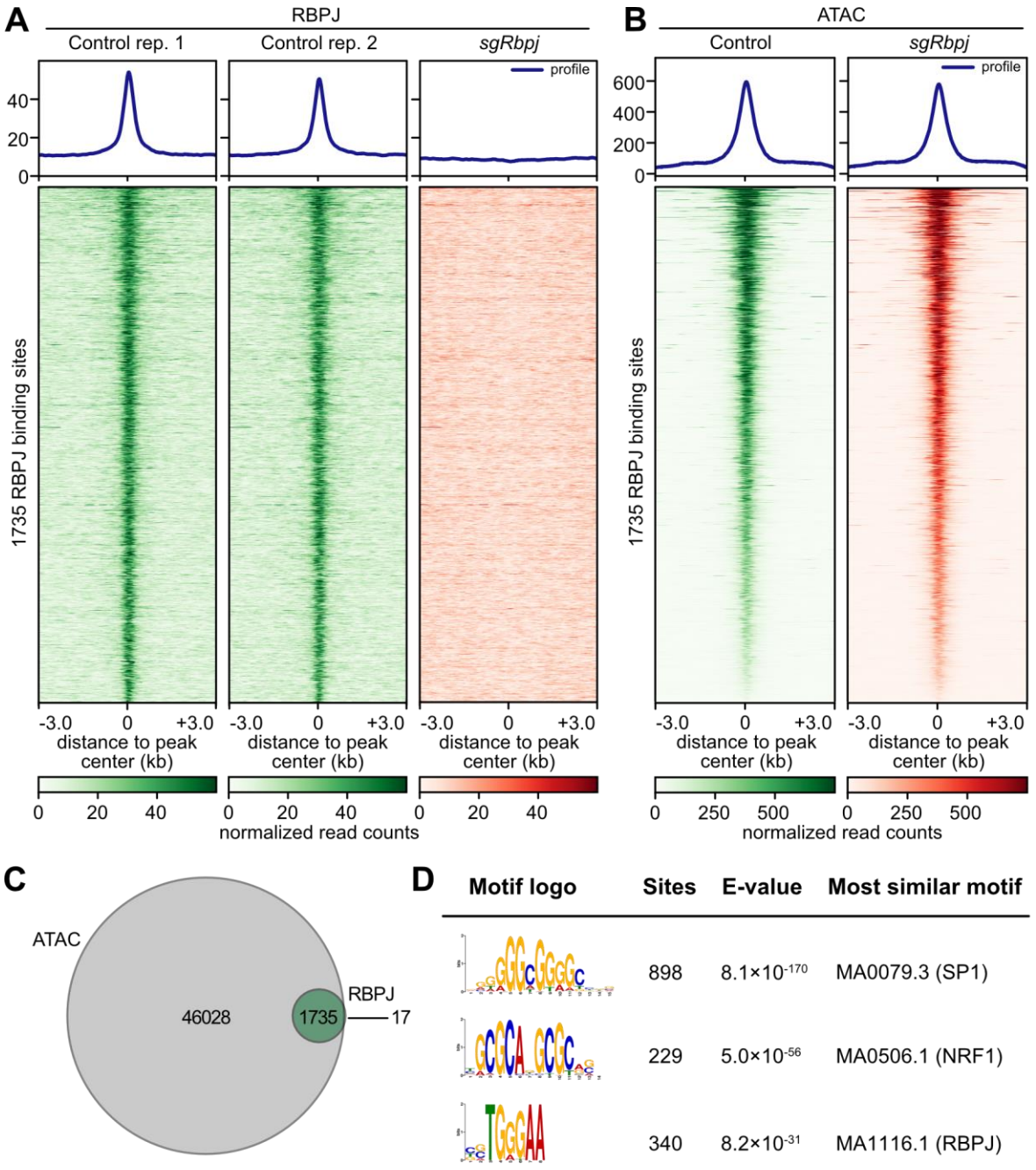


**Figure 9) Characterization of RBPJ binding sites in mature T-cells.** A) Heat map and average binding plot (profile) showing the 1735 RBPJ binding sites in control (green) and RBPJ-depleted (red) mature T-cells by ChIP-seq. B) Heat map and average binding plot (profile) of the chromatin accessibility at 1735 RBPJ sites in control (green) and RBPJ-depleted (red) MT cells. Chromatin accessibility was measured by ATAC-seq. C) Venn diagram depicts the overlap of identified open chromatin regions (ATAC-seq) and RBPJ binding sites (ChIP-seq) in control MT cells. D) Table shows enriched DNA binding motifs at RBPJ sites including the SP1, NRF1 and RBPJ motif. Motif discovery was performed using MEME-ChIP.

It is known that RBPJ can affect the chromatin structure during the regulation of the Notch target genes by recruiting several chromatin modifiers including the acetyltransferase p300 (activator) or the HDAC and histone demethylase recruiting SHARP/NCoR complex (co-repressors) (Oswald et al. 2001; Oswald et al. 2002). This led to the assumption that the RBPJ could lead to repressive chromatin conformation in MT cells. In order to test this, I analyzed ATAC-seq results upon depletion of RBPJ. Surprisingly, the overall chromatin accessibility at RBPJ sites was not affected by the depletion of RBPJ (Fig. 9B, Appendix Fig. 1B).

To characterize the RBPJ-mediated effects in regard to histone marks, I analyzed ChIP-seq data of H3K27ac (active chromatin), H3K4me3 (promoter regions) and H3K4me1 (enhancer regions) in control and RBPJ-depleted MT cells. Overall, RBPJ sites were enriched for H3K27ac (Fig. 10A, Appendix Fig. 2A) and H3K4me3 (Fig. 10B, Appendix Fig. 2B). The typical peak-valley-peak pattern (Pundhir et al. 2016), representing RBPJ binding in the valley and the modifications at the surrounding nucleosomes, was found for both histone marks. Overall, RBPJ binding sites and their proximity showed a decreased level of H3K4me1, compared to the outer regions (+/- 3 kb) surrounding the RBPJ sites (Fig. 10C, Appendix Fig. 2C). Previously, H3K4me1 was shown to be found flanking H3K4me3 at active promoters (Bae and Lesch 2020).This indicated that RBPJ sites are mainly found at active promoter regions.

To test whether RBPJ depletion affects the adjacent chromatin landscape, I compared control MT cells to MT cells depleted of RBPJ. Despite the described function of RBPJ to remodel its adjacent chromatin, the overall level of H3K27ac, H3K4me3 and H3K4me1 at RBPJ were only slightly affected upon RBPJ depletion (Fig. 10A - C). Although RBPJ acts as a repressor in MT cells (Yuan et al. 2019) and should therefore be associated with inactive chromatin, the H3K27ac levels where slightly reduced upon RBPJ depletion. Furthermore, H3K4me3 and H3K4me1 were slightly enriched by the depletion.

In contrast to the overall response, chromatin at some RBPJ sites showed a strong increase of H3K27ac and H3K4me3 levels. These RBPJ sites were mainly in the proximity or directly at known Notch target genes like *Hes1 or DTX1*, but also near *Kcnn1*, which has not yet been associated with Notch signaling (Fig. 10D).

In summary, RBPJ sites were associated with the typical active promoter chromatin marks H3K27ac and H3K4me3. Surprisingly, and in contrast to the described function of RBPJ as a repressor, most RBPJ sites were located in active open chormatin. Overall, the depletion

of RBPJ was not associated with changes of the chromatin modifications. However, a minority of sites showed a strong change upon RBPJ depletion

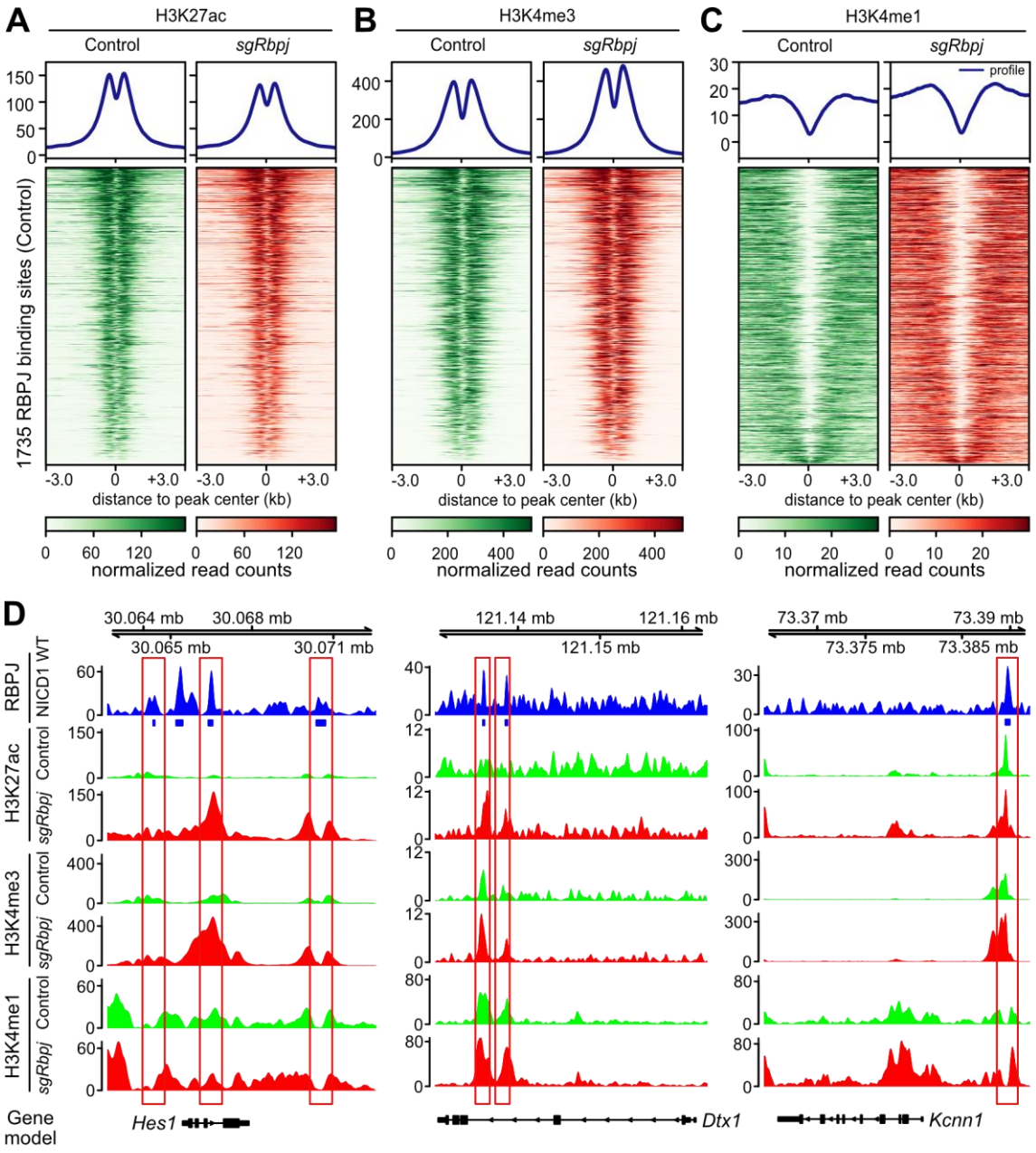


**Figure 10) The chromatin landscape at RBPJ binding sites in mature T-cells.** Heat map and average binding plot (profile) showing the overall enrichment of A) H3K27ac, B) H3K4me3 and C) H3K4me1 at 1735 RBPJ binding sites in control (green) and RBPJ-depleted (red) mature T-cells. D) Genomic snapshots of the gene loci of *Hes1* (left), *Dtx1* (middle) and *Kcnn1* (right) displaying associated histone modifications H3K7ac, H3K4me3 and H3K4me1 for control and RBPJ-depleted MT cells. Histone modifications were analyzed by ChIP-seq.

### 3.1.2. Transcriptional regulation by RBPJ in absence of Notch signaling

After analyzing the effects of RBPJ on surrounding chromatin, the question arose how RBPJ affects transcription, since chromatin conformation and transcription are closely linked. The RBPJ-mediated transcriptional activation of Notch target genes is well described in various cellular systems. However, the RBPJ-mediated repression of genes is less-well understood. Previously, our group published the repressive function of RBPJ on the known Notch target genes *Hes1* and *Hey1* in the absence of active Notch signaling (Yuan et al. 2019). To understand the genome-wide repressive potential of RBPJ, I analyzed RNA-seq data from control and RBPJ-depleted MT cells.

First of all, I identified 509 significantly upregulated ($log_2$ FC > 1 & FDR < 0.05) and 148 significantly downregulated ($log_2$ FC < -1 & FDR < 0.05) genes upon depletion of RBPJ (Fig. 11, Suppl. Table S4). In line with the previous publication (Yuan et al. 2019), *Hes1* and *Hey1*, but also the known Notch target genes *Lgmn* and *Il2ra* were among the significantly upregulated genes. Overall, the depletion of RBPJ resulted in much more upregulated of genes. This is in line with RBPJ's proposed function as a repressor in the absence of an active Notch pathway.

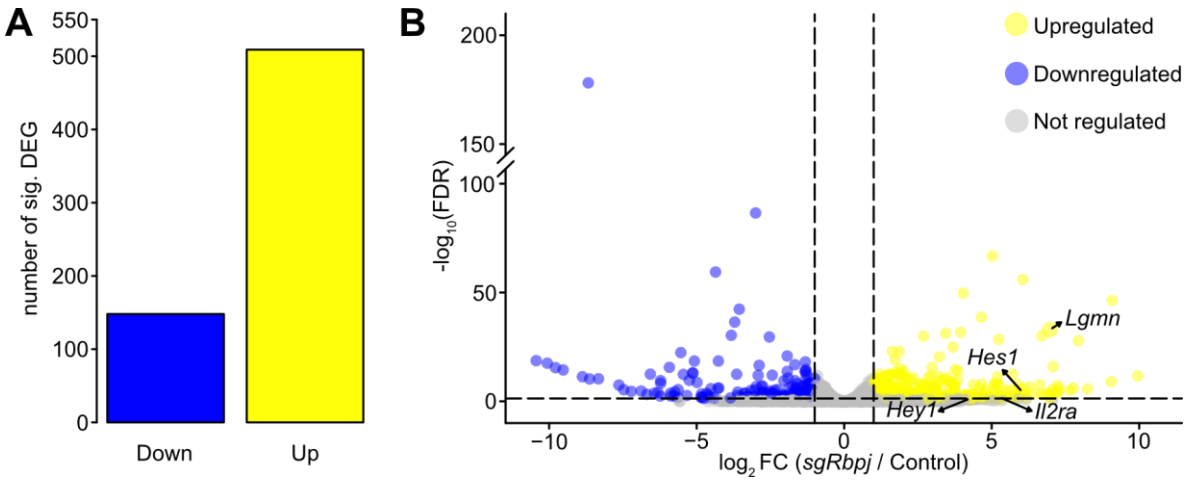


**Figure 11) Overall depletion of RBPJ leads to upregulation of transcription.** A) Bar plot of the 509 significantly upregulated and 109 significantly downregulated genes. Stringency thresholds were $log_2$ FC > 1 (upregulated) or $log_2$ FC < -1 (downregulated) and adjusted p-value (FDR) < 0.05. B) Volcano plot of the transcriptional response upon RBPJ-depletion in mature T-cells measured by RNA-seq. Labeled are the known and significantly upregulated Notch-target genes *Hes1*, *Hey*, *Il2ra* and *Lgmn*.

As described above, it was shown that RBPJ together with co-factors can affect neighboring chromatin regions, which has been shown to be important for transcriptional regulation. In order to find the direct RBPJ target genes and to remove genes that are indirectly regulated by secondary effects, I integrated ChIP-seq and RNA-seq. I defined direct RBPJ target genes as genes associated with an RBPJ binding site that are significantly deregulated upon depletion of RBPJ.

Although there were 1735 RBPJ binding sites and 657 deregulated genes, only 72 genes were fulfilling these criteria (Fig. 12). Both *Hes1* and *Kcnn1,* which showed increased levels of H3K27ac upon depletion of RBPJ (Fig. 10B) and the other well-described Notch target genes *Hey1* and *Lgmn* were found to be direct RBPJ targets. This suggests that in the absence of Notch signaling, RBPJ acts directly as a repressor only on a subset of target genes.

Interestingly, I found a set of 32 (~44%) genes that were bound by RBPJ and showed a repression (downregulation) of transcription upon RBPJ-depletion. This may indicate a yet largely undescribed function of RBPJ as an activator in the absence of Notch.

In summary, depletion of RBPJ resulted in more upregulated genes than downregulated genes, supporting the function of RBPJ as a repressor in cells with an inactive Notch pathway. Only 40 of the 509 significantly upregulated genes were associated with an RBPJ binding site, indicating direct repression by RBPJ. Within those 40 genes were several known Notch target genes, demonstrating the repressive function of RBPJ on a subset of Notch target genes.

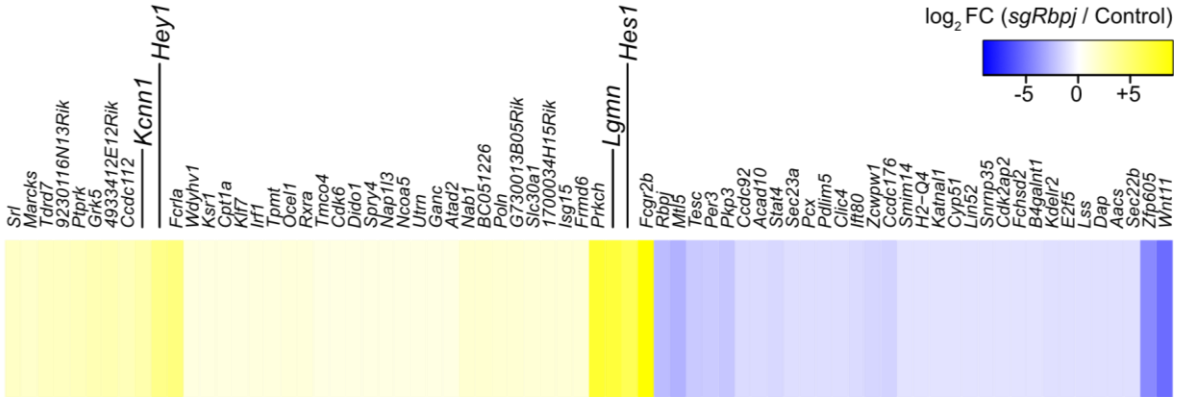


**Figure 12) Identification of 72 direct RBPJ target genes in mature T-cells.** Heat map of the significantly deregulated ($log_2$ FC > 1 or < -1 and adjusted p-value < 0.05) genes upon depletion of RBPJ (RNA-seq) that are associated with an RBPJ binding site (ChIP-seq).

### 3.1.3. Notch-mediated activation of target genes is dependent on RBPJ

Activation of the Notch pathway results in the cleavage of the Notch receptor allowing the translocation of the NICD from the plasma membrane into the nucleus. Here, NICD interacts with DNA-bound RBPJ and switches the function of RBPJ from a repressor to an activator. In order to understand the transcriptional response of activating the Notch pathway in MT cells, I analyzed RNA-seq data sets before and after induction of a tamoxifen (4-OHT)-inducible NICD1 (NICD1-ER) or (Bio-tagged) NICD1 wild type (NICD1 WT) and their controls. Here, the tamoxifen inducible system is used to measure the effects of Notch activation after a specific time point, while the NICD1 WT overexpression results in a constant activation of the Notch pathway.

The cells with a constant activation of the Notch pathway (NICD1 WT) showed 1077 significantly upregulated and 150 significantly downregulated genes compared to their control cells. In comparison, the 24 h of Notch activation by tamoxifen treatment resulted in only to 299 significantly upregulated and 48 significantly downregulated genes (Fig. 13A - B, Suppl. Table S4). This already showed that the constant Notch activation led to much stronger changes in the transcriptome and thus to most likely more secondary effects, compared to 24 h of Notch signaling. To identify the genes directly induced by Notch and rule out secondary or indirect effects, I took the 216 commonly upregulated genes (p-value = $1.9\times10^{-227}$) between NICD-WT and 24 h of NICD1-ER. This minimizes the chance of including indirectly regulated genes since two independent methods of Notch activation were compared. In the literature, NICD is described to act as an activator of transcription. Surprisingly, 15 genes were commonly downregulated (p-value = $1.4\times10^{-21}$). Even though the overlap is statistically significant, the fraction of commonly upregulated genes is much higher than the proportion of commonly downregulated genes, indicating a possible indirect effect.

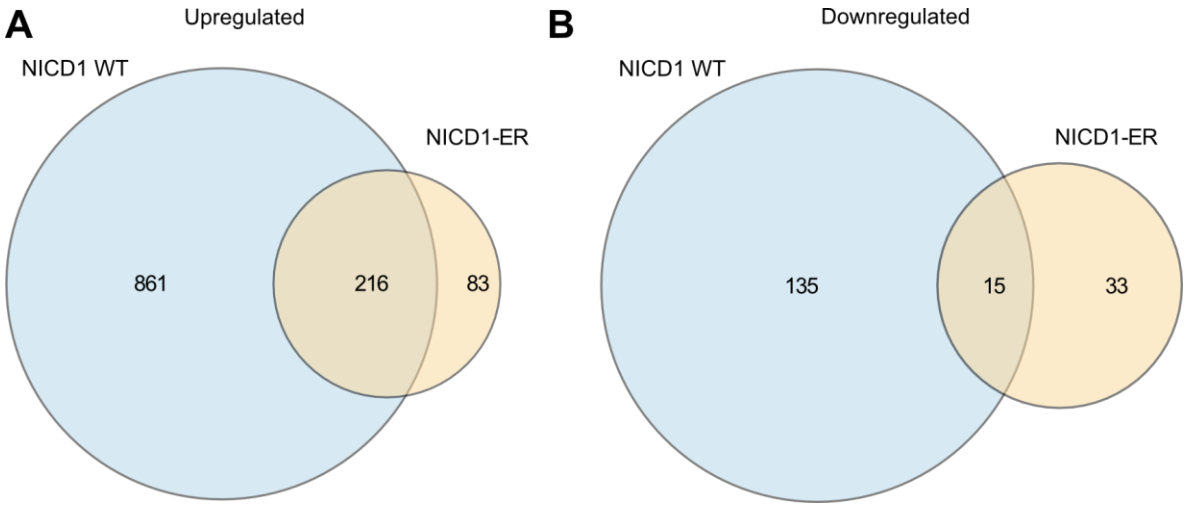


**Figure 13) Identification of Notch target genes.** Venn diagram depicting the overlap of significantly A) upregulated ($log_2$ FC > 1 and adjusted p-value < 0.05) and significantly B) downregulated ($log_2$ FC < -1 and adjusted p-value < 0.05) genes upon constant overexpression of NICD1 WT and 24 h of NICD1-ER. Hypergeometric test: Overlap upregulated: p-value = $1.9\times10^{-227}$; overlap downregulated: p-value = $1.4\times10^{-21}$.

In order to test whether genes previously associated Notch were enriched within the 216 commonly Notch-induced genes, I performed an over representation analysis (ORA) using the GO and KEGG database. Among others, I found three Notch-associated pathways to be significantly overrepresented within the 216 genes (Fig. 14A, Suppl. Table S5). These results confirmed the reliability of the identified Notch-induced genes, the efficacy of both treatments in mimicking Notch activation and further validated the genes as true Notch targets.

It has been previously published that MT cells lack the cleaved NICD1 protein and are therefore Notch inactive (Xu et al. 2017). As additional validation of this finding, I tested the effect of γ-secretase inhibitor (GSI) on MT cells. GSI is a well-established Notch inhibitor that blocks the S3 cleave of the Notch receptor, resulting in downregulation of Notch target genes when cells have active Notch signaling (Olsauskas-Kuprys et al. 2013). As expected, no change in the expression of the 216 Notch target genes (Notch-induced genes) was detectable, confirming that Notch is indeed not active in MT cells (Fig. 14B).

In the canonical model of the Notch pathway, the TF RBPJ is the main transcriptional mediator of the Notch response. This suggest that RBPJ is required for the transcriptional response upon activation Notch pathway. To prove importance of RBPJ for the Notch-

mediated gene activation in MT cells, I analyzed the effect of Notch activation through NICD1 WT overexpression in RBPJ-depleted MT cells. First, these new data sets (called BioeV and BioNICD1 WT) confirmed the previously identified 216 Notch target genes, as they were also strongly upregulated upon BioNICD1 WT compared to their control (BioeV). Second, as suggested by the model, there was no detectable upregulation of the 216 Notch-induced genes in RBPJ-depleted MT cells upon overexpression of NICD1 (BioNICD1 WT) (Fig. 14B, Suppl. Table S4). This confirms that RBPJ is indeed absolutely required for Notch activation.

In summary, the genes commonly upregulated by 24 h of tamoxifen-induced NICD1 (NICD1-ER) and constant overexpression of NICD1 (NICD1 WT) represented a *bona fide* set of direct Notch target genes in MT cells. Furthermore, MT cells had no Notch activity and transcriptional activation of the Notch pathway was absolutely dependent on RBPJ.

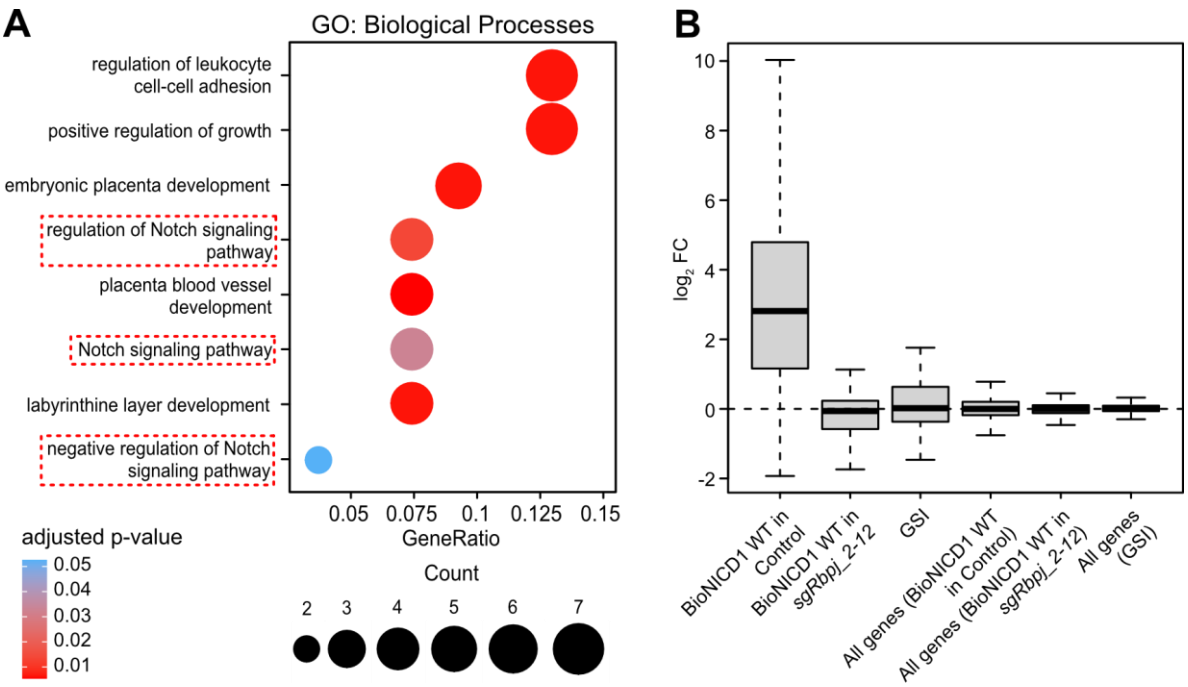


**Figure 14) Notch response in mature T-cells is RBPJ dependent.** A) Dot plot showing that multiple Notch associated pathways are statistically overrepresented within 216 commonly upregulated genes upon constant and 24 h of Notch activation. ORA analysis was performed using the GO "Biological Processes" database. Highlighted are Notch associated pathways. B) Box plot depicting the response of 216 *bona fide* Notch target genes upon BioNICD1 WT (BioNICD1 WT / BioeV) in control or RBPJ-depleted MT cells or upon GSI (GSI / DMSO) treatment. Analysis of transcriptional response was performed by RNA-seq.

### 3.1.4. Notch-activation in MT cells leads to increased RBPJ binding

The above-mentioned experiments, together with the literature, demonstrated the role of the TF RBPJ as an essential mediator of the transcriptional response of the Notch pathway. Several studies indicated that the DNA binding of RBPJ may be dependent on active Notch signaling (Krejčí and Bray 2007; Castel et al. 2013; Wang et al. 2014). Therefore, I focused on the effects of Notch activation on the RBPJ binding. To this end, I analyzed new ChIP-seq data of MT cells overexpressing NICD1 WT (NICD1 WT), a hypoactive NICD1 mutant (NICD1 ΔEP) or BioeV (empty vector) as a control. The NICD1 ΔEP mutant is unable to interact with the histone acetyltransferase EP300, which is described to play an important role in the assembly of the co-activator complex of RBPJ (Oswald et al. 2001). The ΔEP mutant can be used to investigate the function of the coactivator complex on RBPJ binding, as it has been previously described that the MAML/NICD/RBPJ complex increases DNA binding affinity (Wu et al. 2000).

Identification of the RBPJ binding site was repeated using the NICD1 WT data for peak calling. There is evidence in the literature that RBPJ has a stronger DNA-binding in presence of the NICD (Castel et al. 2013), which should allow a more efficient peak calling. Indeed, I was able to detect 3757 binding sites using the RBPJ ChIP-seq in MT cells overexpressing NICD1 WT. Consistent with the above-mentioned literature, the RBPJ binding was stronger in the presence of NICD1 WT compared to their BioeV control cells. Surprisingly, the NICD1 ΔEP mutant showed the overall lowest level of RBPJ binding (Fig. 15A, B & D, Appendix Fig. 3A & B). These findings suggest a potential role for the co-activator complex in the regulation of RBPJ binding to chromatin.

The number of RBPJ binding sites was much higher (2022 new sites) in MT cells overexpressing NICD1 WT (3757 sites) compared to the control MT cells (Fig. 9; 1735 sites). To test how many of the additional 2022 sites were actually not identified with an inactive Notch pathway, I compared both sets of RBPJ binding sites (Fig. 15C, Suppl. Table S2). I found that only 1157 sites were commonly detected in both NICD1 WT and control MT cells. To explain the strong differences in the number of binding sites between NICD1 WT and control cell, I validated the 3757 NICD1 WT sites in control cells (Fig. 15A, Appendix Fig. 3A). Overall, there was a lower binding signal detectable in the control cells, but the pattern was almost identical. Moreover, this signal was completely absent in RBPJ-depleted MT cells. Taken together, the large set of additional binding sites in the presence of NICD1 was most likely due to the stronger binding of RBPJ, resulting in better detectable of the ChIP-seq signals, rather than representing a large set of *de-novo* binding sites.

Furthermore, the detection of DNA binding motifs within the larger set of RBPJ binding sites (3757) in the presence of NICD1 identified similar motifs to those in control cells. These included RBPJ, SP2 and RUNX1 (Suppl. Table S3). This further supports that the larger set of RBPJ binding sites in the presence of NICD1, is overall comparable to the RBPJ sites identified in the absence NICD1.

In summary, the binding of RBPJ to the DNA was significantly stronger in the presence of the NICD1. However, the binding became even weaker upon the overexpression of the hypoactive NICD1 ΔEP mutant, which is unable to interact with EP300. This indicated the importance of the correct forming of the co-activator complex for the RBPJ-DNA binding. Overall, the set of RBPJ binding sites in the presence of NICD1 was comparable to cells without NICD1, indicating that there were not many *de-novo* binding sites.

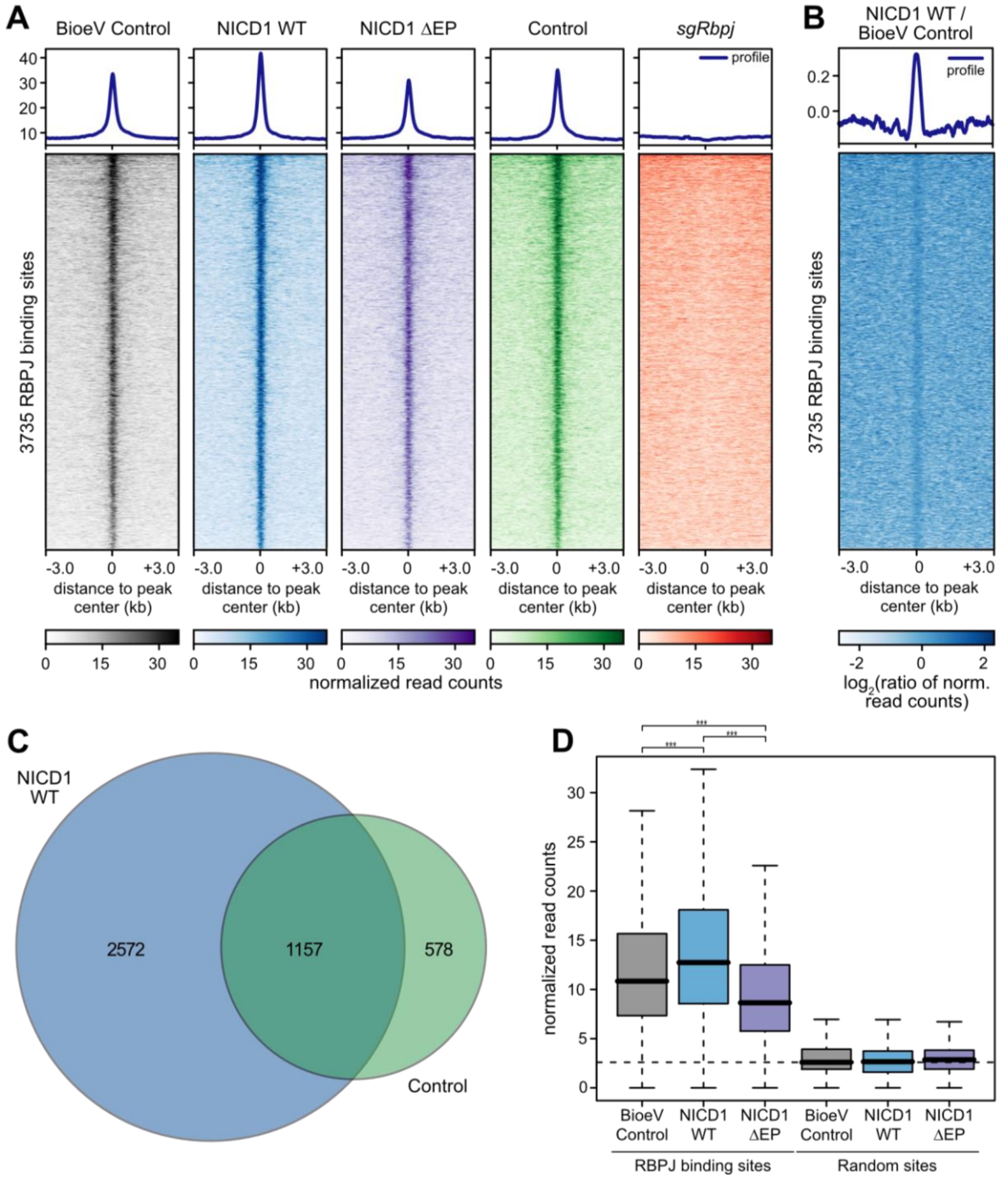


**Figure 15) Notch activation leads to increased RBPJ binding.** A) Heat map and average binding plot (profile) depicting 3735 RBPJ binding sites identified in mature T-cells overexpressing NICD1 WT and their binding strength in BioeV control (grey), NICD1 WT (blue), NICD1 ΔEP (purple), CRISPR control (green) and RBPJ-depleted (red) MT cells. B) Heat map and average binding plot (profile) showing the increase in RBPJ binding at 3735 RBPJ sites upon BioNICD1 WT. C) Venn diagram displaying the overlap of RBPJ binding sites identified in control or BioNICD1 WT overexpressing MT cells. D) Box plot showing the quantification of RBPJ binding at 3757 RBPJ binding sites in control, BioNICD1 WT or BioNICD1 ΔEP and at random control sites. [***] $p < 0.001$; Wilcoxon rank sum test.

### 3.1.5. Identification of *bona fide* Notch target genes in MT cells

After characterization of the Notch-mediated transcriptional activation by 24 h of NICD1-ER or constant overexpression of NICD1 and the effect of NICD1 on the RBPJ binding, I focused on the direct transcriptional Notch response. Consistent with the literature proposing RBPJ as the central transcription factor of Notch signaling, the previous sections showed that RBPJ is essential for the activation of Notch target genes. Therefore, I sought to identify the Notch target genes directly mediated by RBPJ. To this end, I focused on the previously identified 216 Notch-induced genes and selected those associated with at least one of the 3757 RBPJ binding sites in the presence of NICD1. This led to the detection of 65 genes that were induced by Notch-activation and bound by RBPJ (Fig. 16, Suppl. Table S4). These genes included several well-known Notch target genes such as *Hes1*, *Hey1*, *Dtx1* and *Nrarp*.

Taken together, I identified 65 *bona fide* Notch target genes in MT cells. These were defined as genes that are, firstly upregulated by both NICD1 WT and 24 h of NICD1-ER, secondly bound by RBPJ and thirdly this upregulation is dependent on the presence of RBPJ.

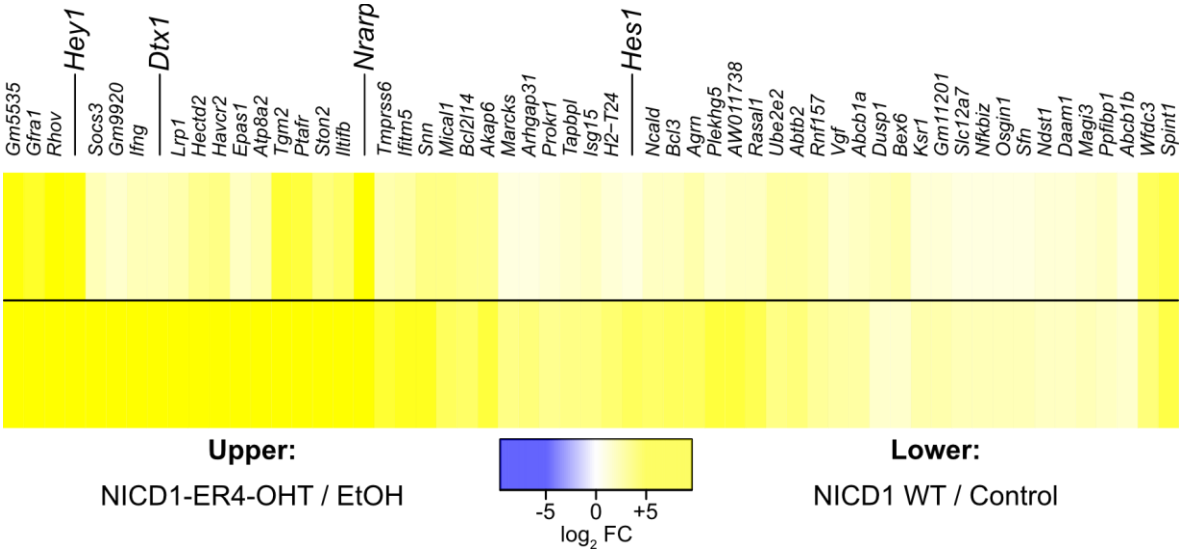


**Figure 16) Identification of direct Notch target genes in MT cells.** Heat map depicting significantly upregulated ($log_2$ FC > 1 and adjusted p-value < 0.05) genes upon 24 h of NICD1-ER (Upper) and constant expression of NICD1 WT (Lower) that are associated with a RBPJ site in MT cells overexpressing NICD1 WT. Analysis of transcriptional response was performed by RNA-seq.

### 3.1.6. Four distinct clusters of RBPJ-Notch target genes

After characterizing both RBPJ-mediated repression and Notch-mediated activation of genes in MT, I wanted to integrate both groups to obtain a genome-wide picture of the overlaps, similarities and differences between the two regulatory mechanisms. Since I was able to show that RBPJ binding is a prerequisite for Notch-mediated gene expression, I focused only on genes associated with an RBPJ-binding site.

In order to better understand the genome-wide regulatory mechanism of RBPJ and Notch, I took all genes that were associated with RBPJ binding in either NICD1 WT overexpressing or control MT cells and that were significantly upregulated by RBPJ depletion (RBPJ-mediated repression), NICD1 WT (constant Notch activation) or NICD1-ER (24 h of Notch activation). Supervised clustering was used to divide these genes into distinct categories (Fig. 17, Suppl. Table S6). The first cluster included all genes upregulated by RBPJ-depletion, NICD1 WT and 24 h of NICD1-ER. These genes were repressed by RBPJ in the absence of Notch and became activated in an RBPJ-mediated manner by Notch signaling. The second cluster was characterized by genes upregulated by RBPJ depletion and NICD1 WT but not by 24 h NICD1-ER. The third cluster comprised genes upregulated by both NICD1 WT and 24 h NICD1-ER but not RBPJ depletion. The fourth cluster consisted of genes upregulated by RBPJ depletion but not with NICD1 WT or 24 h NICD1-ER.

In summary, there were four distinct regulatory patterns of the RBPJ/Notch-mediated transcriptional response. Not all genes activated by Notch signaling were also actively repressed by RBPJ with an inactive Notch pathway. Furthermore, many genes that were actively repressed by RBPJ without Notch signaling were not activated by NICD.

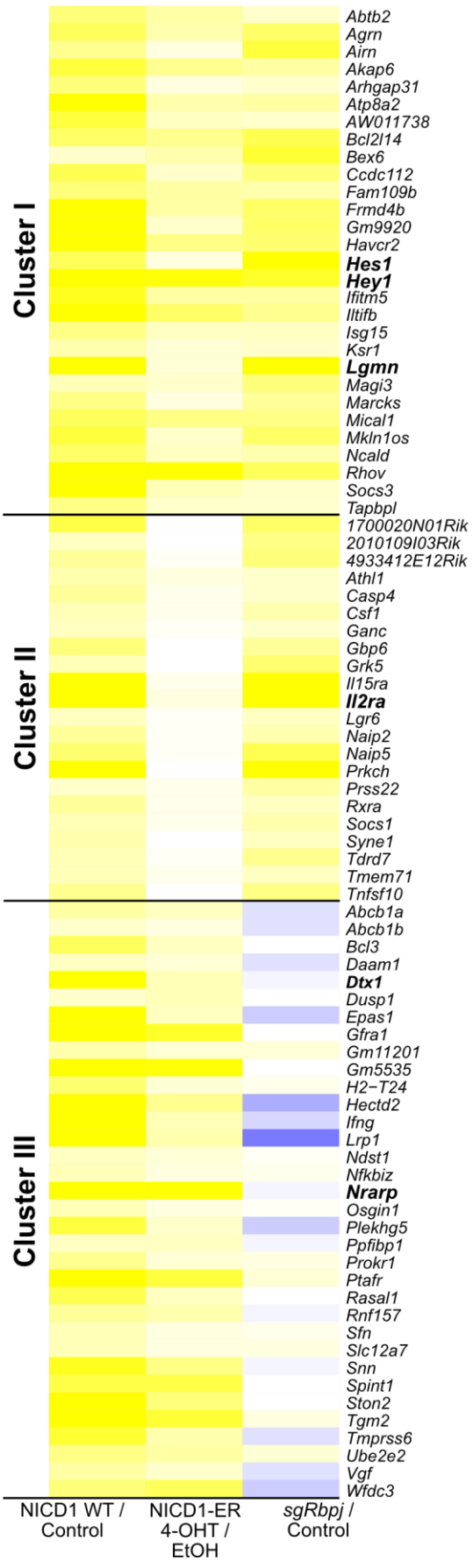
Cluster I
Abtb2
Agrn
Airn
Akap6
Arhgap31
Atp8a2
AW011738
Bcl2l14
Bex6
Ccdc112
Fam109b
Frmd4b
Gm9920
Havcr2
Hes1
Hey1
Ifitm5
Iltifb
Isg15
Ksr1
Lgmn
Magi3
Marcks
Mical1
Mkln1os
Ncald
Rhov
Socs3
Tapbpl
Cluster II
1700020N01Rik
2010109I03Rik
4933412E12Rik
Athl1
Casp4
Csf1
Ganc
Gbp6
Grk5
Il15ra
Il2ra
Lgr6
Naip2
Naip5
Prkch
Prss22
Rxra
Socs1
Syne1
Tdrd7
Tmem71
Tnfsf10
Cluster III
Abcb1a
Abcb1b
Bcl3
Daam1
Dtx1
Dusp1
Epas1
Gfra1
Gm11201
Gm5535
H2−T24
Hectd2
Ifng
Lrp1
Ndst1
Nfkbiz
Nrarp
Osgin1
Plekhg5
Ppfibp1
Prokr1
Ptafr
Rasal1
Rnf157
Sfn
Slc12a7
Snn
Spint1
Ston2
Tgm2
Tmprss6
Ube2e2
Vgf
Wfdc3
NICD1 WT / Control
NICD1-ER 4-OHT / EtOH
sgRbpj / Control

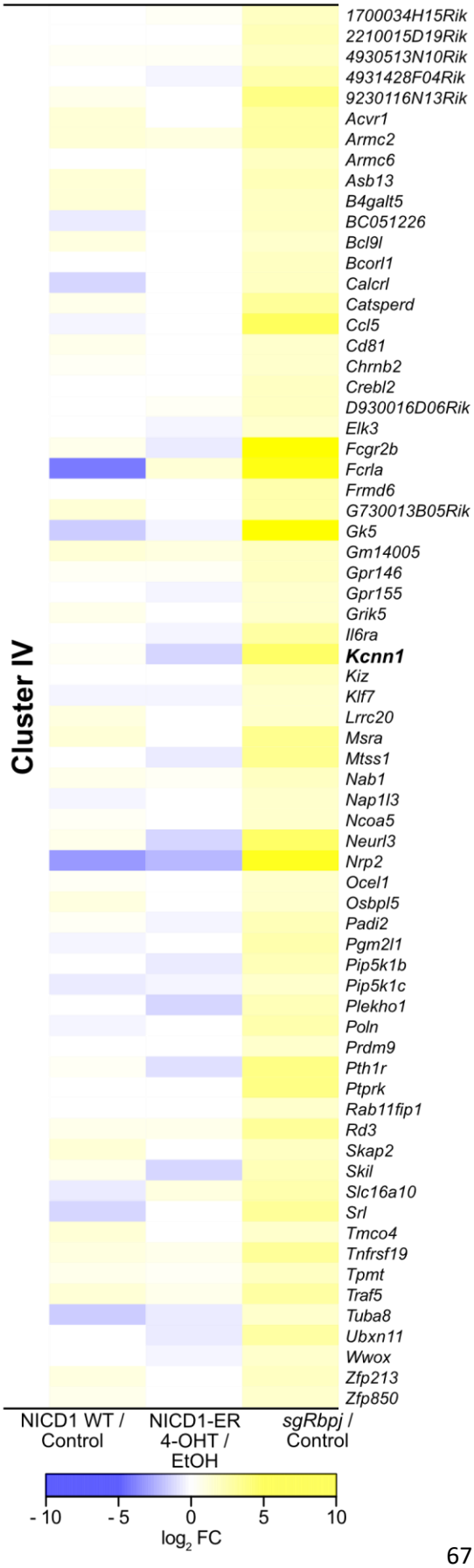
Cluster IV
1700034H15Rik
2210015D19Rik
4930513N10Rik
4931428F04Rik
9230116N13Rik
Acvr1
Armc2
Armc6
Asb13
B4galt5
BC051226
Bcl9l
Bcorl1
Calcrl
Catsperd
Ccl5
Cd81
Chrnb2
Crebl2
D930016D06Rik
Elk3
Fcgr2b
Fcrla
Frmd6
G730013B05Rik
Gk5
Gm14005
Gpr146
Gpr155
Grik5
Il6ra
Kcnn1
Kiz
Klf7
Lrrc20
Msra
Mtss1
Nab1
Nap1l3
Ncoa5
Neurl3
Nrp2
Ocel1
Osbpl5
Padi2
Pgm2l1
Pip5k1b
Pip5k1c
Plekho1
Poln
Prdm9
Pth1r
Ptprk
Rab11fip1
Rd3
Skap2
Skil
Slc16a10
Srl
Tmco4
Tnfrsf19
Tpmt
Traf5
Tuba8
Ubxn11
Wwox
Zfp213
Zfp850
NICD1 WT / Control
NICD1-ER 4-OHT / EtOH
sgRbpj / Control
- 10
- 5
0
5
10
log2 FC

**Figure 17) Four distinct clusters of RBPJ-Notch target genes in MT cells.** Heat map depicting significantly upregulated ($log_2$ FC > 1 and adjusted p-value < 0.05) genes upon 24 h of NICD1-ER or constant expression of NICD1 WT or depletion of RBPJ that are associated with a RBPJ site in MT cells overexpressing BioNICD1 WT or control cells. Heatmap is clustered as followed: I = sig. upregulated in BioNICD1 WT & 24 h of NICD1-ER & RBPJ-depletion, II = sig. upregulated in BioNICD1 WT & RBPJ-depletion, III = sig. upregulated in BioNICD1 WT & 24 h of NICD1-ER, IV = sig. upregulated in RBPJ-depletion.

#### 3.1.6.1. Clusters of target genes represent different genomic features

The previous analysis of histone modifications (Fig. 10) indicated that the vast majority of all RBPJ binding sites were located in promoter regions, as they were strongly enriched for the promoter mark H3K4me3. In order to validate this finding, I analyzed the genomic features associated with RBPJ binding sites. In simple terms, I tested at which previously annotated regions of the genome (e.g. promoter, intronic regions) the RBPJ binding sites were located. Next, I tested whether the RBPJ binding sites associated with the genes from the four clusters show any differences that could explain their distinct transcriptional responses.

As expected by the histone modifications, annotation of RBPJ binding sites showed that the majority (~70%) of RBPJ binding sites were indeed located at promoter regions (Fig. 18). In contrast to this, the RBPJ binding sites associated with the genes from the different clusters were located at promoter regions to a much lesser extent (Fig. 18A). Instead, they were more associated with intronic and intergenic regions. Clusters I and II showed a very similar distribution of genomic features associated with their respective RBPJ-binding sites. Cluster III, which consisted of genes unresponsive to RBPJ-depletion, was highly associated with introns and intergenic regions. This showed that these sites compiled a much higher fraction of enhancers compared to the promoter regions of the other clusters. This finding suggested that RBPJ bound enhancer sites may be less depended on RBPJ-mediated repression. Cluster IV included the highest fraction of promoter sites compared to RBPJ sites from the other clusters. These observations highlighted that the identified clusters have differences in the associated genomic features that could contribute to their distinct transcriptional response upon Notch activation and RBPJ-depletion.

To validate the findings of the different genomic feature associated with RBPJ binding sites, I used the previously analyzed ATAC-seq data and ChIP-seq data for H3K27ac, H3K4me1 and H3K4me3 from control MT cells. These features were used to study the chromatin landscape in the context of RBPJ binding sites associated with the four different clusters.

Using the well-established chromHMM tool, which is capable of identifying different chromatin states based on the combinatory presence of histone marks, I was able to generate a four-state chromatin landscape model (Fig. 18B). In this model, state 1 represented active enhancers, characterized by high levels of H3K4me3, H3K27ac and accessibility but only weak levels of H3K4me1. State 2 lacked any of level of accessibility or the aforementioned histone modifications, indicating gene and enhancer-free regions. State 3 had the same features as state 1 but was more enriched in H3K4me1. This indicated active enhancer regions. State 4 represented poised enhancers, characterized by high levels of H3K4me1, but weak accessibility and minor levels of H3K27ac. Taken together, the generated chromatin states reflected the expected combination of histone modifications associated with the distinct genomic features (promoter, active and poised enhancer).

First of all, the state 2 (gene and enhancer-free) was only weakly enriched at cluster I & IV and nearly not detectable for cluster II & III, indicating that RBPJ sites were mainly located at regulatory regions. As expected by the analysis of the genomic features, the RBPJ binding sites associated with genes from cluster III were more enriched for state 4 (poised enhancers) and less enriched for state 1 (active promoter) compared to the sites from the other clusters in control MT cells. This further validated them as enhancers, which potentially become active upon Notch signaling. In line with the genomic features, sites from cluster IV were the most enriched for state 1 (active promoter) and less enriched for state 2 (active enhancer) or 3 (poised enhancers). This suggested that even when RBPJ acts as a repressor, these genes remain in an overall active chromatin conformation located mainly located at promoters.

In summary, RBPJ sites overall were strongly associated with promoter regions. In contrast to this, RBPJ sites from the genes of the four clusters were much less associated with promoter regions. RBPJ binding sites from all clusters were associated with the active chromatin states 1 and 3. RBPJ sites from cluster III genes were least associated with promoter regions, but more strongly associated with introns and intergenic regions, which was reflected by the enrichment of the poised enhancer chromatin state. Finally, the chromatin states generated reflected the known combinations of histone modifications and were able to further support the identified genomic features at RBPJ sites.

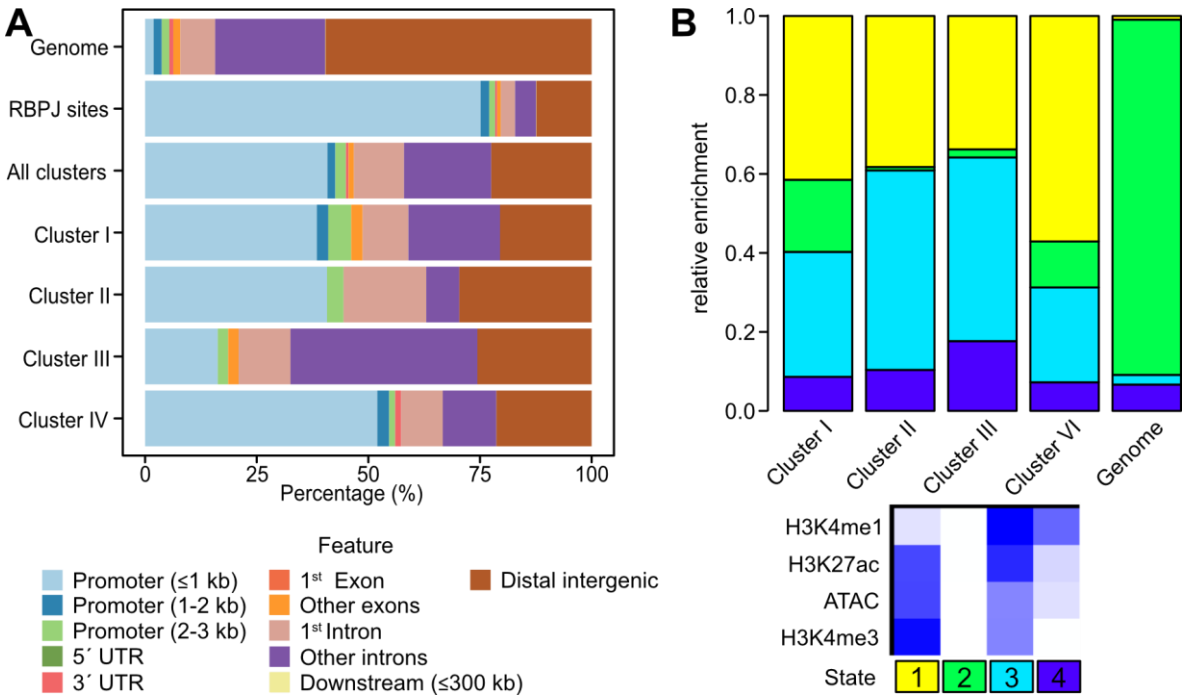


**Figure 18) Cluster of RBPJ binding sites represent different genomic features.** A) Stacked bar plots depicting the genomic features associated with all RBPJ sites or the individual sites from each cluster. B) Stacked bar plot showing the different chromatin states identified by chromHMM associated with the RBPJ binding clusters. Heat map describing the different chromatin states, which were identified based on H3K4me1, H3K4me3, H3K27ac and ATAC-seq.

### 3.1.6.2. Clusters of target genes have distinct functions

The previous chapters highlighted the different transcriptional responses of the four clusters and the different chromatin states at the RBPJ sites associated with the genes of the clusters. However, the actual function of the genes in the different clusters and whether they represent distinct biological functions remained to be investigated.

To this end, I first focused on the genes of cluster I and II because their transcriptional response and binding location were comparable. The main difference was a much weaker response after 24 h of Notch activation. This suggested that these genes may need to be exposed to NICD1 for a longer period of time to be activated compared to cluster I genes. To test this, I analyzed a time-course experiment upon Notch activation. This examined early time points (4 & 8 h) of Notch activation using the same tamoxifen inducible system as it was used for 24 h.

The genes of cluster I and III were already strongly upregulated upon 4 h and even more so after 8 and 24 h of Notch induction. In contrast to this, genes of cluster II showed no expression change upon 4 h of Notch induction. A slight upregulation was detectable after 8 h and a stronger upregulation after 24 h. As expected, genes of cluster IV showed no regulation throughout time-course experiment (Fig. 19, Suppl. Table S4). These results were validated using RT-qPCR (Friedrich et al. 2022).

In summary, genes of cluster I and III responded directly to the induction of the Notch signaling, whereas genes of cluster II needed more time to respond. This suggested that there were early (cluster I & III) and late (cluster II) response genes.

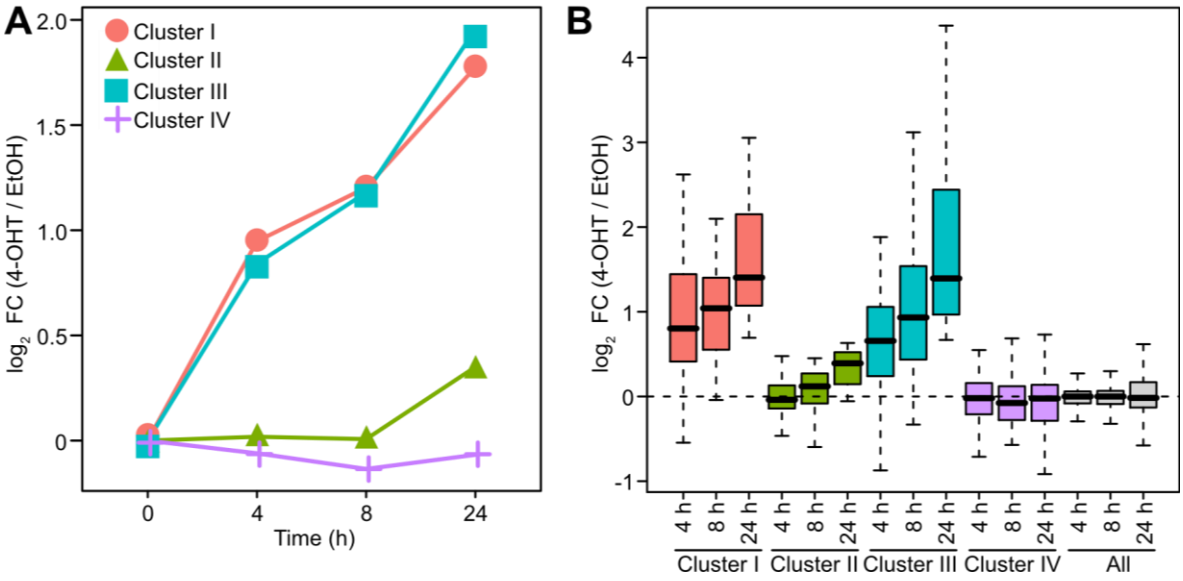


**Figure 19) Genes from RBPJ clusters have different response times upon Notch activation.** A) Line plot depicting different timepoints of the transcriptional response of genes from the different clusters upon NICD1-ER activation. Dots represents the mean $log_2$ FC. B) Box plot quantifying the gene expression changes of the different clusters or all genes upon different time points after NICD1-ER treatment.

After the identification of potential early and late responsive genes, I aimed to elucidate the biological functions of the genes. To this end, I used an ORA with the GO database "Biological Processes" to analyze whether the genes within the four clusters were associated with distinct biological functions.

Genes of cluster I were associated for terms related to development (Fig. 20, Suppl. Table S7). Cluster II genes were enriched for genes associated with inflammatory and cytokine response. In contrast, cluster III were enriched for genes related to T-cell and immune system processes system. The genes of cluster IV were enriched for genes associated with B-cell proliferation and response to growth factor beta. Surprisingly, none individual clusters were significantly enriched for genes from the term “Notch pathway”.

In summary, this indicated that the different clusters not only represented different regulatory mechanims and features, but were also associated with distinct bioloigcal functions.

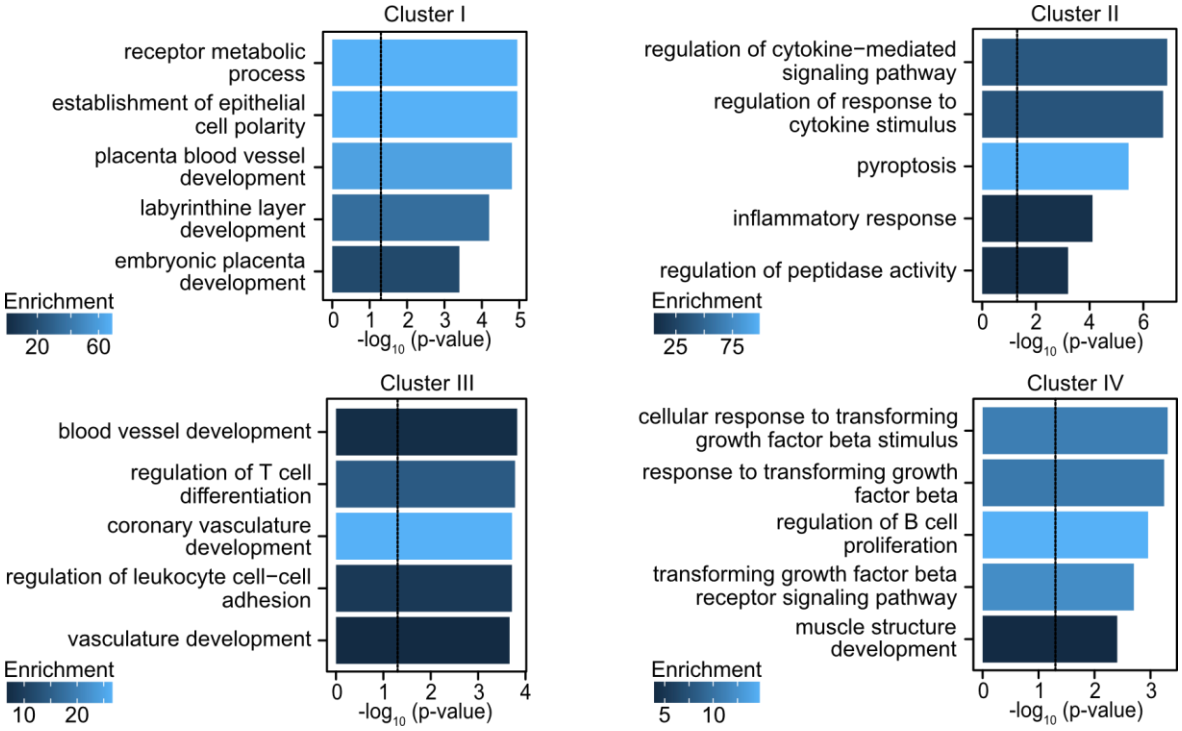


**Figure 20) Different pathways are associated with the four clusters.** Bar plots showing the top five significantly overrepresented pathways from the GO “Biological Processes” database for the genes from the four clusters. Dashed line marking the p-value of 0.05.

### 3.1.6.3. Clusters of target genes are conserved in other cellular systems

In the previous chapters, the four clusters of RBPJ-Notch target genes were characterized in terms of their associated genomic features and potential biological functions. However, the biological mechanism remained unclear. One possible regulatory mechanism could

include the function of the histone variant H2A.Z. A previous publication from our group highlighted that RBPJ and the H2A-Z-chaperone interact and that H2A.Z acts as repressor of Notch target genes in MT cells (Giaimo et al. 2018). Consequently, I focused on the function of histone variant H2A.Z on the genes of the four clusters. To test whether the RBPJ repressed genes (clusters I, II & IV) but not the genes from cluster III (which respond only to Notch) are regulated by H2A.Z, I analyzed RNA-seq data upon H2A.Z depletion.

Only genes from cluster I, II and IV were significantly upregulated upon depletion of H2A.Z, whereas cluster III was not affected (Fig. 21A, Suppl. Table S4). This suggested that not specifically all Notch target genes are activated by depletion of H2A.Z in MT cells but rather RBPJ-repressed genes.

To test whether these four clusters are specific for MT cells or whether they are conserved in other cell types, I analyzed several publicly available RNA-seq data sets. These data sets included T-cell acute lymphoblastic leukemia cells (T-ALL) called T6E and small cell lung cancer (SCLC) called KP1 upon NICD1 overexpression. Both cell lines showed a weak but significant activation of genes from cluster I and III (Fig. 21B & C). This was consistent with the results from MT cells, where clusters I and III also showed the strongest increase in transcription upon Notch activation.

In addition, I analyzed data from primary T-cells (Phase 1: DN1 & DN2a stages and phase 2: DN2b & DN3 stages) that were depleted for both *Notch1* and *Notch2*. Especially, the phase I T-cells showed a strongly reduced transcription of the Notch-depended clusters I and III (Fig. 21D). Phase II T-cells showed a weaker but still significant reduced transcription of cluster I and II genes (Fig. 21E). Of note, phase I T-cells have higher levels of Notch1 compared to phase II T-cells (Romero-Wolf et al. 2020). Taken together, these data suggested that genes from the specific clusters and their responses were at least partially conservation in other cellular systems.

In summary, I was able to identify H2A.Z-dependent repression of genes that are actively repressed by RBPJ in MT cells. This supported a previous publication of our group, which highlighted interaction of the H2A.Z-chaperone and RBPJ in MT cells. Stunningly, the genes from the four clusters identified in MT cells were partially regulated in T-ALL, SCLC and primary T-cells. The perturbation of the Notch pathway by either overexpression of the NICD1 or depletion of *Notch1* and *Notch2* affected mainly the genes from the Notch responsive clusters I, II and III.

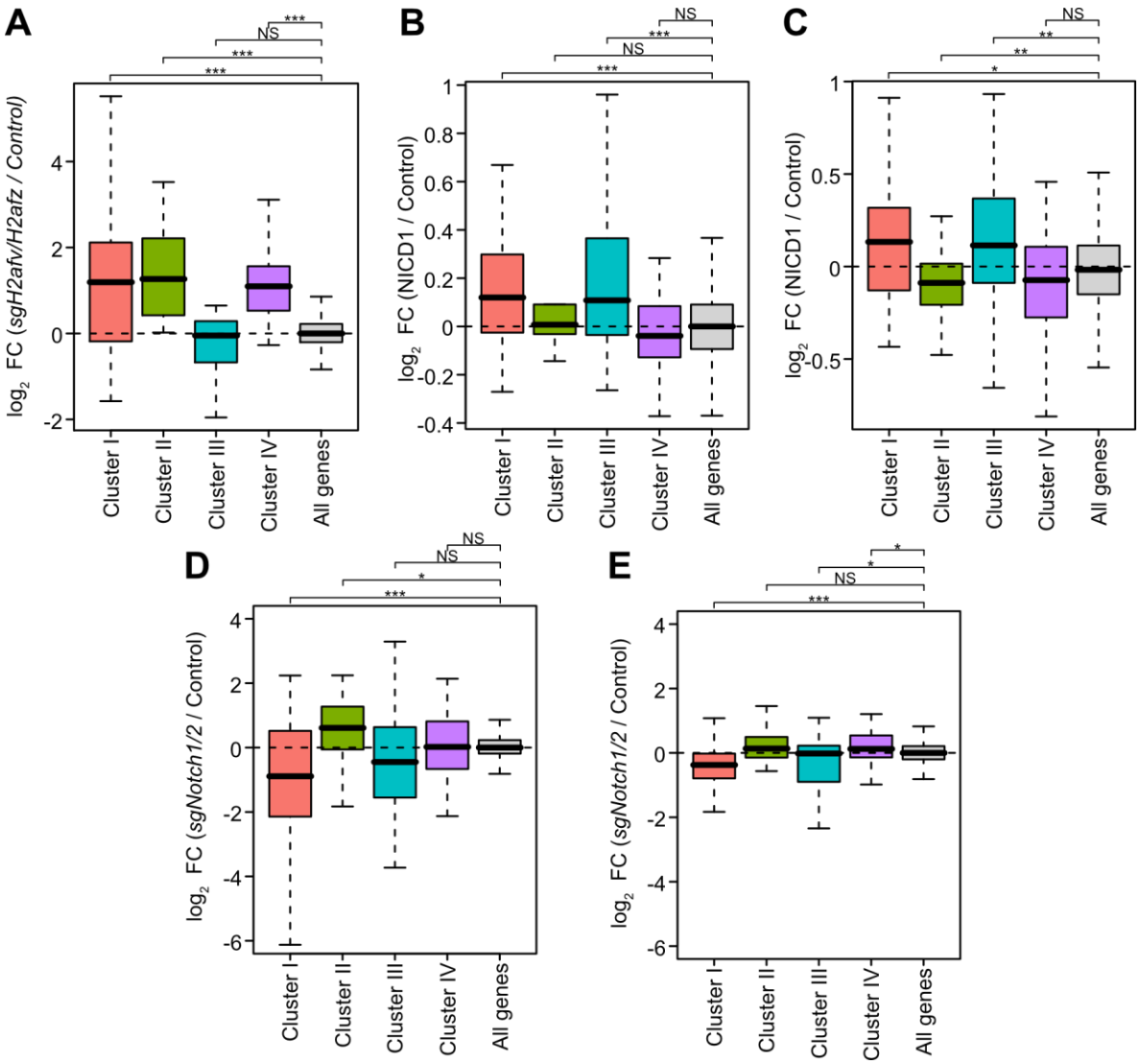


**Figure 21) A comparable transcriptional response of genes from the four RBPJ-Notch-depended clusters is conserved in different cell types.** A) Box plot showing the gene expression changes from genes of the four clusters upon H2A.Z depletion in MT cells. B & C) Box plots depicting the transcriptional effects of the genes from the four clusters upon NICD1 overexpression in B) T6E cells and C) KP1 cells. D & E) Box plots of the gene expression changes of the genes from the four clusters upon depletion of *Notch1* and *Notch2* in D) phase I and E) phase II primary T-cells. [***] $p < 0.001$, [**] $p < 0.01$, [*] $p < 0.5$, [NS] $p > 0.05$; Wilcoxon rank sum test. Data was analyzed by RNA-seq. Data availability: primary T-cells (GSE148441), T6E (GSE97465) and KP1 (GSE69091).

# Chapter II: Predicting dynamic RBPJ binding sites

### 3.2.1. Identification of dynamic RBPJ binding

Previous publications highlighted two different binding behaviors of the TF RBPJ upon changes in the activation state of the Notch pathway. For one set of sites the binding was unaffected (static), while the other sites showed a significantly increased binding (dynamic) in the context of active Notch signaling (Krejčí and Bray 2007; Castel et al. 2013; Wang et al. 2014).

First, I aimed to identify RBPJ binding in a mouse progenitor T-cell line called Beko by analyzing ChIP-seq data. Beko cells are characterized by a constitutive active Notch pathway and are sensitive to gamma secretase inhibitor (GSI), which leads to an inactivation of the Notch pathway (Ferrante et al. 2020). In control Beko cells (DMSO treatment), 3538 RBPJ binding sites were detected as real sites by the MSPC tool (Fig. 22A & B, Appendix Fig. 4, Suppl. Table S9). This number was comparable with the 3757 RBPJ binding sites that were identified in MT cells with an active Notch signaling (Chapter I). To identify different binding behaviors of RBPJ, I compared the RBPJ binding strength to Beko cells with an inactivated Notch pathway by 24 h GSI treatment. The vast majority of sites (3380) where unaffected by the treatment, but a small fraction (158) showed reduced ($log_2$ FC < -0.5) RBPJ binding upon GSI. These sites were designated as dynamic sites and static sites, respectively. Both binding patterns were validated by ChIP-qPCR in control or GSI treated Beko cells (Fig. 22F).

In order to validate static and dynamic binding behavior using additional approaches, I tested both groups upon apicidin treatment and under hypoxic conditions (hypoxia). Both apicidin (HDAC inhibitor) and hypoxic conditions were shown to inactivate the Notch pathway by destabilizing the NICD1 protein (Ferrante et al. 2020; Ferrante et al. 2022) and should therefore reveal dynamic or static binding behavior, comparable to GSI treatment. Consistent with the described functions of both treatments, apicidin (vs. DMSO) and hypoxic conditions (vs. normoxic conditions) resulted in significantly reduced RBPJ binding at dynamic sites, whereas static sites remained unaffected (Fig. 22B - E, Appendix Fig. 4).

In summary, I was able to identify the two different binding behaviors (dynamic and static) of TF RBPJ upon inactivation of the Notch pathway using GSI in Beko cells. Furthermore, both groups could be validated with additional approaches (hypoxia or apicidin).

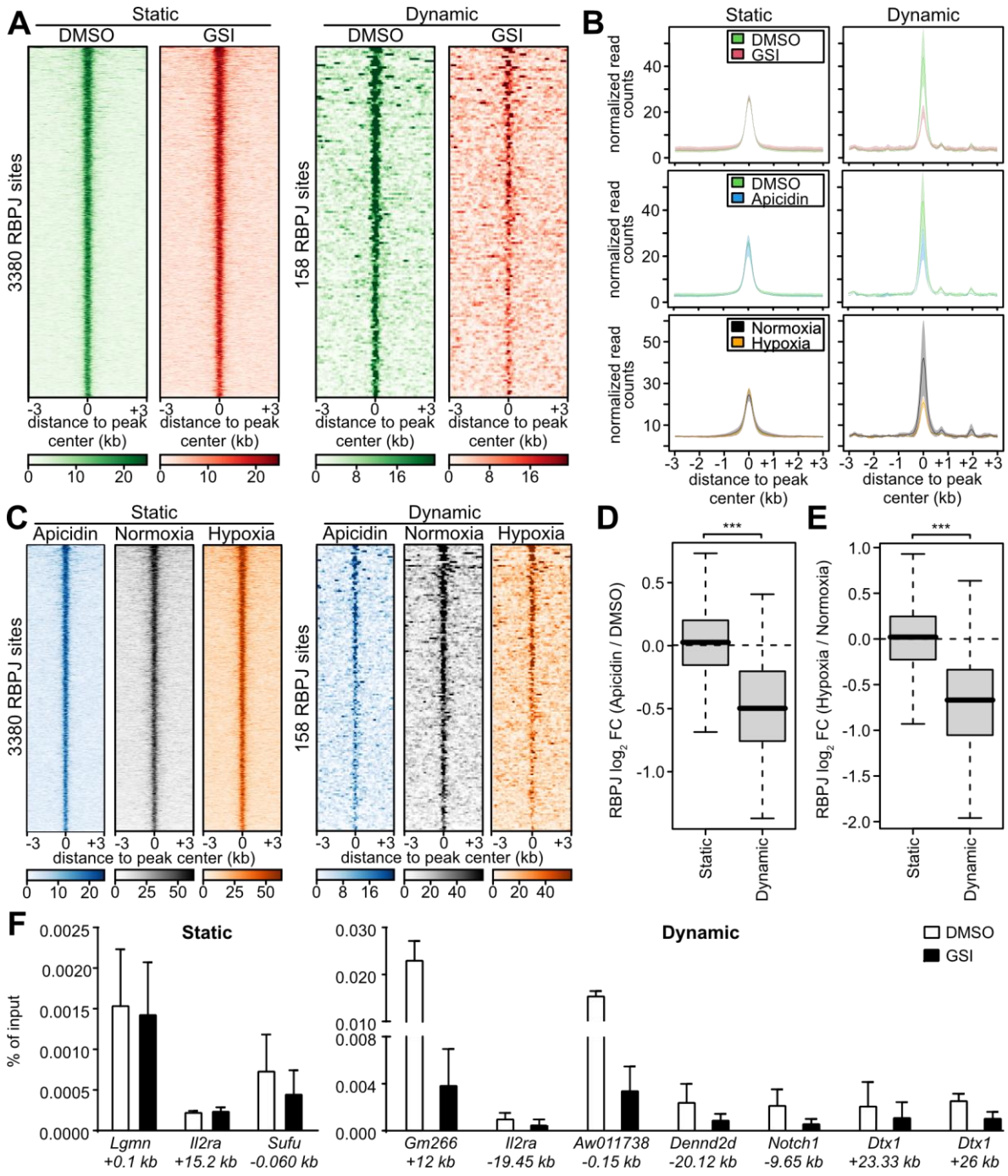


**Figure 22) Identification of dynamic RBPJ binding in Beko cells.** A) Heat map depicting 3380 static ($log_2$ FC > -0.5) and 158 dynamic ($log_2$ FC < -0.5) RBPJ binding sites in DMSO (green) or GSI (red) treated Beko cells. B) Line plot quantifying the average static and dynamic RBPJ binding sites in GSI / DMSO (upper), Apicidin / DMSO (middle) and hypoxia / normoxia (lower). Outline representing the standard deviation of the replicates. C) Heat map showing static and dynamic RBPJ binding sites in Apicidin (blue), hypoxia (orange) and normoxia (grey). D & E) Box plot quantifying the RBPJ binding changes upon D) Apicidin vs DMSO or E) hypoxia vs normoxia. F) Bar plots showing qPCR validation of static or dynamic RBPJ binding sites. qPCR validation was performed by Dr. Benedetto Daniele Giaimo. [***] p < 0.001; Wilcoxon rank sum test.

### 3.2.2. Characterization of dynamic RBPJ binding sites

After identifying dynamic and static RBPJ binding sites in Beko cells, I aimed to characterize the differences between the two groups. The two previous publications that focused on the identification of dynamic RBPJ binding sites identified common features, such as their location at enhancers or stronger enrichment of H3K27ac. However, they also showed some strong discrepancies in terms of the total number of RBPJ binding sites, the proportion of static versus dynamic sites or the overall location of RBPJ sites (Castel et al. 2013; Wang et al. 2014). This demonstrated the complexity of the understanding dynamic and static RBPJ sites. As a starting point for characterizing both groups in Beko cells, I analyzed of RBPJ binding sites themselves, their location and associated motifs.

First, I first examined RBPJ binding strength at dynamic or static sites in control Beko cells with an active Notch signaling (DMSO or normoxia). The dynamic sites showed overall a significantly stronger RBPJ binding compared with static sites (Fig. 22B). The RBPJ binding strength was comparable in Beko cells with an inactive Notch pathway (GSI, apicidin or hypoxia). This indicated a base level of RBPJ binding independent on the Notch pathway activity that increases specific at dynamic sites with active Notch signaling. This was in contrast to a previous publication that showed a comparable level of RBPJ binding with active Notch signaling and only a lower level upon Notch inhibition (Castel et al. 2013).

To examine which DNA-binding motifs were enriched at dynamic and static sites and whether these identified motifs differ between both groups, a *de novo* motif discovery was performed. The most frequently found motif differs between both groups (Fig. 23A, Suppl. Table S10). As expected for RBPJ binding sites, ~81% of the dynamic sites carried the RBPJ motif. In addition, ~18% of RBPJ sites contained the SP1 motif, which is typically enriched at promoter regions (Hasegawa and Struhl 2021) and has been previously found at RBPJ sites in MT cells (Chapter I). Contrary to this, for static sites the SP1 motif was found at ~60% of the sites, while RBPJ was only identified at ~17%. Interestingly, RBPJ motifs identified at static and dynamic sites differed slightly. The static sites were enriched for the canonical RBPJ motif “TGGGAA”. In contrast to this, the RBPJ motif identified at dynamic sites exhibited a relatively lower conservation of the middle “G”, but both purine bases were equally abundant (TGRGAA).

The differences in the occurrence of SP1 binding motifs already indicated a potential difference with respect to the location of dynamic and static RBPJ binding sites. Indeed, analysis of genomic features associated with dynamic and static RBPJ binding sites

revealed that most static sites were located at promoter regions. In contrast, dynamic sites were associated with promoter regions to a much lesser extent but were more frequently found at intronic and intergenic regions (Fig. 23B).

In summary, dynamic binding sites exhibited stronger RBPJ binding in the context of an active Notch signaling pathway, whereas binding remained comparable between the two groups with inhibited Notch signaling. Moreover, static sites mainly represented promoter regions with relatively low enrichment of the RBPJ binding motif, whereas dynamic sites were mainly localized outside of the promoter context and contained the RBPJ motif more frequently than their static counterparts.

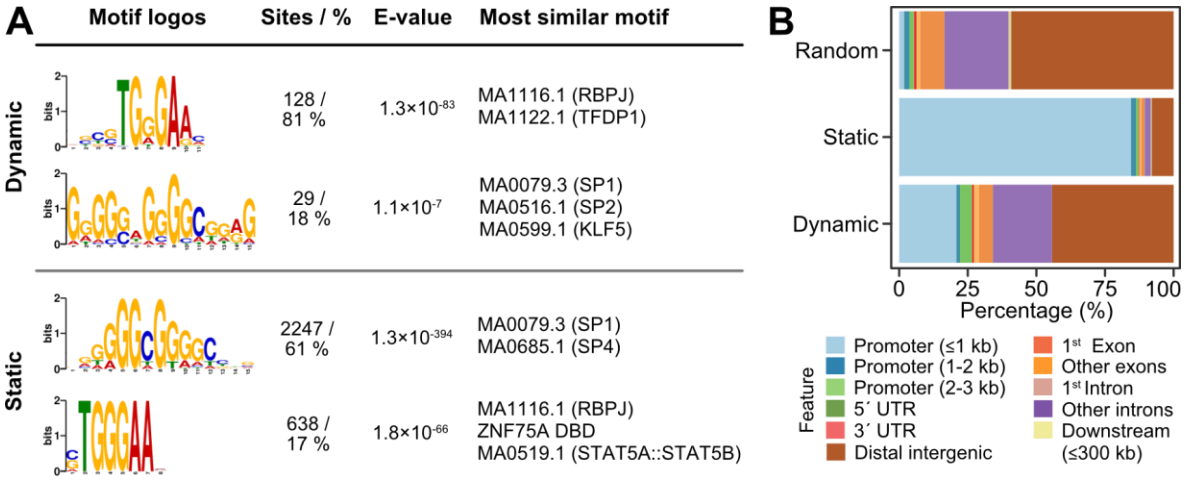


**Figure 23) Dynamic sites are not located at promoter regions.** A) Table showing the top enriched DNA binding motifs for static and dynamic RBPJ binding sites in Beko cells. B) Stacked bar plot depicting the genomic features associated with static and dynamic RBPJ binding sites.

### 3.2.3. Dynamic and static RBPJ sites are associated with a distinct chromatin state

Previous studies indicated distinct chromatin states at static and dynamic RBPJ sites by analyzing the distribution of histone modifications H3K27ac (active chromatin), H3K4me3 (promoter) and H3K4me1 (enhancer) in the vicinity of RBPJ sites (Castel et al. 2013). In order to characterize the chromatin state adjacent to static and dynamic RBPJ binding sites in Beko cells, I analyzed ATAC-seq and ChIP-seq data for the histone modifications H3K27ac, H3K4me1, H4Kme3, H3K18ac and H3K9ac.

Using ATAC-seq, I identified that both groups were strongly associated with open chromatin regions, but overall accessibility was higher in the vicinity of static sites, as compared to dynamic sites (Fig. 24A). In addition, both groups of RBPJ sites were strongly enriched for active chromatin marks H3K27ac and H3K18ac compared with the average H3K27ac and H3K18ac site, respectively. Both static and dynamic sites were comparably enriched for both marks (Fig. 24B & C). To confirm the previous observation that static sites were mainly at promoter regions, while dynamic sites are often located outside of promoter regions, I analyzed H3K4me1, which is characteristic for enhancer regions but absent directly at promoters. As expected, H3K4me1 was highly enriched at dynamic sites, whereas static sites had below average level compared to all H3K4me1 sites (Fig. 24D). In contrast to this, H3K4me3 a marker for promoter regions, was highly enriched at static sites, whereas dynamic sites showed only weak enrichment (Fig. 24E). H3K9ac has been described to co-localized with H3K4me3 at promoter regions (Igolkina et al. 2019). Accordingly, the H3K9ac mirrored the distribution of H3K4me3 (Fig. 24F).

Taken together, static and dynamic RBPJ binding sites in Beko represented a distinct chromatin state. As expected from the previous chapter, static sites were highly enriched for histone modifications found at promoter regions, while dynamic sites were enriched for enhancer marks. Both groups revealed high levels of accessibly and histone modification binding, indicating RBPJ sites at strong and active regulatory regions.

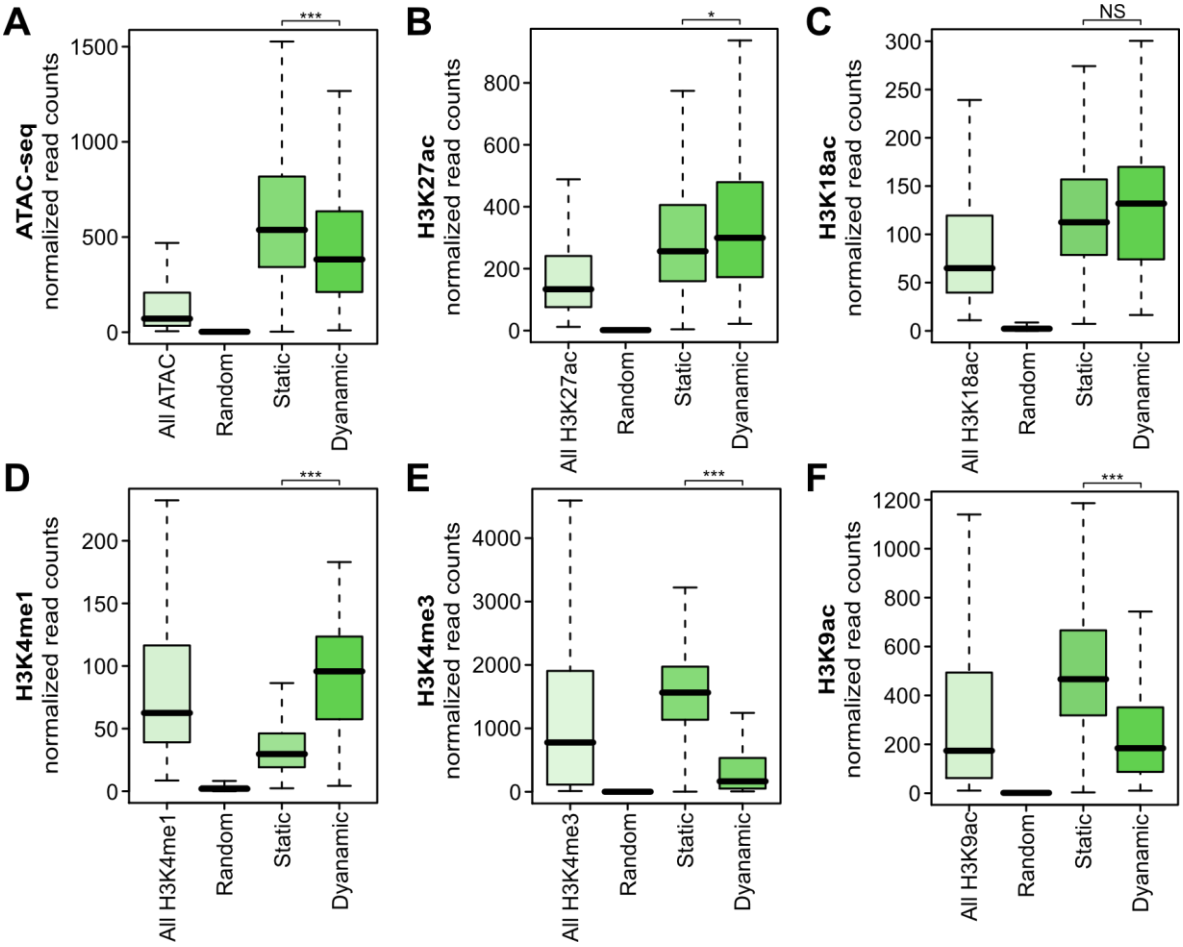


**Figure 24) Chromatin landscape at static vs dynamic RBPJ sites.** A - F) Box plot depicting enrichment of A) chromatin accessibility, B) H3K27ac, C) H3K18ac, D) H3K4me1, E) H3K4me3 and F) H3K9ac at all identified sites of the given mark, random genomic regions, at static RBPJ sites and at dynamic RBPJ binding sites. Chromatin accessibility was measured by ATAC-seq, histone modification enrichment by ChIP-seq. [***] $p < 0.001$, [**] $p < 0.01$, [*] $p < 0.5$, [NS] $p > 0.05$; Wilcoxon rank sum test.

CpG islands are rarely methylated and often found located in the proximity of promoter regions. In contrast, symmetrical CpG dinucleotides, which are not within CpG island are often methylated (Ehrlich et al. 1982; Bird et al. 1985). To test, whether dynamic or static RBPJ binding sites were preferentially or at least partially associated with CpG islands, I analyzed published mouse CpG islands (University of California, Santa Cruz).

As expected by the strong association with promoter sites, a large fraction of RBPJ binding sites (82%) overlapped with known CpG island from the mouse genome (Fig. 25A). To further understand the association of CpG islands and RBPJ binding, I first focused on the

location of CpG islands in general. As expected from the literature, many promoter sites were associated with CpG islands (Saxonov et al. 2006). When testing the promoters enriched for a H3K4me3 signal, the fraction of overlap with CpG islands was even larger (~80%). Consistent with this, static sites, which mainly represent promoters associated with strong enrichment of H3K4me3, showed a comparable overlap with CpG island as the group of H3K4me3-positive promoters (Fig. 25B). In contrast to this, dynamic sites showed only a weak association with CpG islands.

Previous studies identified a dimeric RBPJ complex that has a much higher DNA binding affinity compared to a single RBPJ protein. This complex has been shown to regulate the transcriptional response of Notch target genes. These complexes rely on two RBPJ binding sites in head-to-head (H2H) orientation with a spacing of 15-17 bp (Nam et al. 2007; Liu et al. 2010).

To test if these H2H motifs occur at RBPJ binding sites in Beko and to analyze whether they might contribute to the dynamic and static binding behavior, I investigated the appearance of these H2H motifs within both groups. Since the previous analysis of the RBPJ motif revealed slight variations, I reduced the stringency for the motif identification. To this end, I allowed for either one mismatch (MM) or two mismatches within the two RBPJ binding motifs. Regardless of whether one or two MM were considered, the fraction of RBPJ binding sites with H2H motifs was much higher within dynamic sites (Fig. 25C). With one MM it was about five times higher at dynamic sites; with two MM, it was still four times higher.

In summary, static RBPJ binding sites were stronger associated with CpG islands, further confirming their location at promoter sites. In contrast, dynamic RBPJ binding sites had a much higher occurrence of the dimeric head-to-head RBPJ binding motif, which has been shown to be important for the transcriptional regulation of Notch target genes (Liu et al. 2010).

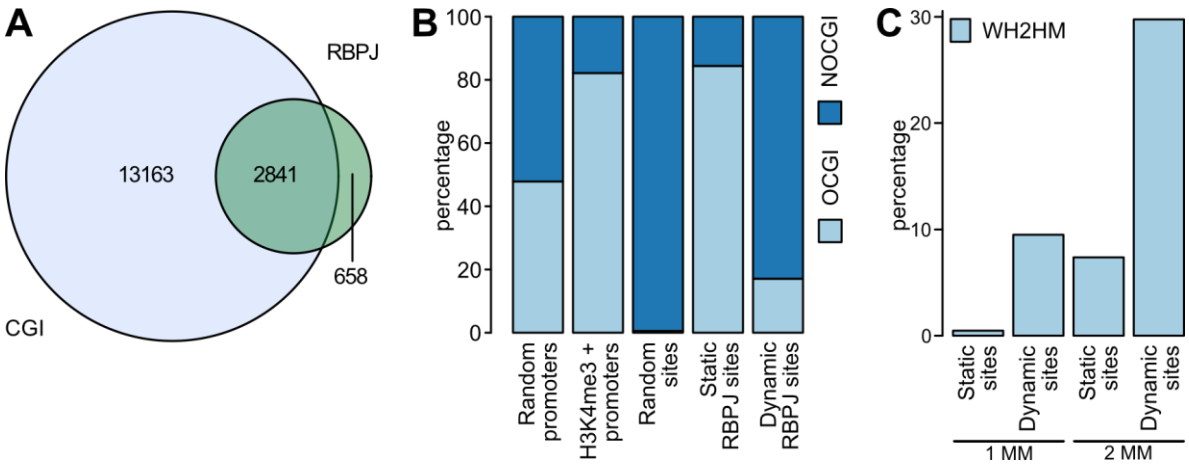


**Figure 25) RBPJ binding sites are associated with CpG island and dimeric RBPJ binding motifs.** A) Venn diagram showing the overlap of known mm9 CpG islands and identified RBPJ binding sites in Beko cells. B) Stacked bar plot depicting the percentage of random promoters, H3K4me3-positive promoters, random sites, static and dynamic RBPJ sites with known CpG islands. NOCGI = not overlapping with CpG island; OCGI = overlapping with CpG island. C) Bar plot showing the percentage of static or dynamic RBPJ binding sites with the dimeric head-to-head RBPJ binding motif, either allowing one mismatch (1MM) or two mismatches (2MM) within the two motifs. WH2HM = with head-to-head RBPJ motif.

### 3.2.4. Inhibition of Notch leads to chromatin changes exclusively at dynamic sites

The characterization of dynamic and static RBPJ sites revealed several differences between the two groups. In particular, it became evident, that the chromatin landscape at both classes differs considerably. The literature suggested that mainly dynamic RBPJ sites were associated with changes of the H3K27ac levels upon switches of the Notch pathway activity, whereas H3K4me1 and H3K4me3 remain unaffected (Castel et al. 2013). To understand the effects on the adjacent chromatin dependent on the Notch pathway activity beyond H3K27ac, I analyzed the changes of the previously described histone modifications and accessibility between compared control cells (Notch active) and GSI treated ones (Notch inactive).

Consistent with the changes of RBPJ binding, chromatin accessibility was reduced mainly at dynamic sites upon inactivation of the Notch signaling (Fig. 26A). Additionally, the active chromatin marks H3K27ac and H3K18ac were strongly reduced at dynamic sites compared to static ones upon GSI treatment (Fig. 26B & C). In line with the literature, the enhancer mark H3K4me1 was not affected by the GSI treatment at both dynamic and static sites (Fig.

26D). In contrast to the literature, the promoter mark H3K4me3, which was weakly associated with dynamic RBPJ sites, showed a reduced level of H3K4me3 at dynamic sites while static sites were overall unaffected upon inactivation of the Notch pathway (Fig. 26E). Noteworthy, Stunnenberg and colleagues found essentially no enrichment for H3K4me3 at either static or dynamic sites (Castel et al. 2013). Finally, H3K9ac that is known to co-localize with H3K4me3 showed a comparable behavior as H3K4me3 (Fig. 26F).

In summary, the chromatin landscape was most responsive to changes in Notch pathway activity at dynamically bound RBPJ sites, whereas chromatin adjacent static sites generally remained unaffected.

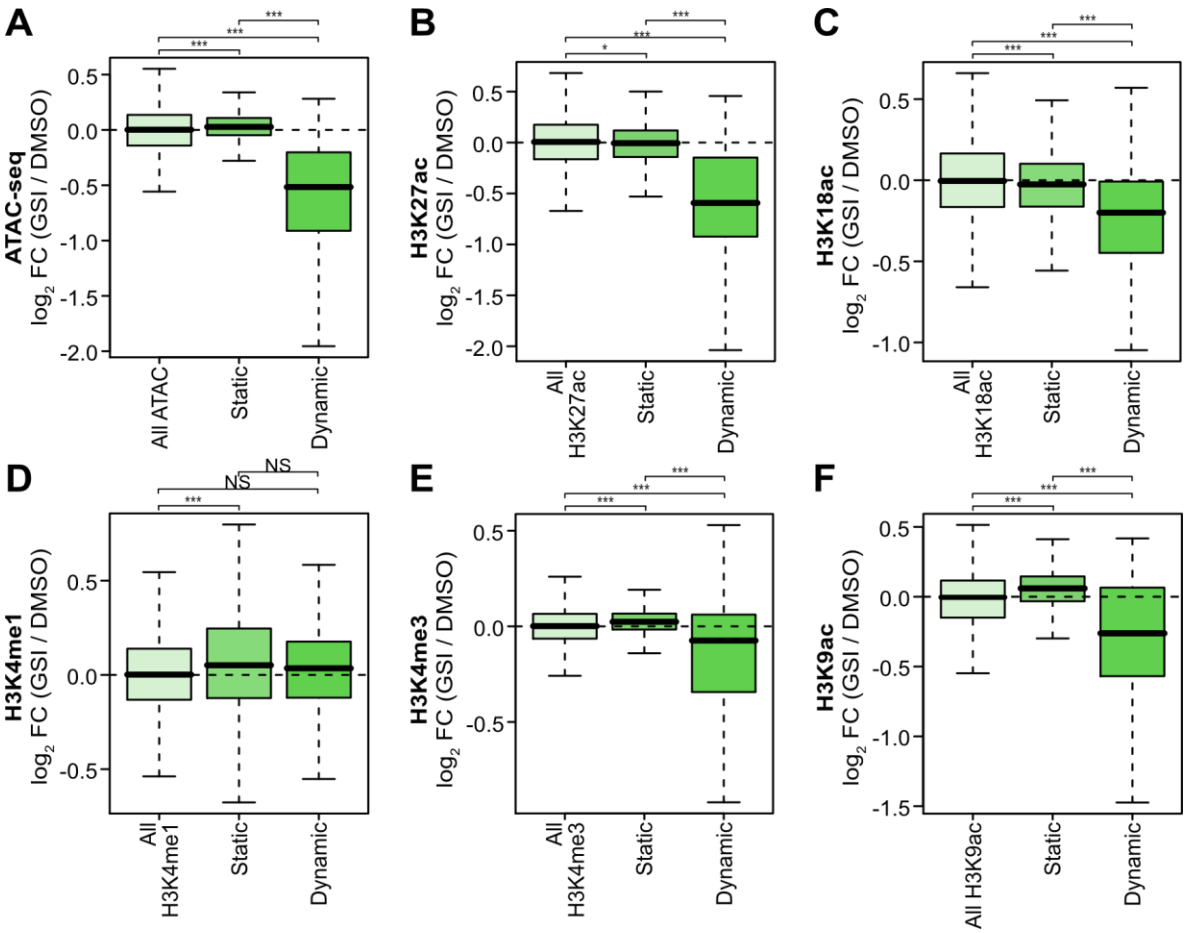


**Figure 26) Changes of the chromatin is mainly found at dynamic sites upon inactivating of the Notch pathway.** A - F) Box plot depicting the changes of A) chromatin accessibility, B) H3K27ac, C) H3K18ac, D) H3K4me1, E) H3K4me3 and F) H3K9ac upon Notch inactivation by GSI treatment at all identified sites of the given mark, at static RBPJ sites and at dynamic RBPJ binding sites. [***] $p < 0.001$, [*] $p < 0.05$, [NS] $p > 0.05$; Wilcoxon rank sum test.

### 3.2.4. CUT&Tag reflects dynamic and static binding behavior

In order to validate the previous findings, which are mainly based on ChIP-seq results, I analyzed CUT&Tag data. CUT&Tag has several described advantages compared to ChIP-seq. In addition to economic advantages, fewer cells required and a potentially optimized signal-to-noise ratio, CUT&Tag has a major biological benefit: it works with live cells or cell nuclei and does not depend on cross-linking with formaldehyde (Kaya-Okur et al. 2019), which is a potential source of experimental artefacts (Gavrilov et al. 2015).

Overall, ChIP-seq (18780 regions) and CUT&Tag (14313 regions) for H3K27ac resulted in comparable numbers of identified peaks (Fig. 27A). The majority of sites (11596) were detected commonly by both techniques. However, 7211 ChIP-seq and 2717 CUT&Tag specific regions were identified. To test whether these specific regions actually had no enrichment with the other technique (or alternatively were just slightly below the detection threshold), I compared all sites with both techniques. While the technique-specific signals were more enriched in the technique used to identify them, there was also weaker, but still detectable, enrichment for these sites in the other technique (Fig. 27A). This suggested that sites specifically identified by only one of the methods were nonetheless genuine H3K27ac signals.

After validating the quality and comparability of the CUT&Tag H3K27ac data, I analyzed the effects of the Notch inhibition on the H3K27ac levels at dynamic and static RBPJ sites using CUT&Tag data. Consistent with the ChIP-seq results, the enrichment of H3K27ac was stronger at both static and dynamic sites compared to the average H3K27ac sites (Fig. 27B). In addition, the enrichment of H3K27ac at dynamic sites was stronger compared to static sites. Finally, the response to Notch pathway inactivation by GSI was clearly detectable exclusively at dynamic sites (Fig. 27C).

In summary, CUT&Tag of H3K27ac yielded a comparable number of enriched sites as ChIP-seq. In addition, CUT&Tag confirmed the previous H3K27ac ChIP-seq results indicating differential binding and regulation of this histone mark particularly at dynamic RBPJ sites.

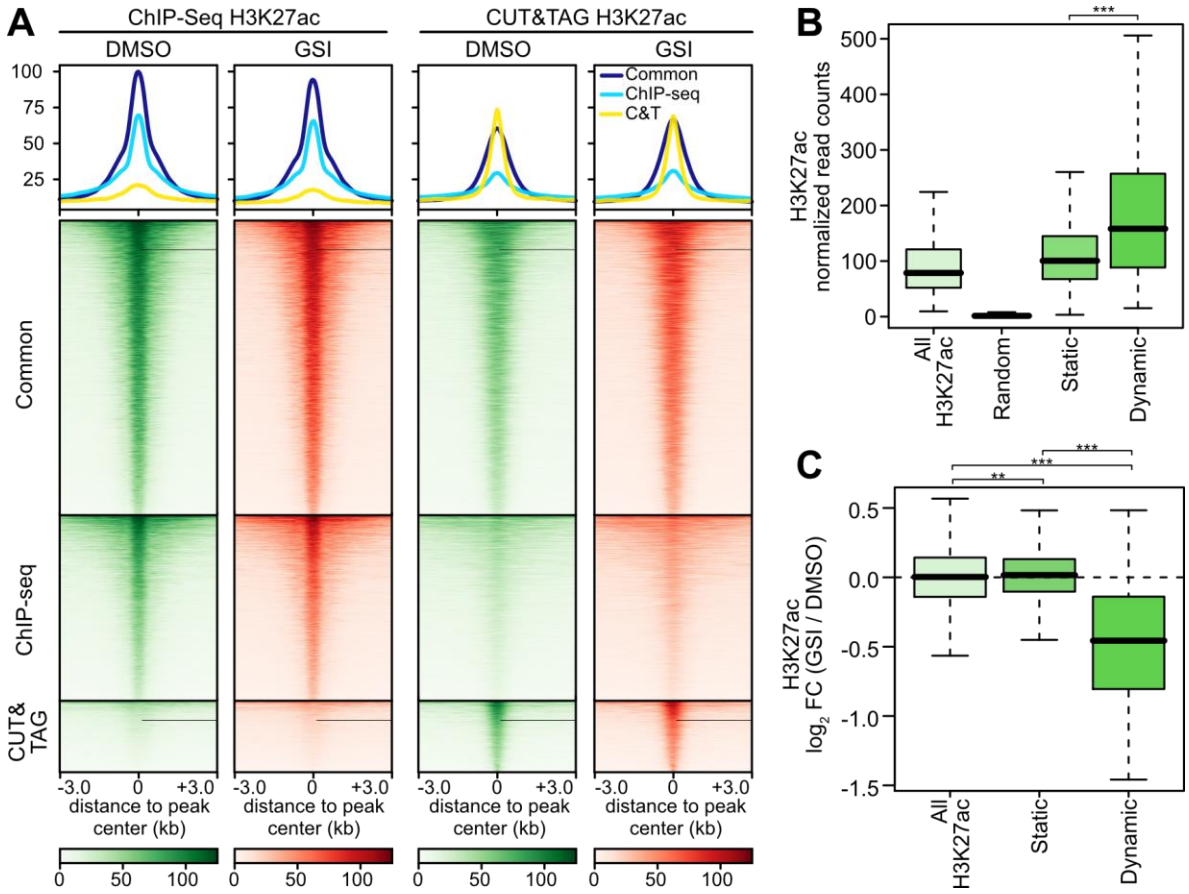


**Figure 27) CUT&Tag confirms dynamic RBPJ binding sites.** A) Heat map and average binding plot showing H3K27ac binding with ChIP-seq and CUT&Tag in Beko cells based on H3K27ac peaks that were identified commonly in ChIP-seq and CUT&Tag, only in ChIP-seq and only in CUT&Tag. B) Box plot depicting enrichment of H3K27ac at all identified H3K27ac sites, random genomic regions, at static RBPJ sites and at dynamic RBPJ binding sites. C) Box plot of the changes of H3K27ac upon Notch inactivation by GSI treatment at all identified H3K27ac sites, at static RBPJ sites and at dynamic RBPJ binding sites. H3K27ac was measured by CUT&Tag. [***] $p < 0.001$, [**] $p < 0.01$; Wilcoxon rank sum test.

### 3.2.5. Transcriptional Notch response is mainly associated with dynamic sites

The previous analysis revealed that chromatin dynamics mediated by the Notch response occur predominantly at dynamic sites. To test the transcriptional response of genes associated with static or dynamic RBPJ sites, I analyzed previous published RNA-seq data from control Beko cells or cells treated with GSI.

First, I examined the biological function of genes associated with either static or dynamic RBPJ sites. After annotating the RBPJ sites to their corresponding genes, an ORA was conducted to investigate whether these genes were associated with different known

biological pathways. For genes associated with dynamic sites, several Notch-associated terms from GO and KEGG databases were identified to be significantly enriched (Fig. 28A & C). Based on the KEGG database, the term “Th1 and Th2 cell differentiation” was significantly enriched. This was consistent with previous publications highlighting the important role of Notch signaling in T helper cell development (Dell'Aringa and Reinhardt 2018). In contrast to this, for genes associated with static sites, only one Notch associated term (“Notch receptor processing”) was identified to be overrepresented based on the GO database (Fig. 28B & D). Instead, several general terms were enriched, this included “DNA repair”, “mRNA processing”, “Histone modification”, “RNA splicing” and more (Suppl. Table S11).

Taken together, these data supported a model in which the typical and expected Notch response appears to be driven primarily by genes associated with dynamic RBPJ sites.

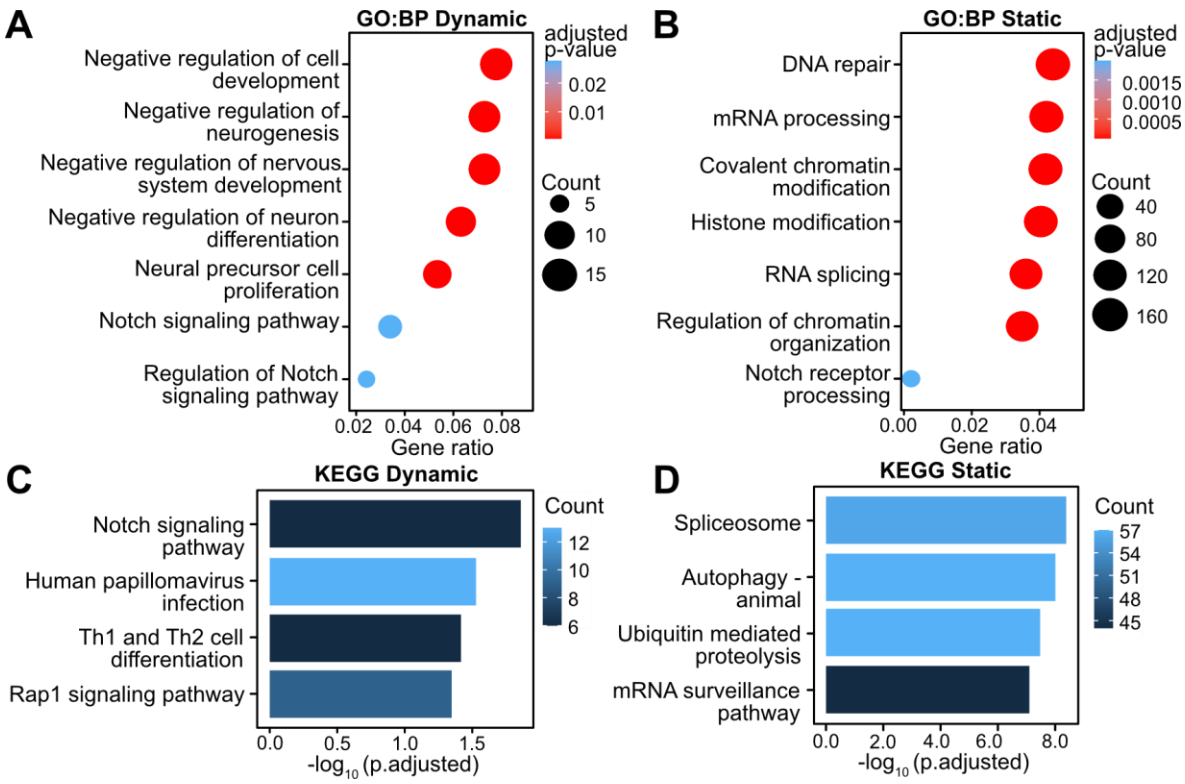


**Figure 28) Genes associated with dynamic RBPJ sites are enriched for Notch terms.** A & B) Dot plot showing terms statistically overrepresented within genes associated with A) dynamic or B) static RBPJ binding. Within the genes associated with dynamic sites multiple Notch associated terms were significantly enriched. ORA analysis was performed using the GO “Biological Process” (BP) database. C & D) Bar plots showing significantly overrepresented terms from the KEGG database for the genes associated with C) dynamic or D) static RBPJ binding.

In order to understand the transcriptional regulation of these genes, I first analyzed the transcript level of the RBPJ associated genes. In general, transcripts for both groups of genes were detectable in Beko control cells, indicating active transcription (Fig. 29A). The genes associated with static and dynamic sites had comparable overall transcript abundance. The patterns between both expression levels were slightly different. Overall genes associated with static sites had a higher median expression and only the lower whiskers contained genes without transcripts. In comparison, genes associated with dynamic sites showed higher variance in the number of transcripts. Noteworthy, the majority of dynamic sites were enhancer regions, which were much more difficult to associate with their target genes, resulting in potentially misassigned genes.

Next, I focused on the expression changes of the genes associated with static or dynamic sites, like it was done in previous studies focusing on RBPJ and Notch induction (Castel et al. 2013; Wang et al. 2014). The reduced level of H3K27ac at dynamic sites upon Notch inactivation already suggested decreased transcription and indeed genes associated with dynamic sites showed significantly reduced transcripts upon GSI treatment (Fig. 29C, Suppl. Table S12). In contrast, the statically bound genes were not affected by GSI, consistent with unaffected H3K27ac levels at static sites.

To relate RBPJ sites to Notch-regulated genes, I tested how many of the significantly differentially expressed genes (DEGs) upon Notch inactivation by GSI were associated with either static or dynamic RBPJ binding sites. The fraction of DEGs overlapping with dynamically bound genes (~11%) was much higher than with static genes (< 1%). As expected, almost all DEGs that were associated with dynamic sites (27 out of 28) were downregulated upon GSI (Fig. 29B, Suppl. Table S12). In comparison, DEGs associated with static sites had a higher fraction of significantly upregulated genes, indicating potentially indirect effects.

In order to test whether the association of DEGs and RBPJ bound genes is statistically robust, I calculated the $\log_2$ (enrichment of DEGs) within both groups of RBPJ sites. Simplified, this calculated how many more DEGs were present within genes associated with static, dynamic or static and dynamic compared to the randomly expected number of overlaps. Strikingly, genes associated with at least one dynamic RBPJ sites had ~8-fold higher chance to be a DEG than expected by chance (Fig. 29D, Suppl. Table S12). In contrast, genes only associated with static sites had even a ~1.4-fold reduced chance to be

a DEG. This confirmed that genes associated with dynamic RBPJ binding were statistically much more strongly associated with the expected Notch response (downregulated by GSI).

Previously, I showed that dynamic sites were characterized by stronger RBPJ binding on average than static sites. To test whether the binding strength plays a role in the likelihood of regulation of associated genes, I divided the RBPJ sites into the strongly bound sites (> median MSPCs p-value) and the weaker bound sites (< median MSPCs p-value) based on untreated cells. Since genes associated only with static sites had a much lower chance of being a DEG, I decided to include all genes that have at least one dynamic site in the dynamic group, regardless of whether they are additionally bound by a static site. Indeed, the strongly bound dynamic sites showed an even higher association with DEGs, compared the weaker dynamic sites (Fig. 29D, Suppl. Table S12). In contrast, even strong static sites were not significantly enriched for DEG.

In summary, genes associated with RBPJ binding sites were actively transcribed, but only the dynamically bound genes were strongly enriched for known Notch target genes. Furthermore, only genes associated with dynamic sites showed robust changes in transcription upon inactivation of the Notch pathway. Finally, genes associated with at least one dynamic site had much higher probability of being a significantly deregulated gene upon GSI.

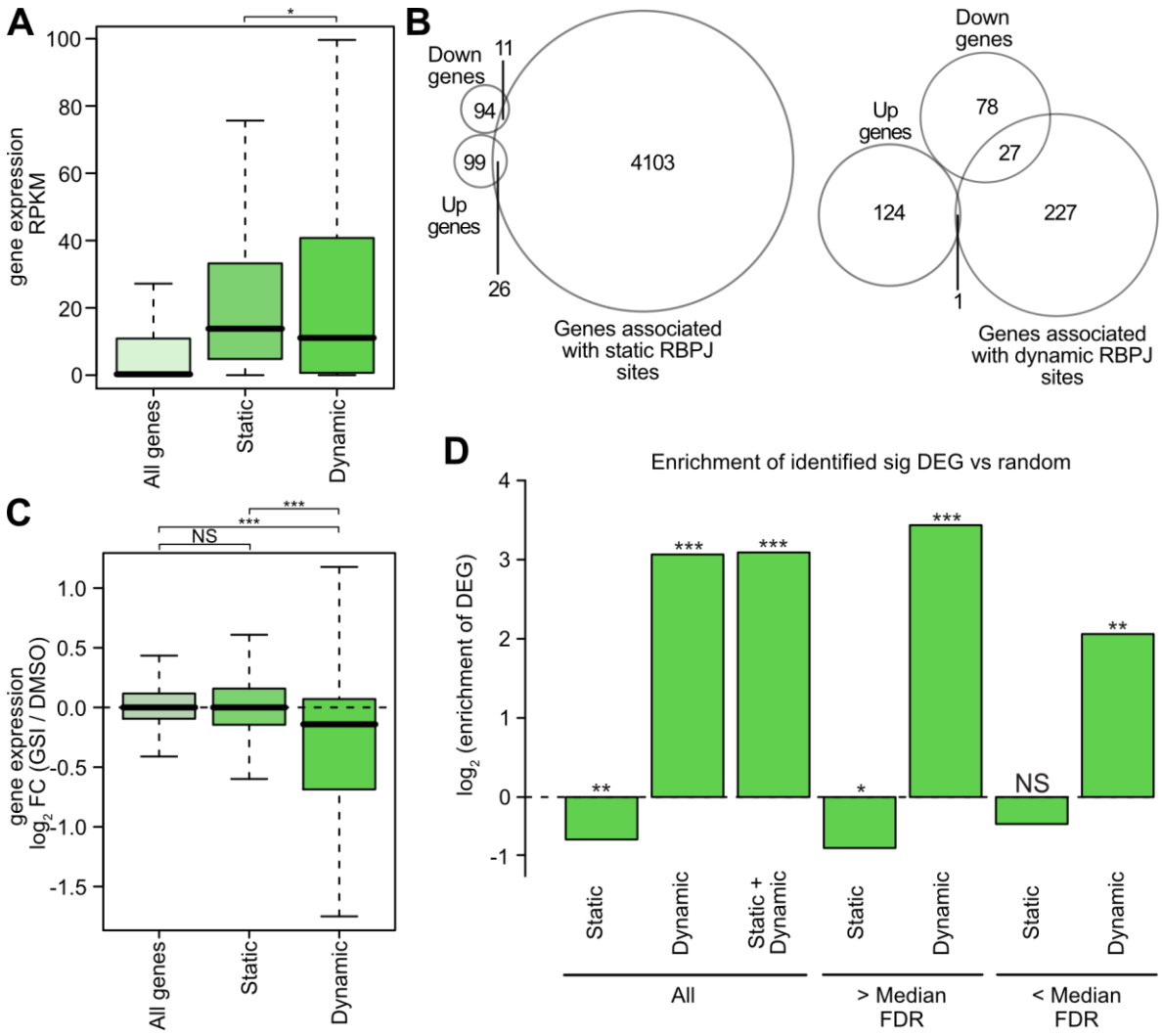


**Figure 29) Transcriptional response upon Notch inactivation occurs mainly at genes associated with dynamic sites.** A) Box plot showing the expression of all genes, genes associated with static or dynamic RBPJ binding sites. B) Venn diagram of the overlap of significantly upregulated ($log_2$ FC > 1 & adjusted p-value < 0.05) genes or significantly downregulated ($log_2$ FC < -1 & adjusted p-value < 0.05) genes with genes associated with static (left) or dynamic (right) RBPJ binding sites. C) Box plot of the expression changes of all genes, genes associated with static or dynamic RBPJ binding sites upon Notch inactivation by GSI treatment. D) Bar plot depicting the enrichment of significantly DEGs within the genes associated with static, dynamic and static & dynamic RBPJ sites. Enrichment is also shown for genes associated with the strongest half (> median MSPCs p-value) or weakest half (< median MSPCs p-value) of static and dynamic RBPJ bound genes. [***] p < 0.001, [*] p < 0.5, [NS] p > 0.05; Wilcoxon rank sum test or hypergeometric test.

### 3.2.6. Washout of GSI leads to strong re-activation of Notch target genes

Previous publications have presented a different approach to study the precise effects of changes in Notch pathway activation (Weng et al. 2006; Liefke et al. 2010; Bailis et al. 2014). The typical method is to measure the effects of blocking the Notch pathway by inhibiting the cleavage of NICD1 from the membrane by GSI. An alternative approach is to keep and subsequently washout the inhibitor, which results in a precise and strong peak of Notch signaling.

Using this washout approach, I analyzed RNA-seq data of Beko cells cultured for 48 h in GSI followed by 24 h of washout of GSI (Suppl. Table S12). Beko cells treated with 10 µg/ml GSI for 48 h showed only minor levels of NICD1 in the nucleus. Upon 24 h of washout of the GSI the NICD1 signal recovered (Fig. 30A). The hypothesis was that the washout leads to an effect opposite to the GSI treatment. Indeed, genes that were significantly upregulated by GSI treatment were significantly downregulated by washout overall and vice versa (Fig. 30B). The washout led to much more genes significantly deregulated (2113) compared to the GSI treatment (230). Despite the function of Notch as an activator, the overlap between genes upregulated in GSI and downregulated in the washout was higher compared genes downregulated in GSI and upregulated in WO, indicating possible indirect effects. Nevertheless, the WO of GSI led to upregulation of genes that were significantly downregulated upon GSI and vice versa (Fig. 30C).

Consistent with my previous findings that only genes associated with dynamic RBPJ sites were downregulated by GSI, the same genes were significantly upregulated after washout of GSI. In contrast, genes with static sites showed only minors changes (Fig. 30D).

Together, the results from the washout experiments showed an overall opposite effect compared to the GSI treatment, which is consistent with my previous results.

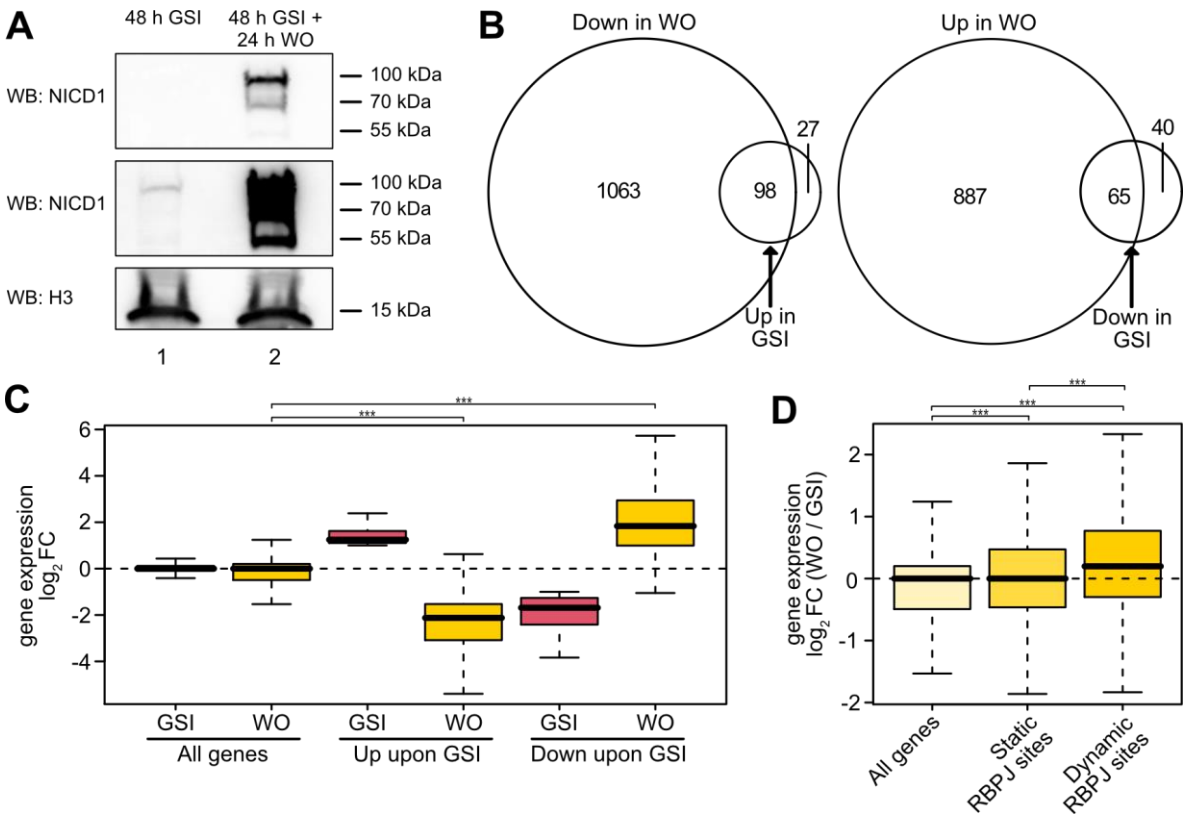


**Figure 30) Washout of GSI leads to re-activation of Notch target genes.** A) Western blot showing the strongly reduced level of NICD1 upon 48 h of GSI (1). NICD1 reappears upon additional 24 h of washout (WO) of GSI (2). Upper box shows short exposure, lower box shows long exposure. Nuclear extract was analyzed for cleaved NICD1 or H3 as loading control. Western blot was performed by Dr. Benedetto Daniele Giaimo. B) Venn diagram depicting the overlap of genes downregulated in washout (WO) and upregulated by GSI or vice versa. C) Box plot of the expression changes of genes significantly upregulated by GSI upon the washout of GSI (WO) and vice versa. Expression changes of all genes upon GSI or washout are plotted as control. D) Box plot depicting the expression changes of genes associated with static or dynamic sites upon washout of GSI. All genes are shown as control. [***] $p < 0.001$, Wilcoxon rank sum test.

### 3.2.7. Identification and characterization of directly regulated Notch target genes

27 genes were identified, which were significantly downregulated upon GSI and associated with dynamic RBPJ sites (Fig. 29B). These genes, which were directly regulated by dynamic RBPJ sites, included several known Notch target genes such as *Ptcra*, *Heyl*, *Hes1*, *Gm266*, *Dtx1*, *Il2ra Hey1* and the *Notch1* gene itself (Fig. 31A, Suppl. Table S12). To further validate these results, I compared my data with other data sets in which Notch signaling was perturbated. I analyzed RNA-seq upon Apicdin treatment, overexpression of a dominant negative mutant of MAML (dnMAML) or washout of GSI. Overall, these genes were downregulated by Apicidin and dnMAML and upregulated by washout of GSI, validating them as *bona fide* Notch target genes.

To further characterize these dynamically bound Notch target genes, I analyzed the accessibility and histone modifications H3K27ac (active chromatin), H3K18ac (active chromatin), H3K4me3 (promoter region), H3K9ac (promoter region) and H3K36me3 (active transcription) (Bannister et al. 2005) at these genes in control Beko cells or upon GSI treatment (Fig. 31B - G). Histone marks were consistent with the expected pattern including high levels of accessibility and all marks except for H3K36me3 at the promoter regions. H3K36me3 gradually increased over the length of the gene, as it was shown in previous studies (Zaidan and Sridharan 2020).

As expected from the reduced transcription, the active marks H3K27ac, H3K18ac and H3K36me3 were strongly reduced upon GSI treatment. Surprisingly, also the promoter mark H3K4me3 and H3K9ac, which co-localizes with H3K4me3, were slightly reduced upon GSI, while the overall accessibility remains unaffected.

In summary, those 27 genes represented a core set of Notch targets genes in Beko cells that were regulated by dynamic RBPJ binding. Moreover, histone modifications at these genes showed the expected pattern with reduced active marks upon GSI. Interestingly, there appeared to be no correlation between accessibility and transcription of these genes.

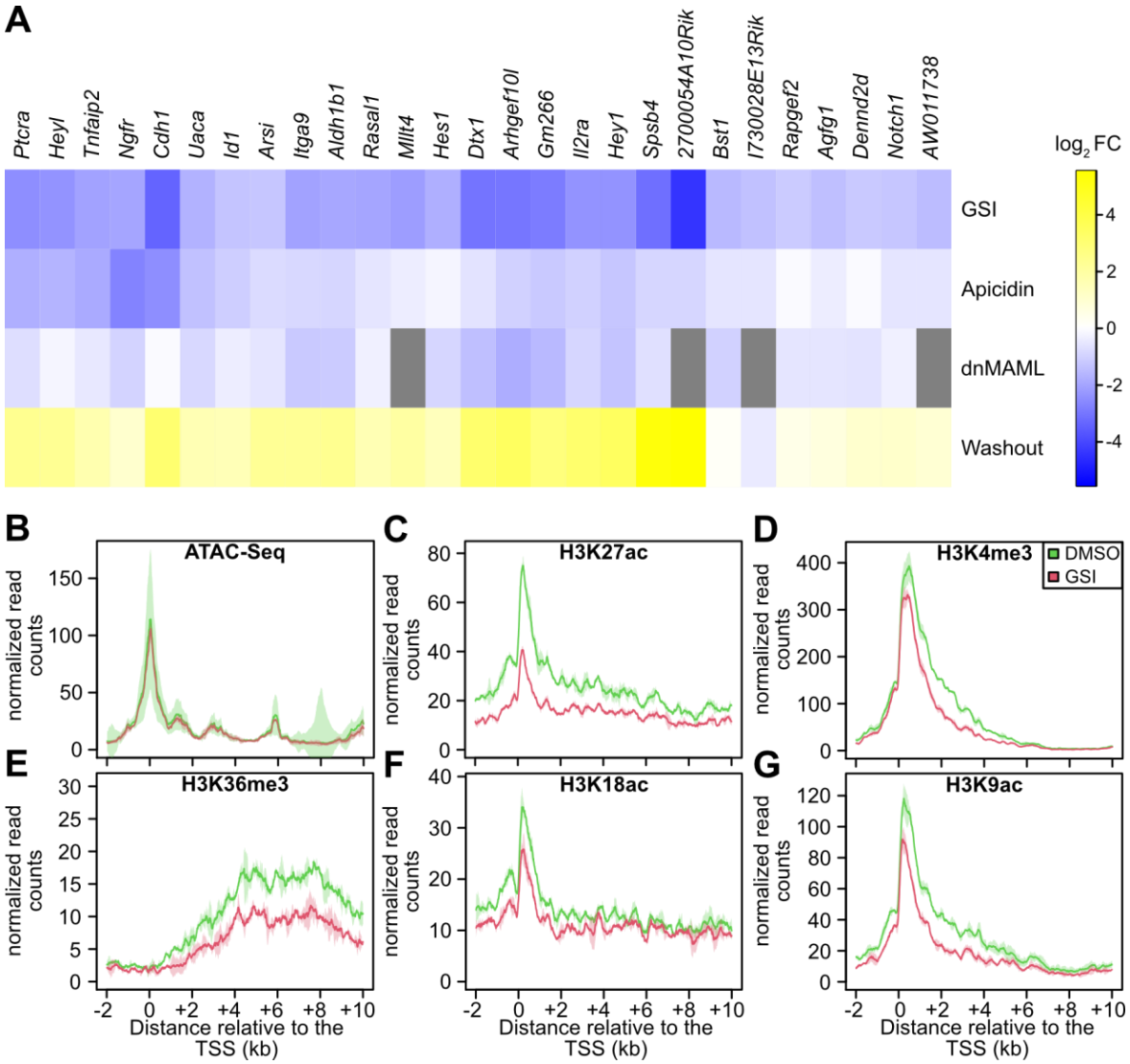


**Figure 31) Genes directly regulated by dynamic RBPJ binding sites.** A) Heat map depicting genes significantly downregulated ($log_2$ FC < -1 & adjusted p-value < 0.05) by GSI and associated with a dynamic RBPJ binding sites. Additionally shown are the expression changes of those genes upon washout of GSI / GSI, dominant negative mutant of MAML (dnMAML) / control and apicidin / DMSO. Grey genes were not represented on the microarray (dnMAML). B - G) Line plots of the enrichment level of B) accessibility (ATAC-seq), C) H3K27ac, D) H3K4me3, E) H3K36me3, D) H3K18ac and G) H3K9ac at identified dynamically bound Notch target genes in control Beko cells (green) or upon GSI treatment (red). Outline representing the standard deviation of the replicates.

### 3.2.8. Super enhancers associated with dynamic RBPJ sites are regulated by GSI

An important regulator of the global transcription are the so-called super enhancers (SEs) (Lovén et al. 2013). SEs have been shown to be important for cell type identity (Hnisz et al. 2013) and a previous publication highlighted a transcriptional regulation of RBPJ via dynamic interactions with SEs (Wang et al. 2014). As described above, the dynamic RBPJ binding sites appeared to be the main mediator of the Notch signaling, which plays a vital role in Beko cells and therefore suggesting a connection of dynamic sites with SEs in Beko cells.

In order to understand the relation between dynamic RBPJ binding and SEs, I used H3K27ac ChIP-seq to identify SEs in Beko cells. Using the well-established ROSE tool, I detected 935 SEs, which is in agreement with other publications (Suppl. Table S13) (Khan and Zhang 2019). As expected, the H3K27ac levels were highly enriched over the entire length of the identified SEs (Fig. 32A). To further characterize the 935 SEs with respect to the associated histone modifications, especially the enrichment of the enhancer mark H3K4me1, I analyzed different histone modification ChIP-seq data sets. The 935 SEs were strongly enriched for the enhancer mark H3K4me1 along the entire length of the SEs (Fig. 32B). Furthermore, they showed enrichment of the histone marks H3K4me3, H3K9ac and H3K18ac and compared to the genomic background (Fig. 32C - E). However, especially the levels of H3K4me3 and H3K9ac showed strong enrichment at the beginning and the end of the SE, whereas the entire length of the SEs was much less enriched. Noteworthy, the strong enrichment at the border of the SEs was most likely a technical artifact due to scaling of multiple SEs.

I previously showed that dynamic RBPJ binding sites were mainly enhancer regions, while static sites represent mainly promoter regions. As expected from these results, a much larger fraction of dynamic RBPJ sites were overlapping with SEs (43%), compared to static RBPJ sites (15%) (Fig. 32F). Interestingly, there were still 442 static RBPJ binding sites overlapping with SEs. A large fraction (29) of SEs were overlapping with both dynamic and static RBPJ sites.

In order to test whether the activation level of the identified SEs is sensitive to changes in the Notch activation, I tested the effect of GSI on the SEs. Surprisingly, GSI treatment resulted in a slight but still significant decrease in the activation level of all SEs as measured by H3K27ac (Fig. 32G). Overall, SEs overlapping exclusively with dynamic RBPJ binding sites showed a much stronger reduction of their activity. SEs with both static and dynamic

RBPJ sites were weaker but still significantly reduced of activity. SEs overlapping only with static RBPJ sites showed no reduction in H3K27ac upon inactivation of the Notch pathway.

In summary, dynamically bound RBPJ sites were much stronger associated with SEs compared to static RBPJ sites and the activity (H3K27ac) of these SEs was reduced upon inactivation of the Notch pathway, while SEs associated with static sites were not affected.

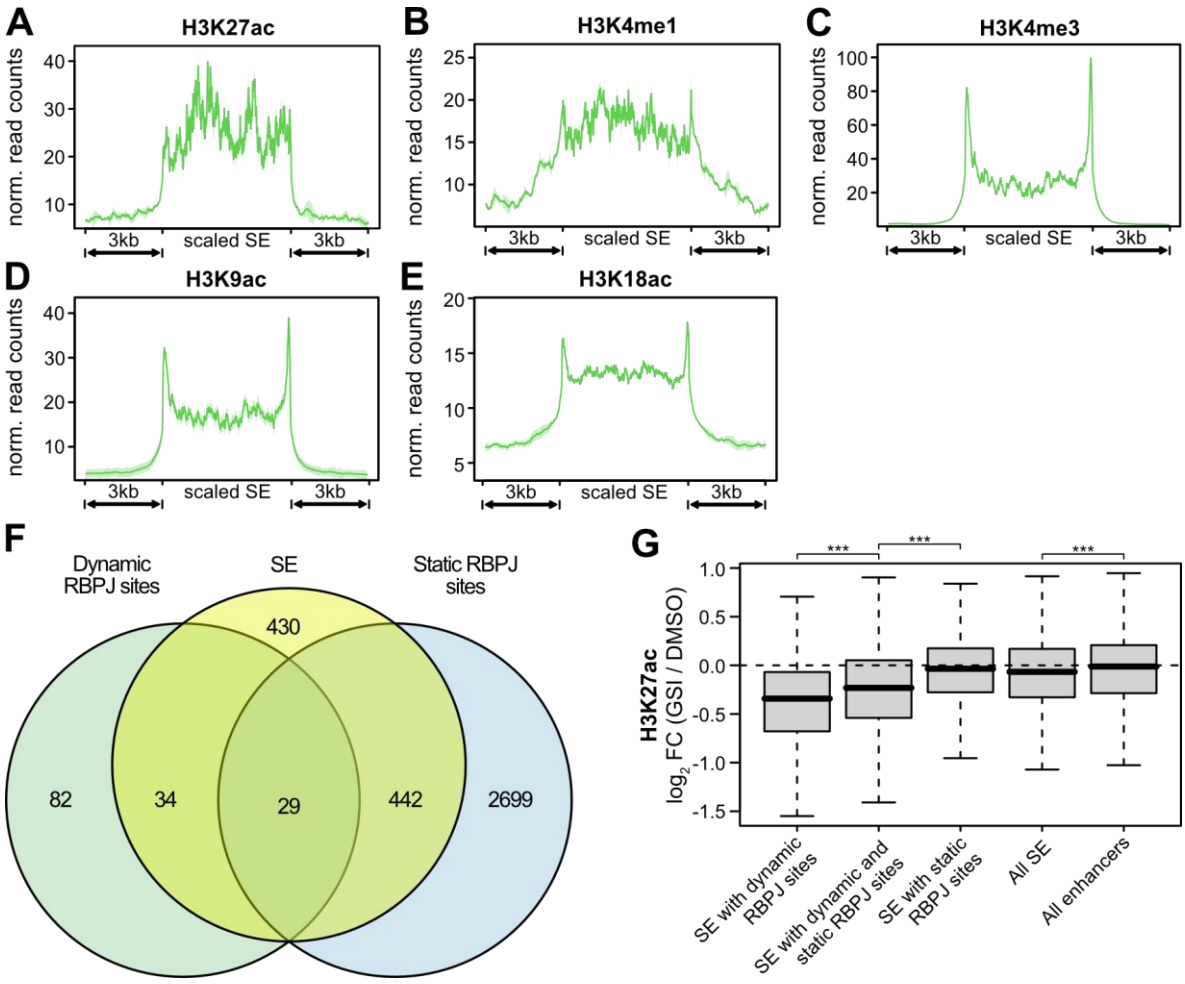


**Figure 32) SEs bound by dynamic RBPJ binding sites are responsive to inactivation of the Notch pathway.** A - E) Line plots of the enrichment level of A) H3K27ac, B) H3K4me1, C) H3K4me3, D) H3K9ac and E) H3K18ac at SEs in control Beko cells (green). Outline representing the standard deviation of the replicates. F) Venn diagram depicting the overlap of identified SEs, dynamic RBPJ binding sites, dynamic + static RBPJ binding sites and static RBPJ binding sites. G) Box plot showing the changes of H3K27ac levels at identified SEs upon Notch inactivation by GSI. Shown are SEs with dynamic RBPJ sites, SEs with static + dynamic RBPJ sites, SEs with static RBPJ sites, all SEs and all individual identifies enhancers in Beko cells. [***] $p < 0.001$; Wilcoxon rank sum test.

### 3.2.9. Dynamic binding behavior is conserved in triple negative breast cancer

Triple negative breast cancer (TNBC) is a specific type of breast cancer that lacks ER, PR, HER2 and is characterized by an active Notch pathway (Abramson et al. 2015). TNBC has an overall poor prognosis compared to other types of breast cancer. Furthermore, a stronger Notch signaling is associated with worse prognosis of the patient (Reedijk et al. 2005). The two TNBC cell lines HCC1599 and MB157 were previously well characterized by Faryabi and colleagues in terms of their transcriptome and epigenome (including RBPJ) upon of the Notch pathway inactivation (Petrovic et al. 2019).

In order to test whether dynamic and static binding behavior is also detectable in TNBC, I reanalyzed several ChIP-seq and RNA-seq data sets from (Petrovic et al. 2019). First, I used the RBPJ ChIP-seq data upon the washout of GSI to identify RBPJ binding sites in both HCC1599 and MB157. As expected from the published results, the numbers of RBPJ binding sites were much higher compared to our Beko cells (3538 sites). Using my own analysis pipeline, I was able to identify 14010 RBPJ binding sites in HC1599 (Fig. 33A) and 7628 in MB157 (Appendix Fig. 5A), respectively. Both numbers of sites were in a comparable range as the published 28365 and 7851, respectively.

Consistent with my findings in Beko cells, both HCC1599 and MB157 showed static and dynamic binding behavior of RBPJ upon washout of GSI. In HCC1599, increased RBPJ binding was detectable for 2607 (~19%) of 14010 sites upon 5 h washout of GSI (Fig. 33A). In MB157, 2040 of 7628 (~27%) sites were stronger bound with a reactivated Notch signaling (Appendix Fig. 5A). These fractions were much higher than in Beko cells, where only < 5% of all RBPJ sites showed dynamic binding behavior.

Additionally, the data included ChIP-seq for NICD1 upon GSI washout. Surprisingly, NICD1 binding was still detectable upon 72 h of GSI treatment (Fig. 33A, Appendix Fig. 5A). As expected, NICD1 binding was located at the RBPJ binding sites. Moreover, the dynamic binding pattern of RBPJ was also detectable in NICD1 binding. For both HCC1599 and MB157 at static RBPJ sites, the NICD1 levels seemed to be unaffected by 72 h of Notch inactivation or by the re-activation of the Notch pathway. In contrast, NICD1 was mainly detectable at dynamic sites with active Notch signaling, whereas NICD1 levels decreased sharply after 72 h of Notch inactivation (Fig. 33A, Appendix Fig. 5A). In Beko cells, H3K27ac was one of the histone marks predominantly affected at dynamic sites upon inactivation of Notch signaling. I evaluated whether H3K27ac was also exclusively regulated at dynamic sites in TNBC upon washout of GSI. Indeed, for both HCC1599 (Fig. 33B) and MB157

(Appendix Fig. 5B), I found a significant increase in H3K27ac levels exclusively at dynamic sites. H3K27ac at static sites or total H3K27ac levels remained largely unchanged.

Next, I investigated the transcriptional response of genes associated with either static or dynamic RBPJ binding sites in HC1599 or MB157. In Beko cells, genes associated with dynamic sites showed a much stronger response of changes in the Notch pathway activity compared to statically bound genes. To compare the TNBC cells to the Beko cells, the enrichment of DEGs was calculated, and consistent with the Beko results, genes associated with at least one dynamic site were much more likely to be a significantly DEG than expected by chance (Fig. 33C). Genes that were only associated with a static site showed no enrichment for DEGs.

The analysis of the MB157 cells revealed a comparable result. In contrast to the HCC1599, the genes associated with static sites were significantly enriched for DEGs. Nevertheless, in both cases, the enrichment of the genes associated with dynamic sites was much higher (Appendix Fig. 5C).

In Beko cells, static sites clearly represented promoter regions, whereas dynamic sites were much stronger associated with intronic or intergenic regions. To test for a similar binding behavior in TNBC, I analyzed the binding position of dynamic and static RBPJ sites in both HCC1599 and MB157. Consistent with the observations made in Beko cells, static sites in TNBC were mainly close to the TSS (0-1 kb) regions, whereas dynamic sites were predominantly far away from the TSS (> 10 kb) (Fig. 33D, Appendix Fig. 5D).

In summary, both TNBC cell lines HCC1599 and MB157 showed dynamic and static binding behavior of RBPJ upon changes of the Notch activation status. Although the fraction of dynamic sites was significantly larger as compared to Beko cells, the basic features such as the binding position and strength of RBPJ sites or the associated changes of H3K27ac were comparable to Beko cells.

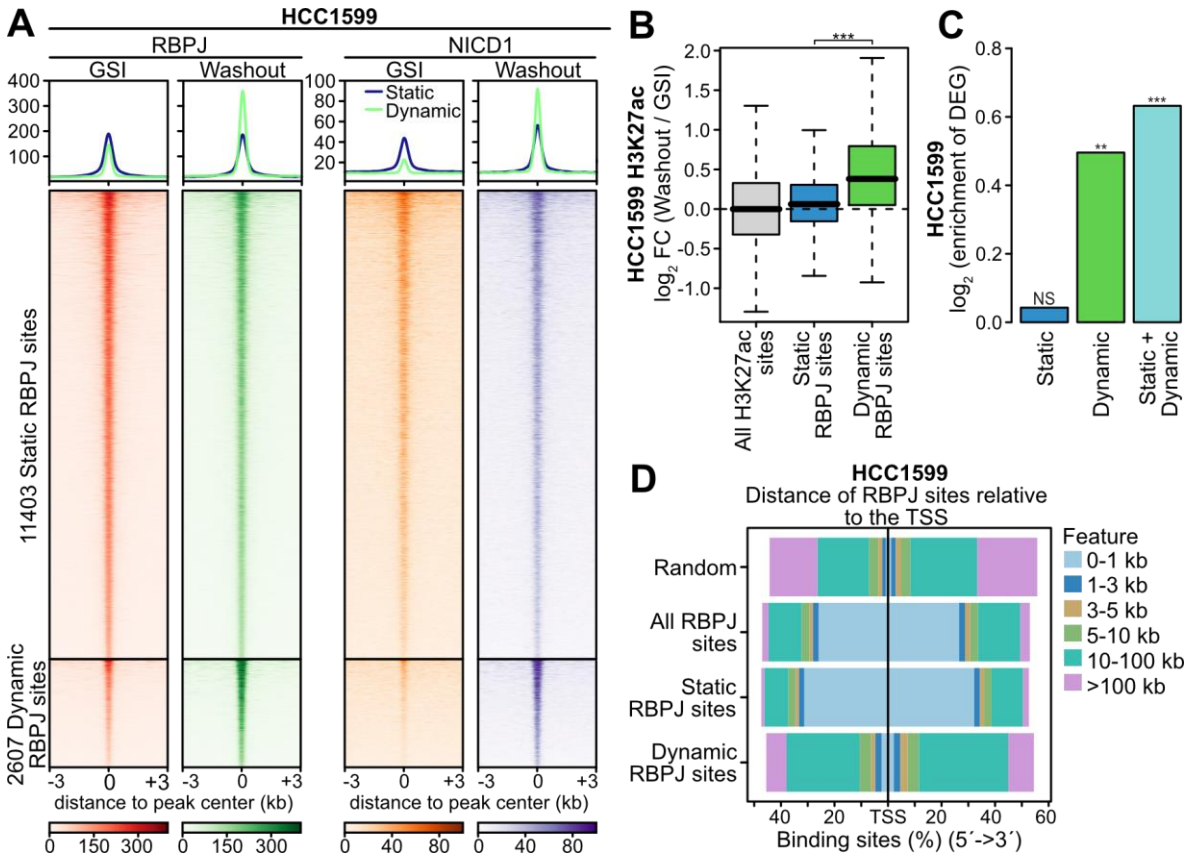


**Figure 33) HCC1599 cells show dynamic and static RBPJ binding behavior.** A) Heat map and average binding plot depicting 11403 static and 2607 dynamic RBPJ binding sites in HCC1599 cells upon 5 h of GSI washout. Shown are RBPJ binding (left) after 72 h of treatment (red) or 5 h of GSI washout (green) and NICD1 binding (right) after 72 h of treatment (orange) or 5 h of GSI washout (purple). B) Box plot of the changes of H3K27ac upon Notch re-activation by washout of GSI at all identified H3K27ac sites, at static RBPJ sites and at dynamic RBPJ binding sites. C) Bar plot depicting the enrichment of significantly DEGs within the genes associated with static, dynamic and static & dynamic RBPJ sites. D) Stacked bar plots showing the distance to the nearest TSS of all RBPJ binding sites, dynamically bound RBPJ sites or statically bound RBPJ sites. Random sites are also shown as a control. [***] $p < 0.001$, [**] $p < 0.01$, [NS] $p > 0.05$; Wilcoxon rank sum test or hypergeometric test.

### 3.2.10. Characteristics of dynamic and static site are conserved in TNBC

The previous sections showed that dynamic and static binding sites are characterized by specific features regardless of cell type. To test and further validate the features for dynamic and static sites, I focused on the two main factors: Binding strength (measured by MSPC's p-value of the peak) and binding position relative to the TSS of the next gene in both TNBC cell lines.

First, I aimed to correlate binding strength and the probability of a binding site to be either dynamic or static. Indeed, the better the p-value of an RBPJ site, the more likely it was to be dynamic (Fig. 34A &D). In HCC1599, the top 1% of all RBPJ binding sites were nearly 70% dynamic, whereas for all sites only about 20% showed dynamic binding behavior. A similar tendency, although somewhat less pronounce, was evident in MB157.

Analyses in Beko cells and TNBC, as well as other publications (Castel et al. 2013; Wang et al. 2014), clearly showed that dynamic RBPJ sites were more strongly associated with the transcriptional Notch response (Fig. 29D & 33C, Appendix Fig. 5C). Moreover, in Beko cells, the strongest dynamic sites showed the highest association with significantly DEGs genes upon Notch pathway inactivation. Next, I tested to see if a similar trend was detectable in TNBC. Indeed, the binding strength of RBPJ had predictive power for the transcriptional Notch response in TNBC as well. Strong dynamic sites had a higher probability of being associated with significantly DEGs compared to weaker bound dynamic sites or static sites (Fig. 34B & E).

Previous analyses in Beko cells and TNBCs had shown that dynamic sites were predominantly associated with enhancers, whereas static sites were mainly at promoter regions. This led to the conclusion that the location of an RBPJ binding site could predict the probability of it being dynamic or static. To test this, I focused on the correlation between the distance of an RBPJ binding site and the probability that it was dynamic. The binding distance clearly correlated with the likelihood of a site to be dynamic (Fig. 34C & F). For both HCC1599 and MB157, sites close to the nearest TSS (< 1 kb) were over 90% static, whereas sites more than 100 kb away from the TSS were about 50% dynamic.

In summary, both distance to the nearest TSS and binding strength correlated with the likelihood that an RBPJ site was dynamic in both TNBC cell lines. In addition, strongly bound dynamic sites had higher probability of being associated with significantly DEGs. This was consistent with my previous results in Beko cells. These correlations suggested that there are general rules that could explain the identity of dynamic and static binding behavior.

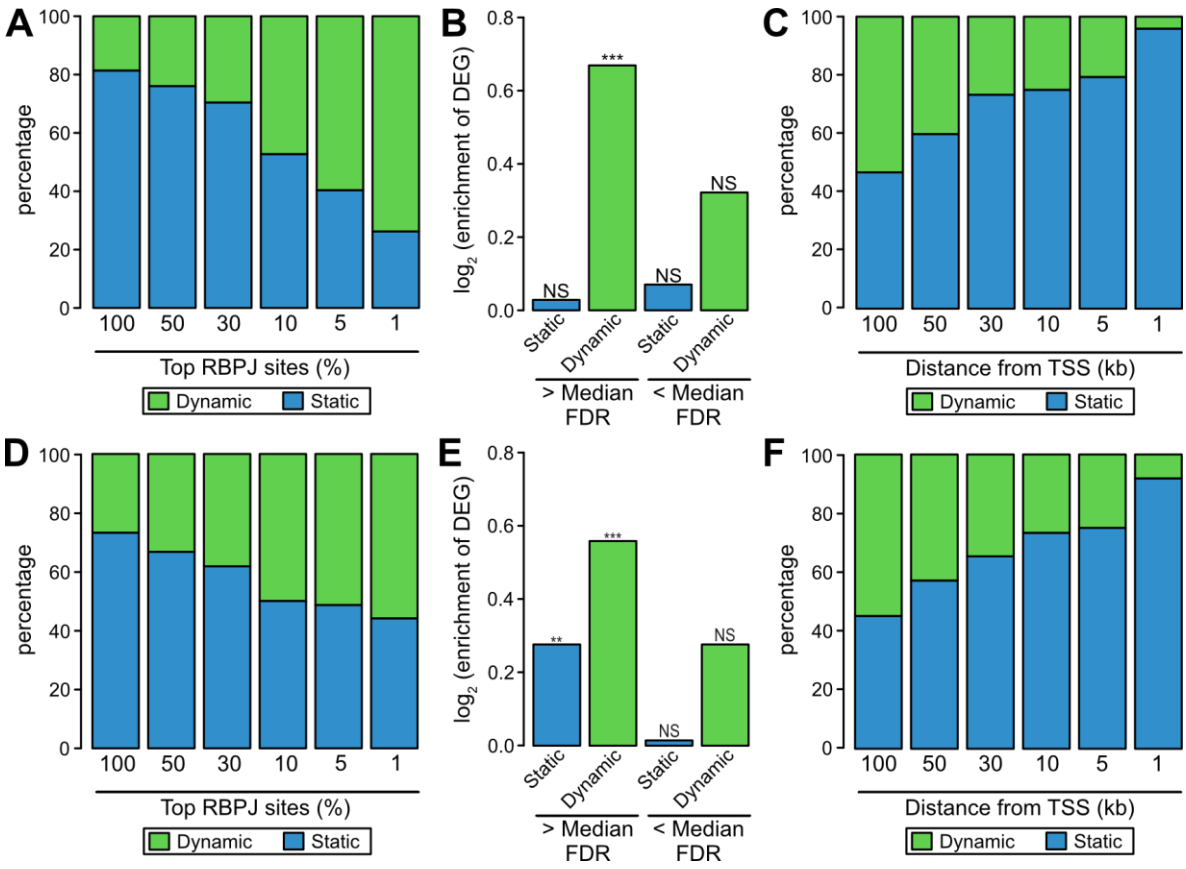


**Figure 34) Binding strength and distance to TSS correlates with static and dynamic binding in HCC1599 and MB157.** A & D) Stacked bar plot depicting the fraction of dynamic and static sites for the top 100, 50, 30, 10, 5 and 1 percent of RBPJ binding sites ranked by their p-values calculated with MSPC in A) HCC1599 or D) MB157. B & E) Bar plot of the enrichment of significantly DEGs within the genes associated with static and static & dynamic RBPJ sites. Sites are divided in to the top 50% and the bottom 50% by their p-values calculated by MSPC in B) HCC1599 or E) MB157. C & F) Stacked bar plot showing the fraction of dynamic and static RBPJ sites sorted for different distances to the next TSS of the site in C) HCC1599 or F) MB157. Shown are the distances: 100-50 kb, 50-30 kb, 30-10 kb, 10-5 kb, 5-1 kb, < 1 kb. [***] $p < 0.001$, [**] $p < 0.01$, [NS] $p > 0.05$; Hypergeometric test.

### 3.2.11. Prediction of dynamic and static RBPJ sites

The previous results underscored the importance of dynamic RBPJ binding as a mediator of the Notch response, in mouse Beko cells and in two human TNBC cell lines. Moreover, these dynamic sites shared several common features in both mouse and human, including their high binding strength and their localization far from the nearest TSS. Since the dynamic sites shared comparable features, I aimed to use a machine learning approach to predict

dynamic and static RBPJ binding sites. First, this would be useful to additionally validate the conserved characteristics of dynamic and static binding sites using an unbiased method. More importantly, this would dramatically minimize the effort required to identify cell type-specific Notch target genes (using only a RBPJ ChIP-seq data set).

To establish the approach, I used Beko's data as the starting point. In order to compensate for the obvious imbalance in classification (bias within the classes: 158 dynamic vs. 3380 static), I took all 158 dynamic sites and 1500 static sites as an input for the prediction model. The random forest approach based on the normalized p-value calculated by MSPC and the genomic feature resulted in the best correct prediction of static and dynamic sites in Beko cells (Fig. 35A & B, Suppl. Table S14). Of the 331 selected training sites (= 20%), over 97% were correctly predicted as either static or dynamic. In more detail, ~89% (41/46) of predicted dynamic sites were actually dynamic sites and ~99% (283/285) of predicted static sites were actually static sites. To ensure the model was not overfitted for the Beko training set (i.e. model works only with the training data set) and to test whether the model created was able to predict dynamic and static sites in other cell types, I validated it on different cell lines.

First, I tested the model on the two TNBC cell lines described above. I was able to correctly predict ~78% of static and dynamic sites in HCC1599 (Fig. 35C, Suppl. Table S14) and ~71% in MB157 (Fig. 35D, Suppl. Table S14), respectively. The main purpose of the model was to predict dynamic sites, as their transcriptional potential for Notch response is higher. For this reason, I focused on correctly predicting dynamic sites rather than static sites. For HCC1599, out of 2425 predicted dynamic sites 1006 (~42%) were observed dynamic sites. This was more than double compared to the randomly expected ~19% (background distribution) of dynamic sites. For MB157, 910 out of 1942 (~47%) predicted dynamic sites were observed dynamic sites. Again, this was significantly more compared to the expected 27%.

To further validate the model, I searched for suitable other data sets and analyzed data from two other cell lines upon GSI washout and finally used a human T-ALL cell line called CUTLL1 and human squamous cell carcinoma cell line called IC8. I was able to predict ~81% of sites in CUTLL1 (Fig. 35E, Suppl. Table S14) and ~75% in IC8 (Fig. 35F, Suppl. Table S14), respectively. Focusing again on the prediction of dynamic sites in CUTLL1, 152 of 285 (~53%) predicted dynamic sites were correctly predicted. This equals more than double compared to the background of ~21% dynamic sites. For IC8, 7762 of 15851 (~49%)

predicted dynamic sites were observed as dynamic sites. This is also more than the expected ~32% of dynamic sites as background.

To further analyze the quality of the predicted dynamic and static sites, I validated the actual measured changes in RBPJ binding upon GSI washout at the predicted static or dynamic RBPJ sites. The definition of a dynamic binding sites was a strong ($log_2FC > 0.5$ for the washout of GSI or < -0.5 for the GSI treatment) change of the RBPJ binding upon changes in the activation state of the Notch pathway. Significant differences between the predicted static and predicted dynamic sites were clearly detectable for HCC1599 (Fig. 36A), MB157 (Fig. 36D) and CUTLL1 (Fig. 36G) as well as IC8 (data not shown). For all cell lines, the predicted dynamic sites showed much stronger change of the RBPJ binding upon washout of GSI compared to the predicted static sites.

The previous analysis revealed a clear difference between H3K27ac at dynamic and static RBPJ binding sites upon changes in the activation state of the Notch pathway. H3K27ac at dynamic sites displayed a clear response, while H3K27ac at static sites remained mainly unaffected. To test, whether these changes in H3K27ac were also observed for the predicted static or dynamic sites, I analyzed H3K27ac upon the washout of GSI in all cell lines. As expected, HC1599 (Fig. 36B), MB157 (Fig. 36E) and CUTLL1 (Fig. 36H) revealed a significant upregulation of the H3K27ac levels at the real dynamic binding sites compared to the static ones. In the IC8 data, H3K27ac showed no changes, indicating a general inconsistency compared to the other data sets and was therefore it was removed from the following analysis. Next, I tested the changes of H3K27ac at predicted dynamic or static sites. In all three data sets, there was a significant different between the H3K27ac response at predicted static or dynamic sites (Fig. 36B, E & H). The differences were minor for HCC1599, but this was to be expected since HC1599 showed overall the weakest response.

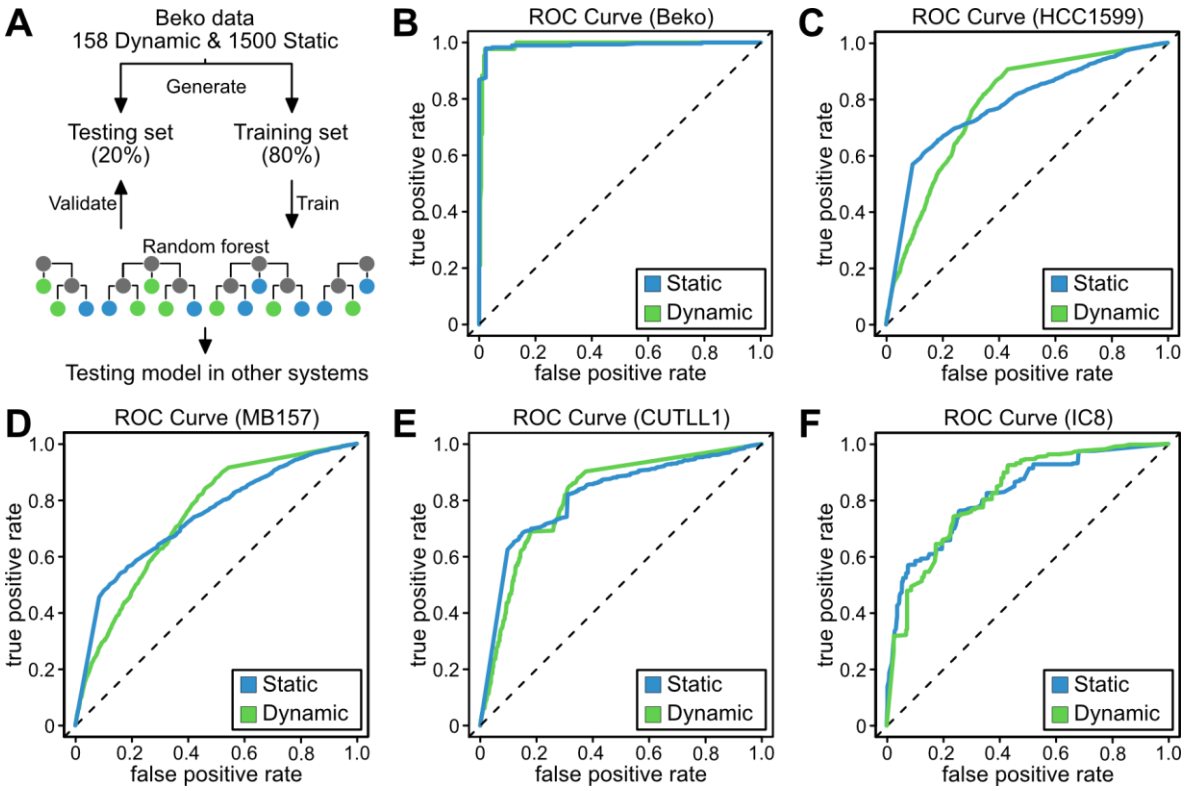


**Figure 35) Prediction of dynamic and static sites.** A) Scheme of the approach to generate the random forest that was used to predict static and dynamic RBPJ sites. B - F) Receiver operating characteristics (ROC) curve depicting the rate of true vs. false positive rate of prediction for static (blue) and dynamic (green) sites in B) Beko, C) HCC1599, D) MB157, E) CUTTL1 and F) IC8. Dashed line indicating the random chance of prediction.

Finally, I analyzed the transcriptional response of genes associated with predicted static and dynamic sites. The previous analysis revealed that genes associated with dynamic sites had a much higher chance to be a significantly DEGs upon the changes in the Notch activity. Therefore, I utilized the previously explained enrichment of DEGs analysis within the groups of predicted static and dynamic RBPJ binding sites. For all four data sets, the enrichment of DEGs was much higher for predicted dynamic sites compared with predicted static sites (Fig. 36C, F & I). This suggested, the capability of the proposed model to increase the chance of identifying significantly DEGs by using only RBPJ binding information. As expected by the strong difference between both groups, the prediction was the most efficient for CUTLL1 data. Enrichment of DEGs in HCC1599 was the least efficient, as the large number of RBPJ binding sites makes it statistically less likely to catch a DEG.

Strikingly, for CUTLL1, when dividing the predicted static and dynamic RBPJ sites into weaker and stronger bound sites (measured as MSPC's p-value; used for the training of the model), the enrichment for DEGs was higher for the weaker predicted dynamic sites compared to the strongest predicted static sites. This showed that the predictive power of the model was greater than its individual input features, indicating a synergistic effect of the individual features.

Taken together, the proposed random forest model validated the existence of static and dynamic sites in an unbiased manner. It provided evidence that dynamic and static sites were characterized by the same features, regardless of cell type or species. Moreover, dynamic sites in all cell types showed a much stronger response to changes in Notch activation status at both chromatin and transcriptional levels. Finally, the model generated was able to predict dynamic sites based on a single RBPJ ChIP-seq experiment with sufficient efficiency in numerous other cell types, even from different species.

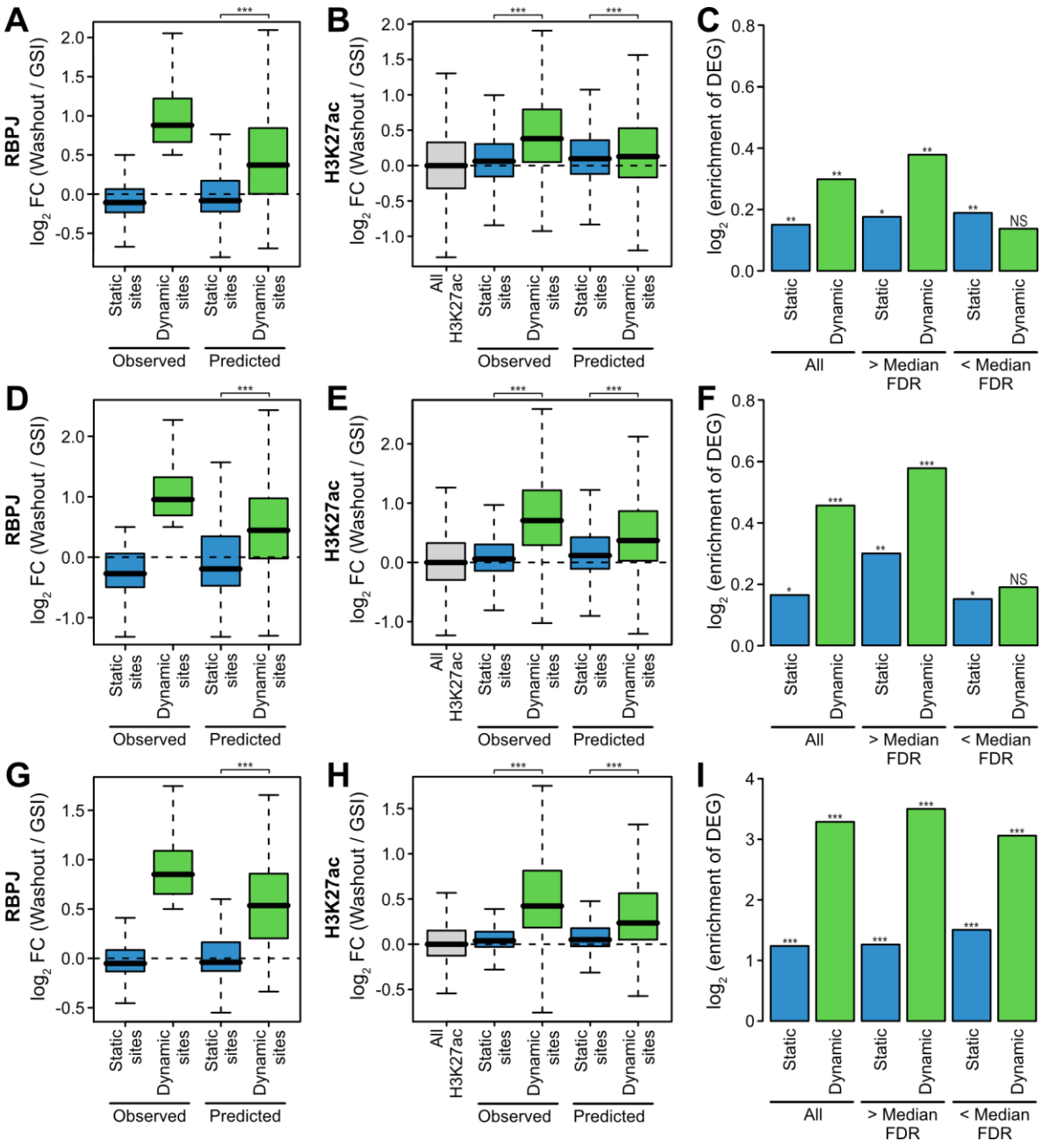


**Figure 36) Predicted dynamic sites are comparable to observed ones.** A, D & G) Box plots depicting the changes of the RBPJ binding upon washout of GSI for observed or predicted static and dynamic sites in A) HCC1599, D) MB157 and G) CUTLL1. B, E & H) Box plot showing the changes of the H3K27ac levels upon GSI washout at observed or predicted static and dynamic RBPJ sites or all H3K27ac sites (control) in B) HCC1599, E) MB157 and H) CUTLL1. C, F & I) Bar plot of the enrichment of significantly DEGs within the genes associated with predicted static (static) and static & dynamic (dynamic) RBPJ sites. Enrichment is also shown for genes associated with the strongest half (> median FDR) or weakest half (< median FDR) of predicted static and dynamic RBPJ bound genes in in C) HCC1599, F) MB157 and I) CUTLL1. [***] $p < 0.001$, [**] $p < 0.01$, [NS] $p > 0.05$; Wilcoxon rank sum test or hypergeometric test.

# 4. Discussion

In this study, I elucidated two aspects of genome-wide regulation of the Notch signaling pathway. First, the Notch-dependent and -independent role of the transcription factor RBPJ was investigated in mature T-cells using a combination of Notch activation and/or depletion of RBPJ. Interestingly, four clusters of different RBPJ/Notch-dependent genes with distinct transcription patterns were detectable. Second, two binding modes of RBPJ were identified in progenitor T-cells upon inactivation of the Notch pathway. Predominantly, dynamically bound genes were associated with the known Notch response. This dynamic binding behavior is conserved in different cell types as well as across species and can be computationally predicted based solely on the position and binding strength of RBPJ binding sites.

## 4.1. Four clusters represent distinct regulatory programs

Integrated ChIP-seq and RNA-seq analyses in mature T-cells revealed four distinct transcriptional responses (clusters) of RBPJ bound genes upon depletion of RBPJ or Notch activation. Cluster I represents the canonical RBPJ/Notch response (Borggrefe and Oswald 2009). In the context of these genes, RBPJ acts as a repressor of transcription without Notch signaling and as an activator with an active Notch pathway. Cluster II is behaving principally similar but is characterized by a delayed transcriptional response. Cluster III consists mainly of genes that are not directly bound to their promoter regions but are regulated by RBPJ via interaction with distal enhancer regions. These genes become activated upon Notch signaling but are not actively repressed by RBPJ in the absence of Notch. Cluster IV includes genes that are upregulated by RBPJ depletion but are not responsive to Notch activation (Fig. 37). Importantly, these different binding responses were conserved in other cell types, supporting the validity of the clusters.

All clusters contained genes previously associated with Notch signaling, confirming the authenticity of the clusters as Notch-associated genes. The first cluster included the well-described Notch target genes *Hes1* (Sasai et al. 1992) and *Hey1* (Iso et al. 2001), but also *Lgmn* (Hall et al. 2022). Both genes coding for the alpha-chain of the interleukin receptors 2 and 15 (*Il2ra* & *Il15ra*) were within the second cluster (Adler et al. 2003; Kornsuthisopon et

al. 2021). Two genes coding for negative feedback regulators of Notch signaling (*Nrarp* & *Dtx1*) (Lamar et al. 2001; Yamamoto et al. 2001) and *Lrp1* (a positive regulator of Notch signaling) were found in the third cluster (Bian et al. 2021). Relative to its size, the fourth cluster contained only few genes previously associated with Notch signaling, including *Ccl5*, *Klf7* and *Padi2* (Wang et al. 2016a; Lin et al. 2017; Bai et al. 2021).

Functional analyses of the genes within each cluster revealed common, but also specific biological pathways to be enriched in individual clusters. In all clusters, except for cluster II, multiple pathways related to developmental processes were enriched. This fits with Notch's described important function in the context of several development processes (Siebel and Lendahl 2017).

The following sections address the potential role of selected candidate genes:

The gene *Atp8a2* (Cluster I) is important for brain development and mutations are associated with cognitive impairment (Onat et al. 2013; McMillan et al. 2018). Comparably, *Tgm2* and *Ifng* (Cluster III) and multiple genes (*Chrnb2*, *Nrp2*, *B4galt5*, *Pip5k1c*, *Klf7*, *Plekho1*) from cluster IV are known to play a role in neural development (Appendix/Tables/ Table_S7_Ch1_GO_Cluster). This is in line with the described function of Notch signaling during neural development, postnatal neuro- and gliogenesis (Siebel and Lendahl 2017).

First, it was already described that *Atp8a2* (Cluster I), coding for ATPase Phospholipid Transporting 8A2, is linked to Notch in the regulation of intestinal intraepithelial lymphocytes (IELs), as the lack of RBPJ led to a strongly decreased level of *Atp8a2*, which in turn resulted in a strongly reduced amount of TCRαβ$^+$CD8αα$^+$ IELs (Ishifune et al. 2019). Furthermore, both Notch1 and Notch2 are required for the correct development of TCRαβ$^+$CD8αα$^+$ IELs. In addition, *Atp8a2* overexpression was able to increase the numbers TCRαβ$^+$CD8αα$^+$ IELs, again (Ishifune et al. 2019). These results suggest that RBPJ-mediated Notch signaling leads to an activation of *Atp8a2*, which is needed for the correct forming of TCRαβ$^+$CD8αα$^+$ IELs. Simplified, the function of Atp8a2, together with other P4-ATPases, is to regulate plasma membrane phospholipid asymmetry, which is important for several cellular functions (Andersen et al. 2016). Whether the same Notch-Atp8a2 regulatory axis described for the development of TCRαβ$^+$CD8αα$^+$ IELs is also crucial for neural development remains to be elucidated.

Next, the gene *Tgm2* (Cluster III), coding for Transglutaminase 2, is highly expressed in neural stem/progenitor cells (NSPCs) (Shi et al. 2023), which are known to be regulated by

Notch signaling (Ehm et al. 2010; Chen et al. 2021; Kang et al. 2022a). Depletion of *Tgm2* led to downregulation of various Notch target genes in both differentiating and proliferating NSPCs, indicating a clear connection between Notch signaling and Transglutaminase 2 (Shi et al. 2023). The analysis of MT cells showed *Tgm2* as a Notch target gene, while Transglutaminase 2 itself regulates Notch target genes in NSPCs (Shi et al. 2023). This would suggest a potentially self-regulating mechanism, as it was previously described for other Notch target genes, like *Nrarp* (Lamar et al. 2001). Whether Transglutaminase 2 is indeed important for Notch-mediated neural development requires further validation. Moreover, it remains unclear how Transglutaminase 2 regulates Notch target genes. Other studies showed that Transglutaminase 2 regulates progression of gastric cancer by activation of the ERK1/2 pathway (Wang et al. 2016b), which is described to promote Notch signaling (Tremblay et al. 2013; Li et al. 2022). However, possible ERK-mediated activation of Notch target genes via Transglutaminase 2 remains highly speculative.

Finally, *B4galt5* (Cluster IV), coding for β1,4-Galactosyltransferase V (B4GalT5), was described to be highly correlated with breast cancer stem cells (BCSCs) and poor prognosis (Tang et al. 2020). B4GalT5 promotes Wnt/β-catenin signaling, which is known to crosstalk with Notch (Borggrefe et al. 2016; Lee et al. 2021). This B4GalT5-mediated crosstalk could be an interesting part of the Wnt-Notch axis, which is also important for neuronal development.

In contrast to the above-mentioned neuronal development associated genes, both cluster III genes *Epas1* (coding for hypoxia-inducible factor-2α) and *Ndst1* are known to contribute to vasculature development (Peng et al. 2000; Adhikari et al. 2010; Rosenblum et al. 2021). Hypoxia-inducible factor-2α (HIF-2α) has previously been shown to be upregulated by Notch signaling in several cancer cells and that activation of some Notch target genes depends on HIF-2α (Mutvei et al. 2018). Furthermore, HIF-2α and *Ndst1*, can activate or enhance Wnt signaling (Yan et al. 2018; Yamamoto et al. 2023) and with this promoting additional targets for the Wnt-Notch axis.

In summary, multiple developmental associated genes are contained within the identified clusters. Many genes associated with neuronal development are found within these clusters. They may not only be regulated by the Notch signaling pathway, may also act as feedback regulators (e.g. *Tgm2*, in addition to the known *Dtx1* or *Nrarp*).

Strikingly, 8 out of 19 genes in cluster II can by associated with cytokine mediated signaling (Appendix/Tables/ Table_S7_Ch1_GO_Cluster). These genes are *Casp4*, *Socs1*, *Csf1*,

*Naip2*, *Naip5*, *Il15ra*, *Il2ra* and *Tnfsf10*. Interestingly, *Casp4* was shown to repress *Notch1* activity by interacting with the catalytic core of γ-secretase (Fan et al. 2022). *Il2ra* has known functions in different T-cells (Ross and Cantrell 2018). *Il15ra* is associated with natural killer cells (Guo et al. 2017) and *Socs1* and *Csf1* are important in macrophages (Jones and Ricardo 2013; Wilson 2014). Due to the longer response time after Notch activation, it can be assumed that the cytokine mediated aspects are a secondary response to the Notch activation. The activation of these genes needs potentially additional factors, which are possibly dependent on the initial Notch response (Cluster I & III). Although the individual functions of the 8 genes appear to be distinct, a clear connection of cytokine-mediated signaling and late response Notch target genes can be made. A comparable connection of Notch signaling and cytokine-mediated transcription was already published for the regulation of neural stem cells (NSCs) (Nagao et al. 2007), T-cell differentiation (Sauma et al. 2012) and oncogenesis in general (Colombo et al. 2018). The interplay between cytokine and Notch signaling remains to be further investigated.

Taken together, the different clusters of RBPJ/Notch target genes are associated with unique and commonly found biological function, indicating a complex regulatory network that is required for the precise and correct functional output upon Notch activation.

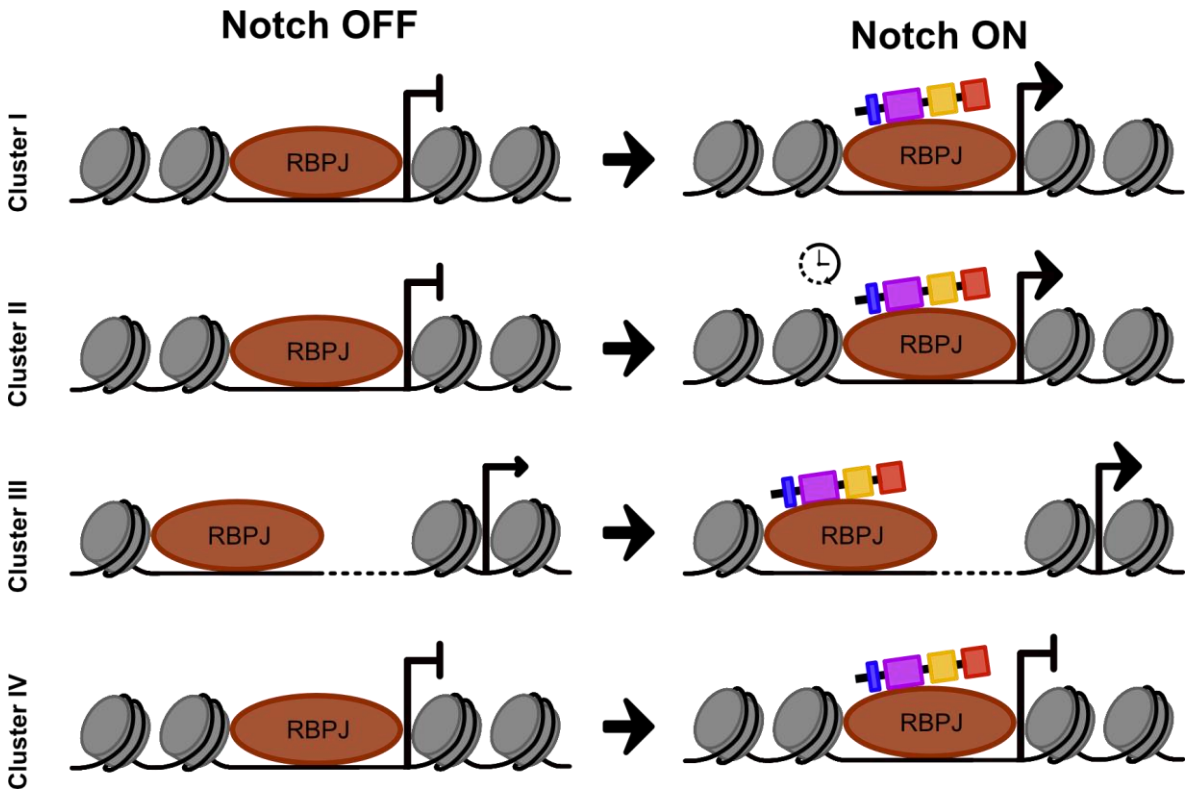


**Figure 37) Schematic representation of the four different RBPJ/Notch target genes.** Cluster I represents the canonical Notch response with RBPJ as either a repressor or an activator, depending on the presence of NICD1. Cluster II shows the same general response but requires longer Notch activation for their response and therefore represents late response targets. Cluster III consists mainly of genes that are not directly bound to their promoter regions, but are regulated by RBPJ via interaction with distal enhancer regions. RBPJ enhances transcription of target genes but acts not as a repressor in the absence of Notch signaling. Cluster IV is composed of genes that are repressed by RBPJ independent of the activation state of the Notch pathway in MT cells.

### 4.2. RBPJ could act as a repressor even in cells with an active Notch signaling

From the literature it is known that RBPJ can act as either an activator or a repressor of Notch target genes, depending on the activation state of Notch signaling (Borggrefe and Oswald 2009; Kopan and Ilagan 2009). Cluster IV genes were clearly bound by RBPJ and actively repressed in MT cells lacking active Notch signaling. Surprisingly, these genes were not upregulated by Notch activation in MT cells, indicating continuous active repression by RBPJ. This suggests that some genes remain repressed by RBPJ even though the Notch pathway is active (Fig. 38) and therefore indicates an additional Notch-independent mechanism of RBPJ that remains to be further explored.

The last chapter (4.1) discussed the potentially different functions of the clusters, including neural development. Interestingly, most of the genes associated with neural development were in cluster IV, i.e. genes that do not respond to Notch activation in mature T-cells. It is well described that Notch signaling plays an important role in neural development, including a regulatory function in NSPCs (Nagao et al. 2007; Siebel and Lendahl 2017). Consistent with this, GSI treatment in iPSC-derived NSPCs resulted in a downregulation not only of expected Notch target genes, but also of cluster IV genes that have been associated with neural development (*Nrp2*, *B4galt5* and *Pip5k1c*) (Okubo et al. 2016). This corroborates the functional relevance of the genes in cluster IV and their Notch-dependent regulation in other physiological contexts (NSPCs). It may be that these genes require additional factors, for example neuronal-specific TFs. Moreover, this would suggest that RBPJ actively represses neural development-related genes in mature T-cells.

A comparable phenomenon of active repression of neuronal genes in non-neuronal tissues is described for the well-characterized transcription factor RE1-Silencing Transcription factor (REST) (Hwang and Zukin 2018). REST forms complexes with other factors, including HDACs, to compact adjacent chromatin, resulting in transcriptional repression (Andrés et al. 1999; Grimes et al. 2000; Rodenas-Ruano et al. 2012). It could be speculated that RBPJ have similar functions or even cooperate with REST to suppress these genes. In line with that, early genome-wide studies of RBPJ binding sites in two mouse T-ALL cell lines already identified the REST binding motif as highly enriched at RBPJ binding sites (Wang et al. 2011), providing further evidence for the REST and RBPJ/Notch connection. Motif analysis for REST in MT cells revealed that approximately 10% of all RBPJ sites carry the REST motif. Moreover, a recent study showed an additional connection of Notch and REST, demonstrating repression of the neuroendocrine cell fate by Notch-mediated activation of REST in the lung (Shue et al. 2022).

Together, the above findings further validate that the RBPJ/Notch regulation is context specific. Specifically, it suggests that RBPJ may also retain its function as a repressor of cell type-specific genes even in presence of active Notch signaling. However, it remains to be elucidated how RBPJ directly represses some target genes independently of the active Notch pathway and whether other factors (e.g. REST) are involved in this repression.

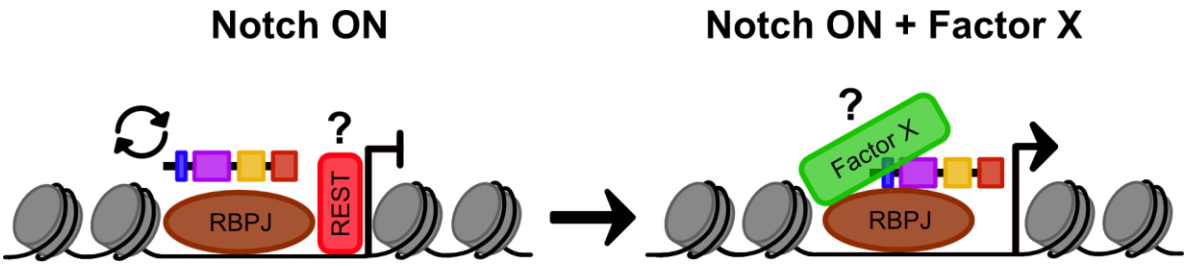


**Figure 38) Schematic representation of RBPJ dependent repression, despite an active Notch signal.** Independent of an active Notch pathway, RBPJ remains its function as a repressor, potentially by interacting with other repressors (e.g. REST) or the NICD cannot bind properly to RBPJ. Potentially, RBPJ could act as an activator at these sites in combination with an unknown cell type specific factor.

### 4.3. RBPJ may be a Notch-independent activator

The canonical model assumes that RBPJ acts as an activator only in the presence of the NICD, whereas it actively represses genes in the absence of NICD. Consistent with this, depletion of RBPJ in MT cells (Notch inactive) resulted in a predominant (> 85%) activation of transcription, confirming its function as a repressor. However, the integration of RBPJ binding to identify direct targets led to a surprising result. Nearly 45% of all direct RBPJ targets were downregulated by the removal of RBPJ, indicating an activation function of RBPJ in the absence of NICD1 (Fig. 12). Based on the function of RBPJ, it can be hypothesized that the interaction with other factors besides NICD1 could lead to this activation. Consistent with this hypothesis, the activation of Notch led to slight downregulation of these genes, suggesting competitive binding of NICD1 and the assumed factor (Fig. 39).

In a previous study, RBPJ was shown to interact directly with Pancreas Associated Transcription Factor 1a (PTF1A) using yeast-2-hybrid screen (Obata et al. 2001). In a later study, RBPJ was found to be critical for early pancreatic development within a stable trimeric DNA-binding complex. This complex binds to promoter regions and is required for the activation of target genes including *RBPJL*, a pancreas-specific paralog of RBPJ (Masui et al. 2007). Furthermore, the interaction of PTF1A and RBPJ has been shown to be important in the neural development (Hori et al. 2008). If there is a comparable factor in T-cells, which would explain the NICD-independent activation by RBPJ, needs to be explored.

Another explanation could be the described function of RBPJ as a pioneer or bookmarking factor (Miele 2011; Lake et al. 2014; Rozenberg et al. 2018; Dreval et al. 2022). It is possible

that RBPJ does not activate these genes directly, but rather primes their promoter regions for other TFs, allowing active transcription.

Finally, the question remains whether the Notch-independent activation is actually directly RBPJ-mediated or just an indirect effect. Just because RBPJ binding is associated with these genes and the depletion of RBPJ resulted in an activation does not necessarily mean that this is due to RBPJ itself.

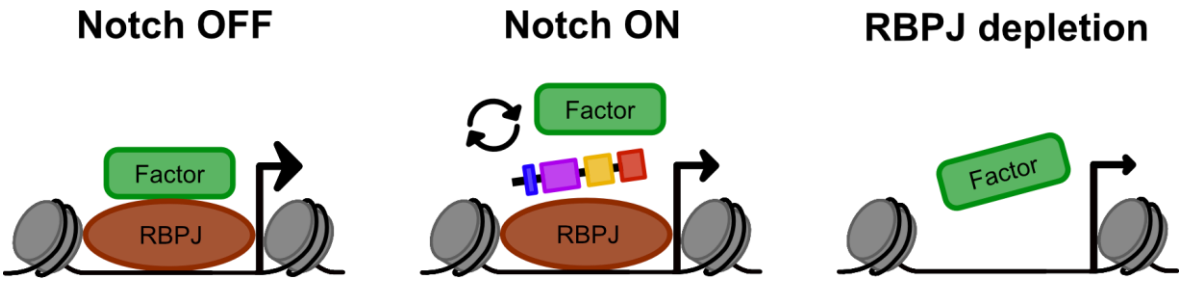


**Figure 39) Schematic representation of the possible NICD-independent activator function of RBPJ**. In this scenario RBPJ acts as an activator without NICD (Notch OFF) by interacting with another factor, a reduced transcription is detectable with NICD (Notch ON) and finally genes are very weak expressed without RBPJ (RBPJ depletion).

### 4.4. The Notch activation state influences the RBPJ binding

Several studies have shown that RBPJ is not constantly bound to DNA but rather binds dynamically dependent on the activation state of the Notch pathway. The precise function of this dynamic binding and the molecular explanation remained elusive. The groups of both Stunnenberg and Aster have shown that dynamically bound sites are the major contributors to the transcriptional Notch response in mammals (Castel et al. 2013; Wang et al. 2014). Furthermore, Sarah Bray's group showed that RBPJ is actively loaded to the DNA in *Drosophila* and that this prolonged binding results in an active transcription (Krejčí and Bray 2007; Gomez-Lamarca et al. 2018). The interpretation of these results was that the transcription of Notch target genes can be indirectly repressed by short binding time of RBPJ, which is insufficient for the recruitment of the RNA polymerase transcription machinery. Various other studies in mammalian systems showed that RBPJ actively recruits co-repressors including HDACs; here the interpretation was that the co-repressors affect the surrounding chromatin to repress transcription (Taniguchi et al. 1998; Oswald et al. 2002;

Wacker et al. 2011; Xu et al. 2017). Both mechanisms, short DNA occupancy of RBPJ or HDAC-mediated chromatin changes, are not mutually exclusive.

In line with the results published by the groups of Stunnenberg and Aster (Castel et al. 2013; Wang et al. 2014), my analysis of mature T-cells and Beko cells showed that the Notch status affects the RBPJ binding (Fig. 15 & 22). Interestingly, the activation of Notch in MT cells led to an overall increase of RBPJ binding, whereas the inactivation of Notch in Beko cells affected only a minority of binding sites. Regardless of this difference, a subset of sites in MT and Beko cells were much more responsive to changes in Notch activity compared to all other sites. Previous publications showed that a dimerized RBPJ binding, based on a head-to-head RBPJ motif, leads to a drastically increased DNA binding (Nam et al. 2007; Liu et al. 2010). In line with this, these head-to-head binding motifs were much stronger associated with the dynamically bound RBPJ sites in Beko cells. The expression of NICD ΔEP, a mutant that is not able to interact with the co-activator complex (Oswald et al. 2001), resulted in weaker binding of RBPJ in MT cells compared with cells lacking NICD (Fig. 15). This is further evidence that proper formation of the co-activator complex is critical for increased RBPJ binding.

Surprisingly, previously published data from human TNBC cells revealed that upon 72 h of Notch inactivation by GSI, NICD was still detectable at static sites. In contrast, dynamic sites showed a strong reduction of NICD binding. It is possible that the NICD is in a large multiprotein complex at static RBPJ binding sites, making these sites much less sensitive to GSI treatment. In line with this, static sites are mainly found at promoter regions, which is known to be broadly occupied by many factors including general TFs and TFs (Thomas and Chiang 2006; Partridge et al. 2020). Previous global studies highlighted that broad regulatory regions tend to be more resistant to expression changes compared to smaller regions (Sigalova et al. 2020).

Another important observation was that a few sites were exclusively bound when Notch signaling is active, thus representing *de-novo* binding sites. The RBPJ binding site upstream of the genes *Il2ra* and *Ptcra* were good examples. Consistent with this, the chromatin accessibility as strongly reduced in the absence of Notch signaling, even though a weak ATAC-seq signals persists. This indicates that the chromatin is not completely closed at these sites, even without any detectable RBPJ binding. Taken together, NICD is required for the binding of RBPJ in a minority of sites. One explanation could be that other factors

compete with RBPJ at these sites and only the enhanced binding in combination with NICD and MAML allows RBPJ to displace the other factor.

In summary, there are several possible causes for the dynamic binding behavior of RBPJ. However, the predominant location at enhancer sites seems to be a major predictor of dynamic sites.

### 4.5. Adjacent chromatin is altered only at a subset of RBPJ sites

In the canonical model, activation of Notch target genes is mediated by recruitment of co-activators. These include histone acetyl transferases like p300, which acetylates histones and thus contributes to an active chromatin conformation (Oswald et al. 2001). It has further been shown that RBPJ is associated with super enhancer (large cluster of strong enhancers) and that the reduced RBPJ binding (dynamic) at these SEs leads to overall reduced activation levels (Wang et al. 2014). Consistent with these results, inactivation of Notch in Beko cells resulted in a specific loss of H3K27ac at dynamically bound RBPJ sites, whereas overall H3K27ac levels were not affected. In line with the study of Aster's group (Wang et al. 2014), dynamic RBPJ sites were much stronger associated with SEs as compared to the static sites. In addition, the functional spectrum of RBPJ also involves active repression of Notch target genes through recruitment of co-repressors such as HDACs (Kao et al. 1998; Oswald et al. 2002). This led to the hypothesis of an on/off switch function of RBPJ mediated in part by chromatin modification by HAT or HDACs. However, the studies by Stunnenberg and Aster (Castel et al. 2013; Wang et al. 2014), as well as the results of this study, suggest that this change is more complex.

Static RBPJ sites did not appear to affect surrounding chromatin, as switching the activity of the Notch signaling pathway did not result in a change in active chromatin marks. Among the motifs enriched at the static sites was the Thap11 / Ronin motif, which is frequently found at housekeeping genes (Dejosez et al. 2023). Housekeeping genes maintain expression and are largely resistant to perturbations (Iyer et al. 2017) and a similar behavior is detectable for static sites upon Notch perturbation.

Furthermore, the studies by Aster's and Faryabi's groups also included ChIP-seq for NICD1, which had a comparable binding pattern to RBPJ (Wang et al. 2014; Petrovic et al. 2019). This leads to the hypothesis that the static RBPJ sites are still bound by NICD1 after 72

hours of GSI and therefore remain active and do not alter chromatin. However, genome-wide analysis of RBPJ binding in mature T-cells showed that loss of RBPJ also did not result in alteration of chromatin marks at the vast majority of RBPJ sites. These findings imply that only a subset of RBPJ sites, mainly dynamic ones, can alter surrounding chromatin.

In contrast, dynamic RBPJ sites showed a strong effect on surrounding chromatin upon changes in the Notch signaling pathway. This raises the question of why only some sites are responsive. The strong overlap of dynamic RBPJ with SEs could explain their stronger regulatory potential. Different studies highlight that SEs in general are very vulnerable to perturbation of their components, which can result in a collapse of the entire SE. This phenomenon can be explained as SEs form phase-separated multi-component complex and therefore are dependent on the integrity of their components (Hnisz et al. 2017; Sabari et al. 2018). In line with this, changes in Notch signaling in both Aster's and my data resulted in widespread alteration of the chromatin surrounding dynamic sites. The level of H3K27ac was strongly reduced upon Notch inactivation by GSI, even at peaks far away from the RBPJ site itself. This was especially prominent at the *Notch1* locus, where a whole 180 kb SE showed a reduced activity upon inactivation of the Notch pathway. Noteworthy, strong levels of H3K27ac were detectable at five RBPJ binding sites within this SE. This perturbation of the whole SE as a result of the reduced RBPJ binding could be explained by the absence of co-activators, like p300, which is associated with the formation SEs (Hnisz et al. 2017; Sen et al. 2019).

Another explanation for the responsive subset could be the interaction of RBPJ with its co-factors, as this interaction is crucial for the regulation of transcription and adjacent chromatin. Both, the groups of Stunnenberg and Aster, have shown that the HAT p300 is much stronger associated with dynamic sites (Castel et al. 2013; Wang et al. 2014). In addition to the co-activators, several co-repressors are known to interact with RBPJ for active repression of Notch target genes. These include SHARP, L3MBTL3 and KyoT2 (Taniguchi et al. 1998; Oswald et al. 2002; Xu et al. 2017). Genome-wide studies of L3MBTL3 and RBPJ binding in *Drosophila* showed that only a fraction of RBPJ sites are associated with L3MBTL3 binding (Xu et al. 2017). It remains to be seen, whether other co-repressors like SHARP have a larger co-occupancy with RBPJ.

Based on these results, it appears that the architecture of the chromatin is crucial for the responsiveness of RBPJ sites. It seems that responsive dynamic sites are mainly associated with broad enhancer regions, which are described to be sensitive to perturbations of factors

like p300. The unresponsive static sites are mainly associated with promoter regions, which are described to less vulnerable to perturbations. Lastly, the occupancy of co-factors remains to be elucidated.

### 4.6. Dynamic sites as a predictor of Notch target genes

A major challenge of studying the Notch signaling pathway is the diversity of its target genes. Different cell types or even just the crosstalk with other pathways strongly influence the transcriptional outcome of Notch signaling (Siebel and Lendahl 2017). Here it is important to note, that classical Notch target genes like *Hes1* are also regulated by other pathways (Borggrefe et al. 2016; Zheng et al. 2017). Therefore, defining general Notch target genes remains extremely difficult. This is particularly problematic because Notch signaling plays an important role in many types of cancer and thus understanding the transcriptional Notch response is important (Aster et al. 2017).

Different data sets showed that dynamic RBPJ sites are clearly associated with the major transcriptional response of the Notch pathway. These dynamic sites were mainly enhancer regions, suggesting that RBPJ binding to enhancers is likely more important for the transcriptional Notch response than binding to promoter regions (Fig. 40). This finding is in line by the work of Aster's group, which showed that dynamic binding at super-enhancers is a key factor in Notch-dependent regulation (Wang et al. 2014). An important question is how these dynamic RBPJ binding sites may affect the surrounding chromatin and genes in distances up to 100 kb from the actual binding site. The last chapter (4.5) already explained how whole SEs might be affected by reduced RBPJ binding and thus reduced p300 level. Furthermore, Faryabi's group has already shed light on the wide-ranging interactions associated with the Notch signaling pathway. They described the capability of Notch to regulate expression by directing the repositioning of enhancers and forming spatial hubs, adding another mechanism to Notch-mediated long-range regulation of transcription (Petrovic et al. 2019).

One alternative scenario is that another factor apart from RBPJ itself drives or influences these widespread chromatin changes. CTCF could potentially take this role. CTCF acts as an insulator for the spread of chromatin changes (Narendra et al. 2015) and is crucial for enhancer-promoter interactions (Ren et al. 2017). Furthermore, the Faryabi group showed

that approximately 50% of cohesin and CTCF-bound sites are overlapping with RBPJ binding sites, highlighting their importance for the long-term regulatory potential of RBPJ (Petrovic et al. 2019). It remains to be seen whether CTCF is regulating looping especially at dynamic RBPJ bound sites and therefore shape the regulatory potential of RBPJ sites.

Overall, there are several mechanisms that could contribute to RBPJ's remote regulatory potential, mainly related to the 3D chromatin architecture at RBPJ sites. To this end, the correct formation of regulatory hubs seems to be a key mechanism.

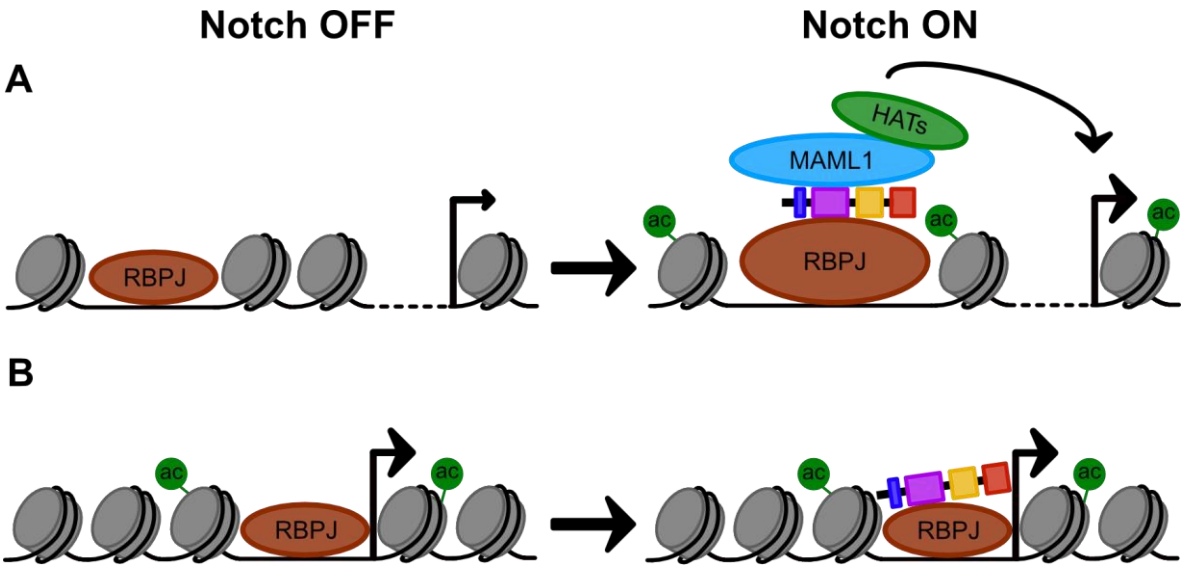


**Figure 40) Schematic representation of dynamic and static RBPJ binding sites.** A) Dynamic sites are mainly at enhancer regions and show increased binding and H3K27ac levels upon Notch activation. B) Static sites are mainly at promoter sites and the RBPJ binding level and H3K27ac are not affected by the Notch pathway. HAT = histone acetyltransferase; ac = acetylation of histone tails.

The number and fraction of dynamic binding sites differed greatly between the cell types analyzed, which can be due to technical reasons. Irrespective of this, they were characterized by comparable features. This leads to the question why the numbers differ that much. The different number of dynamic RBPJ sites can be easily explained by the strong differences in detectable RBPJ binding sites. Surprisingly, only ~1500 RBPJ binding sites were detectable in CUTLL1 cells, whereas IC8 cells had >45000 sites. An explanation for these differences could be a general more open chromatin conformation in some cell types, which would result in more accessible RBPJ sites and therefore more binding. The

different fraction of static and dynamic RBPJ sites could be explained by a different dose of Notch signaling between Beko (<5%) and other cell types (>18%). While Beko cells were treated with GSI for the detection of dynamic sites, all other cell types were cultured in GSI and the effects were measured after the washout of GSI. This method is described to result in a stronger peak of Notch signaling (intranuclear NICD1), as result of the accumulation of partially cleaved (NICD & TM without NECD) Notch proteins at the membrane upon extended exposure to GSI (Weng et al. 2006). The stronger peak of NICD1 and therefore an increased Notch response could explain the higher fraction of dynamic sites. Lasty, the availability of co-factors like p300 might also contribute to the different fractions of dynamic RBPJ sites, as p300 seems to be a characteristic for dynamic sites (Castel et al. 2013).

Surprisingly, regardless of the differences in number of dynamic RBPJ sites in various cell types, they can be predicted by a relatively simple approach using only RBPJ ChIP-seq data with a high accuracy and without any treatment (Fig. 35 & 36). Therefore, they might be suitable for identifying Notch target genes in cellular systems that are less well studied. The high variability of Notch target genes in different tissues makes the identification of specific Notch target genes challenging. In the past, the best way to identify Notch target genes was to test already known genes from other tissues or to perform various experiments, e.g. by RNA-seq upon inactivation or activation of the Notch pathway. This has led to problems in identifying Notch targets in different cancers. Daniel Mertens' group found that only 11 of the 35 postulated Notch target genes were significantly differentially expressed between patients with Notch1 activation mutation and patients without it in primary chronic lymphocytic leukemia data (Close et al. 2019). This further highlights the difficulty of precisely determining Notch target genes. Here, computational prediction of potential Notch target genes provides a useful tool for pre-selection of candidate genes. This will lead to easier and more efficient prediction of Notch target genes which in turn could be used as biomarkers for clinical use in the future.

### 4.7. A redefined model of the Notch pathway regulation

In this study, two different approaches were used to decipher the Notch signaling pathway. In chapter I, I have shown that there are different types of RBPJ/Notch target genes with distinct biological functions. In chapter II, I identified dynamic and static RBPJ binding sites and characterized their impact on chromatin and transcription. In order to get the holistic

picture of the Notch pathway, I combined both approaches. However, combining the two approaches is quite complicated because they do not involve the same biological set of methods. Nevertheless, several aspects are comparable.

First, the overlap of significantly deregulated genes upon Notch activation (MT cells) or inactivation (Beko cells) and RBPJ-associated genes was rather small in both cell types and publicly available data, suggesting that only a minority of RBPJ sites have a regulatory function for transcription in the Notch context. This was also supported by the observation that most sites were not able to affect surrounding chromatin. Consistent with this, the literature highlighted differences in occurrence of co-factors at RBPJ sites (Castel et al. 2013; Xu et al. 2017). Based on the complete absence of signals in MT cells depleted for RBPJ, it can be concluded that all sites are indeed genuine and do not reflect ChIP-seq artifacts like phantom peaks (Jain et al. 2015). In line with this, NICD1 ChIP-seq analysis showed clear co-localization of RBPJ and NICD1 at all RBPJ sites (Petrovic et al. 2019). Furthermore, the majority of RBPJ sites are located at promoter regions. In all analyzed systems, the transcriptional responsive sites are less associated with promoter sites. In summary, a large fraction of the promoter regions bound by RBPJ do not represent the classical Notch response. Exactly why this is the case remains speculative. One possibility is that these regions are so heavily populated with other factors that a RBPJ alone is not sufficient to affect the transcriptional response of these promoters.

Another group of RBPJ binding sites responds only to removal of RBPJ in MT cells but not to activation of Notch signaling (Fig. 38). Surprisingly, some of these genes were responsive to changes in the Notch pathway in other cellular systems. This indicates a set of cell type specific set of Notch-target genes, which remain repressed by RBPJ in other cell types.

A consistent feature of transcriptional-responsive RBPJ sites in Beko and MT cells, as well as in the other data sets analyzed, was a lower association with promoter sites compared to the unresponsive RBPJ sites. Dynamic sites in Beko cells were mainly (~75%) located at enhancer sites. Interestingly, cluster III in MT cells was also much more strongly associated with enhancer sites. However, the assumption that these are the only dynamically bound sites is too simplistic. Even though Beko and MT cells are both T-cell lines, only five Notch target genes (*Rasal1*, *Hes1*, *Dtx1*, *Il2ra*, *Hey1*) from Beko cells were found within the four clusters in MT cells. Surprisingly, only *Rasal1* and *Dtx1* were within the third cluster. Interestingly, RBPJ binding sites in I, II and III cluster showed overall an increased binding of RBPJ upon constant overexpression of NICD1, indicating some kind of dynamic binding.

Consistent with this, RBPJ binding sites with an increased binding upon Notch activation in MT cells were less associated with promoter regions and stronger associated with DEG. Taken together, dynamic RBPJ binding plays an important role in Notch-mediated transcriptional activation (Fig. 40). However, the question whether the enhanced binding contributes to activation or is a consequence of proper formation of the activator complex remains still open.

Finally, the group of Notch-responsive RBPJ-bound target genes can be divided into two groups. First, genes where RBPJ act as a repressor of transcription in the absence of Notch signaling like *Hes1* and *Hey1*. These sites are located predominantly in the proximity of promoter regions and have different response times upon Notch signaling. Second, RBPJ bound enhancers (e.g. at *Dtx1* and *Nrarp*), where RBPJ does not act as a repressor without Notch signaling, but merely enhances transcription upon Notch activation.

### 4.8. Computationally prediction of transcription factor targets

The majority of RBPJ binding sites were not associated with differentially expressed genes upon changes in the Notch pathway activity. This phenomenon was detectable in all cell types analyzed. As statistically expected, the cell types with higher numbers of RBPJ binding sites had an even lower association with DEGs. This is also obvious with other TFs, which have more than ten thousand binding sites, which most likely cannot regulate several thousand genes (Kang et al. 2022b). To disentangle the relation between TFs binding and gene expression is a challenging task. For individual sites, this is relatively easy, as one can mutate the binding site and measure the effect on the associated genes or use targeted CRISPR approaches (Pihlajamaa et al. 2023). A genome-wide approach is way more challenging, labor-intensive and costly because it requires different techniques such as RNA-seq, ChIP-seq and ideally long-range interaction studies (e.g. HiChIP). In this study, I developed a computational approach to narrow down and identify potential target genes. As shown in this work, this approach worked for Notch/RBPJ in many cell types, despite the fact that the different cell types had a high variation of the number of RBPJ binding sites (~1500 - ~45000). Based on these results the question arises whether a comparable approach could be applied to other TFs. This would be particularly useful for TFs, which have a wide variety of target genes depending on cell type or with different regulatory networks. A generally applicable prediction tool developed in one cell type could be useful

for the prediction in other cell types and furthermore increase the understanding of the regulatory mechanism of the given TF.

Wnt/β-catenin signaling represents a promising candidate for a comparable approach. This highly conserved pathway regulates its target genes primarily through interaction with TF of the T-cell factor (TCF) (Archbold et al. 2012). Comparably to RBPJ, TCF can switch is function from a repressor (in absence of Wnt signaling) to an activator (Ramakrishnan et al. 2018). Moreover, the transcriptional response of Wnt/β-catenin signaling is highly variable and dependent on the cellular context (Ramakrishnan and Cadigan 2017). Several genome-wide studies have shown that only a small subset of genes associated with β-cat binding sites were regulated by Wnt/β-catenin signaling (Watanabe et al. 2014; Nakamura et al. 2016). These results show a transcriptional phenomenon comparable to Notch/RBPJ and therefore the prediction of functional TCF/Wnt target genes may be feasible.

A similar problem is evident with one of the best characterized and studied TFs, p53. In a comprehensive study analyzing p53 binding sites in 12 cell lines, more than 8500 p53 binding signals were identified, of which 95% were conserved between cell types. Although the p53 binding motif was enriched in all peaks indicative of true p53 sites, the overall transcriptional response to ionizing radiation was not statistically correlated with the binding sites (Hafner et al. 2020). Consistent with this observation, another study showed that only a minority of previously identified p53 target genes are conserved between different cell types (Fischer 2017). Overall, p53 binding and transcriptional response are weakly linked, again demonstrating the importance of cell type-specific detection of TF target genes.

Several databases aim to summarize the information of TF binding and their corresponding target genes e.g. (Liska et al. 2022). This provides a useful tool for the understanding of transcription factor interactions with their target genes. However, to date, these databases are mainly based on manually annotated information, resulting in a severely limited number of TFs analyzed. In addition, cell type specific interactions of TFs add another layer of complexity, as many TFs have cell type specific target genes. Therefore, the cross-cell type annotation of TFs to their target genes lacks much of the information required to understand TF-mediated regulation in a cell type specific manner. In contrast, a computationally prediction for TF interactions would be useful for different TFs and could be applied in a cell type specific manner.

In summary, computational prediction of target genes would not only decrease the amount of work that is needed to identify target genes in new cell types but could also be useful to

elucidate general rules for how TFs interact with their target genes. Most likely, TF binding and its transcriptional outcome are subject to general rules, such as the importance of binding strength or the position of TF binding sites.

# 5. Outlook

This study provides an in-depth genome-wide analysis of the RBPJ/Notch target gene regulation. However, there are still several questions remaining. First, many of the findings put forward require further validation, in particular the function of RBPJ as a Notch-independent activator of transcription. Does RBPJ contribute to the transcription of these genes or is this finding a coincidence? Potential tissue specific interactors of RBPJ need be identified to understand the Notch-independent function of RBPJ.

One of the most fundamental questions is how specificity of Notch target genes is achieved and why only these target genes of Notch are responsive. So far, dynamic sites are essentially a category of RBPJ binding sites that are identifiable in different cell types and organisms. However, why dynamic sites in particular regulate transcription and chromatin remains to be elucidated. To answer this, the canonical and well-described regulatory potential of RBPJ/Notch needs to be further studied, for example with an inducible depletion of RBPJ. Furthermore, the correct forming of the co-factor complexes seems to be important, e.g. for the formation of phase-separated enhancer hubs. To this end, genome-wide binding of the known co-factors like SHARP, L3MBTL3, KyoT2 or p300, MAML in both Notch on and off systems may elucidate and explain the regulatory potential of RBPJ. In addition, acute depletion of certain co-factors may help to understand their function in a Notch-context dependent manner. It is likely that the chromatin environment is central, which needs to be further investigated by e.g. HiChIP. This could ultimately decipher how the Notch signaling pathway regulates so many different genes depending on the cellular context.

Finally, it needs to be tested whether a comparable predictive model to that developed in this study can be established for other transcription factors that regulate inducible gene expression.

# 6. Abbreviations

| | |
|---|---|
| °C | Degree Celsius |
| 4-OHT | (Z)-4-hydroxytamoxifen |
| ac | Acetylation of histone tails |
| ADAM | A disintegrin and metalloprotease |
| ANK | Ankyrin repeats |
| ATAC-seq | Assay for Transposase-Accessible Chromatin using sequencing |
| BAM | Binary Alignment Map |
| BC | Breast cancer |
| BHLH | Basic helix-loop-helix |
| bp | Base pairs |
| BP | Biological Process |
| BTD | β-trefoil domain |
| CGI | CpG islands |
| ChIP | Chromatin immunoprecipitation |
| ChIP-seq | Chromatin immunoprecipitation sequencing |
| CoR | Co-repressors |
| CSL | CBF1/Su(H)/Lag-1 |
| CTCF | CCCTC-binding factor |
| CTD | C-terminal domain |
| CUT&Tag | Cleavage Under Targets and Tagmentation |
| Cys | Cysteine |
| DAR | Differential accessibility region |
| DBR | Differentially bound region |
| DEG | Differentially expressed gene |
| DLL | Delta-like ligand |
| DN | Double negative |
| DNA | Deoxyribonucleic acid |
| dnMAML | Dominant negative mutant of MAML |
| DP | Double positive |
| DSL | Delta/Serrate/LAG-2 domain |
| EGF | Epidermal growth factor |
| EMSA | Electrophoretic mobility shift assay |
| ENCODE | ENCyclopedia Of DNA Elements |
| ER | Estrogen receptor |
| ETP | Early T-cell precursors |
| FC | Fold change |
| FCS | Fetal calf serum |
| g | Gramm |
| GEO | Gene Expression Omnibus |
| GFF | General Feature Format |
| GO | Gene Ontology |
| GRN | Gene regulatory network |
| GSEA | Gene set enrichment analysis |
| GSI | γ-secretase inhibitor |
| GTF | Genome transfer file |
| h | Hour |
| H2H | Head-to-head |
| HAT | Histone acetyltransferases |
| HD | Heterodimerization domain |
| HDAC | Histone deacetylases |
| HER2 | Human epidermal growth factor receptor 2 |
| HSC | Hematopoietic stem cell |
| IEL | Intestinal intraepithelial lymphocyte |
| IgG | Immunoglobulin G |
| iPSC | Induced pluripotent stem cells |

| | |
|---|---|
| JAG | Jagged |
| L | Liter |
| L3MBTL3 | Lethal(3)Malignant Brain Tumor-Like Protein 3 |
| LNR | Lin12 Notch repeats |
| M | Mol |
| MAML | Mastermind-like |
| me | Methylation of histone tails |
| min | Minutes |
| MM | Mismatch |
| MNNL | NOTCH ligand N-terminal domain |
| mRNA | Messenger ribonucleic acid |
| NCR | NOTCH cytokine response |
| NECD | Notch extracellular domain |
| NEXT | NOTCH extracellular truncation |
| NGS | Next generation sequencing |
| NICD | Notch intracellular domain |
| NICD1-ER | tamoxifen (4-OHT)-inducible NICD1 |
| NOCGI | Not overlapping with CpG island |
| NRR | Negative regulatory region |
| NSC | Neural stem cell |
| NSPC | Neural stem/progenitor cell |
| NTD | N-terminal domain |
| OCGI | Overlapping with CpG island |
| ORA | Over representation analysis |
| PCC | Pearson correlation coefficient |
| PDZL | Post-synaptic density protein ligand |
| PEST | Proline/glutamic acid/serine/threonine |
| PR | Progesterone receptor |
| PTF1A | Pancreas Associated Transcription Factor 1a |
| PTM | Posttranslational modification |
| RAM | Recombination binding protein-J -associated module |
| RBPJ | Recombination binding protein-J |
| REST | RE1-Silencing Transcription factor |
| ROC | Receiver operating characteristic |
| SAM | Sequence Alignment Maps |
| SBS | Sequencing by synthesis |
| SE | Super-enhancer |
| SHARP | SMRT/HDAC1 Associated Repressor Protein |
| SP | Single positive |
| SP1 | Specificity protein 1 |
| SPa | Single-pass |
| SUMO | Small ubiquitin-related modifier |
| TAD | Transactivation domain |
| T-ALL | T-cell acute lymphoblastic leukemia |
| TCF | T-cell factor |
| TCR | T-cell receptor |
| TEC | Thymic epithelial cell |
| TF | Transcription factor |
| TM | Transmembrane domain |
| TNBC | Triple negative breast cancer |
| TSS | Transcription start site |
| WH2HM | With head-to-head RBPJ motif |
| WT | Wild type |

# 7. Publication bibliography

Abramson, Vandana G.; Lehmann, Brian D.; Ballinger, Tarah J.; Pietenpol, Jennifer A. (2015): Subtyping of triple-negative breast cancer: implications for therapy. In *Cancer* 121 (1), pp. 8–16. DOI: 10.1002/cncr.28914.

Adhikari, Neeta; Basi, David L.; Townsend, Dewayne; Rusch, Melissa; Mariash, Ami; Mullegama, Sureni et al. (2010): Heparan sulfate Ndst1 regulates vascular smooth muscle cell proliferation, vessel size and vascular remodeling. In *Journal of molecular and cellular cardiology* 49 (2), pp. 287–293. DOI: 10.1016/j.yjmcc.2010.02.022.

Adler, Scott H.; Chiffoleau, Elise; Xu, Lanwei; Dalton, Nicole M.; Burg, Jennifer M.; Wells, Andrew D. et al. (2003): Notch signaling augments T cell responsiveness by enhancing CD25 expression. In *Journal of immunology (Baltimore, Md. : 1950)* 171 (6), pp. 2896–2903. DOI: 10.4049/jimmunol.171.6.2896.

Agrawal, Smita; Archer, Colin; Schaffer, David V. (2009): Computational models of the Notch network elucidate mechanisms of context-dependent signaling. In *PLoS computational biology* 5 (5), e1000390. DOI: 10.1371/journal.pcbi.1000390.

Ahrendt, S. A.; Halachmi, S.; Chow, J. T.; Wu, L.; Halachmi, N.; Yang, S. C. et al. (1999): Rapid p53 sequence analysis in primary lung cancer using an oligonucleotide probe array. In *Proceedings of the National Academy of Sciences of the United States of America* 96 (13), pp. 7382–7387. DOI: 10.1073/pnas.96.13.7382.

Alberts, Bruce; Johnson, Alexander; Lewis, Julian; Raff, Martin; Roberts, Keith; Walter, Peter (2002): Chromosomal DNA and Its Packaging in the Chromatin Fiber: Garland Science.

Alitalo, K.; Bishop, J. M.; Smith, D. H.; Chen, E. Y.; Colby, W. W.; Levinson, A. D. (1983): Nucleotide sequence to the v-myc oncogene of avian retrovirus MC29. In *Proceedings of the National Academy of Sciences of the United States of America* 80 (1), pp. 100–104. DOI: 10.1073/pnas.80.1.100.

Allfrey, V.G; Faulker, R.; Mirsky, A. E. (1964): Acetylation and Methylation of Histones and their possible role in the regulation of RNA synthesis. In *Proceedings of the National Academy of Sciences of the United States of America* 51, pp. 786–794. DOI: 10.1073/pnas.51.5.786.

Amemiya, Haley M.; Kundaje, Anshul; Boyle, Alan P. (2019): The ENCODE Blacklist: Identification of Problematic Regions of the Genome. In *Sci Rep* 9 (1). DOI: 10.1038/s41598-019-45839-z.

Andersen, Jens P.; Vestergaard, Anna L.; Mikkelsen, Stine A.; Mogensen, Louise S.; Chalat, Madhavan; Molday, Robert S. (2016): P4-ATPases as Phospholipid Flippases-Structure, Function, and Enigmas. In *Frontiers in physiology* 7, p. 275. DOI: 10.3389/fphys.2016.00275.

Andrés, M. E.; Burger, C.; Peral-Rubio, M. J.; Battaglioli, E.; Anderson, M. E.; Grimes, J. et al. (1999): CoREST: a functional corepressor required for regulation of neural-specific gene expression. In *Proceedings of the National Academy of Sciences of the United States of America* 96 (17), pp. 9873–9878. DOI: 10.1073/pnas.96.17.9873.

Andrews, S.; Krueger, F.; Segonds-Pichon, A.; Biggins, L.; Krueger, C.; Wingett, S. (2020): FastQC: a quality control tool for high throughput sequence data [Online]. 2010. In *Avilable from: http://www. bioinformatics. babraham. ac. uk/projects/fastqc/. Accessed* 27.

Archbold, H. C.; Yang, Y. X.; Chen, L.; Cadigan, K. M. (2012): How do they do Wnt they do?: regulation of transcription by the Wnt/β-catenin pathway. In *Acta physiologica (Oxford, England)* 204 (1), pp. 74–109. DOI: 10.1111/j.1748-1716.2011.02293.x.

Arruga, Francesca; Vaisitti, Tiziana; Deaglio, Silvia (2018): The NOTCH Pathway and Its Mutations in Mature B Cell Malignancies. In *Frontiers in oncology* 8, p. 550. DOI: 10.3389/fonc.2018.00550.

Artavanis-Tsakonas, S.; Muskavitch, M. A.; Yedvobnick, B. (1983): Molecular cloning of Notch, a locus affecting neurogenesis in Drosophila melanogaster. In *Proceedings of the National Academy of Sciences* 80 (7), pp. 1977–1981. DOI: 10.1073/pnas.80.7.1977.

Artavanis-Tsakonas, S.; Rand, M. D.; Lake, R. J. (1999): Notch signaling: cell fate control and signal integration in development. In *Science (New York, N.Y.)* 284 (5415), pp. 770–776. DOI: 10.1126/science.284.5415.770.

Aster, J.; Pear, W.; Hasserjian, R.; Erba, H.; Davi, F.; Luo, B. et al. (1994): Functional analysis of the TAN-1 gene, a human homolog of Drosophila notch. In *Cold Spring Harbor symposia on quantitative biology* 59, pp. 125–136.

Aster, Jon C.; Pear, Warren S.; Blacklow, Stephen C. (2017): The Varied Roles of Notch in Cancer. In *Annual review of pathology* 12, pp. 245–275. DOI: 10.1146/annurev-pathol-052016-100127.

Austin, J.; Kimble, J. (1989): Transcript analysis of glp-1 and lin-12, homologous genes required for cell interactions during development of C. elegans. In *Cell* 58 (3), pp. 565–571. DOI: 10.1016/0092-8674(89)90437-6.

Axelrod, J. D.; Matsuno, K.; Artavanis-Tsakonas, S.; Perrimon, N. (1996): Interaction between Wingless and Notch signaling pathways mediated by dishevelled. In *Science (New York, N.Y.)* 271 (5257), pp. 1826–1832. DOI: 10.1126/science.271.5257.1826.

Bae, Sunhee; Lesch, Bluma J. (2020): H3K4me1 Distribution Predicts Transcription State and Poising at Promoters. In *Frontiers in cell and developmental biology* 8, p. 289. DOI: 10.3389/fcell.2020.00289.

Bai, Jing; Khajavi, Mehrdad; Sui, Lufei; Fu, Haojie; Tarakkad Krishnaji, Subrahmanian; Birsner, Amy E. et al. (2021): Angiogenic responses in a 3D micro-engineered environment of primary endothelial cells and pericytes. In *Angiogenesis* 24 (1), pp. 111–127. DOI: 10.1007/s10456-020-09746-6.

Bailey, Timothy L.; Boden, Mikael; Buske, Fabian A.; Frith, Martin; Grant, Charles E.; Clementi, Luca et al. (2009): MEME SUITE: tools for motif discovery and searching. In *Nucleic acids research* 37 (Web Server issue), W202-8. DOI: 10.1093/nar/gkp335.

Bailis, Will; Yashiro-Ohtani, Yumi; Pear, Warren S. (2014): Identifying direct Notch transcriptional targets using the GSI-washout assay. In *Methods in molecular biology (Clifton, N.J.)* 1187, pp. 247–254. DOI: 10.1007/978-1-4939-1139-4_19.

Bannister, Andrew J.; Kouzarides, Tony (2011): Regulation of chromatin by histone modifications. In *Cell research* 21 (3), pp. 381–395. DOI: 10.1038/cr.2011.22.

Bannister, Andrew J.; Schneider, Robert; Myers, Fiona A.; Thorne, Alan W.; Crane-Robinson, Colyn; Kouzarides, Tony (2005): Spatial distribution of di- and tri-methyl lysine 36 of histone H3 at active genes. In *The Journal of biological chemistry* 280 (18), pp. 17732–17736. DOI: 10.1074/jbc.M500796200.

Bartels, Stefanie J. J.; Spruijt, Cornelia G.; Brinkman, Arie B.; Jansen, Pascal W. T. C.; Vermeulen, Michiel; Stunnenberg, Hendrik G. (2011): A SILAC-based screen for Methyl-CpG binding proteins identifies RBP-J as a DNA methylation and sequence-specific binding protein. In *PloS one* 6 (10), e25884. DOI: 10.1371/journal.pone.0025884.

Benjamini, Yoav; Hochberg, Yosef (1995): Controlling the False Discovery Rate: A Practical and Powerful Approach to Multiple Testing. In *Journal of the Royal Statistical Society: Series B (Methodological)* 57 (1), pp. 289–300. DOI: 10.1111/j.2517-6161.1995.tb02031.x.

Bernasconi-Elias, P.; Hu, T.; Jenkins, D.; Firestone, B.; Gans, S.; Kurth, E. et al. (2016): Characterization of activating mutations of NOTCH3 in T-cell acute lymphoblastic leukemia and anti-leukemic activity of NOTCH3 inhibitory antibodies. In *Oncogene* 35 (47), pp. 6077–6086. DOI: 10.1038/onc.2016.133.

Bestor, T.; Laudano, A.; Mattaliano, R.; Ingram, V. (1988): Cloning and sequencing of a cDNA encoding DNA methyltransferase of mouse cells. The carboxyl-terminal domain of the mammalian enzymes is related to bacterial restriction methyltransferases. In *Journal of molecular biology* 203 (4), pp. 971–983. DOI: 10.1016/0022-2836(88)90122-2.

Beverly, Levi J.; Capobianco, Anthony J. (2003): Perturbation of Ikaros isoform selection by MLV integration is a cooperative event in Notch(IC)-induced T cell leukemogenesis. In *Cancer cell* 3 (6), pp. 551–564. DOI: 10.1016/S1535-6108(03)00137-5.

Bian, Weixiang; Tang, Mengfan; Jiang, Hua; Xu, Wenyan; Hao, Wanyu; Sui, Yue et al. (2021): Low-density-lipoprotein-receptor-related protein 1 mediates Notch pathway activation. In *Developmental cell* 56 (20), 2902-2919.e8. DOI: 10.1016/j.devcel.2021.09.015.

Bird, A.; Taggart, M.; Frommer, M.; Miller, O. J.; Macleod, D. (1985): A fraction of the mouse genome that is derived from islands of nonmethylated, CpG-rich DNA. In *Cell* 40 (1), pp. 91–99. DOI: 10.1016/0092-8674(85)90312-5.

Blokzijl, Andries; Dahlqvist, Camilla; Reissmann, Eva; Falk, Anna; Moliner, Annalena; Lendahl, Urban; Ibáñez, Carlos F. (2003): Cross-talk between the Notch and TGF-beta signaling pathways mediated by interaction of the Notch intracellular domain with Smad3. In *The Journal of cell biology* 163 (4), pp. 723–728. DOI: 10.1083/jcb.200305112.

Bloomfield, V. A. (1996): DNA condensation. In *Current opinion in structural biology* 6 (3), pp. 334–341. DOI: 10.1016/s0959-440x(96)80052-2.

Boeger, Hinrich; Bushnell, David A.; Davis, Ralph; Griesenbeck, Joachim; Lorch, Yahli; Strattan, J. Seth et al. (2005): Structural basis of eukaryotic gene transcription. In *FEBS letters* 579 (4), pp. 899–903. DOI: 10.1016/j.febslet.2004.11.027.

Borggrefe, T.; Oswald, F. (2009): The Notch signaling pathway: transcriptional regulation at Notch target genes. In *Cellular and molecular life sciences : CMLS* 66 (10), pp. 1631–1646. DOI: 10.1007/s00018-009-8668-7.

Borggrefe, Tilman; Lauth, Matthias; an Zwijsen; Huylebroeck, Danny; Oswald, Franz; Giaimo, Benedetto Daniele (2016): The Notch intracellular domain integrates signals from Wnt, Hedgehog, TGFβ/BMP and hypoxia pathways. In *Biochimica et biophysica acta* 1863 (2), pp. 303–313. DOI: 10.1016/j.bbamcr.2015.11.020.

Brasset, E.; Vaury, C. (2005): Insulators are fundamental components of the eukaryotic genomes. In *Heredity* 94 (6), pp. 571–576. DOI: 10.1038/sj.hdy.6800669.

Brou, C.; Logeat, F.; Gupta, N.; Bessia, C.; LeBail, O.; Doedens, J. R. et al. (2000): A novel proteolytic cleavage involved in Notch signaling: the role of the disintegrin-metalloprotease TACE. In *Molecular cell* 5 (2), pp. 207–216.

Brown, S. W. (1966): Heterochromatin. In *Science (New York, N.Y.)* 151 (3709), pp. 417–425. DOI: 10.1126/science.151.3709.417.

Buenrostro, Jason D.; Wu, Beijing; Chang, Howard Y.; Greenleaf, William J. (2015): ATAC-seq: A Method for Assaying Chromatin Accessibility Genome-Wide. In *Current protocols in molecular biology* 109, 21.29.1-21.29.9. DOI: 10.1002/0471142727.mb2129s109.

Bumgarner, Roger (2013): Overview of DNA microarrays: types, applications, and their future. In *Current protocols in molecular biology* Chapter 22, Unit 22.1. DOI: 10.1002/0471142727.mb2201s101.

Buschbeck, Marcus; Hake, Sandra B. (2017): Variants of core histones and their roles in cell fate decisions, development and cancer. In *Nature reviews. Molecular cell biology* 18 (5), pp. 299–314. DOI: 10.1038/nrm.2016.166.

Bushweller, John H. (2019): Targeting transcription factors in cancer - from undruggable to reality. In *Nature reviews. Cancer* 19 (11), pp. 611–624. DOI: 10.1038/s41568-019-0196-7.

Canté-Barrett, Kirsten; Holtzer, Laurent; van Ooijen, Henk; Hagelaar, Rico; Cordo', Valentina; Verhaegh, Wim et al. (2020): A Molecular Test for Quantifying Functional Notch Signaling Pathway Activity in Human Cancer. In *Cancers* 12 (11). DOI: 10.3390/cancers12113142.

Carrieri, Francesca A.; Dale, Jacqueline Kim (2016): Turn It Down a Notch. In *Frontiers in cell and developmental biology* 4, p. 151. DOI: 10.3389/fcell.2016.00151.

Castel, David; Mourikis, Philippos; Bartels, Stefanie J. J.; Brinkman, Arie B.; Tajbakhsh, Shahragim; Stunnenberg, Hendrik G. (2013): Dynamic binding of RBPJ is determined by Notch signaling status. In *Genes & development* 27 (9), pp. 1059–1071. DOI: 10.1101/gad.211912.112.

Chen, Junchen; Dong, Xiaoxue; Cheng, Xuejun; Zhu, Qiang; Zhang, Jinyu; Li, Qian et al. (2021): Ogt controls neural stem/progenitor cell pool and adult neurogenesis through modulating Notch signaling. In *Cell reports* 34 (13), p. 108905. DOI: 10.1016/j.celrep.2021.108905.

Cheung, P.; Allis, C. D.; Sassone-Corsi, P. (2000): Signaling to chromatin through histone modifications. In *Cell* 103 (2), pp. 263–271. DOI: 10.1016/S0092-8674(00)00118-5.

Ciofani, Maria; Knowles, Gisèle C.; Wiest, David L.; Boehmer, Harald von; Zúñiga-Pflücker, Juan Carlos (2006): Stage-specific and differential notch dependency at the alphabeta and gammadelta T lineage bifurcation. In *Immunity* 25 (1), pp. 105–116. DOI: 10.1016/j.immuni.2006.05.010.

Close, Viola; Close, William; Kugler, Sabrina Julia; Reichenzeller, Michaela; Yosifov, Deyan Yordanov; Bloehdorn, Johannes et al. (2019): FBXW7 mutations reduce binding of NOTCH1, leading to cleaved NOTCH1 accumulation and target gene activation in CLL. In *Blood* 133 (8), pp. 830–839. DOI: 10.1182/blood-2018-09-874529.

Coffman, C.; Harris, W.; Kintner, C. (1990): Xotch, the Xenopus homolog of Drosophila notch. In *Science (New York, N.Y.)* 249 (4975), pp. 1438–1441. DOI: 10.1126/science.2402639.

Colombo, Michela; Mirandola, Leonardo; Chiriva-Internati, Maurizio; Basile, Andrea; Locati, Massimo; Lesma, Elena et al. (2018): Cancer Cells Exploit Notch Signaling to Redefine a Supportive Cytokine Milieu. In *Frontiers in immunology* 9. DOI: 10.3389/fimmu.2018.01823.

Crick, F. H. C.; Barnett, L, Brenner, S.; Watts-Tobin, R. J. (1961): General Nature of the Genetic Code for Proteins. In *Nature* 192, pp. 1227–1232. DOI: 10.1038/1921227a0.

Curry, Christine L.; Reed, Laura L.; Nickoloff, Brian J.; Miele, Lucio; Foreman, Kimberly E. (2006): Notch-independent regulation of Hes-1 expression by c-Jun N-terminal kinase signaling in human endothelial cells. In *Laboratory investigation; a journal of technical methods and pathology* 86 (8), pp. 842–852. DOI: 10.1038/labinvest.3700442.

Davis, Sean; Meltzer, Paul S. (2007): GEOquery: a bridge between the Gene Expression Omnibus (GEO) and BioConductor. In *Bioinformatics (Oxford, England)* 23 (14), pp. 1846–1847. DOI: 10.1093/bioinformatics/btm254.

Dejosez, Marion; Dall'Agnese, Alessandra; Ramamoorthy, Mahesh; Platt, Jesse; Yin, Xing; Hogan, Megan et al. (2023): Regulatory architecture of housekeeping genes is driven by promoter assemblies. In *Cell reports* 42 (5), p. 112505. DOI: 10.1016/j.celrep.2023.112505.

del Amo, F. F.; Gendron-Maguire, M.; Swiatek, P. J.; Jenkins, N. A.; Copeland, N. G.; Gridley, T. (1993): Cloning, analysis, and chromosomal localization of Notch-1, a mouse homolog of Drosophila Notch. In *Genomics* 15 (2), pp. 259–264. DOI: 10.1006/geno.1993.1055.

Dell'Aringa, Mark; Reinhardt, R. Lee (2018): Notch signaling represents an important checkpoint between follicular T-helper and canonical T-helper 2 cell fate. In *Mucosal immunology* 11 (4), pp. 1079–1091. DOI: 10.1038/s41385-018-0012-9.

Dent, Rebecca; Trudeau, Maureen; Pritchard, Kathleen I.; Hanna, Wedad M.; Kahn, Harriet K.; Sawka, Carol A. et al. (2007): Triple-negative breast cancer: clinical features and patterns of recurrence. In *Clinical cancer research : an official journal of the American Association for Cancer Research* 13 (15 Pt 1), pp. 4429–4434. DOI: 10.1158/1078-0432.CCR-06-3045.

Dexter, John S. (1914): The Analysis of a Case of Continuous Variation in Drosophila by a Study of Its Linkage Relations. In *The American Naturalist* 48 (576), pp. 712–758. DOI: 10.1086/279446.

Dray, Nicolas; Mancini, Laure; Binshtok, Udi; Cheysson, Felix; Supatto, Willy; Mahou, Pierre et al. (2021): Dynamic spatiotemporal coordination of neural stem cell fate decisions occurs through local feedback in the adult vertebrate brain. In *Cell stem cell* 28 (8), 1457-1472.e12. DOI: 10.1016/j.stem.2021.03.014.

Dreval, Kostiantyn; Lake, Robert J.; Fan, Hua-Ying (2022): Analyzing the Interaction of RBPJ with Mitotic Chromatin and Its Impact on Transcription Reactivation upon Mitotic Exit. In *Methods in molecular biology (Clifton, N.J.)* 2472, pp. 95–108. DOI: 10.1007/978-1-0716-2201-8_9.

D'Souza, Brendan; Meloty-Kapella, Laurence; Weinmaster, Gerry (2010): Canonical and non-canonical Notch ligands. In *Current topics in developmental biology* 92, pp. 73–129. DOI: 10.1016/S0070-2153(10)92003-6.

Dumortier, Alexis; Jeannet, Robin; Kirstetter, Peggy; Kleinmann, Eva; Sellars, MacLean; dos Santos, Nuno R. et al. (2006): Notch activation is an early and critical event during T-Cell leukemogenesis in Ikaros-deficient mice. In *Molecular and cellular biology* 26 (1), pp. 209–220. DOI: 10.1128/MCB.26.1.209-220.2006.

Edgar, Ron; Domrachev, Michael; Lash, Alex E. (2002): Gene Expression Omnibus: NCBI gene expression and hybridization array data repository. In *Nucleic acids research* 30 (1), pp. 207–210. DOI: 10.1093/nar/30.1.207.

Ehm, Oliver; Göritz, Christian; Covic, Marcela; Schäffner, Iris; Schwarz, Tobias J.; Karaca, Esra et al. (2010): RBPJkappa-dependent signaling is essential for long-term maintenance of neural stem cells in the adult hippocampus. In *The Journal of neuroscience : the official journal of the Society for Neuroscience* 30 (41), pp. 13794–13807. DOI: 10.1523/JNEUROSCI.1567-10.2010.

Ehrlich, M.; Gama-Sosa, M. A.; Huang, L. H.; Midgett, R. M.; Kuo, K. C.; McCune, R. A.; Gehrke, C. (1982): Amount and distribution of 5-methylcytosine in human DNA from different types of tissues of cells. In *Nucleic acids research* 10 (8), pp. 2709–2721. DOI: 10.1093/nar/10.8.2709.

Ellisen, L. W.; Bird, J.; West, D. C.; Soreng, A. L.; Reynolds, T. C.; Smith, S. D.; Sklar, J. (1991): TAN-1, the human homolog of the Drosophila notch gene, is broken by chromosomal translocations in T lymphoblastic neoplasms. In *Cell* 66 (4), pp. 649–661. DOI: 10.1016/0092-8674(91)90111-b.

ENCODE Project Consortium (2012): An integrated encyclopedia of DNA elements in the human genome. In *Nature* 489 (7414), pp. 57–74. DOI: 10.1038/nature11247.

Ernst, Jason; Kellis, Manolis (2017): Chromatin-state discovery and genome annotation with ChromHMM. In *Nature protocols* 12 (12), pp. 2478–2492. DOI: 10.1038/nprot.2017.124.

Fan, Linlin; Liu, Hao; Zhu, Guofu; Singh, Shekhar; Yu, Ze; Wang, Shumin et al. (2022): Caspase-4/11 is critical for angiogenesis by repressing Notch1 signalling via inhibiting γ-secretase activity. In *British journal of pharmacology* 179 (20), pp. 4809–4828. DOI: 10.1111/bph.15904.

Feng, Xin; Grossman, Robert; Stein, Lincoln (2011): PeakRanger: a cloud-enabled peak caller for ChIP-seq data. In *BMC bioinformatics* 12, p. 139. DOI: 10.1186/1471-2105-12-139.

Fernández-Majada, V.; Aguilera, C.; Villanueva, A.; Vilardell, F.; Robert-Moreno, A.; Aytés, A. et al. (2007): Nuclear IKK activity leads to dysregulated notch-dependent gene expression in colorectal cancer. In *Proceedings of the National Academy of Sciences of the United States of America* 104 (1), pp. 276–281. DOI: 10.1073/pnas.0606476104.

Ferrante, Francesca; Giaimo, Benedetto Daniele; Bartkuhn, Marek; Zimmermann, Tobias; Close, Viola; Mertens, Daniel et al. (2020): HDAC3 functions as a positive regulator in Notch signal transduction. In *Nucleic acids research* 48 (7), pp. 3496–3512. DOI: 10.1093/nar/gkaa088.

Ferrante, Francesca; Giaimo, Benedetto Daniele; Friedrich, Tobias; Sugino, Toshiya; Mertens, Daniel; Kugler, Sabrina et al. (2022): Hydroxylation of the NOTCH1 intracellular domain regulates Notch signaling dynamics. In *Cell death & disease* 13 (7), p. 600. DOI: 10.1038/s41419-022-05052-9.

Filippova, G. N.; Fagerlie, S.; Klenova, E. M.; Myers, C.; Dehner, Y.; Goodwin, G. et al. (1996): An exceptionally conserved transcriptional repressor, CTCF, employs different combinations of zinc fingers to bind diverged promoter sequences of avian and mammalian c-myc oncogenes. In *Molecular and cellular biology* 16 (6), pp. 2802–2813. DOI: 10.1128/MCB.16.6.2802.

Finch, J. T.; Klug, A. (1976): Solenoidal model for superstructure in chromatin. In *Proceedings of the National Academy of Sciences of the United States of America* 73 (6), pp. 1897–1901. DOI: 10.1073/pnas.73.6.1897.

Fischer, Andreas; Gessler, Manfred (2007): Delta-Notch--and then? Protein interactions and proposed modes of repression by Hes and Hey bHLH factors. In *Nucleic acids research* 35 (14), pp. 4583–4596. DOI: 10.1093/nar/gkm477.

Fischer, M. (2017): Census and evaluation of p53 target genes. In *Oncogene* 36 (28), pp. 3943–3956. DOI: 10.1038/onc.2016.502.

Friedrich, Tobias; Ferrante, Francesca; Pioger, Léo; Nist, Andrea; Stiewe, Thorsten; Andrau, Jean-Christophe et al. (2022): Notch-dependent and -independent functions of transcription factor RBPJ. In *Nucleic acids research* 50 (14), pp. 7925–7937. DOI: 10.1093/nar/gkac601.

Fryer, Christy J.; White, J. Brandon; Jones, Katherine A. (2004): Mastermind recruits CycC:CDK8 to phosphorylate the Notch ICD and coordinate activation with turnover. In *Molecular cell* 16 (4), pp. 509–520. DOI: 10.1016/j.molcel.2004.10.014.

Furey, Terrence S. (2012): ChIP-seq and beyond: new and improved methodologies to detect and characterize protein-DNA interactions. In *Nature reviews. Genetics* 13 (12), pp. 840–852. DOI: 10.1038/nrg3306.

Furriols, M.; Bray, S. (2001): A model Notch response element detects Suppressor of Hairless-dependent molecular switch. In *Current biology : CB* 11 (1), pp. 60–64. DOI: 10.1016/S0960-9822(00)00044-0.

Gallahan, D.; Callahan, R. (1997): The mouse mammary tumor associated gene INT3 is a unique member of the NOTCH gene family (NOTCH4). In *Oncogene* 14 (16), pp. 1883–1890. DOI: 10.1038/sj.onc.1201035.

Gao, Fei; Zhang, YuQin; Wang, ShengChun; Liu, YuanQiang; Zheng, Lin; Yang, JianQuan et al. (2014): Hes1 is involved in the self-renewal and tumourigenicity of stem-like cancer cells in colon cancer. In *Sci Rep* 4, p. 3963. DOI: 10.1038/srep03963.

Garbe, Annette I.; Krueger, Andreas; Gounari, Fotini; Zúñiga-Pflücker, Juan Carlos; Boehmer, Harald von (2006): Differential synergy of Notch and T cell receptor signaling determines alphabeta versus gammadelta lineage fate. In *The Journal of experimental medicine* 203 (6), pp. 1579–1590. DOI: 10.1084/jem.20060474.

García-Peydró, Marina; Fuentes, Patricia; Mosquera, Marta; García-León, María J.; Alcain, Juan; Rodríguez, Antonio et al. (2018): The NOTCH1/CD44 axis drives pathogenesis in a T cell acute lymphoblastic leukemia model. In *The Journal of clinical investigation* 128 (7), pp. 2802–2818. DOI: 10.1172/JCI92981.

Gaston, K.; Jayaraman, P. S. (2003): Transcriptional repression in eukaryotes: repressors and repression mechanisms. In *Cellular and molecular life sciences : CMLS* 60 (4), pp. 721–741. DOI: 10.1007/s00018-003-2260-3.

Gavrilov, Alexey; Razin, Sergey V.; Cavalli, Giacomo (2015): In vivo formaldehyde cross-linking: it is time for black box analysis. In *Briefings in functional genomics* 14 (2), pp. 163–165. DOI: 10.1093/bfgp/elu037.

Gazave, Eve; Lapébie, Pascal; Richards, Gemma S.; Brunet, Frédéric; Ereskovsky, Alexander V.; Degnan, Bernard M. et al. (2009): Origin and evolution of the Notch signalling pathway: an overview from eukaryotic genomes. In *BMC evolutionary biology* 9, p. 249. DOI: 10.1186/1471-2148-9-249.

George, Julie; Lim, Jing Shan; Jang, Se Jin; Cun, Yupeng; Ozretić, Luka; Kong, Gu et al. (2015): Comprehensive genomic profiles of small cell lung cancer. In *Nature* 524 (7563), pp. 47–53. DOI: 10.1038/nature14664.

Giaimo, Benedetto Daniele; Ferrante, Francesca; Borggrefe, Tilman (2017): Chromatin Immunoprecipitation (ChIP) in Mouse T-cell Lines. In *Journal of visualized experiments : JoVE* (124). DOI: 10.3791/55907.

Giaimo, Benedetto Daniele; Ferrante, Francesca; Herchenröther, Andreas; Hake, Sandra B.; Borggrefe, Tilman (2019): The histone variant H2A.Z in gene regulation. In *Epigenetics & chromatin* 12 (1), p. 37. DOI: 10.1186/s13072-019-0274-9.

Giaimo, Benedetto Daniele; Ferrante, Francesca; Vallejo, Diana M.; Hein, Kerstin; Gutierrez-Perez, Irene; Nist, Andrea et al. (2018): Histone variant H2A.Z deposition and acetylation directs the canonical Notch signaling response. In *Nucleic acids research* 46 (16), pp. 8197–8215. DOI: 10.1093/nar/gky551.

Giebel, B.; Campos-Ortega, J. A. (1997): Functional dissection of the Drosophila enhancer of split protein, a suppressor of neurogenesis. In *Proceedings of the National Academy of Sciences of the United States of America* 94 (12), pp. 6250–6254. DOI: 10.1073/pnas.94.12.6250.

Gillette, Thomas G.; Hill, Joseph A. (2015): Readers, writers, and erasers: chromatin as the whiteboard of heart disease. In *Circulation research* 116 (7), pp. 1245–1253. DOI: 10.1161/CIRCRESAHA.116.303630.

Gomez-Lamarca, Maria J.; Falo-Sanjuan, Julia; Stojnic, Robert; Abdul Rehman, Sohaib; Muresan, Leila; Jones, Matthew L. et al. (2018): Activation of the Notch Signaling Pathway In Vivo Elicits Changes in CSL Nuclear Dynamics. In *Developmental cell* 44 (5), 611-623.e7. DOI: 10.1016/j.devcel.2018.01.020.

González-García, Sara; García-Peydró, Marina; Martín-Gayo, Enrique; Ballestar, Esteban; Esteller, Manel; Bornstein, Rafael et al. (2009): CSL-MAML-dependent Notch1 signaling controls T lineage-specific IL-7R{alpha} gene expression in early human thymopoiesis and leukemia. In *The Journal of experimental medicine* 206 (4), pp. 779–791. DOI: 10.1084/jem.20081922.

Gordon, Wendy R.; Arnett, Kelly L.; Blacklow, Stephen C. (2008): The molecular logic of Notch signaling--a structural and biochemical perspective. In *Journal of cell science* 121 (Pt 19), pp. 3109–3119. DOI: 10.1242/jcs.035683.

Grimes, J. A.; Nielsen, S. J.; Battaglioli, E.; Miska, E. A.; Speh, J. C.; Berry, D. L. et al. (2000): The co-repressor mSin3A is a functional component of the REST-CoREST repressor complex. In *The Journal of biological chemistry* 275 (13), pp. 9461–9467. DOI: 10.1074/jbc.275.13.9461.

Guarani, Virginia; Deflorian, Gianluca; Franco, Claudio A.; Krüger, Marcus; Phng, Li-Kun; Bentley, Katie et al. (2011): Acetylation-dependent regulation of endothelial Notch signalling by the SIRT1 deacetylase. In *Nature* 473 (7346), pp. 234–238. DOI: 10.1038/nature09917.

Guo, Yin; Luan, Liming; Patil, Naeem K.; Sherwood, Edward R. (2017): Immunobiology of the IL-15/IL-15Rα complex as an antitumor and antiviral agent. In *Cytokine & growth factor reviews* 38, pp. 10–21. DOI: 10.1016/j.cytogfr.2017.08.002.

Gupta-Rossi, N.; Le Bail, O.; Gonen, H.; Brou, C.; Logeat, F.; Six, E. et al. (2001): Functional interaction between SEL-10, an F-box protein, and the nuclear form of activated Notch1 receptor. In *The Journal of biological chemistry* 276 (37), pp. 34371–34378. DOI: 10.1074/jbc.M101343200.

Gustafsson, Maria V.; Zheng, Xiaowei; Pereira, Teresa; Gradin, Katarina; Jin, Shaobo; Lundkvist, Johan et al. (2005): Hypoxia requires notch signaling to maintain the undifferentiated cell state. In *Developmental cell* 9 (5), pp. 617–628. DOI: 10.1016/j.devcel.2005.09.010.

H Backman, Tyler W.; Girke, Thomas (2016): systemPipeR: NGS workflow and report generation environment. In *BMC bioinformatics* 17, p. 388. DOI: 10.1186/s12859-016-1241-0.

Hafner, Antonina; Kublo, Lyubov; Tsabar, Michael; Lahav, Galit; Stewart-Ornstein, Jacob (2020): Identification of universal and cell-type specific p53 DNA binding. In *BMC molecular and cell biology* 21 (1), p. 5. DOI: 10.1186/s12860-020-00251-8.

Hahne, Florian; Ivanek, Robert (2016): Visualizing Genomic Data Using Gviz and Bioconductor. In *Methods in molecular biology (Clifton, N.J.)* 1418, pp. 335–351. DOI: 10.1007/978-1-4939-3578-9_16.

Hall, Daniel; Giaimo, Benedetto Daniele; Park, Sung-Soo; Hemmer, Wiebke; Friedrich, Tobias; Ferrante, Francesca et al. (2022): The structure, binding and function of a Notch transcription complex involving RBPJ and the epigenetic reader protein L3MBTL3. In *Nucleic acids research* 50 (22), pp. 13083–13099. DOI: 10.1093/nar/gkac1137.

Hamaguchi, Y.; Yamamoto, Y.; Iwanari, H.; Maruyama, S.; Furukawa, T.; Matsunami, N.; Honjo, T. (1992): Biochemical and immunological characterization of the DNA binding protein (RBP-J kappa) to mouse J kappa recombination signal sequence. In *Journal of biochemistry* 112 (3), pp. 314–320. DOI: 10.1093/oxfordjournals.jbchem.a123898.

Han, Hua; Tanigaki, Kenji; Yamamoto, Norio; Kuroda, Kazuki; Yoshimoto, Momoko; Nakahata, Tatsutoshi et al. (2002): Inducible gene knockout of transcription factor recombination signal binding protein-J reveals its essential role in T versus B lineage decision. In *International immunology* 14 (6), pp. 637–645. DOI: 10.1093/intimm/dxf030.

Hanahan, Douglas; Weinberg, Robert A. (2011): Hallmarks of cancer: the next generation. In *Cell* 144 (5), pp. 646–674. DOI: 10.1016/j.cell.2011.02.013.

Hasegawa, Yuko; Struhl, Kevin (2021): Different SP1 binding dynamics at individual genomic loci in human cells. In *Proceedings of the National Academy of Sciences of the United States of America* 118 (46). DOI: 10.1073/pnas.2113579118.

Hassed, Susan J.; Wiley, Graham B.; Wang, Shaofeng; Lee, Ji-Yun; Li, Shibo; Xu, Weihong et al. (2012): RBPJ mutations identified in two families affected by Adams-Oliver syndrome. In *American Journal of Human Genetics* 91 (2), pp. 391–395. DOI: 10.1016/j.ajhg.2012.07.005.

Hatakeyama, Jun; Bessho, Yasumasa; Katoh, Kazuo; Ookawara, Shigeo; Fujioka, Makio; Guillemot, François; Kageyama, Ryoichiro (2004): Hes genes regulate size, shape and histogenesis of the nervous system by control of the timing of neural stem cell differentiation. In *Development (Cambridge, England)* 131 (22), pp. 5539–5550. DOI: 10.1242/dev.01436.

Hayward, Penny; Brennan, Keith; Sanders, Phil; Balayo, Tina; DasGupta, Ramanuj; Perrimon, Norbert; Martinez Arias, Alfonso (2005): Notch modulates Wnt signalling by associating with Armadillo/beta-catenin and regulating its transcriptional activity. In *Development (Cambridge, England)* 132 (8), pp. 1819–1830. DOI: 10.1242/dev.01724.

Hebbes, T. R.; Thorne, A. W.; Crane-Robinson, C. (1988): A direct link between core histone acetylation and transcriptionally active chromatin. In *The EMBO Journal* 7 (5), pp. 1395–1402.

Heintzman, Nathaniel D.; Stuart, Rhona K.; Hon, Gary; Fu, Yutao; Ching, Christina W.; Hawkins, R. David et al. (2007): Distinct and predictive chromatin signatures of transcriptional promoters and enhancers in the human genome. In *Nature genetics* 39 (3), pp. 311–318. DOI: 10.1038/ng1966.

Heitz, Emil (1928): Das heterochromatin der moose.

Heitz, Emil (1929): Heterochromatin, chromocentren, chromomeren: Komm. Fischer.

Herranz, Daniel; Ambesi-Impiombato, Alberto; Palomero, Teresa; Schnell, Stephanie A.; Belver, Laura; Wendorff, Agnieszka A. et al. (2014): A NOTCH1-driven MYC enhancer promotes T cell development, transformation and acute lymphoblastic leukemia. In *Nature medicine* 20 (10), pp. 1130–1137. DOI: 10.1038/nm.3665.

Hnisz, Denes; Abraham, Brian J.; Lee, Tong Ihn; Lau, Ashley; Saint-André, Violaine; Sigova, Alla A. et al. (2013): Super-enhancers in the control of cell identity and disease. In *Cell* 155 (4), pp. 934–947. DOI: 10.1016/j.cell.2013.09.053.

Hnisz, Denes; Shrinivas, Krishna; Young, Richard A.; Chakraborty, Arup K.; Sharp, Phillip A. (2017): A Phase Separation Model for Transcriptional Control. In *Cell* 169 (1), pp. 13–23. DOI: 10.1016/j.cell.2017.02.007.

Hori, Kei; Cholewa-Waclaw, Justyna; Nakada, Yuji; Glasgow, Stacey M.; Masui, Toshihiko; Henke, R. Michael et al. (2008): A nonclassical bHLH Rbpj transcription factor complex is required for specification

of GABAergic neurons independent of Notch signaling. In *Genes & development* 22 (2), pp. 166–178. DOI: 10.1101/gad.1628008.

Horikoshi, M.; Hai, T.; Lin, Y. S.; Green, M. R.; Roeder, R. G. (1988): Transcription factor ATF interacts with the TATA factor to facilitate establishment of a preinitiation complex. In *Cell* 54 (7), pp. 1033–1042. DOI: 10.1016/0092-8674(88)90118-3.

Hossain, Fokhrul; Sorrentino, Claudia; Ucar, Deniz A.; Peng, Yin; Matossian, Margarite; Wyczechowska, Dorota et al. (2018): Notch Signaling Regulates Mitochondrial Metabolism and NF-κB Activity in Triple-Negative Breast Cancer Cells via IKKα-Dependent Non-canonical Pathways. In *Frontiers in oncology* 8, p. 575. DOI: 10.3389/fonc.2018.00575.

Hsieh, J. J.; Henkel, T.; Salmon, P.; Robey, E.; Peterson, M. G.; Hayward, S. D. (1996): Truncated mammalian Notch1 activates CBF1/RBPJk-repressed genes by a mechanism resembling that of Epstein-Barr virus EBNA2. In *Molecular and cellular biology* 16 (3), pp. 952–959. DOI: 10.1128/MCB.16.3.952.

Hu, Taishan; Chitnis, Nilesh; Monos, Dimitri; Dinh, Anh (2021): Next-generation sequencing technologies: An overview. In *Human immunology* 82 (11), pp. 801–811. DOI: 10.1016/j.humimm.2021.02.012.

Huang, Chang; Zhu, Bing (2018): Roles of H3K36-specific histone methyltransferases in transcription: antagonizing silencing and safeguarding transcription fidelity. In *Biophysics reports* 4 (4), pp. 170–177. DOI: 10.1007/s41048-018-0063-1.

Hwang, Jee-Yeon; Zukin, R. Suzanne (2018): REST, a master transcriptional regulator in neurodegenerative disease. In *Current opinion in neurobiology* 48, pp. 193–200. DOI: 10.1016/j.conb.2017.12.008.

Igolkina, Anna A.; Zinkevich, Arsenii; Karandasheva, Kristina O.; Popov, Aleksey A.; Selifanova, Maria V.; Nikolaeva, Daria et al. (2019): H3K4me3, H3K9ac, H3K27ac, H3K27me3 and H3K9me3 Histone Tags Suggest Distinct Regulatory Evolution of Open and Condensed Chromatin Landmarks. In *Cells* 8 (9). DOI: 10.3390/cells8091034.

Ishifune, Chieko; Tsukumo, Shin-Ichi; Maekawa, Yoichi; Hozumi, Katsuto; Chung, Doo Hyun; Motozono, Chihiro et al. (2019): Regulation of membrane phospholipid asymmetry by Notch-mediated flippase expression controls the number of intraepithelial TCRαβ+CD8αα+ T cells. In *PLoS biology* 17 (5), e3000262. DOI: 10.1371/journal.pbio.3000262.

Iso, T.; Sartorelli, V.; Poizat, C.; Iezzi, S.; Wu, H. Y.; Chung, G. et al. (2001): HERP, a novel heterodimer partner of HES/E(spl) in Notch signaling. In *Molecular and cellular biology* 21 (17), pp. 6080–6089. DOI: 10.1128/MCB.21.17.6080-6089.2001.

Iso, Tatsuya; Kedes, Larry; Hamamori, Yasuo (2003): HES and HERP families: multiple effectors of the Notch signaling pathway. In *Journal of cellular physiology* 194 (3), pp. 237–255. DOI: 10.1002/jcp.10208.

Itoh, Fumiko; Itoh, Susumu; Goumans, Marie-José; Valdimarsdottir, Gudrun; Iso, Tatsuya; Dotto, G. Paolo et al. (2004): Synergy and antagonism between Notch and BMP receptor signaling pathways in endothelial cells. In *The EMBO Journal* 23 (3), pp. 541–551. DOI: 10.1038/sj.emboj.7600065.

Iyer, Gopal; Wang, Albert R.; Brennan, Sean R.; Bourgeois, Shay; Armstrong, Eric; Shah, Pari; Harari, Paul M. (2017): Identification of stable housekeeping genes in response to ionizing radiation in cancer research. In *Sci Rep* 7. DOI: 10.1038/srep43763.

Izon, David J.; Aster, Jon C.; He, Yiping; Weng, Andrew; Karnell, Fredrick G.; Patriub, Vytas et al. (2002): Deltex1 redirects lymphoid progenitors to the B cell lineage by antagonizing Notch1. In *Immunity* 16 (2), pp. 231–243. DOI: 10.1016/s1074-7613(02)00271-6.

Jacob, F.; Monod, J. (1961): Genetic regulatory mechanisms in the synthesis of proteins. In *Journal of molecular biology* 3, pp. 318–356. DOI: 10.1016/s0022-2836(61)80072-7.

Jain, Dhawal; Baldi, Sandro; Zabel, Angelika; Straub, Tobias; Becker, Peter B. (2015): Active promoters give rise to false positive 'Phantom Peaks' in ChIP-seq experiments. In *Nucleic acids research* 43 (14), pp. 6959–6968. DOI: 10.1093/nar/gkv637.

Jalili, Vahid; Matteucci, Matteo; Masseroli, Marco; Morelli, Marco J. (2015): Using combined evidence from replicates to evaluate ChIP-seq peaks. In *Bioinformatics (Oxford, England)* 31 (17), pp. 2761–2769. DOI: 10.1093/bioinformatics/btv293.

Jarrett, Sanchez M.; Seegar, Tom C. M.; Andrews, Mark; Adelmant, Guillaume; Marto, Jarrod A.; Aster, Jon C.; Blacklow, Stephen C. (2019): Extension of the Notch intracellular domain ankyrin repeat stack by NRARP promotes feedback inhibition of Notch signaling. In *Science signaling* 12 (606). DOI: 10.1126/scisignal.aay2369.

Jeffries, Shawn; Robbins, David J.; Capobianco, Anthony J. (2002): Characterization of a high-molecular-weight Notch complex in the nucleus of Notch(ic)-transformed RKE cells and in a human T-cell leukemia cell line. In *Molecular and cellular biology* 22 (11), pp. 3927–3941. DOI: 10.1128/MCB.22.11.3927-3941.2002.

Jian, Yunqing; Liu, Zunyong; Wang, Haixia; Chen, Yun; Yin, Yanni; Zhao, Youfu; Ma, Zhonghua (2021): Interplay of two transcription factors for recruitment of the chromatin remodeling complex modulates fungal nitrosative stress response. In *Nature communications* 12 (1), p. 2576. DOI: 10.1038/s41467-021-22831-8.

Jin, S.; Mutvei, A. P.; Chivukula, I. V.; Andersson, E. R.; Ramsköld, D.; Sandberg, R. et al. (2013): Non-canonical Notch signaling activates IL-6/JAK/STAT signaling in breast tumor cells and is controlled by p53 and IKKα/IKKβ. In *Oncogene* 32 (41), pp. 4892–4902. DOI: 10.1038/onc.2012.517.

Jones, Christina V.; Ricardo, Sharon D. (2013): Macrophages and CSF-1: implications for development and beyond. In *Organogenesis* 9 (4), pp. 249–260. DOI: 10.4161/org.25676.

Joutel, A.; Corpechot, C.; Ducros, A.; Vahedi, K.; Chabriat, H.; Mouton, P. et al. (1996): Notch3 mutations in CADASIL, a hereditary adult-onset condition causing stroke and dementia. In *Nature* 383 (6602), pp. 707–710. DOI: 10.1038/383707a0.

Kang, Xin; Zhang, Zheng-Ping; Song, Chang-Geng; Liu, Long; Zhao, Yan; Du, Jin-Le et al. (2022a): γ-secretase inhibitor disturbs the morphological development of differentiating neurons through affecting Notch/miR-342-5p. In *Neuroscience letters* 778, p. 136603. DOI: 10.1016/j.neulet.2022.136603.

Kang, Yiming; Jung, Wooseok J.; Brent, Michael R. (2022b): Predicting which genes will respond to transcription factor perturbations. In *G3 (Bethesda, Md.)* 12 (8). DOI: 10.1093/g3journal/jkac144.

Kao, H. Y.; Ordentlich, P.; Koyano-Nakagawa, N.; Tang, Z.; Downes, M.; Kintner, C. R. et al. (1998): A histone deacetylase corepressor complex regulates the Notch signal transduction pathway. In *Genes & development* 12 (15), pp. 2269–2277. DOI: 10.1101/gad.12.15.2269.

Kaya-Okur, Hatice S.; Wu, Steven J.; Codomo, Christine A.; Pledger, Erica S.; Bryson, Terri D.; Henikoff, Jorja G. et al. (2019): CUT&Tag for efficient epigenomic profiling of small samples and single cells. In *Nature communications* 10 (1), p. 1930. DOI: 10.1038/s41467-019-09982-5.

Khan, Aziz; Zhang, Xuegong (2019): Integrative modeling reveals key chromatin and sequence signatures predicting super-enhancers. In *Sci Rep* 9 (1), p. 2877. DOI: 10.1038/s41598-019-38979-9.

Kiaris, Hippokratis; Politi, Katerina; Grimm, Lisa M.; Szabolcs, Matthias; Fisher, Peter; Efstratiadis, Argiris; Artavanis-Tsakonas, Spyros (2004): Modulation of notch signaling elicits signature tumors and inhibits hras1-induced oncogenesis in the mouse mammary epithelium. In *The American journal of pathology* 165 (2), pp. 695–705. DOI: 10.1016/S0002-9440(10)63333-0.

Kidd, S.; Kelley, M. R.; Young, M. W. (1986): Sequence of the notch locus of Drosophila melanogaster: relationship of the encoded protein to mammalian clotting and growth factors. In *Molecular and cellular biology* 6 (9), pp. 3094–3108. DOI: 10.1128/mcb.6.9.3094.

Kim, Daehwan; Paggi, Joseph M.; Park, Chanhee; Bennett, Christopher; Salzberg, Steven L. (2019): Graph-based genome alignment and genotyping with HISAT2 and HISAT-genotype. In *Nature biotechnology* 37 (8), pp. 907–915. DOI: 10.1038/s41587-019-0201-4.

Kim, Daehwan; Pertea, Geo; Trapnell, Cole; Pimentel, Harold; Kelley, Ryan; Salzberg, Steven L. (2013): TopHat2: accurate alignment of transcriptomes in the presence of insertions, deletions and gene fusions. In *Genome biology* 14 (4), R36. DOI: 10.1186/gb-2013-14-4-r36.

Koch, Ute; Fiorini, Emma; Benedito, Rui; Besseyrias, Valerie; Schuster-Gossler, Karin; Pierres, Michel et al. (2008): Delta-like 4 is the essential, nonredundant ligand for Notch1 during thymic T cell lineage commitment. In *The Journal of experimental medicine* 205 (11), pp. 2515–2523. DOI: 10.1084/jem.20080829.

Kojika, S.; Griffin, J. D. (2001): Notch receptors and hematopoiesis. In *Experimental hematology* 29 (9), pp. 1041–1052. DOI: 10.1016/S0301-472X(01)00676-2.

Kopan, Raphael; Ilagan, Maria Xenia G. (2009): The canonical Notch signaling pathway: unfolding the activation mechanism. In *Cell* 137 (2), pp. 216–233. DOI: 10.1016/j.cell.2009.03.045.

Kornberg, R. D. (1974): Chromatin structure: a repeating unit of histones and DNA. In *Science (New York, N.Y.)* 184 (4139), pp. 868–871. DOI: 10.1126/science.184.4139.868.

Kornberg, Roger D. (2007): The molecular basis of eukaryotic transcription. In *Proceedings of the National Academy of Sciences of the United States of America* 104 (32), pp. 12955–12961. DOI: 10.1073/pnas.0704138104.

Kornsuthisopon, Chatvadee; Manokawinchoke, Jeeranan; Sonpoung, Opor; Osathanon, Thanaphum; Damrongsri, Damrong (2021): Interleukin 15 participates in Jagged1-induced mineralization in human dental pulp cells. In *Archives of oral biology* 128, p. 105163. DOI: 10.1016/j.archoralbio.2021.105163.

Kouzarides, Tony (2007): Chromatin modifications and their function. In *Cell* 128 (4), pp. 693–705. DOI: 10.1016/j.cell.2007.02.005.

Krejčí, Alena; Bray, Sarah (2007): Notch activation stimulates transient and selective binding of Su(H)/CSL to target enhancers. In *Genes & development* 21 (11), pp. 1322–1327. DOI: 10.1101/gad.424607.

Krueger, F. (2019): Trim Galore! Available online at http://www.bioinformatics.babraham.ac.uk/projects/trim_galore/.

Kuhn, Max (2008): Building Predictive Models in R Using the caret Package. In *J. Stat. Soft.* 28 (5). DOI: 10.18637/jss.v028.i05.

Kuramoto, Takuya; Goto, Hisatsugu; Mitsuhashi, Atsushi; Tabata, Sho; Ogawa, Hirohisa; Uehara, Hisanori et al. (2012): Dll4-Fc, an inhibitor of Dll4-notch signaling, suppresses liver metastasis of small cell lung cancer cells through the downregulation of the NF-κB activity. In *Molecular cancer therapeutics* 11 (12), pp. 2578–2587. DOI: 10.1158/1535-7163.MCT-12-0640.

Lake, Robert J.; Grimm, Lisa M.; Veraksa, Alexey; Banos, Andrew; Artavanis-Tsakonas, Spyros (2009): In vivo analysis of the Notch receptor S1 cleavage. In *PloS one* 4 (8), e6728. DOI: 10.1371/journal.pone.0006728.

Lake, Robert J.; Tsai, Pei-Fang; Choi, Inchan; Won, Kyoung-Jae; Fan, Hua-Ying (2014): RBPJ, the major transcriptional effector of Notch signaling, remains associated with chromatin throughout mitosis, suggesting a role in mitotic bookmarking. In *PLoS genetics* 10 (3), e1004204. DOI: 10.1371/journal.pgen.1004204.

Lamar, E.; Deblandre, G.; Wettstein, D.; Gawantka, V.; Pollet, N.; Niehrs, C.; Kintner, C. (2001): Nrarp is a novel intracellular component of the Notch signaling pathway. In *Genes & development* 15 (15), pp. 1885–1899. DOI: 10.1101/gad.908101.

Lander, E. S.; Linton, L. M.; Birren, B.; Nusbaum, C.; Zody, M. C.; Baldwin, J. et al. (2001): Initial sequencing and analysis of the human genome. In *Nature* 409 (6822), pp. 860–921. DOI: 10.1038/35057062.

Langmead, Ben; Salzberg, Steven L. (2012): Fast gapped-read alignment with Bowtie 2. In *Nature methods* 9 (4), pp. 357–359. DOI: 10.1038/nmeth.1923.

Lardelli, M.; Dahlstrand, J.; Lendahl, U. (1994): The novel Notch homologue mouse Notch 3 lacks specific epidermal growth factor-repeats and is expressed in proliferating neuroepithelium. In *Mechanisms of development* 46 (2), pp. 123–136. DOI: 10.1016/0925-4773(94)90081-7.

Larsson, C.; Lardelli, M.; White, I.; Lendahl, U. (1994): The human NOTCH1, 2, and 3 genes are located at chromosome positions 9q34, 1p13-p11, and 19p13.2-p13.1 in regions of neoplasia-associated translocation. In *Genomics* 24 (2), pp. 253–258. DOI: 10.1006/geno.1994.1613.

Latchman, D. S. (1993): Transcription factors: an overview. In *International Journal of Experimental Pathology* 74 (5), pp. 417–422.

Lawrence, Michael; Huber, Wolfgang; Pagès, Hervé; Aboyoun, Patrick; Carlson, Marc; Gentleman, Robert et al. (2013): Software for computing and annotating genomic ranges. In *PLoS computational biology* 9 (8), e1003118. DOI: 10.1371/journal.pcbi.1003118.

Lee, S.; Remark, L. H.; Josephson, A. M.; Leclerc, K.; Lopez, E. Muiños; Kirby, D. J. et al. (2021): Notch-Wnt signal crosstalk regulates proliferation and differentiation of osteoprogenitor cells during intramembranous bone healing. In *NPJ Regenerative medicine* 6 (1), p. 29. DOI: 10.1038/s41536-021-00139-x.

Lee, Tong Ihn; Young, Richard A. (2013): Transcriptional regulation and its misregulation in disease. In *Cell* 152 (6), pp. 1237–1251. DOI: 10.1016/j.cell.2013.02.014.

Li, Heng; Handsaker, Bob; Wysoker, Alec; Fennell, Tim; Ruan, Jue; Homer, Nils et al. (2009): The Sequence Alignment/Map format and SAMtools. In *Bioinformatics (Oxford, England)* 25 (16), pp. 2078–2079. DOI: 10.1093/bioinformatics/btp352.

Li, Hui; Lan, Tian; Xu, Lin; Liu, Hailing; Wang, Jinju; Li, Jiaxin et al. (2020): NCSTN promotes hepatocellular carcinoma cell growth and metastasis via β-catenin activation in a Notch1/AKT dependent manner. In *Journal of experimental & clinical cancer research : CR* 39 (1), p. 128. DOI: 10.1186/s13046-020-01638-3.

Li, L.; Krantz, I. D.; Deng, Y.; Genin, A.; Banta, A. B.; Collins, C. C. et al. (1997): Alagille syndrome is caused by mutations in human Jagged1, which encodes a ligand for Notch1. In *Nature genetics* 16 (3), pp. 243–251. DOI: 10.1038/ng0797-243.

Li, Li-Jie; Chang, Peter Mu-Hsin; Li, Chien-Hsiu; Chang, Yu-Chan; Lai, Tsung-Ching; Su, Chia-Yi et al. (2022): FAS receptor regulates NOTCH activity through ERK-JAG1 axis activation and controls oral cancer stemness ability and pulmonary metastasis. In *Cell death discovery* 8 (1), p. 101. DOI: 10.1038/s41420-022-00899-5.

Liefke, Robert; Oswald, Franz; Alvarado, Cristobal; Ferres-Marco, Dolores; Mittler, Gerhard; Rodriguez, Patrick et al. (2010): Histone demethylase KDM5A is an integral part of the core Notch–RBP-J repressor complex. In *Genes & development* 24 (6), pp. 590–601. DOI: 10.1101/gad.563210.

Lin, Sensen; Sun, Li; Lyu, Xiaodan; Ai, Xiongfei; Du, Danyu; Su, Nan et al. (2017): Lactate-activated macrophages induced aerobic glycolysis and epithelial-mesenchymal transition in breast cancer by regulation of CCL5-CCR5 axis: a positive metabolic feedback loop. In *Oncotarget* 8 (66), pp. 110426–110443. DOI: 10.18632/oncotarget.22786.

Liska, Orsolya; Bohár, Balázs; Hidas, András; Korcsmáros, Tamás; Papp, Balázs; Fazekas, Dávid; Ari, Eszter (2022): TFLink: an integrated gateway to access transcription factor-target gene interactions for multiple species. In *Database : the journal of biological databases and curation* 2022. DOI: 10.1093/database/baac083.

Liu, Beibei; Liu, Xinhua; Han, Lulu; Chen, Xing; Wu, Xiaodi; Wu, Jiajing et al. (2022): BRD4-directed super-enhancer organization of transcription repression programs links to chemotherapeutic efficacy in breast cancer. In *Proceedings of the National Academy of Sciences of the United States of America* 119 (6). DOI: 10.1073/pnas.2109133119.

Liu, Hudan; Chi, Anthony W. S.; Arnett, Kelly L.; Chiang, Mark Y.; Xu, Lanwei; Shestova, Olga et al. (2010): Notch dimerization is required for leukemogenesis and T-cell development. In *Genes & development* 24 (21), pp. 2395–2407. DOI: 10.1101/gad.1975210.

Lockhart, D. J.; Dong, H.; Byrne, M. C.; Follettie, M. T.; Gallo, M. V.; Chee, M. S. et al. (1996): Expression monitoring by hybridization to high-density oligonucleotide arrays. In *Nature biotechnology* 14 (13), pp. 1675–1680. DOI: 10.1038/nbt1296-1675.

Lopes, Rui; Agami, Reuven; Korkmaz, Gozde (2017): GRO-seq, A Tool for Identification of Transcripts Regulating Gene Expression. In *Methods in molecular biology (Clifton, N.J.)* 1543, pp. 45–55. DOI: 10.1007/978-1-4939-6716-2_3.

Love, Michael I.; Huber, Wolfgang; Anders, Simon (2014): Moderated estimation of fold change and dispersion for RNA-seq data with DESeq2. In *Genome biology* 15 (12), p. 550. DOI: 10.1186/s13059-014-0550-8.

Lovén, Jakob; Hoke, Heather A.; Lin, Charles Y.; Lau, Ashley; Orlando, David A.; Vakoc, Christopher R. et al. (2013): Selective inhibition of tumor oncogenes by disruption of super-enhancers. In *Cell* 153 (2), pp. 320–334. DOI: 10.1016/j.cell.2013.03.036.

Lun, Aaron T. L.; Smyth, Gordon K. (2016): csaw: a Bioconductor package for differential binding analysis of ChIP-seq data using sliding windows. In *Nucleic acids research* 44 (5), e45. DOI: 10.1093/nar/gkv1191.

Maemura, Kentaro; Yoshikawa, Hirohide; Yokoyama, Kazutake; Ueno, Teruo; Kurose, Hitomi; Uchiyama, Kazuhisa; Otsuki, Yoshinori (2013): Delta-like 3 is silenced by methylation and induces apoptosis in human hepatocellular carcinoma. In *International journal of oncology* 42 (3), pp. 817–822. DOI: 10.3892/ijo.2013.1778.

Mangolini, Maurizio; Götte, Frederik; Moore, Andrew; Ammon, Tim; Oelsner, Madlen; Lutzny-Geier, Gloria et al. (2018): Notch2 controls non-autonomous Wnt-signalling in chronic lymphocytic leukaemia. In *Nature communications* 9 (1), p. 3839. DOI: 10.1038/s41467-018-06069-5.

Martin, Marcel (2011): Cutadapt removes adapter sequences from high-throughput sequencing reads. In *EMBnet j.* 17 (1), p. 10. DOI: 10.14806/ej.17.1.200.

Martini, Simone; Bernoth, Kristina; Main, Heather; Ortega, German Dario Camargo; Lendahl, Urban; Just, Ursula; Schwanbeck, Ralf (2013): A critical role for Sox9 in notch-induced astrogliogenesis and stem cell maintenance. In *Stem cells (Dayton, Ohio)* 31 (4), pp. 741–751. DOI: 10.1002/stem.1320.

Masui, Toshihiko; Long, Qiaoming; Beres, Thomas M.; Magnuson, Mark A.; Macdonald, Raymond J. (2007): Early pancreatic development requires the vertebrate Suppressor of Hairless (RBPJ) in the PTF1 bHLH complex. In *Genes & development* 21 (20), pp. 2629–2643. DOI: 10.1101/gad.1575207.

Matsui, T.; Segall, J.; Weil, P. A.; Roeder, R. G. (1980): Multiple factors required for accurate initiation of transcription by purified RNA polymerase II. In *The Journal of biological chemistry* 255 (24), pp. 11992–11996.

McCombie, W. Richard; McPherson, John D.; Mardis, Elaine R. (2019): Next-Generation Sequencing Technologies. In *Cold Spring Harbor perspectives in medicine* 9 (11). DOI: 10.1101/cshperspect.a036798.

McLean, Cory Y.; Bristor, Dave; Hiller, Michael; Clarke, Shoa L.; Schaar, Bruce T.; Lowe, Craig B. et al. (2010): GREAT improves functional interpretation of cis-regulatory regions. In *Nature biotechnology* 28 (5), pp. 495–501. DOI: 10.1038/nbt.1630.

McMillan, Hugh J.; Telegrafi, Aida; Singleton, Amanda; Cho, Megan T.; Lelli, Daniel; Lynn, Francis C. et al. (2018): Recessive mutations in ATP8A2 cause severe hypotonia, cognitive impairment, hyperkinetic

movement disorders and progressive optic atrophy. In *Orphanet journal of rare diseases* 13 (1), p. 86. DOI: 10.1186/s13023-018-0825-3.

Miele, Lucio (2011): Transcription factor RBPJ/CSL: a genome-wide look at transcriptional regulation. In *Proceedings of the National Academy of Sciences of the United States of America* 108 (36), pp. 14715–14716. DOI: 10.1073/pnas.1110570108.

Miller, Jaime L.; Grant, Patrick A. (2013): The role of DNA methylation and histone modifications in transcriptional regulation in humans. In *Sub-cellular biochemistry* 61, pp. 289–317. DOI: 10.1007/978-94-007-4525-4_13.

Minnis-Lyons, Sarah E.; Ferreira-González, Sofía; Aleksieva, Niya; Man, Tak Yung; Gadd, Victoria L.; Williams, Michael J. et al. (2021): Notch-IGF1 signaling during liver regeneration drives biliary epithelial cell expansion and inhibits hepatocyte differentiation. In *Science signaling* 14 (688). DOI: 10.1126/scisignal.aay9185.

Mishra, A.; Agrawal, N.; Banerjee, S.; Sardesai, D.; Dalal, J. S.; Bhojwani, J.; Sinha, P. (2001): Spatial regulation of DELTA expression mediates NOTCH signalling for segmentation of Drosophila legs. In *Mechanisms of development* 105 (1-2), pp. 115–127. DOI: 10.1016/s0925-4773(01)00387-2.

Morgan, Martin; Pagès, Hervé; Obenchain, Valerie; Hayden, Nathaniel (2017): Rsamtools: Bioconductor.

Morgan, T. H. (1917): The Theory of the Gene. In *The American Naturalist* 51 (609), pp. 513–544. DOI: 10.1086/279629.

Mumbach, Maxwell R.; Rubin, Adam J.; Flynn, Ryan A.; Dai, Chao; Khavari, Paul A.; Greenleaf, William J.; Chang, Howard Y. (2016): HiChIP: efficient and sensitive analysis of protein-directed genome architecture. In *Nature methods* 13 (11), pp. 919–922. DOI: 10.1038/nmeth.3999.

Mumm, J. S.; Schroeter, E. H.; Saxena, M. T.; Griesemer, A.; Tian, X.; Pan, D. J. et al. (2000): A ligand-induced extracellular cleavage regulates gamma-secretase-like proteolytic activation of Notch1. In *Molecular cell* 5 (2), pp. 197–206.

Murata, Kaoru; Hattori, Masakazu; Hirai, Norihito; Shinozuka, Yoriko; Hirata, Hiromi; Kageyama, Ryoichiro et al. (2005): Hes1 directly controls cell proliferation through the transcriptional repression of p27Kip1. In *Molecular and cellular biology* 25 (10), pp. 4262–4271. DOI: 10.1128/MCB.25.10.4262-4271.2005.

Mutvei, Anders P.; Landor, Sebastian K-J; Fox, Rhys; Braune, Eike-Benjamin; Tsoi, Yat Long; Phoon, Yee Peng et al. (2018): Notch signaling promotes a HIF2α-driven hypoxic response in multiple tumor cell types. In *Oncogene* 37 (46), pp. 6083–6095. DOI: 10.1038/s41388-018-0400-3.

Nagao, Motoshi; Sugimori, Michiya; Nakafuku, Masato (2007): Cross talk between notch and growth factor/cytokine signaling pathways in neural stem cells. In *Molecular and cellular biology* 27 (11), pp. 3982–3994. DOI: 10.1128/MCB.00170-07.

Nakamura, Y.; Sakakibara, S. i.; Miyata, T.; Ogawa, M.; Shimazaki, T.; Weiss, S. et al. (2000): The bHLH gene hes1 as a repressor of the neuronal commitment of CNS stem cells. In *The Journal of neuroscience : the official journal of the Society for Neuroscience* 20 (1), pp. 283–293. DOI: 10.1523/JNEUROSCI.20-01-00283.2000.

Nakamura, Yukio; Paiva Alves, Eduardo de; Veenstra, Gert Jan C.; Hoppler, Stefan (2016): Tissue- and stage-specific Wnt target gene expression is controlled subsequent to β-catenin recruitment to cis-regulatory modules. In *Development (Cambridge, England)* 143 (11), pp. 1914–1925. DOI: 10.1242/dev.131664.

Nam, Yunsun; Sliz, Piotr; Pear, Warren S.; Aster, Jon C.; Blacklow, Stephen C. (2007): Cooperative assembly of higher-order Notch complexes functions as a switch to induce transcription. In *Proceedings of the National Academy of Sciences of the United States of America* 104 (7), pp. 2103–2108. DOI: 10.1073/pnas.0611092104.

Nam, Yunsun; Sliz, Piotr; Song, Luyan; Aster, Jon C.; Blacklow, Stephen C. (2006): Structural basis for cooperativity in recruitment of MAML coactivators to Notch transcription complexes. In *Cell* 124 (5), pp. 973–983. DOI: 10.1016/j.cell.2005.12.037.

Nanney, D. L. (1958): EPIGENETIC CONTROL SYSTEMS*. In *Proceedings of the National Academy of Sciences of the United States of America* 44 (7), pp. 712–717.

Narendra, Varun; Rocha, Pedro P.; An, Disi; Raviram, Ramya; Skok, Jane A.; Mazzoni, Esteban O.; Reinberg, Danny (2015): CTCF establishes discrete functional chromatin domains at the Hox clusters during differentiation. In *Science (New York, N.Y.)* 347 (6225), pp. 1017–1021. DOI: 10.1126/science.1262088.

Ngondo-Mbongo, Richard Patryk; Myslinski, Evelyne; Aster, Jon C.; Carbon, Philippe (2013): Modulation of gene expression via overlapping binding sites exerted by ZNF143, Notch1 and THAP11. In *Nucleic acids research* 41 (7), pp. 4000–4014. DOI: 10.1093/nar/gkt088.

Obata, J.; Yano, M.; Mimura, H.; Goto, T.; Nakayama, R.; Mibu, Y. et al. (2001): p48 subunit of mouse PTF1 binds to RBP-Jkappa/CBF-1, the intracellular mediator of Notch signalling, and is expressed in the neural tube of early stage embryos. In *Genes to cells : devoted to molecular & cellular mechanisms* 6 (4), pp. 345–360. DOI: 10.1046/j.1365-2443.2001.00422.x.

Ohkuma, Y.; Horikoshi, M.; Roeder, R. G.; Desplan, C. (1990): Engrailed, a homeodomain protein, can repress in vitro transcription by competition with the TATA box-binding protein transcription factor IID. In *Proceedings of the National Academy of Sciences of the United States of America* 87 (6), pp. 2289–2293. DOI: 10.1073/pnas.87.6.2289.

Oka, C.; Nakano, T.; Wakeham, A.; La Pompa, J. L. de; Mori, C.; Sakai, T. et al. (1995): Disruption of the mouse RBP-J kappa gene results in early embryonic death. In *Development (Cambridge, England)* 121 (10), pp. 3291–3301. DOI: 10.1242/dev.121.10.3291.

Okubo, Toshiki; Iwanami, Akio; Kohyama, Jun; Itakura, Go; Kawabata, Soya; Nishiyama, Yuichiro et al. (2016): Pretreatment with a γ-Secretase Inhibitor Prevents Tumor-like Overgrowth in Human iPSC-Derived Transplants for Spinal Cord Injury. In *Stem cell reports* 7 (4), pp. 649–663. DOI: 10.1016/j.stemcr.2016.08.015.

Olave, I.; Reinberg, D.; Vales, L. D. (1998): The mammalian transcriptional repressor RBP (CBF1) targets TFIID and TFIIA to prevent activated transcription. In *Genes & development* 12 (11), pp. 1621–1637. DOI: 10.1101/gad.12.11.1621.

Olins, A. L.; Olins, D. E. (1974): Spheroid chromatin units (v bodies). In *Science (New York, N.Y.)* 183 (4122), pp. 330–332. DOI: 10.1126/science.183.4122.330.

Olins, Donald E.; Olins, Ada L. (2003): Chromatin history: our view from the bridge. In *Nature reviews. Molecular cell biology* 4 (10), pp. 809–814. DOI: 10.1038/nrm1225.

Olsauskas-Kuprys, Roma; Zlobin, Andrei; Osipo, Clodia (2013): Gamma secretase inhibitors of Notch signaling. In *OncoTargets and therapy* 6, pp. 943–955. DOI: 10.2147/OTT.S33766.

Onat, Onur Emre; Gulsuner, Suleyman; Bilguvar, Kaya; Nazli Basak, Ayse; Topaloglu, Haluk; Tan, Meliha et al. (2013): Missense mutation in the ATPase, aminophospholipid transporter protein ATP8A2 is associated with cerebellar atrophy and quadrupedal locomotion. In *European journal of human genetics : EJHG* 21 (3), pp. 281–285. DOI: 10.1038/ejhg.2012.170.

Oswald, F.; Täuber, B.; Dobner, T.; Bourteele, S.; Kostezka, U.; Adler, G. et al. (2001): p300 acts as a transcriptional coactivator for mammalian Notch-1. In *Molecular and cellular biology* 21 (22), pp. 7761–7774. DOI: 10.1128/MCB.21.22.7761-7774.2001.

Oswald, Franz; Kostezka, Ulrike; Astrahantseff, Kathy; Bourteele, Soizic; Dillinger, Karin; Zechner, Ulrich et al. (2002): SHARP is a novel component of the Notch/RBP-Jkappa signalling pathway. In *The EMBO Journal* 21 (20), pp. 5417–5426. DOI: 10.1093/emboj/cdf549.

Oswald, Franz; Rodriguez, Patrick; Giaimo, Benedetto Daniele; Antonello, Zeus A.; Mira, Laura; Mittler, Gerhard et al. (2016): A phospho-dependent mechanism involving NCoR and KMT2D controls a

permissive chromatin state at Notch target genes. In *Nucleic acids research* 44 (10), pp. 4703–4720. DOI: 10.1093/nar/gkw105.

Palstra, Robert-Jan; Grosveld, Frank (2012): Transcription factor binding at enhancers: shaping a genomic regulatory landscape in flux. In *Frontiers in genetics* 3, p. 195. DOI: 10.3389/fgene.2012.00195.

Pan, Li; Lemieux, Madeleine E.; Thomas, Tom; Rogers, Julia M.; Lipper, Colin H.; Lee, Winston et al. (2020): IER5, a DNA damage response gene, is required for Notch-mediated induction of squamous cell differentiation. In *eLife* 9. DOI: 10.7554/eLife.58081.

Parker, Stephen C. J.; Stitzel, Michael L.; Taylor, D. Leland; Orozco, Jose Miguel; Erdos, Michael R.; Akiyama, Jennifer A. et al. (2013): Chromatin stretch enhancer states drive cell-specific gene regulation and harbor human disease risk variants. In *Proceedings of the National Academy of Sciences of the United States of America* 110 (44), pp. 17921–17926. DOI: 10.1073/pnas.1317023110.

Partridge, E. Christopher; Chhetri, Surya B.; Prokop, Jeremy W.; Ramaker, Ryne C.; Jansen, Camden S.; Goh, Say-Tar et al. (2020): Occupancy maps of 208 chromatin-associated proteins in one human cell type. In *Nature* 583 (7818), pp. 720–728. DOI: 10.1038/s41586-020-2023-4.

Pear, W. S.; Aster, J. C.; Scott, M. L.; Hasserjian, R. P.; Soffer, B.; Sklar, J.; Baltimore, D. (1996): Exclusive development of T cell neoplasms in mice transplanted with bone marrow expressing activated Notch alleles. In *The Journal of experimental medicine* 183 (5), pp. 2283–2291. DOI: 10.1084/jem.183.5.2283.

Peng, J.; Zhang, L.; Drysdale, L.; Fong, G. H. (2000): The transcription factor EPAS-1/hypoxia-inducible factor 2alpha plays an important role in vascular remodeling. In *Proceedings of the National Academy of Sciences of the United States of America* 97 (15), pp. 8386–8391. DOI: 10.1073/pnas.140087397.

Pennisi, E. (2001): The human genome. In *Science (New York, N.Y.)* 291 (5507), pp. 1177–1180. DOI: 10.1126/science.291.5507.1177.

Perenthaler, Elena; Yousefi, Soheil; Niggl, Eva; Barakat, Tahsin Stefan (2019): Beyond the Exome: The Non-coding Genome and Enhancers in Neurodevelopmental Disorders and Malformations of Cortical Development. In *Frontiers in cellular neuroscience* 13, p. 352. DOI: 10.3389/fncel.2019.00352.

Petrovic, Jelena; Zhou, Yeqiao; Fasolino, Maria; Goldman, Naomi; Schwartz, Gregory W.; Mumbach, Maxwell R. et al. (2019): Oncogenic Notch Promotes Long-Range Regulatory Interactions within Hyperconnected 3D Cliques. In *Molecular cell* 73 (6), 1174-1190.e12. DOI: 10.1016/j.molcel.2019.01.006.

Pickering, Curtis R.; Zhou, Jane H.; Lee, J. Jack; Drummond, Jennifer A.; Peng, S. Andrew; Saade, Rami E. et al. (2014): Mutational landscape of aggressive cutaneous squamous cell carcinoma. In *Clinical cancer research : an official journal of the American Association for Cancer Research* 20 (24), pp. 6582–6592. DOI: 10.1158/1078-0432.CCR-14-1768.

Pihlajamaa, Päivi; Kauko, Otto; Sahu, Biswajyoti; Kivioja, Teemu; Taipale, Jussi (2023): A competitive precision CRISPR method to identify the fitness effects of transcription factor binding sites. In *Nature biotechnology* 41 (2), pp. 197–203. DOI: 10.1038/s41587-022-01444-6.

Pillidge, Zoe; Bray, Sarah J. (2019): SWI/SNF chromatin remodeling controls Notch-responsive enhancer accessibility. In *EMBO reports* 20 (5). DOI: 10.15252/embr.201846944.

Pott, Sebastian; Lieb, Jason D. (2015): What are super-enhancers? In *Nature genetics* 47 (1), pp. 8–12. DOI: 10.1038/ng.3167.

Poulson, D. F. (1937): Chromosomal Deficiencies and the Embryonic Development of Drosophila Melanogaster. In *Proceedings of the National Academy of Sciences of the United States of America* 23 (3), pp. 133–137. DOI: 10.1073/pnas.23.3.133.

Pugh, B. F.; Tjian, R. (1990): Mechanism of transcriptional activation by Sp1: evidence for coactivators. In *Cell* 61 (7), pp. 1187–1197. DOI: 10.1016/0092-8674(90)90683-6.

Pui, J. C.; Allman, D.; Xu, L.; DeRocco, S.; Karnell, F. G.; Bakkour, S. et al. (1999): Notch1 expression in early lymphopoiesis influences B versus T lineage determination. In *Immunity* 11 (3), pp. 299–308. DOI: 10.1016/S1074-7613(00)80105-3.

Pundhir, Sachin; Bagger, Frederik O.; Lauridsen, Felicia B.; Rapin, Nicolas; Porse, Bo T. (2016): Peak-valley-peak pattern of histone modifications delineates active regulatory elements and their directionality. In *Nucleic acids research* 44 (9), pp. 4037–4051. DOI: 10.1093/nar/gkw250.

R Core Team (2022): R: A Language and Environment for Statistical Computing. Vienna, Austria. Available online at https://www.R-project.org/.

Radtke, F.; Wilson, A.; Stark, G.; Bauer, M.; van Meerwijk, J.; MacDonald, H. R.; Aguet, M. (1999): Deficient T cell fate specification in mice with an induced inactivation of Notch1. In *Immunity* 10 (5), pp. 547–558. DOI: 10.1016/S1074-7613(00)80054-0.

Raisner, Ryan M.; Hartley, Paul D.; Meneghini, Marc D.; Bao, Marie Z.; Liu, Chih Long; Schreiber, Stuart L. et al. (2005): Histone Variant H2A.Z Marks the 5′ Ends of Both Active and Inactive Genes in Euchromatin. In *Cell* 123 (2), pp. 233–248. DOI: 10.1016/j.cell.2005.10.002.

Ramakrishnan, Aravinda-Bharathi; Cadigan, Ken M. (2017): Wnt target genes and where to find them. In *F1000Research* 6, p. 746. DOI: 10.12688/f1000research.11034.1.

Ramakrishnan, Aravinda-Bharathi; Sinha, Abhishek; Fan, Vinson B.; Cadigan, Ken M. (2018): The Wnt Transcriptional Switch: TLE Removal or Inactivation? In *BioEssays : news and reviews in molecular, cellular and developmental biology* 40 (2). DOI: 10.1002/bies.201700162.

Ramírez, Fidel; Dündar, Friederike; Diehl, Sarah; Grüning, Björn A.; Manke, Thomas (2014): deepTools: a flexible platform for exploring deep-sequencing data. In *Nucleic acids research* 42 (Web Server issue), W187-91. DOI: 10.1093/nar/gku365.

Ravasi, Timothy; Suzuki, Harukazu; Cannistraci, Carlo Vittorio; Katayama, Shintaro; Bajic, Vladimir B.; Tan, Kai et al. (2010): An atlas of combinatorial transcriptional regulation in mouse and man. In *Cell* 140 (5), pp. 744–752. DOI: 10.1016/j.cell.2010.01.044.

Razumilava, Nataliya; Gores, Gregory J. (2013): Notch-driven carcinogenesis: the merging of hepatocellular cancer and cholangiocarcinoma into a common molecular liver cancer subtype. In *Journal of hepatology* 58 (6), pp. 1244–1245. DOI: 10.1016/j.jhep.2013.01.017.

Rea, S.; Eisenhaber, F.; O'Carroll, D.; Strahl, B. D.; Sun, Z. W.; Schmid, M. et al. (2000): Regulation of chromatin structure by site-specific histone H3 methyltransferases. In *Nature* 406 (6796), pp. 593–599. DOI: 10.1038/35020506.

Rebay, I.; Fleming, R. J.; Fehon, R. G.; Cherbas, L.; Cherbas, P.; Artavanis-Tsakonas, S. (1991): Specific EGF repeats of Notch mediate interactions with Delta and Serrate: implications for Notch as a multifunctional receptor. In *Cell* 67 (4), pp. 687–699. DOI: 10.1016/0092-8674(91)90064-6.

Rechsteiner, Martin; Rogers, Scott W. (1996): PEST sequences and regulation by proteolysis. In *Trends in Biochemical Sciences* 21 (7), pp. 267–271. DOI: 10.1016/S0968-0004(96)10031-1.

Reedijk, Michael; Odorcic, Silvia; Chang, Lynn; Zhang, Hui; Miller, Naomi; McCready, David R. et al. (2005): High-level coexpression of JAG1 and NOTCH1 is observed in human breast cancer and is associated with poor overall survival. In *Cancer research* 65 (18), pp. 8530–8537. DOI: 10.1158/0008-5472.CAN-05-1069.

Rekhtman, Natasha; Pietanza, Maria C.; Hellmann, Matthew D.; Naidoo, Jarushka; Arora, Arshi; Won, Helen et al. (2016): Next-Generation Sequencing of Pulmonary Large Cell Neuroendocrine Carcinoma Reveals Small Cell Carcinoma-like and Non-Small Cell Carcinoma-like Subsets. In *Clinical cancer research : an official journal of the American Association for Cancer Research* 22 (14), pp. 3618–3629. DOI: 10.1158/1078-0432.CCR-15-2946.

Ren, Gang; Jin, Wenfei; Cui, Kairong; Rodrigez, Joseph; Hu, Gangqing; Zhang, Zhiying et al. (2017): CTCF-Mediated Enhancer-Promoter Interaction Is a Critical Regulator of Cell-to-Cell Variation of Gene Expression. In *Molecular cell* 67 (6), 1049-1058.e6. DOI: 10.1016/j.molcel.2017.08.026.

Reyes, Alexis A.; Marcum, Ryan D.; He, Yuan (2021): Structure and Function of Chromatin Remodelers. In *Journal of molecular biology* 433 (14), p. 166929. DOI: 10.1016/j.jmb.2021.166929.

Richter, A.; Schwager, C.; Hentze, S.; Ansorge, W.; Hentze, M. W.; Muckenthaler, M. (2002): Comparison of fluorescent tag DNA labeling methods used for expression analysis by DNA microarrays. In *BioTechniques* 33 (3), 620-8, 630. DOI: 10.2144/02333rr05.

Ritchie, Matthew E.; Phipson, Belinda; Di Wu; Hu, Yifang; Law, Charity W.; Shi, Wei; Smyth, Gordon K. (2015): limma powers differential expression analyses for RNA-sequencing and microarray studies. In *Nucleic acids research* 43 (7), e47. DOI: 10.1093/nar/gkv007.

Robbins, J.; Blondel, B. J.; Gallahan, D.; Callahan, R. (1992): Mouse mammary tumor gene int-3: a member of the notch gene family transforms mammary epithelial cells. In *Journal of virology* 66 (4), pp. 2594–2599. DOI: 10.1128/JVI.66.4.2594-2599.1992.

Robinson, James T.; Thorvaldsdóttir, Helga; Winckler, Wendy; Guttman, Mitchell; Lander, Eric S.; Getz, Gad; Mesirov, Jill P. (2011): Integrative genomics viewer. In *Nature biotechnology* 29 (1), pp. 24–26. DOI: 10.1038/nbt.1754.

Rodenas-Ruano, Alma; Chávez, Andrés E.; Cossio, Maria J.; Castillo, Pablo E.; Zukin, R. Suzanne (2012): REST-dependent epigenetic remodeling promotes the developmental switch in synaptic NMDA receptors. In *Nature neuroscience* 15 (10), pp. 1382–1390. DOI: 10.1038/nn.3214.

Roeder, R. G.; Rutter, W. J. (1969): Multiple forms of DNA-dependent RNA polymerase in eukaryotic organisms. In *Nature* 224 (5216), pp. 234–237. DOI: 10.1038/224234a0.

Rogers, Julia M.; Guo, Bingqian; Egan, Emily D.; Aster, Jon C.; Adelman, Karen; Blacklow, Stephen C. (2020): MAML1-Dependent Notch-Responsive Genes Exhibit Differing Cofactor Requirements for Transcriptional Activation. In *Molecular and cellular biology* 40 (11). DOI: 10.1128/MCB.00014-20.

Romero-Wolf, Maile; Shin, Boyoung; Zhou, Wen; Koizumi, Maria; Rothenberg, Ellen V.; Hosokawa, Hiroyuki (2020): Notch2 complements Notch1 to mediate inductive signaling that initiates early T cell development. In *The Journal of cell biology* 219 (10). DOI: 10.1083/jcb.202005093.

Rosenblum, Jared S.; Wang, Herui; Dmitriev, Pauline M.; Cappadona, Anthony J.; Mastorakos, Panagiotis; Xu, Chen et al. (2021): Developmental vascular malformations in EPAS1 gain-of-function syndrome. In *JCI insight* 6 (5). DOI: 10.1172/jci.insight.144368.

Ross, Sarah H.; Cantrell, Doreen A. (2018): Signaling and Function of Interleukin-2 in T Lymphocytes. In *Annual review of immunology* 36, pp. 411–433. DOI: 10.1146/annurev-immunol-042617-053352.

Rothenberg, Ellen V.; Moore, Jonathan E.; Yui, Mary A. (2008): Launching the T-cell-lineage developmental programme. In *Nature reviews. Immunology* 8 (1), pp. 9–21. DOI: 10.1038/nri2232.

Rozenberg, Julian M.; Taylor, Joan M.; Mack, Christopher P. (2018): RBPJ binds to consensus and methylated cis elements within phased nucleosomes and controls gene expression in human aortic smooth muscle cells in cooperation with SRF. In *Nucleic acids research* 46 (16), pp. 8232–8244. DOI: 10.1093/nar/gky562.

Rozenberg, Julian M.; Tesfu, Daniel B.; Musunuri, Srilaxmi; Taylor, Joan M.; Mack, Christopher P. (2014): DNA methylation of a GC repressor element in the smooth muscle myosin heavy chain promoter facilitates binding of the Notch-associated transcription factor, RBPJ/CSL1. In *Arteriosclerosis, thrombosis, and vascular biology* 34 (12), pp. 2624–2631. DOI: 10.1161/ATVBAHA.114.304634.

RStudio Team (2022): RStudio: Integrated Development Environment for R. Boston, MA. Available online at http://www.rstudio.com/.

Rustighi, Alessandra; Tiberi, Luca; Soldano, Alessia; Napoli, Marco; Nuciforo, Paolo; Rosato, Antonio et al. (2009): The prolyl-isomerase Pin1 is a Notch1 target that enhances Notch1 activation in cancer. In *Nature cell biology* 11 (2), pp. 133–142. DOI: 10.1038/ncb1822.

Sabari, Benjamin R.; Dall'Agnese, Alessandra; Boija, Ann; Klein, Isaac A.; Coffey, Eliot L.; Shrinivas, Krishna et al. (2018): Coactivator condensation at super-enhancers links phase separation and gene control. In *Science (New York, N.Y.)* 361 (6400). DOI: 10.1126/science.aar3958.

Saksouk, Nehmé; Simboeck, Elisabeth; Déjardin, Jérôme (2015): Constitutive heterochromatin formation and transcription in mammals. In *Epigenetics & chromatin* 8, p. 3. DOI: 10.1186/1756-8935-8-3.

Sánchez-Iranzo, Héctor; Halavatyi, Aliaksandr; Diz-Muñoz, Alba (2022): Strength of interactions in the Notch gene regulatory network determines patterning and fate in the notochord. In *eLife* 11. DOI: 10.7554/eLife.75429.

Sanger, F.; Nicklen, S.; Coulson, A. R. (1977): DNA sequencing with chain-terminating inhibitors. In *Proceedings of the National Academy of Sciences of the United States of America* 74 (12), pp. 5463–5467. DOI: 10.1073/pnas.74.12.5463.

Sanz-Ezquerro, Juan J.; Münsterberg, Andrea E.; Stricker, Sigmar (2017): Editorial: Signaling Pathways in Embryonic Development. In *Frontiers in cell and developmental biology* 5, p. 76. DOI: 10.3389/fcell.2017.00076.

Sasai, Y.; Kageyama, R.; Tagawa, Y.; Shigemoto, R.; Nakanishi, S. (1992): Two mammalian helix-loop-helix factors structurally related to Drosophila hairy and Enhancer of split. In *Genes & development* 6 (12B), pp. 2620–2634. DOI: 10.1101/gad.6.12b.2620.

Sauma, D.; Ramirez, A.; Alvarez, K.; Rosemblatt, M.; Bono, M. R. (2012): Notch signalling regulates cytokine production by CD8+ and CD4+ T cells. In *Scandinavian journal of immunology* 75 (4), pp. 389–400. DOI: 10.1111/j.1365-3083.2012.02673.x.

Saxonov, Serge; Berg, Paul; Brutlag, Douglas L. (2006): A genome-wide analysis of CpG dinucleotides in the human genome distinguishes two distinct classes of promoters. In *Proceedings of the National Academy of Sciences of the United States of America* 103 (5), pp. 1412–1417. DOI: 10.1073/pnas.0510310103.

Schmitt, Thomas M.; Ciofani, Maria; Petrie, Howard T.; Zúñiga-Pflücker, Juan Carlos (2004): Maintenance of T cell specification and differentiation requires recurrent notch receptor-ligand interactions. In *The Journal of experimental medicine* 200 (4), pp. 469–479. DOI: 10.1084/jem.20040394.

Sedat, J.; Manuelidis, L. (1978): A direct approach to the structure of eukaryotic chromosomes. In *Cold Spring Harbor symposia on quantitative biology* 42 Pt 1, pp. 331–350. DOI: 10.1101/sqb.1978.042.01.035.

Sen, Payel; Lan, Yemin; Li, Catherine Y.; Sidoli, Simone; Donahue, Greg; Dou, Zhixun et al. (2019): Histone Acetyltransferase p300 Induces De Novo Super-Enhancers to Drive Cellular Senescence. In *Molecular cell* 73 (4), 684-698.e8. DOI: 10.1016/j.molcel.2019.01.021.

Severson, Eric; Arnett, Kelly L.; Wang, Hongfang; Zang, Chongzhi; Taing, Len; Liu, Hudan et al. (2017): Genome-wide identification and characterization of Notch transcription complex-binding sequence-paired sites in leukemia cells. In *Science signaling* 10 (477). DOI: 10.1126/scisignal.aag1598.

Sherwood, D. R.; McClay, D. R. (1997): Identification and localization of a sea urchin Notch homologue: insights into vegetal plate regionalization and Notch receptor regulation. In *Development (Cambridge, England)* 124 (17), pp. 3363–3374.

Shi, Ruo-Xi; Liu, Cong; Xu, Ya-Jie; Wang, Ying-Ying; He, Bao-Dong; He, Xuan-Cheng et al. (2023): The Role and Mechanism of Transglutaminase 2 in Regulating Hippocampal Neurogenesis after Traumatic Brain Injury. In *Cells* 12 (4). DOI: 10.3390/cells12040558.

Shi, Yujiang; Lan, Fei; Matson, Caitlin; Mulligan, Peter; Whetstine, Johnathan R.; Cole, Philip A. et al. (2004): Histone demethylation mediated by the nuclear amine oxidase homolog LSD1. In *Cell* 119 (7), pp. 941–953. DOI: 10.1016/j.cell.2004.12.012.

Shue, Yan Ting; Drainas, Alexandros P.; Li, Nancy Yanzhe; Pearsall, Sarah M.; Morgan, Derrick; Sinnott-Armstrong, Nasa et al. (2022): A conserved YAP/Notch/REST network controls the

neuroendocrine cell fate in the lungs. In *Nature communications* 13 (1), p. 2690. DOI: 10.1038/s41467-022-30416-2.

Siebel, Chris; Lendahl, Urban (2017): Notch Signaling in Development, Tissue Homeostasis, and Disease. In *Physiological reviews* 97 (4), pp. 1235–1294. DOI: 10.1152/physrev.00005.2017.

Sigalova, Olga M.; Shaeiri, Amirreza; Forneris, Mattia; Furlong, Eileen Em; Zaugg, Judith B. (2020): Predictive features of gene expression variation reveal mechanistic link with differential expression. In *Molecular systems biology* 16 (8), e9539. DOI: 10.15252/msb.20209539.

Sing, Tobias; Sander, Oliver; Beerenwinkel, Niko; Lengauer, Thomas (2005): ROCR: visualizing classifier performance in R. In *Bioinformatics (Oxford, England)* 21 (20), pp. 3940–3941. DOI: 10.1093/bioinformatics/bti623.

Slatko, Barton E.; Gardner, Andrew F.; Ausubel, Frederick M. (2018): Overview of Next-Generation Sequencing Technologies. In *Current protocols in molecular biology* 122 (1), e59. DOI: 10.1002/cpmb.59.

Solomon, M. J.; Larsen, P. L.; Varshavsky, A. (1988): Mapping protein-DNA interactions in vivo with formaldehyde: evidence that histone H4 is retained on a highly transcribed gene. In *Cell* 53 (6), pp. 937–947. DOI: 10.1016/s0092-8674(88)90469-2.

Sonawane, Abhijeet Rajendra; Platig, John; Fagny, Maud; Chen, Cho-Yi; Paulson, Joseph Nathaniel; Lopes-Ramos, Camila Miranda et al. (2017): Understanding Tissue-Specific Gene Regulation. In *Cell reports* 21 (4), pp. 1077–1088. DOI: 10.1016/j.celrep.2017.10.001.

Song, L. L.; Peng, Y.; Yun, J.; Rizzo, P.; Chaturvedi, V.; Weijzen, S. et al. (2008): Notch-1 associates with IKKalpha and regulates IKK activity in cervical cancer cells. In *Oncogene* 27 (44), pp. 5833–5844. DOI: 10.1038/onc.2008.190.

Speiser, Jodi; Foreman, Kimberly; Drinka, Eva; Godellas, Constantine; Perez, Claudia; Salhadar, Alia et al. (2012): Notch-1 and Notch-4 biomarker expression in triple-negative breast cancer. In *International journal of surgical pathology* 20 (2), pp. 139–145. DOI: 10.1177/1066896911427035.

Spitz, François; Furlong, Eileen E. M. (2012): Transcription factors: from enhancer binding to developmental control. In *Nature reviews. Genetics* 13 (9), pp. 613–626. DOI: 10.1038/nrg3207.

Stephenson, Natalie L.; Avis, Johanna M. (2012): Direct observation of proteolytic cleavage at the S2 site upon forced unfolding of the Notch negative regulatory region. In *Proceedings of the National Academy of Sciences of the United States of America* 109 (41), E2757-65. DOI: 10.1073/pnas.1205788109.

Sterner, David E.; Berger, Shelley L. (2000): Acetylation of Histones and Transcription-Related Factors. In *Microbiology and Molecular Biology Reviews* 64 (2), pp. 435–459.

Stittrich, Anna-Barbara; Lehman, Anna; Bodian, Dale L.; Ashworth, Justin; Zong, Zheyuan; Li, Hong et al. (2014): Mutations in NOTCH1 cause Adams-Oliver syndrome. In *American Journal of Human Genetics* 95 (3), pp. 275–284. DOI: 10.1016/j.ajhg.2014.07.011.

Strahl, B. D.; Allis, C. D. (2000): The language of covalent histone modifications. In *Nature* 403 (6765), pp. 41–45. DOI: 10.1038/47412.

Stylianou, Spyros; Clarke, Rob B.; Brennan, Keith (2006): Aberrant activation of notch signaling in human breast cancer. In *Cancer research* 66 (3), pp. 1517–1525. DOI: 10.1158/0008-5472.CAN-05-3054.

Sugaya, K.; Sasanuma, S.; Nohata, J.; Kimura, T.; Fukagawa, T.; Nakamura, Y. et al. (1997): Gene organization of human NOTCH4 and (CTG)n polymorphism in this human counterpart gene of mouse proto-oncogene Int3. In *Gene* 189 (2), pp. 235–244. DOI: 10.1016/s0378-1119(96)00857-8.

Swygert, Sarah G.; Peterson, Craig L. (2014): Chromatin dynamics: interplay between remodeling enzymes and histone modifications. In *Biochimica et biophysica acta* 1839 (8), pp. 728–736. DOI: 10.1016/j.bbagrm.2014.02.013.

Taghon, Tom N.; David, Elizabeth-Sharon; Zúñiga-Pflücker, Juan Carlos; Rothenberg, Ellen V. (2005): Delayed, asynchronous, and reversible T-lineage specification induced by Notch/Delta signaling. In *Genes & development* 19 (8), pp. 965–978. DOI: 10.1101/gad.1298305.

Tahiliani, Mamta; Koh, Kian Peng; Shen, Yinghua; Pastor, William A.; Bandukwala, Hozefa; Brudno, Yevgeny et al. (2009): Conversion of 5-methylcytosine to 5-hydroxymethylcytosine in mammalian DNA by MLL partner TET1. In *Science (New York, N.Y.)* 324 (5929), pp. 930–935. DOI: 10.1126/science.1170116.

Tamura, K.; Taniguchi, Y.; Minoguchi, S.; Sakai, T.; Tun, T.; Furukawa, T.; Honjo, T. (1995): Physical interaction between a novel domain of the receptor Notch and the transcription factor RBP-J kappa/Su(H). In *Current biology : CB* 5 (12), pp. 1416–1423. DOI: 10.1016/s0960-9822(95)00279-x.

Tang, Wei; Li, Meng; Qi, Xin; Li, Jing (2020): β1,4-Galactosyltransferase V Modulates Breast Cancer Stem Cells through Wnt/β-catenin Signaling Pathway. In *Cancer research and treatment* 52 (4), pp. 1084–1102. DOI: 10.4143/crt.2020.093.

Taniguchi, Y.; Furukawa, T.; Tun, T.; Han, H.; Honjo, T. (1998): LIM protein KyoT2 negatively regulates transcription by association with the RBP-J DNA-binding protein. In *Molecular and cellular biology* 18 (1), pp. 644–654. DOI: 10.1128/MCB.18.1.644.

The ENCODE (ENCyclopedia Of DNA Elements) Project (2004). In *Science (New York, N.Y.)* 306 (5696), pp. 636–640.

Theodosiou, Athina; Arhondakis, Stilianos; Baumann, Marc; Kossida, Sophia (2009): Evolutionary scenarios of Notch proteins. In *Molecular biology and evolution* 26 (7), pp. 1631–1640. DOI: 10.1093/molbev/msp075.

Thomas, Mary C.; Chiang, Cheng-Ming (2006): The general transcription machinery and general cofactors. In *Critical reviews in biochemistry and molecular biology* 41 (3), pp. 105–178. DOI: 10.1080/10409230600648736.

Thompson, John F.; Steinmann, Kathleen E. (2010): Single molecule sequencing with a HeliScope genetic analysis system. In *Current protocols in molecular biology* Chapter 7, Unit7.10. DOI: 10.1002/0471142727.mb0710s92.

Thorne, A. W.; Kmiciek, D.; Mitchelson, K.; Sautiere, P.; Crane-Robinson, C. (1990): Patterns of histone acetylation. In *European journal of biochemistry* 193 (3), pp. 701–713. DOI: 10.1111/j.1432-1033.1990.tb19390.x.

Tokunaga, Akinori; Kohyama, Jun; Yoshida, Tetsu; Nakao, Keiko; Sawamoto, Kazunobu; Okano, Hideyuki (2004): Mapping spatio-temporal activation of Notch signaling during neurogenesis and gliogenesis in the developing mouse brain. In *Journal of neurochemistry* 90 (1), pp. 142–154. DOI: 10.1111/j.1471-4159.2004.02470.x.

Tremblay, Isabelle; Paré, Emanuel; Arsenault, Dominique; Douziech, Mélanie; Boucher, Marie-Josée (2013): The MEK/ERK pathway promotes NOTCH signalling in pancreatic cancer cells. In *PloS one* 8 (12), e85502. DOI: 10.1371/journal.pone.0085502.

Trojer, Patrick; Reinberg, Danny (2007): Facultative heterochromatin: is there a distinctive molecular signature? In *Molecular cell* 28 (1), pp. 1–13. DOI: 10.1016/j.molcel.2007.09.011.

Tsai, F. T.; Sigler, P. B. (2000): Structural basis of preinitiation complex assembly on human pol II promoters. In *The EMBO Journal* 19 (1), pp. 25–36. DOI: 10.1093/emboj/19.1.25.

Tsompana, Maria; Buck, Michael J. (2014): Chromatin accessibility: a window into the genome. In *Epigenetics & chromatin* 7 (1), p. 33. DOI: 10.1186/1756-8935-7-33.

Um, M.; Li, C.; Manley, J. L. (1995): The transcriptional repressor even-skipped interacts directly with TATA-binding protein. In *Molecular and cellular biology* 15 (9), pp. 5007–5016. DOI: 10.1128/MCB.15.9.5007.

Uyttendaele, H.; Marazzi, G.; Wu, G.; Yan, Q.; Sassoon, D.; Kitajewski, J. (1996): Notch4/int-3, a mammary proto-oncogene, is an endothelial cell-specific mammalian Notch gene. In *Development (Cambridge, England)* 122 (7), pp. 2251–2259. DOI: 10.1242/dev.122.7.2251.

van Tetering, Geert; van Diest, Paul; Verlaan, Ingrid; van der Wall, Elsken; Kopan, Raphael; Vooijs, Marc (2009): Metalloprotease ADAM10 is required for Notch1 site 2 cleavage. In *The Journal of biological chemistry* 284 (45), pp. 31018–31027. DOI: 10.1074/jbc.M109.006775.

VanDussen, Kelli L.; Carulli, Alexis J.; Keeley, Theresa M.; Patel, Sanjeevkumar R.; Puthoff, Brent J.; Magness, Scott T. et al. (2012): Notch signaling modulates proliferation and differentiation of intestinal crypt base columnar stem cells. In *Development (Cambridge, England)* 139 (3), pp. 488–497. DOI: 10.1242/dev.070763.

Venter, J. C.; Adams, M. D.; Myers, E. W.; Li, P. W.; Mural, R. J.; Sutton, G. G. et al. (2001): The sequence of the human genome. In *Science (New York, N.Y.)* 291 (5507), pp. 1304–1351. DOI: 10.1126/science.1058040.

Wacker, Stephan Armin; Alvarado, Cristobal; Wichert, Götz von; Knippschild, Uwe; Wiedenmann, Jörg; Clauss, Karen et al. (2011): RITA, a novel modulator of Notch signalling, acts via nuclear export of RBP-J. In *The EMBO Journal* 30 (1), pp. 43–56. DOI: 10.1038/emboj.2010.289.

Wallberg, Annika E.; Pedersen, Kia; Lendahl, Urban; Roeder, Robert G. (2002): p300 and PCAF act cooperatively to mediate transcriptional activation from chromatin templates by notch intracellular domains in vitro. In *Molecular and cellular biology* 22 (22), pp. 7812–7819. DOI: 10.1128/MCB.22.22.7812-7819.2002.

Wang, D. G.; Fan, J. B.; Siao, C. J.; Berno, A.; Young, P.; Sapolsky, R. et al. (1998): Large-scale identification, mapping, and genotyping of single-nucleotide polymorphisms in the human genome. In *Science (New York, N.Y.)* 280 (5366), pp. 1077–1082. DOI: 10.1126/science.280.5366.1077.

Wang, Daojing; Bodovitz, Steven (2010): Single cell analysis: the new frontier in 'omics'. In *Trends in biotechnology* 28 (6), pp. 281–290. DOI: 10.1016/j.tibtech.2010.03.002.

Wang, Hongfang; Zang, Chongzhi; Taing, Len; Arnett, Kelly L.; Wong, Yinling Joey; Pear, Warren S. et al. (2014): NOTCH1-RBPJ complexes drive target gene expression through dynamic interactions with superenhancers. In *Proceedings of the National Academy of Sciences of the United States of America* 111 (2), pp. 705–710. DOI: 10.1073/pnas.1315023111.

Wang, Hongfang; Zou, James; Zhao, Bo; Johannsen, Eric; Ashworth, Todd; Wong, Hoifung et al. (2011): Genome-wide analysis reveals conserved and divergent features of Notch1/RBPJ binding in human and murine T-lymphoblastic leukemia cells. In *Proceedings of the National Academy of Sciences of the United States of America* 108 (36), pp. 14908–14913. DOI: 10.1073/pnas.1109023108.

Wang, Kai; Zhang, Qin; Li, Danan; Ching, Keith; Zhang, Cathy; Zheng, Xianxian et al. (2015): PEST domain mutations in Notch receptors comprise an oncogenic driver segment in triple-negative breast cancer sensitive to a γ-secretase inhibitor. In *Clinical cancer research : an official journal of the American Association for Cancer Research* 21 (6), pp. 1487–1496. DOI: 10.1158/1078-0432.CCR-14-1348.

Wang, Xiaobin; Shen, Qingwu W.; Wang, Jie; Zhang, Zhiguo; Feng, Fu; Chen, Ting et al. (2016a): KLF7 Regulates Satellite Cell Quiescence in Response to Extracellular Signaling. In *Stem cells (Dayton, Ohio)* 34 (5), pp. 1310–1320. DOI: 10.1002/stem.2346.

Wang, Xiaofeng; Yu, Zhenjia; Zhou, Quan; Wu, Xiongyan; Chen, Xuehua; Li, Jianfang et al. (2016b): Tissue transglutaminase-2 promotes gastric cancer progression via the ERK1/2 pathway. In *Oncotarget* 7 (6), pp. 7066–7079. DOI: 10.18632/oncotarget.6883.

Wang, Zhong; Gerstein, Mark; Snyder, Michael (2009): RNA-Seq: a revolutionary tool for transcriptomics. In *Nature reviews. Genetics* 10 (1), pp. 57–63. DOI: 10.1038/nrg2484.

Watanabe, Kazuhide; Biesinger, Jacob; Salmans, Michael L.; Roberts, Brian S.; Arthur, William T.; Cleary, Michele et al. (2014): Integrative ChIP-seq/microarray analysis identifies a CTNNB1 target

signature enriched in intestinal stem cells and colon cancer. In *PloS one* 9 (3), e92317. DOI: 10.1371/journal.pone.0092317.

Weber, Christopher M.; Henikoff, Steven (2014): Histone variants: dynamic punctuation in transcription. In *Genes & development* 28 (7), pp. 672–682. DOI: 10.1101/gad.238873.114.

Wendorff, Agnieszka A.; Koch, Ute; Wunderlich, F. Thomas; Wirth, Silvia; Dubey, Christelle; Brüning, Jens C. et al. (2010): Hes1 is a critical but context-dependent mediator of canonical Notch signaling in lymphocyte development and transformation. In *Immunity* 33 (5), pp. 671–684. DOI: 10.1016/j.immuni.2010.11.014.

Weng, Andrew P.; Ferrando, Adolfo A.; Lee, Woojoong; Morris, John P.; Silverman, Lewis B.; Sanchez-Irizarry, Cheryll et al. (2004): Activating mutations of NOTCH1 in human T cell acute lymphoblastic leukemia. In *Science (New York, N.Y.)* 306 (5694), pp. 269–271. DOI: 10.1126/science.1102160.

Weng, Andrew P.; Millholland, John M.; Yashiro-Ohtani, Yumi; Arcangeli, Marie Laure; Lau, Arthur; Wai, Carol et al. (2006): c-Myc is an important direct target of Notch1 in T-cell acute lymphoblastic leukemia/lymphoma. In *Genes & development* 20 (15), pp. 2096–2109. DOI: 10.1101/gad.1450406.

Wharton, Kristi A.; Johansen, Kristen M.; Xu, Tian; Artavanis-Tsakonas, Spyros (1985): Nucleotide sequence from the neurogenic locus Notch implies a gene product that shares homology with proteins containing EGF-like repeats. In *Cell* 43 (3), pp. 567–581. DOI: 10.1016/0092-8674(85)90229-6.

Whetstine, Johnathan R.; Nottke, Amanda; Lan, Fei; Huarte, Maite; Smolikov, Sarit; Chen, Zhongzhou et al. (2006): Reversal of histone lysine trimethylation by the JMJD2 family of histone demethylases. In *Cell* 125 (3), pp. 467–481. DOI: 10.1016/j.cell.2006.03.028.

Whyte, Warren A.; Orlando, David A.; Hnisz, Denes; Abraham, Brian J.; Lin, Charles Y.; Kagey, Michael H. et al. (2013): Master transcription factors and mediator establish super-enhancers at key cell identity genes. In *Cell* 153 (2), pp. 307–319. DOI: 10.1016/j.cell.2013.03.035.

Wickham, Hadley (2016): ggplot2: Elegant Graphics for Data Analysis: Springer-Verlag New York. Available online at https://ggplot2.tidyverse.org.

Wiese, Cornelia; Heisig, Julia; Gessler, Manfred (2010): Hey bHLH factors in cardiovascular development. In *Pediatric cardiology* 31 (3), pp. 363–370. DOI: 10.1007/s00246-009-9609-9.

William, Dilusha A.; Saitta, Biagio; Gibson, Joshua D.; Traas, Jeremy; Markov, Vladimir; Gonzalez, Dorian M. et al. (2007): Identification of oscillatory genes in somitogenesis from functional genomic analysis of a human mesenchymal stem cell model. In *Developmental biology* 305 (1), pp. 172–186. DOI: 10.1016/j.ydbio.2007.02.007.

Wilson, Heather M. (2014): SOCS Proteins in Macrophage Polarization and Function. In *Frontiers in immunology* 5, p. 357. DOI: 10.3389/fimmu.2014.00357.

Wilson, Jeffrey J.; Kovall, Rhett A. (2006): Crystal structure of the CSL-Notch-Mastermind ternary complex bound to DNA. In *Cell* 124 (5), pp. 985–996. DOI: 10.1016/j.cell.2006.01.035.

Woodcock, C. L.; Safer, J. P.; Stanchfield, J. E. (1976): Structural repeating units in chromatin. I. Evidence for their general occurrence. In *Experimental cell research* 97, pp. 101–110. DOI: 10.1016/0014-4827(76)90659-5.

Wu, L.; Aster, J. C.; Blacklow, S. C.; Lake, R.; Artavanis-Tsakonas, S.; Griffin, J. D. (2000): MAML1, a human homologue of Drosophila mastermind, is a transcriptional co-activator for NOTCH receptors. In *Nature genetics* 26 (4), pp. 484–489. DOI: 10.1038/82644.

Wu, Lin; Williams, P. Mickey; Koch, Walter (2005): Clinical applications of microarray-based diagnostic tests. In *BioTechniques* 39 (10 Suppl), S577-82. DOI: 10.2144/000112046.

Xu, Tao; Park, Sung-Soo; Giaimo, Benedetto Daniele; Hall, Daniel; Ferrante, Francesca; Ho, Diana M. et al. (2017): RBPJ/CBF1 interacts with L3MBTL3/MBT1 to promote repression of Notch signaling via histone demethylase KDM1A/LSD1. In *The EMBO Journal* 36 (21), pp. 3232–3249. DOI: 10.15252/embj.201796525.

Xue, Dongyun; Li, Dong; Dou, Cong; Li, Junshan (2021): A Comprehensive Bioinformatic Analysis of NOTCH Pathway Involvement in Stomach Adenocarcinoma. In *Disease markers* 2021, p. 4739868. DOI: 10.1155/2021/4739868.

Yamamoto, N.; Yamamoto, S.; Inagaki, F.; Kawaichi, M.; Fukamizu, A.; Kishi, N. et al. (2001): Role of Deltex-1 as a transcriptional regulator downstream of the Notch receptor. In *The Journal of biological chemistry* 276 (48), pp. 45031–45040. DOI: 10.1074/jbc.M105245200.

Yamamoto, Takayoshi; Kambayashi, Yuta; Tsukano, Kohei; Michiue, Tatsuo (2023): Ndst1, a heparan sulfate modification enzyme, regulates neuroectodermal patterning by enhancing Wnt signaling in Xenopus. In *Development, growth & differentiation* 65 (3), pp. 153–160. DOI: 10.1111/dgd.12843.

Yan, Yuanyuan; Liu, Fangxiao; Han, Li; Zhao, Lin; Chen, Jianjun; Olopade, Olufunmilayo I. et al. (2018): HIF-2α promotes conversion to a stem cell phenotype and induces chemoresistance in breast cancer cells by activating Wnt and Notch pathways. In *Journal of experimental & clinical cancer research : CR* 37 (1), p. 256. DOI: 10.1186/s13046-018-0925-x.

Yashiro-Ohtani, Yumi; He, Yiping; Ohtani, Takuya; Jones, Mary E.; Shestova, Olga; Xu, Lanwei et al. (2009): Pre-TCR signaling inactivates Notch1 transcription by antagonizing E2A. In *Genes & development* 23 (14), pp. 1665–1676. DOI: 10.1101/gad.1793709.

Yochem, J.; Weston, K.; Greenwald, I. (1988): The Caenorhabditis elegans lin-12 gene encodes a transmembrane protein with overall similarity to Drosophila Notch. In *Nature* 335 (6190), pp. 547–550. DOI: 10.1038/335547a0.

Yoshino, Seiko; Suzuki, Hiroshi I. (2022): The molecular understanding of super-enhancer dysregulation in cancer. In *Nagoya journal of medical science* 84 (2), pp. 216–229. DOI: 10.18999/nagjms.84.2.216.

Yu, Guangchuang; Wang, Li-Gen; Han, Yanyan; He, Qing-Yu (2012): clusterProfiler: an R package for comparing biological themes among gene clusters. In *Omics : a journal of integrative biology* 16 (5), pp. 284–287. DOI: 10.1089/omi.2011.0118.

Yu, Guangchuang; Wang, Li-Gen; He, Qing-Yu (2015): ChIPseeker: an R/Bioconductor package for ChIP peak annotation, comparison and visualization. In *Bioinformatics (Oxford, England)* 31 (14), pp. 2382–2383. DOI: 10.1093/bioinformatics/btv145.

Yuan, Zhenyu; VanderWielen, Bradley D.; Giaimo, Benedetto Daniele; Pan, Leiling; Collins, Courtney E.; Turkiewicz, Aleksandra et al. (2019): Structural and Functional Studies of the RBPJ-SHARP Complex Reveal a Conserved Corepressor Binding Site. In *Cell reports* 26 (4), 845-854.e6. DOI: 10.1016/j.celrep.2018.12.097.

Yue, Feng; Bi, Pengpeng; Wang, Chao; Shan, Tizhong; Nie, Yaohui; Ratliff, Timothy L. et al. (2017): Pten is necessary for the quiescence and maintenance of adult muscle stem cells. In *Nature communications* 8, p. 14328. DOI: 10.1038/ncomms14328.

Yun, Theodore J.; Bevan, Michael J. (2003): Notch-regulated ankyrin-repeat protein inhibits Notch1 signaling: multiple Notch1 signaling pathways involved in T cell development. In *Journal of immunology (Baltimore, Md. : 1950)* 170 (12), pp. 5834–5841. DOI: 10.4049/jimmunol.170.12.5834.

Zaidan, Nur Zafirah; Sridharan, Rupa (2020): HP1γ regulates H3K36 methylation and pluripotency in embryonic stem cells. In *Nucleic acids research* 48 (22), pp. 12660–12674. DOI: 10.1093/nar/gkaa1091.

Zaret, Kenneth S. (2020): Pioneer Transcription Factors Initiating Gene Network Changes. In *Annual review of genetics* 54, pp. 367–385. DOI: 10.1146/annurev-genet-030220-015007.

Zaret, Kenneth S.; Carroll, Jason S. (2011): Pioneer transcription factors: establishing competence for gene expression. In *Genes & development* 25 (21), pp. 2227–2241. DOI: 10.1101/gad.176826.111.

Zavadil, Jiri; Cermak, Lukas; Soto-Nieves, Noemi; Böttinger, Erwin P. (2004): Integration of TGF-beta/Smad and Jagged1/Notch signalling in epithelial-to-mesenchymal transition. In *The EMBO Journal* 23 (5), pp. 1155–1165. DOI: 10.1038/sj.emboj.7600069.

Zhang, Jun; Chiodini, Rod; Badr, Ahmed; Zhang, Genfa (2011): The impact of next-generation sequencing on genomics. In *Journal of genetics and genomics = Yi chuan xue bao* 38 (3), pp. 95–109. DOI: 10.1016/j.jgg.2011.02.003.

Zhang, Lirong; Xue, Gaogao; Liu, Junjie; Li, Qianzhong; Wang, Yong (2018): Revealing transcription factor and histone modification co-localization and dynamics across cell lines by integrating ChIP-seq and RNA-seq data. In *BMC genomics* 19 (Suppl 10), p. 914. DOI: 10.1186/s12864-018-5278-5.

Zhang, Qikai; Zhu, Zongsi; Guan, Jiaqiang; Hu, Yingying; Zhou, Wenjin; Ye, Wanchun et al. (2022): Hes1 Controls Proliferation and Apoptosis in Chronic Lymphoblastic Leukemia Cells by Modulating PTEN Expression. In *Molecular biotechnology* 64 (12), pp. 1419–1430. DOI: 10.1007/s12033-022-00476-2.

Zhang, Yong; Liu, Tao; Meyer, Clifford A.; Eeckhoute, Jérôme; Johnson, David S.; Bernstein, Bradley E. et al. (2008): Model-based Analysis of ChIP-Seq (MACS). In *Genome biology* 9 (9), R137. DOI: 10.1186/gb-2008-9-9-r137.

Zheng, Xiaofeng; Narayanan, Sampath; Zheng, Xiaowei; Luecke-Johansson, Sandra; Gradin, Katarina; Catrina, Sergiu-Bogdan et al. (2017): A Notch-independent mechanism contributes to the induction of Hes1 gene expression in response to hypoxia in P19 cells. In *Experimental cell research* 358 (2), pp. 129–139. DOI: 10.1016/j.yexcr.2017.06.006.

Zhou, Binghan; Lin, Wanling; Long, Yaling; Yang, Yunkai; Zhang, Huan; Wu, Kongming; Chu, Qian (2022): Notch signaling pathway: architecture, disease, and therapeutics. In *Signal transduction and targeted therapy* 7 (1), p. 95. DOI: 10.1038/s41392-022-00934-y.

Zhou, Mi; Yan, Jun; Ma, Zhaowu; Zhou, Yang; Abbood, Nibras Najm; Liu, Jianfeng et al. (2012): Comparative and evolutionary analysis of the HES/HEY gene family reveal exon/intron loss and teleost specific duplication events. In *PloS one* 7 (7), e40649. DOI: 10.1371/journal.pone.0040649.

Zhou, Quan; Liu, Mingwei; Xia, Xia; Gong, Tongqing; Feng, Jinwen; Liu, Wanlin et al. (2017): A mouse tissue transcription factor atlas. In *Nature communications* 8, p. 15089. DOI: 10.1038/ncomms15089.

Zhu, Changyu; Ho, Yu-Jui; Salomao, Marcela A.; Dapito, Dianne H.; Bartolome, Alberto; Schwabe, Robert F. et al. (2021): Notch activity characterizes a common hepatocellular carcinoma subtype with unique molecular and clinicopathologic features. In *Journal of hepatology* 74 (3), pp. 613–626. DOI: 10.1016/j.jhep.2020.09.032.

Zhu, He; Bhaijee, Feriyl; Ishaq, Nivin; Pepper, Dominique J.; Backus, Kandis; Brown, Alexandra S. et al. (2013): Correlation of Notch1, pAKT and nuclear NF-κB expression in triple negative breast cancer. In *American Journal of Cancer Research* 3 (2), pp. 230–239.

# 8. Appendix

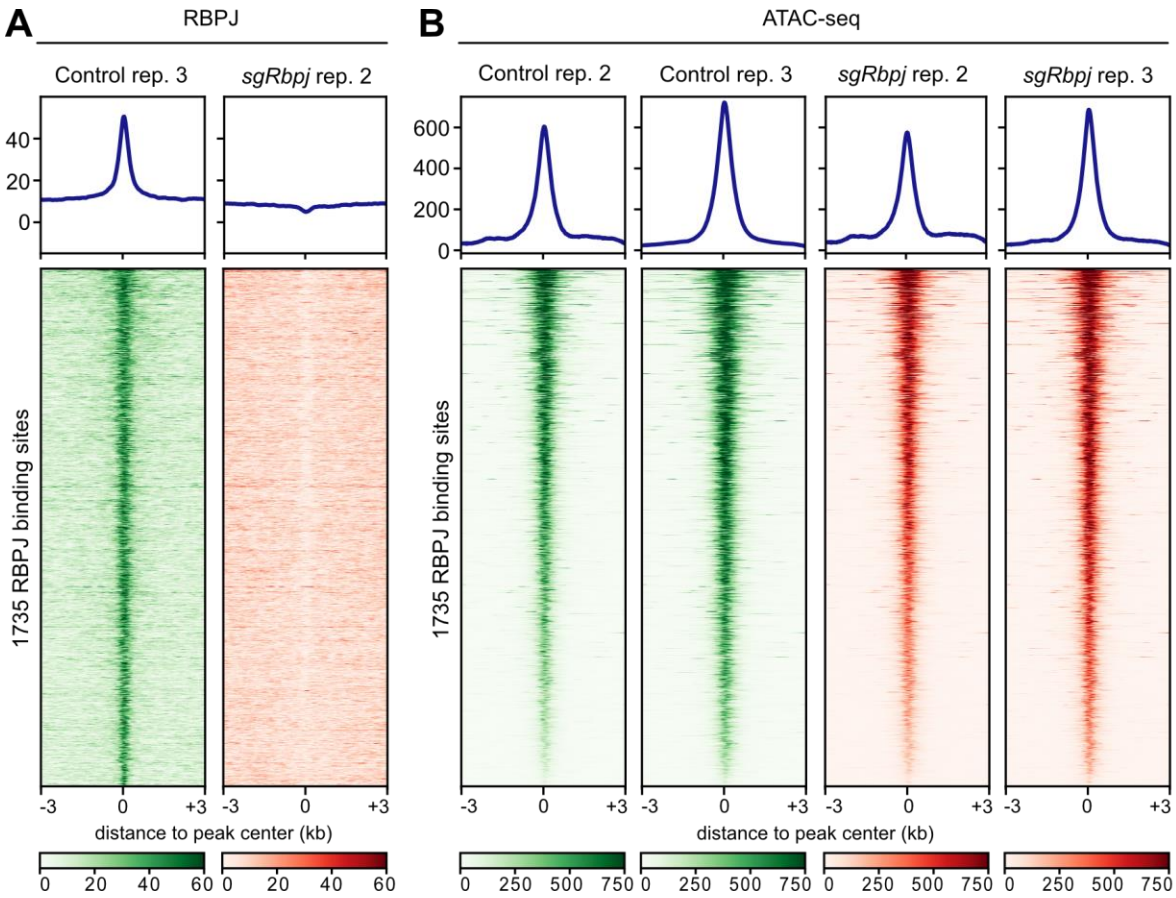


**App. Figure 1) Characterization of RBPJ binding sites in mature T-cells.** A) Heat map and average binding plot (profile) showing the 1735 RBPJ binding sites in control (green) and RBPJ-depleted (red) mature T-cells analyzed by ChIP-seq. B) Heat map and average binding plot (profile) of the chromatin accessibility at 1735 RBPJ sites in control (green) and RBPJ-depleted (red) MT cells. Chromatin accessibility was measured by ATAC-seq.

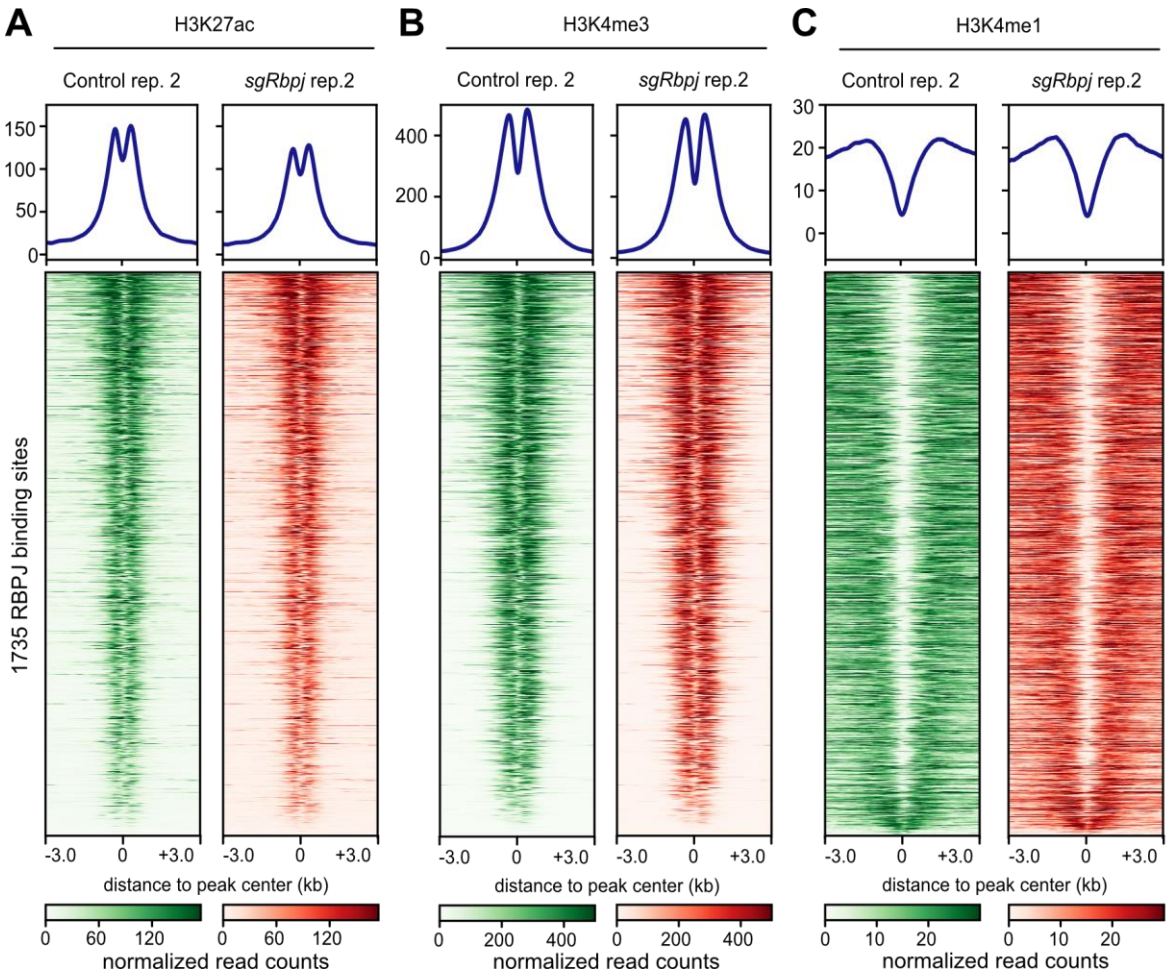


**App. Figure 2) The chromatin landscape at RBPJ binding sites in mature T-cells.** Heat map and average binding plot (profile) showing the overall enrichment of A) H3K27ac, B) H3K4me3 and C) H3K4me1 at 1735 RBPJ binding sites in control (green) and RBPJ-depleted (red) mature T-cells analyzed by ChIP-seq.

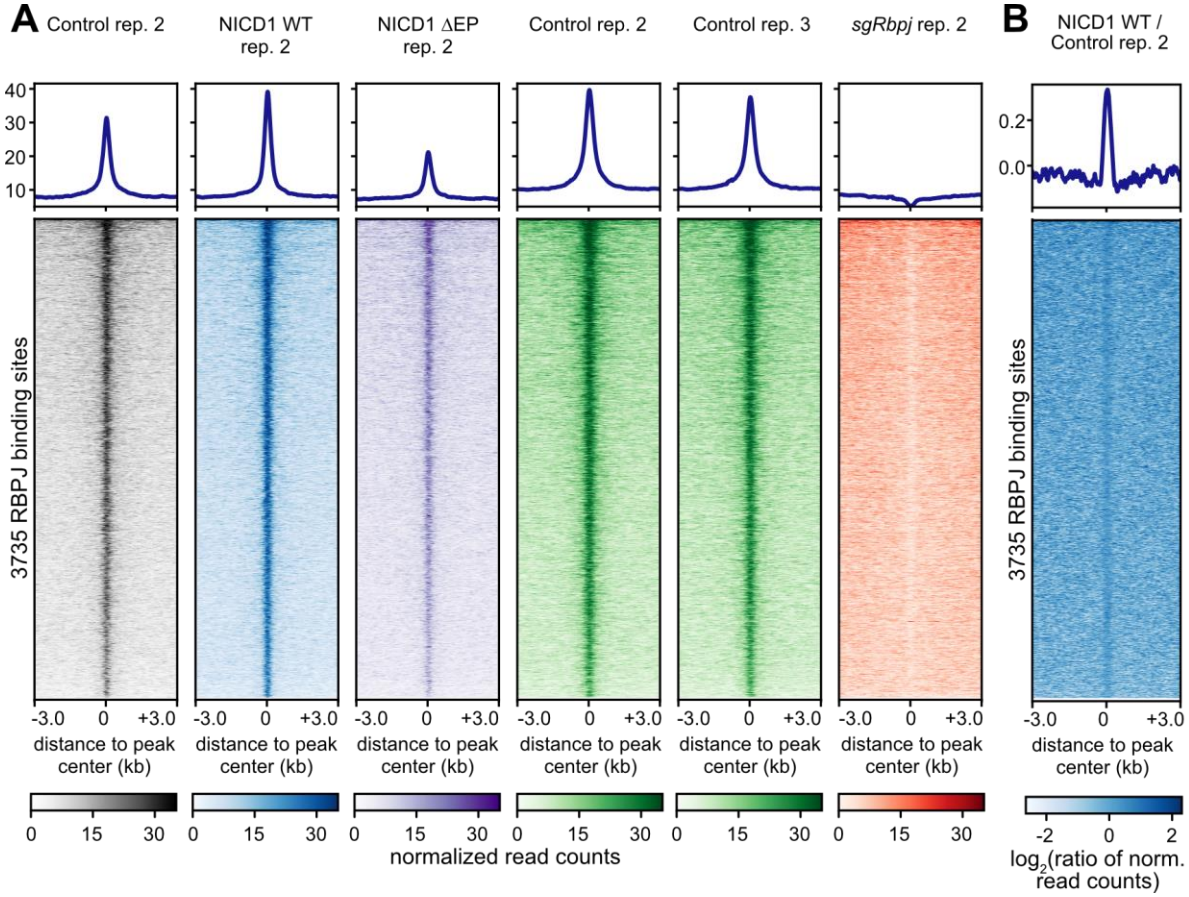


**App. Figure 3) Notch activation leads to increased RBPJ binding.** A) Heat map and average binding plot (profile) depicting 3735 RBPJ binding sites identified in mature T-cells overexpressing NICD1 WT and their binding strength in BioeV control (grey), BioNICD1 WT (blue), BioNICD1 ΔEP (purple), CRISPR control (green) and RBPJ-depleted (red) MT cells. B) Heat map and average binding plot (profile) showing the increase in RBPJ binding at 3735 RBPJ sites upon BioNICD1 WT.

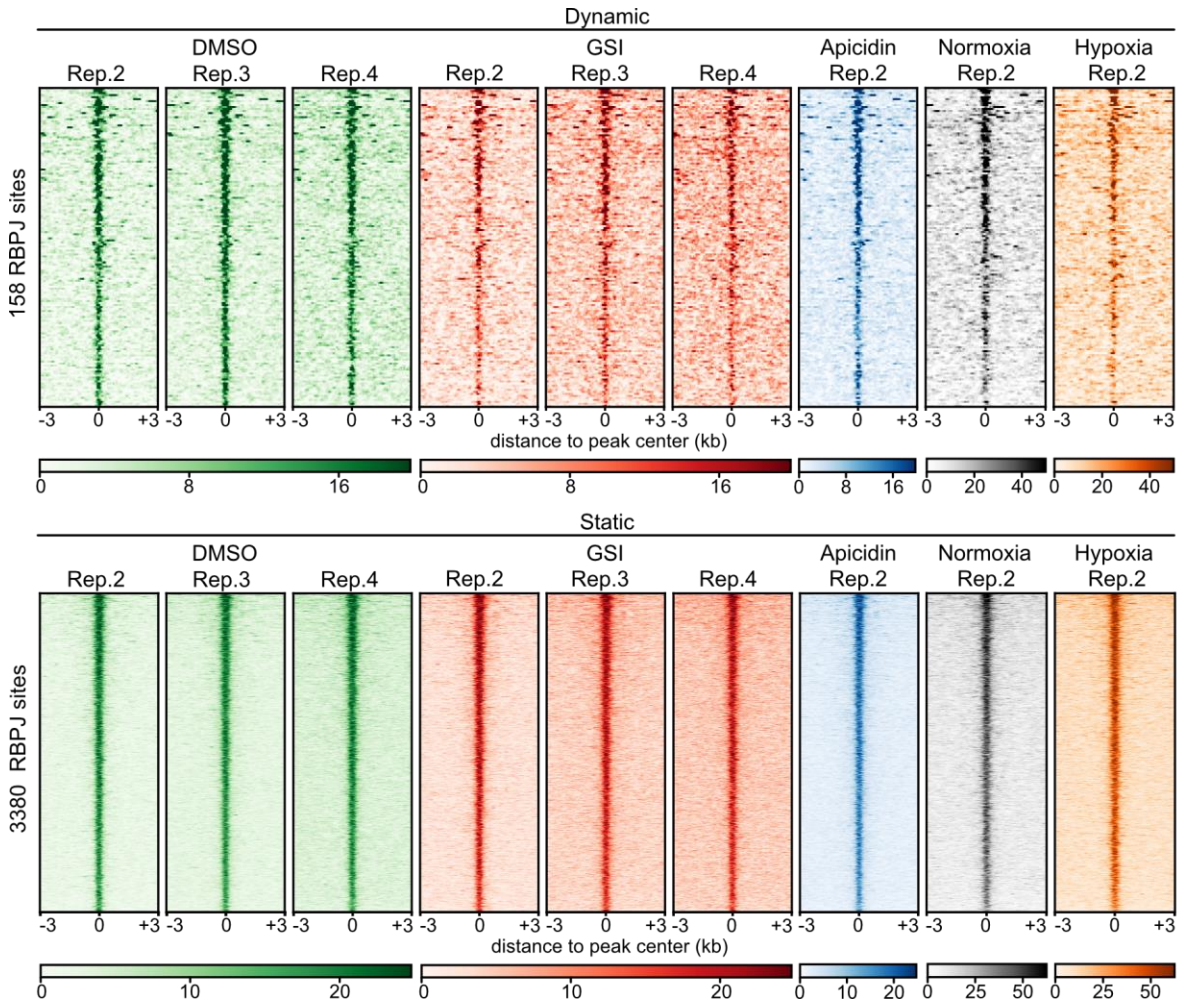


**App. Figure 4) Identification of dynamic RBPJ binding in Beko cells.** Heat map depicting 3380 static ($log_2$ FC > -0.5) and 158 dynamic ($log_2$ FC < -0.5) RBPJ binding sites in DMSO (green), GSI (red), Apicidin (blue), normoxia (grey) and hypoxia (orange).

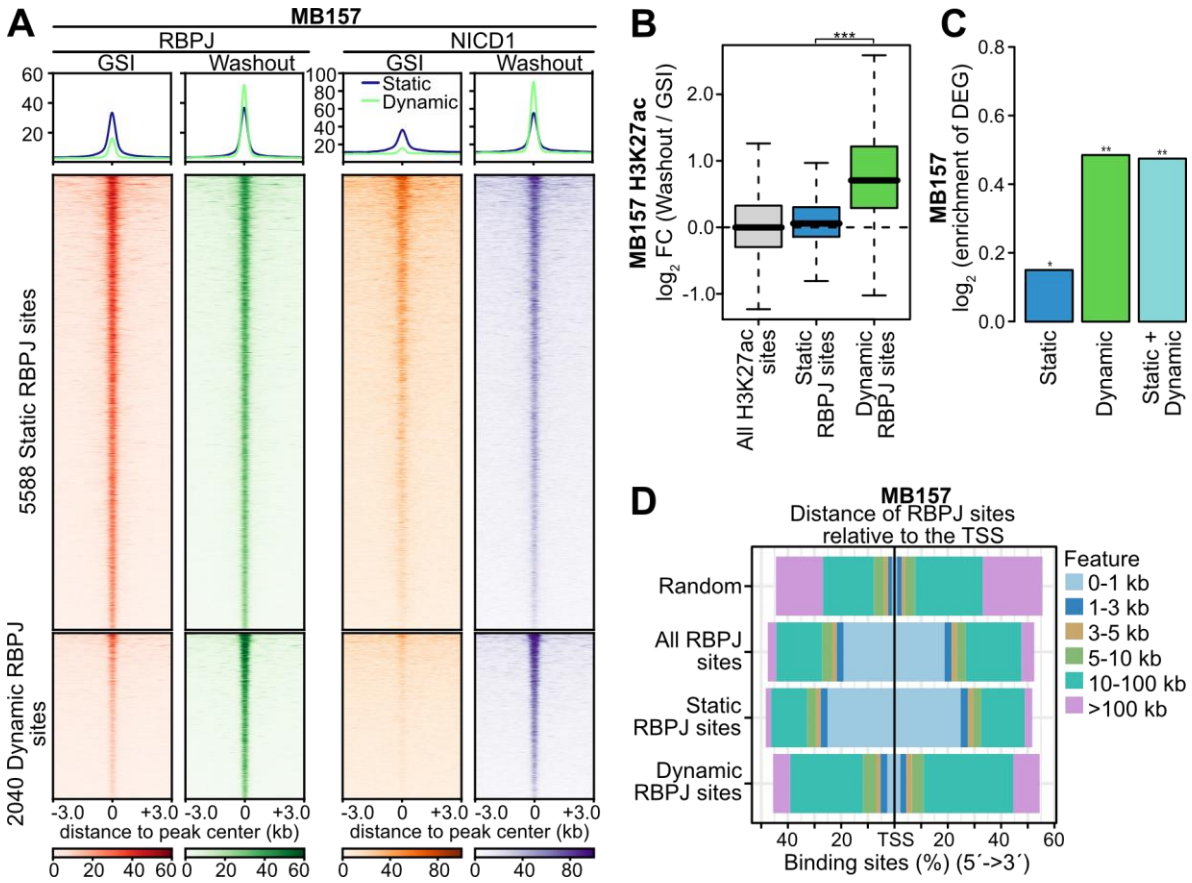


**App. Figure 5) MB157 cells show a dynamic and static RBPJ binding behavior.** A) Heat map and average binding plot depicting 5588 static and 2040 dynamic RBPJ binding sites in MB157 cells upon 5 h of GSI washout. Shown are RBPJ binding (left) after 72 h of treatment (red) or 5 h of GSI washout (green) and NICD1 binding (right) after 72 h of treatment (orange) or 5 h of GSI washout (purple). B) Box plot of the changes of H3K27ac upon Notch re-activation by washout of GSI at all identified H3K27ac sites, at static RBPJ sites and at dynamic RBPJ binding sites. C) Bar plot depicting the enrichment of significantly DEGs within the genes associated with static, dynamic and static & dynamic RBPJ sites. D) Stacked bar plots showing the distance to the nearest TSS of all RBPJ binding sites, dynamically bound RBPJ sites or statically bound RBPJ sites. Random sites are shown as a control. [***] $p < 0.001$, [**] $p < 0.01$, [*] $p < 0.05$; Wilcoxon rank sum test or hypergeometric test.